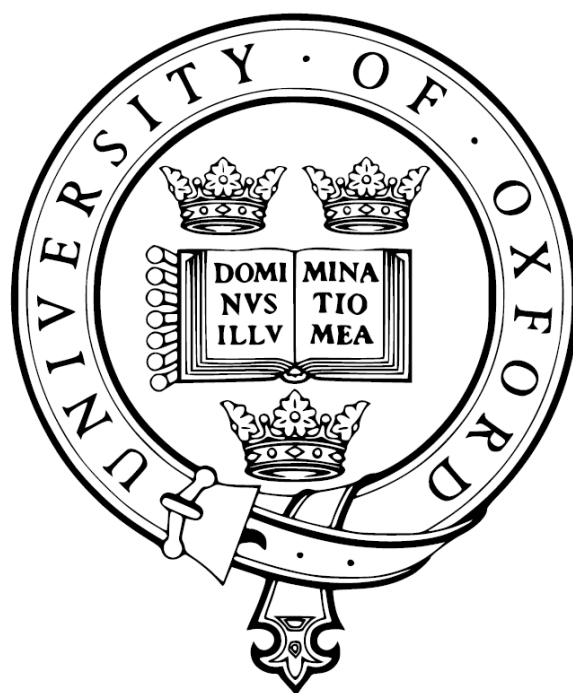


Development of New Multicomponent Reactions for 1,3,4-Oxadiazole Synthesis



A thesis submitted in partial fulfilment of the requirement
for the degree of Doctor of Philosophy (DPhil)

Daniel Matheau-Raven

Supervisor: Prof. Darren J. Dixon

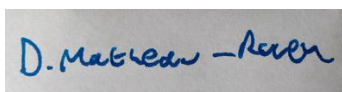
Merton College

University of Oxford

Trinity Term 2022

Declaration

The work described in this thesis was carried out in the Chemistry Research Laboratory, University of Oxford, from June 2018 until April 2022, under the supervision of Professor Darren J. Dixon. All of the work within this thesis is my own unless otherwise stated and has not been submitted previously for any other degree at this or any other university. Work that was done as part of a collaboration with research colleagues has been fully acknowledged and referenced within the text. All compounds synthesized by myself are shown and characterized in the experimental section (chapter 5), but data for compounds synthesized by other colleagues are not reported.

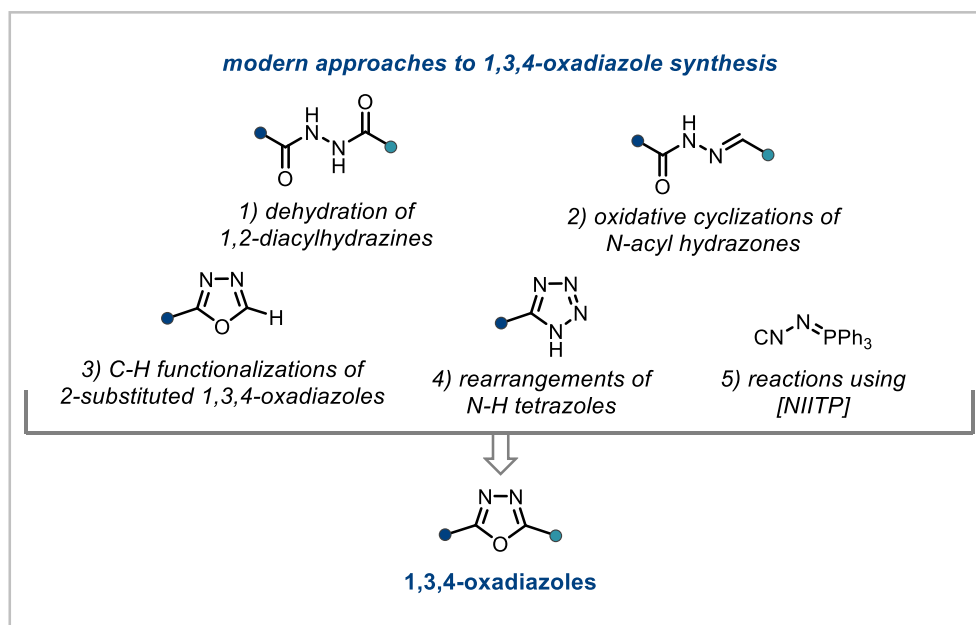


Daniel Matheau-Raven

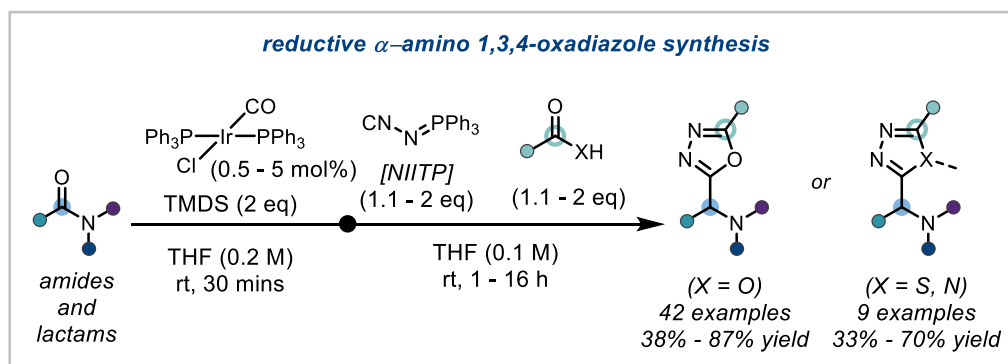
April 2022

Abstract

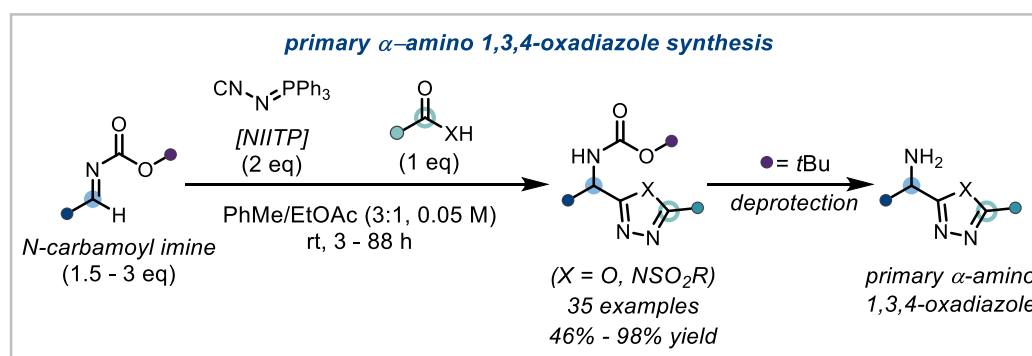
Chapter 1 introduces the chemistry of 1,3,4-oxadiazoles with a specific focus on currently available strategies, and methodologies for their synthesis. Five distinct synthetic approaches – 1) dehydration of 1,2-diacylhydrazines; 2) oxidative cyclizations of *N*-acyl hydrazones; 3) C-H functionalization of 2-substituted 1,3,4-oxadiazoles; 4) rearrangements of *N*-H tetrazoles; 5) reactions using (*N*-isocyanoimino)triphenylphosphorane (NIITP) as a three atom *CNN* source – are discussed in detail and their limitations evaluated.



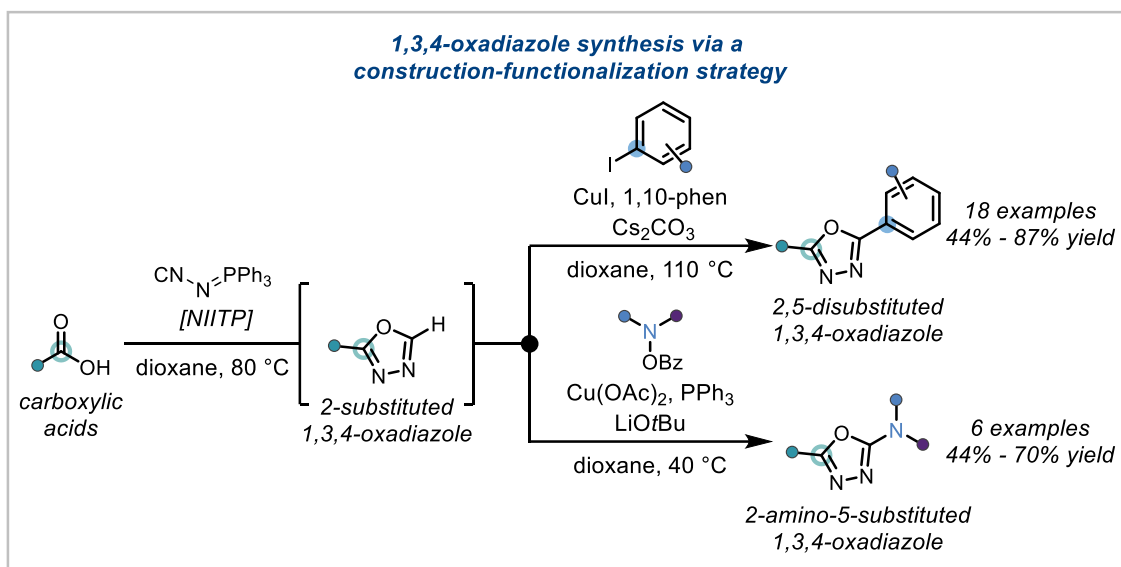
Chapter 2 focuses on a novel three-component reaction for the reductive synthesis of α -amino 1,3,4-oxadiazoles (or heterodiazoles), from tertiary amides and lactams, feedstock carboxylic acids (or appropriate C-, S-, N-Brønsted acids), and NIITP. Taking advantage of the mild and chemoselective reductive activation of tertiary amides provided by the combination of Vaska's complex and 1,1,3,3-tetramethyldisiloxane (TMDS) the reaction was applied to the late-stage functionalization of ten drug-like amides and carboxylic acids and culminated in the synthesis of three heterodiazole-fused drug-drug conjugates.



Chapter 3 demonstrates that *N*-carbamoyl imines, with carboxylic acid (or *N*-acyl sulfonamide) coupling partners and NIITP, can efficiently generate *N*-carbamoyl α -amino 1,3,4-oxadiazole (or 1,2,4-triazole) structures in a three-component reaction – expanding the existing scope of C=N electrophiles used with NIITP. A successful scale-up of this methodology allowed the gram-scale synthesis of a primary α -amino 1,3,4-oxadiazole, and a subsequent investigation into its derivatization.



Chapter 4 presents the merger of two modern approaches for 1,3,4-oxadiazole synthesis – 2-substituted 1,3,4-oxadiazole construction using NIITP and the C-H functionalization of 2-substituted 1,3,4-oxadiazoles – into a one-pot and multicomponent protocol for synthesis of 2,5-disubstituted, or 2-amino-5-substituted, 1,3,4-oxadiazoles. A preliminary investigation into the use of nucleophilic secondary amine coupling partners for synthesis of 2-amino-5-substituted 1,3,4-oxadiazoles is additionally discussed.



Acknowledgements

Firstly, I want to thank Darren for his encouragement, guidance, and continuous ideas throughout my DPhil, including those which didn't work out and eventually led to the ones that did. Your enthusiasm and knowledge of chemistry was endlessly helpful, and your group is a continually engaging and fun place to work and filled with excellent chemists and people.

I'd like to extend my thanks to all who made my DPhil memorable with their ideas and advice, laughter, countless pub trips and one group retreat, including: Jamie, Bran, Phillip, Sam, Yao, Pablo, Pete, Jonny, Mix, Connor, Thomas, Ken, Lucia, Guanglong, Tanya, Andrew, Dan R, Roman, Charmaine, Ben, Tim, Tom, Jack, Molly, Maddy, James, Edvinas, Dan, and Ian.

Special thanks must go to people I've had the pleasure of collaborating with or supervising – Ricardo, Yutao, Tanya, and Lizzie – for making those projects successful, or not, more enjoyable to work on. And to those who lent their time to proofread and correct this thesis – Andrew, Ben, Dan R, Jamie, and Pablo.

My parents and my family must be thanked for their love and unconditional support throughout all my studies.

Lastly, I'd like to thank Miranda, and our cat Dipper, for all their love and support throughout my studies and especially during the uncertainty of the COVID-19 pandemic, I can't wait to continue our life together.

Dedicated to the memory of Andromachi Matbeau-raven

Abbreviations

(R)-TRIP	(R)-3,3'-Bis(2,4,6-triisopropylphenyl)-1,1'-bi-2-naphthol cyclic monophosphate
~	Approximately
1,10-phen	1,10-Phenanthroline
4CR	Four component reaction
Ac	Acetyl
AIDS	Acquired immunodeficiency syndrome
APIs	Active Pharmaceutical Ingredients
Ar	Unspecified aromatic group
aq.	Aqueous
BEMP	2- <i>tert</i> -Butylimino-2-diethylamino-1,3-dimethylperhydro-1,3,2-diazaphosphorine
BINAP	(2,2'-bis(diphenylphosphino)-1,1'-binaphthyl)
BINOL	1,1'-Bi-2-naphthol
Bn	Benzyl
Boc	<i>tert</i> -Butoxycarbonyl
Boc-Gly-OH	(<i>tert</i> -Butoxycarbonyl)glycine
bpy	2,2'-Bipyridine
BQ	Benzoquinone
Bz	Benzoyl

(BzO) ₂	Dibenzoyl peroxide
CAN	Ceric ammonium nitrate
Cbz	Carboxybenzyl
Chloramine-T	Sodium chloro(4-methylbenzene-1-sulfonyl)azanide
cod	1,5-Cyclooctadiene
COVID-19	Coronavirus disease 2019
CRL	Chemistry Research Laboratories, University of Oxford
CuTC	Copper(I) thiophene-2-carboxylate
CyJohnPhos	(2-Biphenyl)dicyclohexylphosphine
d.r.	Diastereomeric ratio
DABCO	1,4-diazabicyclo[2.2.2]octane
DB-18-C-6	Dibenzo-18-crown-6
DBU	1,8-Diazabicyclo[5.4.0]undec-7-ene
DCE	1,2-Dichloroethane
dcype	Bis(dicyclohexylphosphino)ethane
DDQ	2,3-Dichloro-5,6-dicyano-1,4-benzoquinone
DEE	1,2-Diethoxyethane
Difluorphos	5,5'-Bis(diphenylphosphino)-2,2,2',2'-tetrafluoro-4,4'-bi-1,3-benzodioxole
DIPEA	<i>N,N</i> -Diisopropylethylamine
DMAc	Dimethylacetamide

DMAP	4-Dimethylaminopyridine
DME	Dimethoxyethane
DMEDA	1,2-Dimethylethylenediamine
DMF	<i>N,N</i> -dimethylformamide
DMP	Dess–Martin periodinane
DMSO	Dimethyl sulfoxide
DPEphos	Bis(2-diphenylphosphinophenyl)ether
DPPBz	1,2-Bis(diphenylphosphino)benzene
dppe	1,2-Bis(diphenylphosphino)ethane
dppf	1,1'-Bis(diphenylphosphino)ferrocene
dppp	1,3-Bis(diphenylphosphino)propane
DTBP	Di- <i>tert</i> -butyl peroxide
EDC	1-Ethyl-3-(3-dimethylaminopropyl)carbodiimide
ee	Enantiomeric excess
eq	Equivalents
<i>E</i>	<i>Entgegen</i>
EDC	1-Ethyl-3-(3-dimethylaminopropyl)carbodiimide
Et	Ethyl
EtOH	Ethanol
ESI	Electrospray ionization

Et	Ethyl
FCC	Flash column chromatography
FDA	U.S. Food and Drug Administration
Fmoc	9-Fluorenylmethoxycarbonyl
GSK	GlaxoSmithKline
HFIP	Hexafluoroisopropanol
HIV	Human immunodeficiency virus
HMDS	Bis(trimethylsilyl)amine
HPLC	High-performance liquid chromatography
IMes	1,3-Bis(2,4,6-trimethylphenyl)-1,3-dihydro-2H-imidazol-2-ylidene
<i>i</i> Pr	<i>iso</i> -propyl
KHMDS	Potassium bis(trimethylsilyl)amide
LAH	Lithium aluminum hydride
LSF	Late-stage functionalization
MCHr1	Melanin-concentrating hormone receptor 1
MCR	Multicomponent reaction
<i>m</i>	<i>Meta</i>
Me	Methyl
MeOH	Methanol
mins	Minutes

MSD	Merck, Sharp & Dohme
MTBE	Methyl <i>tert</i> -butyl ether
NHC	<i>N</i> -Heterocyclic carbene
NIITP	(<i>N</i> -Isocyanoimino)triphenylphosphorane
NMI	<i>N</i> -Methyl imidazole
NMP	<i>N</i> -Methyl-2-pyrrolidone
NMR	Nuclear magnetic resonance
Nu	Unspecified nucleophilic species
<i>n</i> Bu	<i>Normal</i> -butyl
<i>n</i> Pr	<i>Normal</i> -propyl
<i>o</i>	<i>Ortho</i>
<i>o</i> -DCB	1,2-Dichlorobenzene
<i>p</i>	<i>Para</i>
Pg	Protecting group
Ph	Phenyl
PIDA	(Diacetoxyiodo)benzene
PIFA	(Bis(trifluoroacetoxy)iodo)benzene
PPTS	Pyridinium <i>p</i> -toluenesulfonate
PS	Polymer-supported
PTABS	Phosphotriazene butane sulfonate

PTLC	Preparative thin layer chromatography
PTSA	<i>p</i> -Toluenesulfonic acid
py	pyridine
R	Unspecified organic group
rbf	Round-bottom flask
rt	Room temperature
RuPhos	2-Dicyclohexylphosphino-2',6'-diisopropoxybiphenyl
SAR	Structure-activity relationship
Selectfluor	1-Chloromethyl-4-fluoro-1,4-diazoniabicyclo[2.2.2]octane bis(tetrafluoroborate)
SET	Single-electron transfer
SM	Starting material
Synphos	6,6'-Bis(diphenylphosphino)-2,2',3,3'-tetrahydro-5,5'-bi-1,4-benzodioxin
T ₃ P	Propylphosphonic anhydride
TBAB	Tetra- <i>n</i> -butylammonium bromide
TBAF	Tetra- <i>n</i> -butylammonium fluoride
TBAI	Tetra- <i>n</i> -butylammonium iodide
TBHP	<i>tert</i> -Butyl hydroperoxide
<i>t</i> Bu	<i>Tert</i> -butyl
<i>t</i> BuDavePhos	2-Di- <i>tert</i> -butylphosphino-2'-(<i>N,N</i> -dimethylamino)biphenyl
<i>t</i> BuPHOX	4-(<i>tert</i> -butyl)-2-(2-(diphenylphosphaneyl)phenyl)-4,5-dihydrooxazole

TCCA	Trichloroisocyanuric acid
TEMP	2,2,6,6-tetramethylpiperidine
TEMPO	(2,2,6,6-Tetramethylpiperidin-1-yl)oxyl
Tf	Triflic
TFA	Trifluoroacetic acid
TFE	2,2,2-Trifluoroethanol
THF	Tetrahydrofuran
TM	Transition metal
TMDS	1,1,3,3-Tetramethyldisiloxane
TMG	1,1,3,3-Tetramethylguanidine
TMP-H	2,2,6,6-tetramethylpiperidine
TMS	Trimethylsilyl
<i>t</i> Oct	<i>Tert</i> -octyl
TosMIC	toluenesulfonylmethyl isocyanide
TPPO	Triphenylphosphine oxide
Ts	Tosyl
VT	Variable temperature
w.r.t	With respect to
X	Unspecified atom
Xantphos	4,5-Bis(diphenylphosphino)-9,9-dimethylxanthene

XtalFluor-E *N*-(Difluoro- λ 4-sulfanylidene)-*N*-ethyl-ethanaminium tetrafluoroborate

Z *Zusammen*

Z-Gly-OH ((Benzyloxy)carbonyl)glycine

δ NMR chemical shift

Table of Contents

Chapter 1: Introduction	20
1.1 General Introduction to 1,3,4-Oxadiazoles	20
1.2 Strategies for 2,5-Disubstituted 1,3,4-Oxadiazole Synthesis	23
1.2.1 Dehydrative Approaches	24
1.2.2 Oxidative Approaches	26
1.2.3 C-H Functionalizations of 2-Substituted 1,3,4-Oxadiazoles.....	28
1.2.3.1 Carbon-Carbon Bond Forming Methodologies	29
Arylations of 2-Substituted 1,3,4-Oxadiazoles	29
Alkenylations of 2-Substituted 1,3,4-Oxadiazoles.....	32
Alkynylations of 2-Substituted 1,3,4-Oxadiazoles	35
Alkylations of 2-Substituted 1,3,4-Oxadiazoles.....	36
Domino Reactions Involving 2-Substituted 1,3,4-Oxadiazoles	38
1.2.3.2 Carbon-Nitrogen Bond Forming Methodologies.....	40
1.2.3.3 Carbon-Sulfur and Carbon-Selenium Bond Forming Methodologies.....	45
1.2.3.4 C-H Functionalizations of 2-Substituted 1,3,4-Oxadiazoles <i>via</i> C-H Silylation	46
1.2.4 Synthesis of 1,3,4-Oxadiazoles <i>via</i> the Huisgen Tetrazole Rearrangement	47
1.2.5 Reactions using (<i>N</i> -Isocyanoimino)triphenylphosphorane (NIITP)	50
1.2.5.1 Reactivity with Carboxylic Acids.....	51
1.2.5.2 Reactivity with C=O Electrophiles	53
1.2.5.3 Reactivity with C=N Electrophiles	55
1.2.5.4 Reactivity with Acyl Chlorides	57
1.3 Limitations of Current 1,3,4-Oxadiazole Syntheses	58
1.4 Conclusion and Thesis Aims	60
Chapter 2: Catalytic Reductive Amide Functionalization for Late-Stage α-Amino 1,3,4-Oxadiazole Synthesis	62
2.1 Introduction to Reductive Amide Functionalization	62

2.1.1 General Concept and First Reports	62
2.1.2 Catalytic Reductive Amide Functionalization using Vaska's Complex	65
2.1.3 Catalytic Reductive Amide Functionalizations Involving Isocyanide Nucleophiles	71
2.2 Current Approaches to α-Amino 1,3,4-Oxadiazole Synthesis	73
2.3 Project Concept	74
2.4 Reaction Discovery and Optimization	75
2.5 Reaction Scope	78
2.5.1 Carboxylic Acid Scope	78
2.5.2 Extension to α -Amino Heterodiazole Synthesis	81
2.5.3 Amide and Lactam Scope	84
2.6 Scale-up and Product Derivatization	90
2.7 Synthesis of Heterodiazole-Fused Drug-Drug Conjugates	94
2.8 Conclusions	96
Chapter 3: Primary α-Amino 1,3,4-Oxadiazole Synthesis via an Ugi-Type	
Reaction of <i>N</i>-Carbamoyl Imines with NIITP	97
3.1 Introduction – Project Concept	97
3.2 Reaction Discovery	98
3.2.1 Investigation into the Reactivity of <i>N</i> -H Imines with NIITP	98
3.2.2 Investigation into the Reactivity of Neutral C=N Electrophiles with NIITP	100
3.3 Reaction Optimization	103
3.4 Reaction Scope	107
3.4.1 Scope of Carboxylic Acids	107
3.4.2 Scope of <i>N</i> -Carbamoyl Imines	110
3.4.3 Extension to <i>N</i> -Boc α -Amino Heterodiazole Synthesis	112
3.5 Scale-up and Product Derivatization	115
3.6 Future work – Investigations into an Enantioselective Reaction Variant and the Use of <i>N</i>-	
Acyl Iminium Ion Electrophiles	119
3.6.1 Investigation into an Enantioselective Reaction Variant	119

3.6.2 Investigation into the Use of <i>N</i> -Acyl Iminium Ion Electrophiles	123
3.7 Conclusion	125
Chapter 4: 2,5-Disubstituted 1,3,4-Oxadiazole Synthesis via a One-pot	
Construction-Functionalization Strategy	126
4.1 Introduction – Project Concept.....	126
4.1.1 Initial Investigations	128
4.2 Pursuit of a One-Pot 1,3,4-Oxadiazole Construction-Functionalization Protocol	130
4.3 Development of a One-Pot 1,3,4-Oxadiazole Construction-Arylation.....	131
4.3.1 Optimization of the 2-Substituted 1,3,4-Oxadiazole Synthesis	131
4.3.2 Optimization of the One-Pot 1,3,4-Oxadiazole Construction-Arylation Protocol.....	134
4.3.3 Reaction Scope of the 1,3,4-Oxadiazole Construction-Arylation Protocol.....	136
4.4 Development of a 1,3,4-Oxadiazole Construction-Amination Using Electrophilic Amine	
Coupling Partners	140
4.4.1 Concept	140
4.4.2 Initial Experiments and Optimization	141
4.4.3 Reaction Scope of the 1,3,4-Oxadiazole Construction-Amination Protocol.....	144
4.5 Development of a 1,3,4-Oxadiazole Construction-Amination Using Nucleophilic Amine	
Coupling Partners	146
4.5.1 Concept	146
4.5.2 Optimization of the Nucleophilic 1,3,4-Oxadiazole Ring-Opening	147
4.5.3 Investigations into the Oxidative Ring-Closure	149
4.5.4 Proof-of-Concept of a Three-Stage One-Pot Protocol	150
4.6 Conclusion and Future Work	151
Chapter 5: Experimental Section	152
5.1 General Experimental Details.....	152
5.2 Experimental Details for Chapter 2	155
5.2.1 General Procedure A: Reductive Synthesis of α -Amino Heterodiazoles	155
5.2.2 Synthesis of Starting Materials.....	156

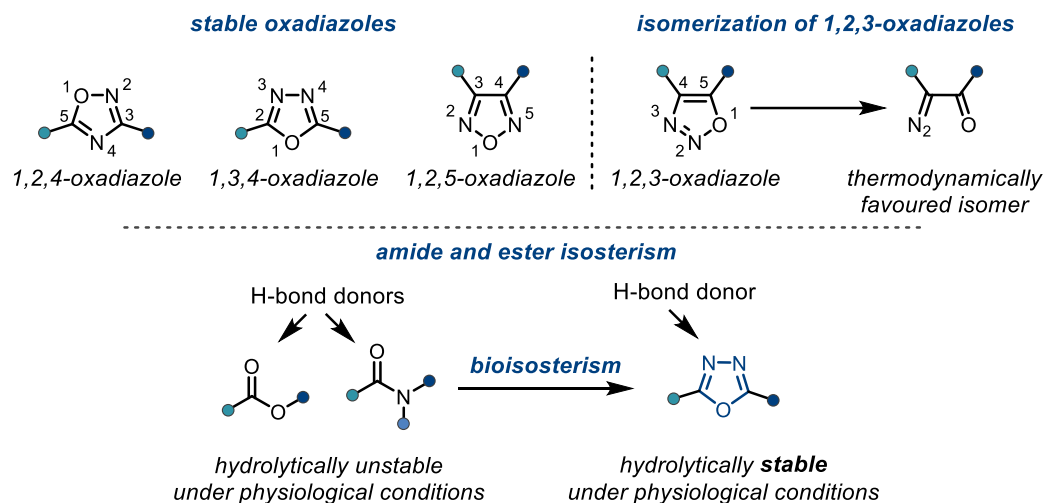
5.2.3 Synthesis of α -Amino Heterodiazole Products.....	168
5.3 Experimental Details for Chapter 3	231
5.3.1 General Procedure B: Synthesis of <i>N</i> -Carbamoyl α -Amino Heterodiazoles.....	231
5.3.2 Synthesis of Starting Materials.....	232
5.3.3 Synthesis of <i>N</i> -Carbamoyl α -Amino Heterodiazoles Products	243
5.3.4 Derivatization of α -Amino 1,3,4-Oxadiazole Products	266
5.4 Experimental Details for Chapter 4	276
5.4.1 General Procedure C: One-Pot 1,3,4-Oxadiazole Construction-Arylation.....	276
5.4.2 General Procedure D: One-Pot 1,3,4-Oxadiazole Construction-Amination.....	277
5.4.3 Synthesis of Starting Materials.....	278
5.4.4 Synthesis of 2,5-Disubstituted 1,3,4-Oxadiazole Products	285
5.4.5 Synthesis of 2-Amino-5-substituted 1,3,4-Oxadiazole Products.....	304
Chapter 6: References	312

Chapter 1: Introduction

1.1 General Introduction to 1,3,4-Oxadiazoles

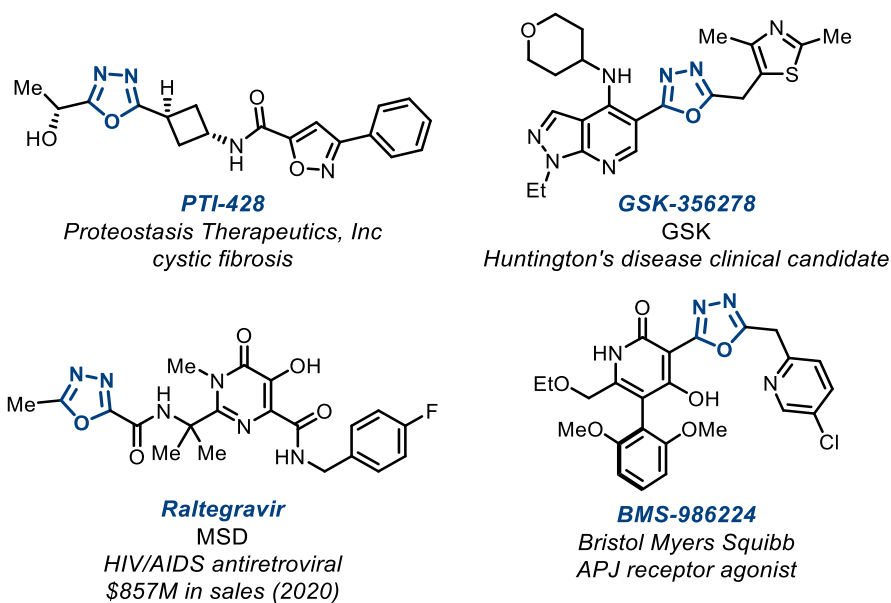
Oxadiazoles are a family of heterocycles that commonly feature as ester and amide bioisosteres¹ in pharmaceuticals and other biologically-active compounds.¹⁻⁵ They can theoretically exist as four structural isomers (scheme 1.1). In reality however, only 1,2,4-, 1,3,4-, and 1,2,5-oxadiazoles can be isolated, with the remaining 1,2,3-oxadiazole isomer readily isomerizing into the thermodynamically more stable α -diazo carbonyl compound – with a computational study suggesting that an unsubstituted 1,2,3-oxadiazole “cannot be isolated as a discrete species even in an inert matrix at low temperature”.⁶ The key features that allow oxadiazoles to be excellent bioisosters are their hydrolytic stability under physiological conditions, and ability to conserve hydrogen bonding interactions within receptor sites, with their physical and pharmaceutical properties being modulated by their H-bond acceptor and donor strengths which vary between the isomers.^{2, 7, 8} Additionally, the orientation of the side chains is of importance with 1,2,5-oxadiazoles appearing less frequently in patented pharmaceuticals. Furthermore, 1,3,4-oxadiazoles have been demonstrated to have lower lipophilicity than 1,2,4-oxadiazoles despite the relative orientation of the side chains remaining constant.² As lower lipophilicity can reduce toxicity, improve solubility, slow metabolic processes, and give higher oral absorption, it is considered an important property during development of pharmaceuticals.^{9, 10}

¹ I.e., structurally diverse classes of compounds that convey similar biological properties to the parent functionality.



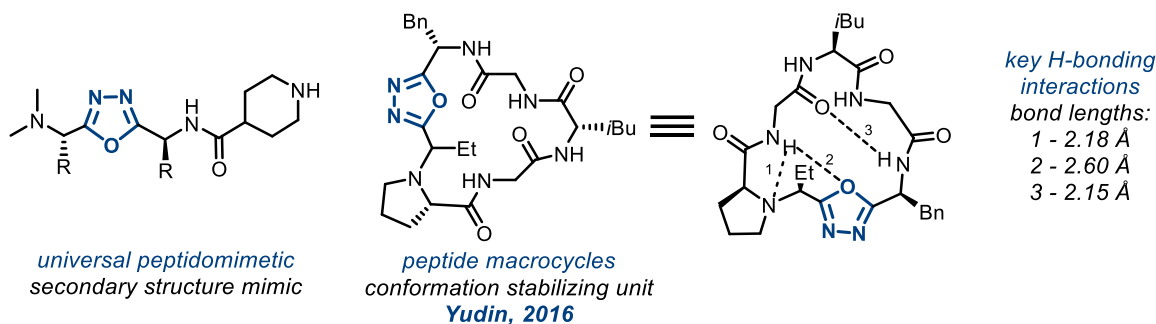
Scheme 1.1: Structural isomers of oxadiazoles, and their amide and ester isosterism.

The benefits of oxadiazoles as bioisosteres has meant that they have been investigated for their activity as anti-inflammatory,¹¹⁻¹⁵ anti-cancer,¹⁶⁻²² and antibacterial agents,²³⁻²⁶ and for many other diverse biological activities.^{9, 16, 27-35} The Drugbank database reveals that there are 18, 10, and 7 compounds currently under investigation containing 1,2,4-, 1,2,5-, and 1,3,4-oxadiazoles respectively.³⁶⁻⁴⁰ The diversity of these indications can also be seen in the subset of pharmaceutical molecules containing 1,3,4-oxadiazole motifs show in scheme 1.2. Notably, Raltegravir is currently FDA approved as a HIV anti-retroviral and made \$857 M in sales revenue in 2020, with the other compounds at various stages of Phase I/II/III clinical trials.⁴¹



Scheme 1.2: 1,3,4-Oxadiazoles in pharmaceutical molecules.

Beyond pharmaceuticals and simple isosterism, α -amino 1,3,4-oxadiazoles have been shown to be capable of imitating “any local pair of amino acids, in any secondary structure” – making them universal peptidomimetics (scheme 1.3).^{42–43} This property has been exploited by the Yudin group for the conformational stabilization of peptide macrocycles. Their investigations using VT NMR and computational studies concluded that internal hydrogen bonds, from the oxygen atom of the 1,3,4-oxadiazole, provided stabilization of the type II β -turn secondary structure.^{44, 45} This stabilization of turn motifs provided by the 1,3,4-oxadiazole helped to significantly improve the passive membrane permeability of 1,3,4-oxadiazole containing macrocycles when compared to their cyclic counterparts that did not contain the 1,3,4-oxadiazole motif.

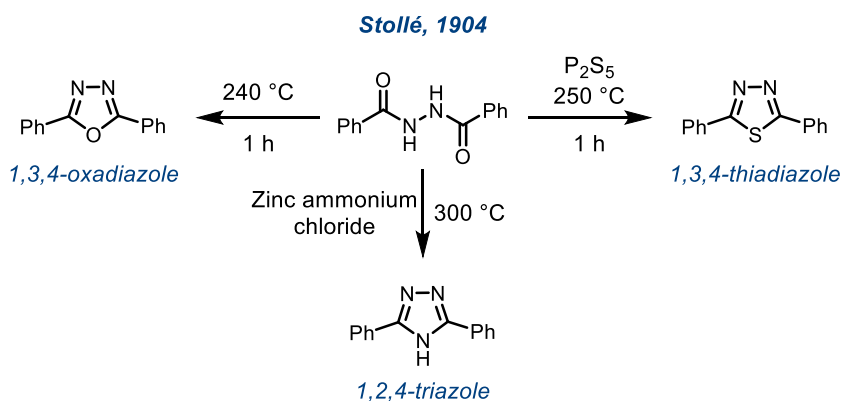


Scheme 1.3: α -Amino 1,3,4-oxadiazoles as peptidomimetics.

The wide-ranging applications of α -amino 1,3,4-oxadiazoles, and 2,5-disubstituted 1,3,4-oxadiazoles, in the pharmaceutical industry and the broader chemical sciences, attracted our interest in pursuing the development of new and efficient strategies for their synthesis.

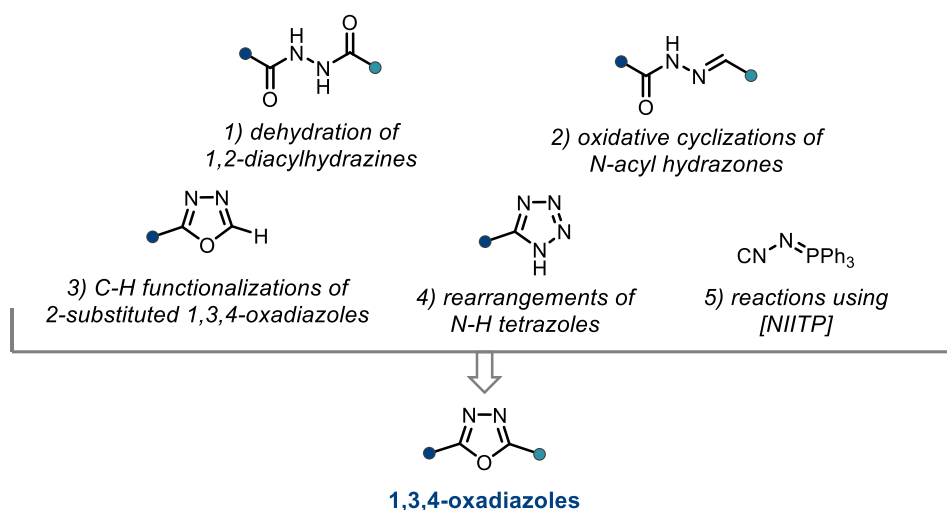
1.2 Strategies for 2,5-Disubstituted 1,3,4-Oxadiazole Synthesis

The first synthesis of a 1,3,4-oxadiazole was achieved by Stollé in 1904 (scheme 1.4).⁴⁶ They found that heating 1,2-dibenzoylhydrazine at 240 °C for 1 h achieved a thermal dehydration and afforded the desired 2,5-diphenyl-1,3,4-oxadiazole. In the same report, 2,5-diphenyl-1,3,5-thiadiazole and the 3,5-diphenyl-1,2,4-triazole could be accessed in a divergent fashion by heating 1,2-dibenzoylhydrazine with either phosphorous pentasulfide, or zinc ammonium chloride respectively.



Scheme 1.4: Heterodiazole synthesis by dehydration of 1,2-dibenzoylhydrazine.

As the conditions reported by Stollé are not suitable for many functionalized molecules, due to the high temperatures used, in the years since their discovery, new methods for 2,5-disubstituted 1,3,4-oxadiazole synthesis have focused on providing improved functional group tolerance, allowing for the 1,3,4-oxadiazole construction to occur in a variety of synthetic contexts. Modern approaches to 2,5-disubstituted 1,3,4-oxadiazole synthesis can be broadly categorised into five strategies based on the disconnections used: 1) dehydrations of 1,2-diacylhydrazines; 2) oxidative cyclizations of *N*-acyl hydrazones; 3) C-H functionalizations of 2-substituted 1,3,4-oxadiazoles; 4) rearrangements of *N*-H tetrazoles; 5) reactions using (*N*-isocyanoimino)triphenylphosphorane (NIITP) as a three atom *CNN* source (scheme 1.5).

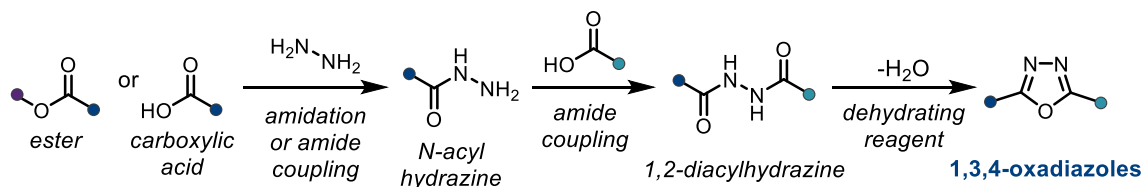


Scheme 1.5: Modern strategies for 2,5-disubstituted 1,3,4-oxadiazole synthesis.

1.2.1 Dehydrative Approaches

The most straightforward approach to 1,3,4-oxadiazole synthesis is through dehydration of 1,2-diacylhydrazines using stoichiometric dehydrating reagents. Retrosynthetically, the 1,2-diacylhydrazines are available by the stepwise coupling of hydrazine with two carboxylic acids (scheme 1.6). Their forward synthesis typically involves formation of the first amide bond by amidation of an ester with hydrazine, to avoid overreaction and formation of an unwanted symmetric 1,2-diacylhydrazine, with the remaining carboxylic acid being subsequently coupled

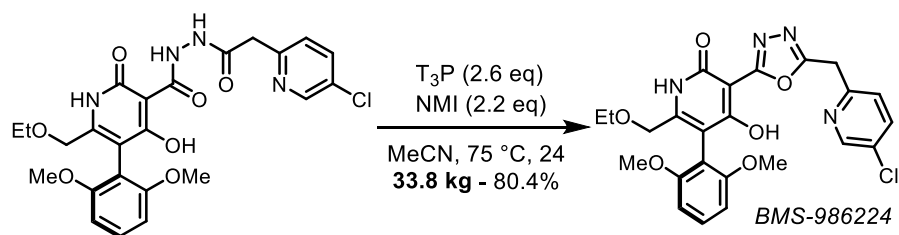
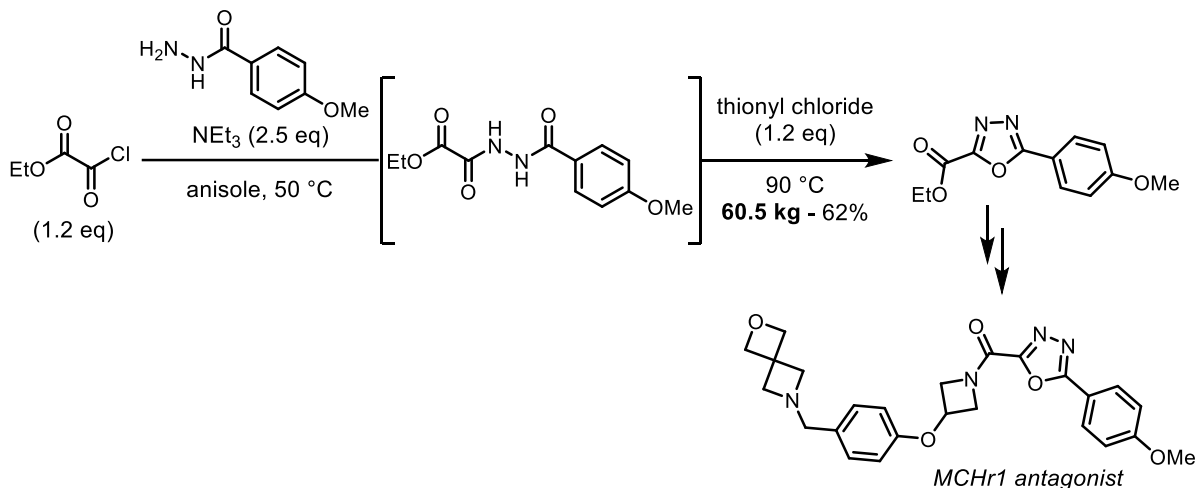
to the mono-acylated hydrazine using a traditional amide coupling reagent. The ease of retrosynthetic analysis and the availability of carboxylic acids as starting materials has led to this approach being widespread in medicinal chemistry reports and is logical when a 1,3,4-oxadiazole is being used to replace an existing amide or ester group – routinely synthesized from carboxylic acids.



Scheme 1.6: General overview of a dehydrative 1,3,4-oxadiazole synthesis.

Advances beyond Stollé's original thermal dehydration conditions were made in the 1950s and 1960s using reagents such as phosphorous(V) oxychloride,⁴⁷ sulfur trioxide,⁴⁸ and thionyl chloride;⁴⁹ however, these methods still required elevated temperatures. Since then, many methods have made use of milder and more effective dehydrating reagents such as T_3P ,⁵⁰ EDC,⁵¹ and tosyl chloride⁵² to improve the scope of tolerated substrates.^{9, 47-70} Furthermore, T_3P has been shown to be effective for a one-pot synthesis of 1,3,4-oxadiazoles from an *N*-acyl hydrazine and a carboxylic acid, acting in the reaction as both an amide coupling agent and a dehydrating reagent.⁵⁰

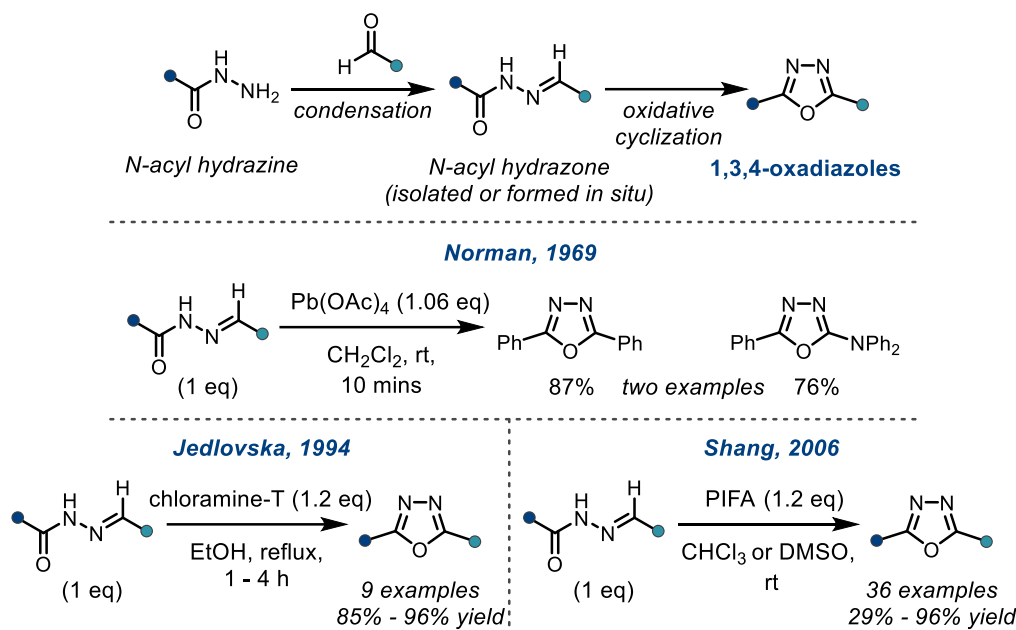
For the synthesis of 1,3,4-oxadiazole-containing pharmaceuticals T_3P and thionyl chloride remain the dehydrating reagents of choice due to each reagent's low cost, wide availability, and ease of by-product removal during purification. Their utility is demonstrated by their application in process chemistry – T_3P has been used to synthesise 33.8 kg of BMS-986224, an APJ receptor agonist,^{50, 71} and thionyl chloride has been used to synthesise 60.5 kg of an 1,3,4-oxadiazole building block in the synthesis of an MCHR1 Antagonist (scheme 1.7).^{49, 72, 73}

synthesis of BMS-986224**synthesis of an MCHR1 antagonist**

Scheme 1.7: Kilogram scale synthesis of 1,3,4-oxadiazoles using a dehydrative approach.

1.2.2 Oxidative Approaches

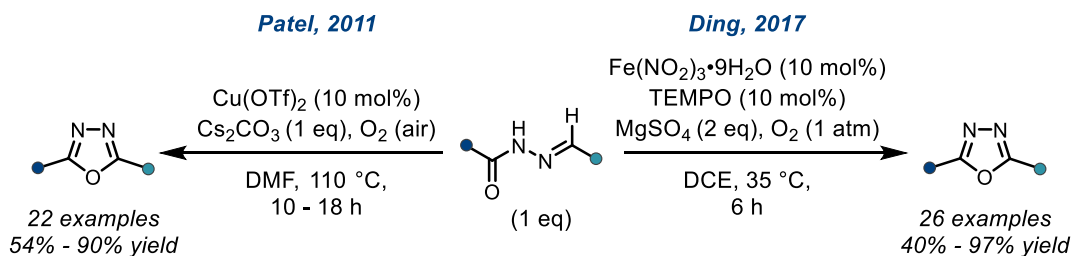
The next earliest described approach to 1,3,4-oxadiazole synthesis was an oxidative cyclization reaction of an *N*-acyl hydrazone, either preformed (and isolated) or generated *in situ* from a hydrazine and an aldehyde (scheme 1.8, top). The first report of such an oxidative cyclization came from Norman *et al* in 1969 using lead(IV) acetate as the oxidant to achieve the synthesis of 2,5-diphenyl 1,3,4-oxadiazole in 87% yield (scheme 1.8, middle).⁷⁴ Additionally, using the same strategy, they disclosed the synthesis of a 2-amino-5-substituted 1,3,4-oxadiazole in 76% yield.



Scheme 1.8: General overview of oxidative 1,3,4-oxadiazole syntheses, first reported oxidative synthesis, and selected examples of modern methodologies.

In the decades that followed, alternative strong oxidants such as lead(IV) oxide,⁷⁵ potassium manganate(VII),⁷⁶ iron(III) chloride,⁷⁷ iodine,⁷⁸ and bromine were reported as able to accomplish this transformation.⁷⁹ Later, stoichiometric hypervalent iodine based reagents including PIDA,⁸⁰ PIFA,⁸¹ and DMP,⁸² were reported to achieved the desired oxidative cyclization under mild conditions, however the cost of these reagents can be prohibitive. Additionally, chloramine-T has been used as a mild, and inexpensive oxidant for this transformation (scheme 1.8, bottom).⁸³

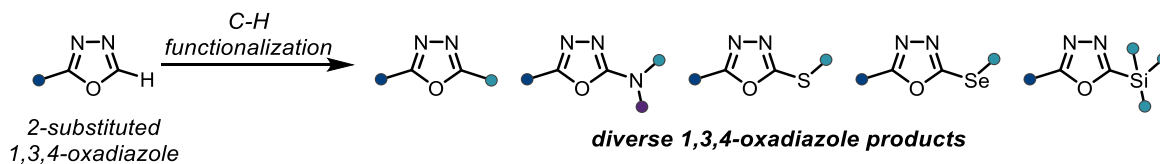
The first report of using dioxygen as the terminal oxidant for this transformation came from the Patel group in 2011, using copper(II) triflate as a catalyst (scheme 1.9, left).⁸⁴ Since then, dioxygen has been employed as the terminal oxidant for 1,3,4-oxadiazole synthesis – *via* oxidative cyclization of *N*-acyl hydrazones – under copper,⁸⁵ iron,⁸⁶ photoredox,⁸⁷ or iodoarene catalysis (scheme 1.9, right).⁸⁸



Scheme 1.9: Selected examples of transition metal catalyzed oxidative cyclizations using dioxygen as the terminal oxidant.

1.2.3 C-H Functionalizations of 2-Substituted 1,3,4-Oxadiazoles

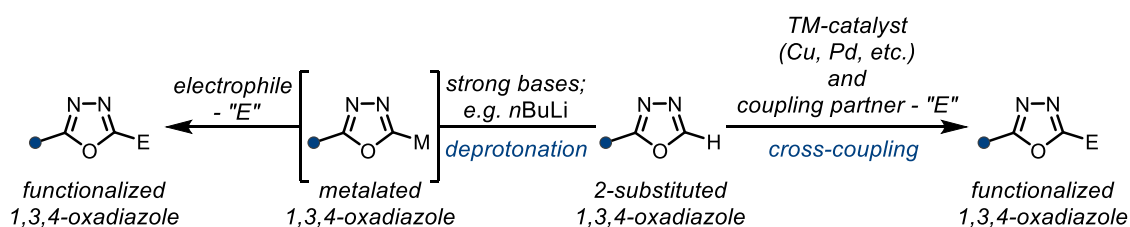
The development of C-H functionalization methodologies utilizing azoles, and 2-substituted 1,3,4-oxadiazoles, has provided a effective platform for the synthesis of complex molecules from unfunctionalized starting materials, and has been the focus of recent reviews.^{89, 90} The key advantage of a C-H functionalization strategy for 2,5-disubstituted 1,3,4-oxadiazole synthesis is that the choice of reagents used dictates the nature of the new substituent installed. With methods for the installation of C-C, C-N, C-S, C-Se, and C-Si bonds being available, diverse products can be synthesized from a singular starting compound (scheme 1.10). Within the context of modern 1,3,4-oxadiazole syntheses this approach remains a powerful tool; however, it suffers from the need for synthesis of the 2-substituted 1,3,4-oxadiazole starting materials which can take multiple synthetic steps.



Scheme 1.10: Diverse 1,3,4-oxadiazoles available via a C-H functionalization strategy.

In practice, the C-H functionalization of 2-substituted 1,3,4-oxadiazoles can be achieved by either: stoichiometric deprotonation of the 1,3,4-oxadiazole C-H bond using a strong organometallic base, for example *n*BuLi or Zn(tmp)₂, and a subsequent reaction with an

appropriate electrophile (scheme 1.11, left); or, more commonly, by a cross-coupling approach using transition metal catalysts to enable the C-H functionalization of 2-substituted 1,3,4-oxadiazoles (scheme 1.11, right). Although methodologies involving the stoichiometric deprotonation of a 2-substituted 1,3,4-oxadiazole have been successfully used by the Knochel group, and others, for the alkylation,⁹¹⁻⁹⁵ amination,⁹⁶⁻⁹⁸ halogenation,^{99, 100} and thiolation of 2-substituted 1,3,4-oxadiazoles,⁹⁹ they will not be discussed here in favour of focusing on transition metal catalyzed C-H functionalization methodologies due to their prevalence in the literature. Additionally, the synthetic studies discussed in this section frequently utilize a range of azoles during a typical reaction scope, and as such vary in the extent of their exploration of a 1,3,4-oxadiazole scope – with generally only 2-aryl 1,3,4-oxadiazole substrates being used – and as such will be categorized and discussed broadly based on the transformation achieved.



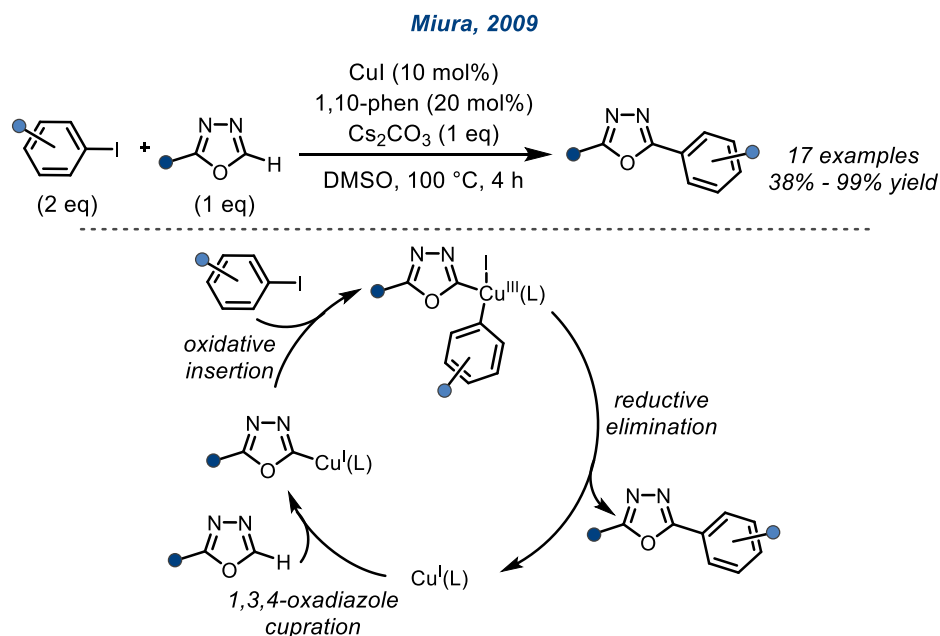
Scheme 1.11: Two approaches to 1,3,4-oxadiazole C-H functionalization.

1.2.3.1 Carbon-Carbon Bond Forming Methodologies

Arylations of 2-Substituted 1,3,4-Oxadiazoles

Of the types of C-H functionalizations possible from 2-substituted 1,3,4-oxadiazoles, those resulting in formation of a new C-C bond are the most investigated and have made use of a wide variety of catalysts and carbon-based coupling partners. In particular, the most studied reaction of this type is the arylation of 2-substituted 1,3,4-oxadiazoles. The first report of such an arylation came from the Miura group in 2009, using aryl iodide electrophiles, copper(I) iodide as a catalyst, and 1,10-phenanthroline as a ligand (scheme 1.12).¹⁰¹ Although the reaction mechanism was not investigated, the authors suggested it could plausibly proceed by a base-

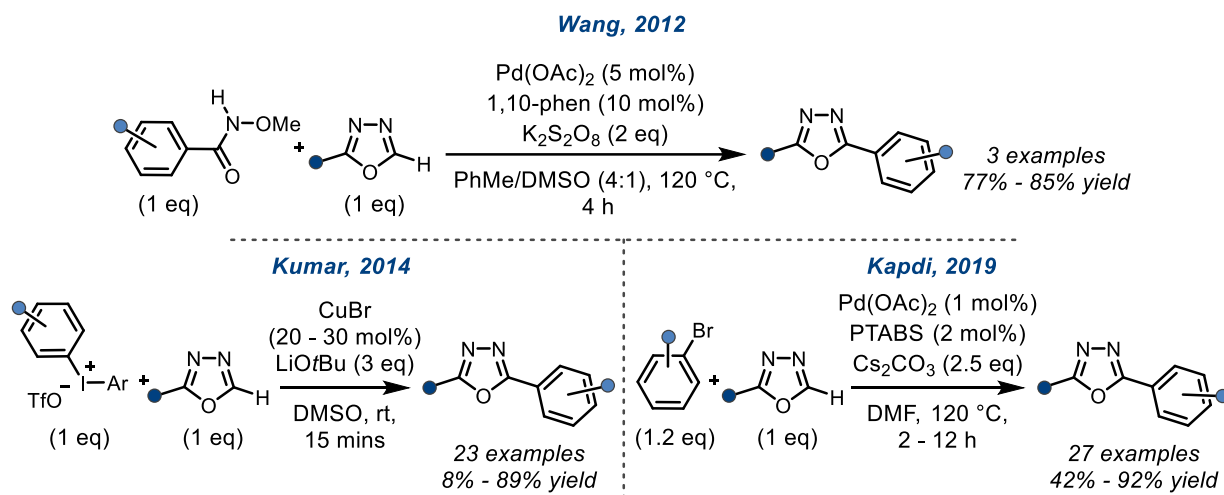
assisted cupration of the 1,3,4-oxadiazole, followed by oxidative addition into the aryl iodide C-I bond to afford a copper(III) intermediate. A C-C bond forming reductive elimination then delivers the product and regenerates the copper(I) catalytic species.



Scheme 1.12: First reported example of the C-H arylation of 2-substituted 1,3,4-oxadiazoles, and a possible reaction mechanism.

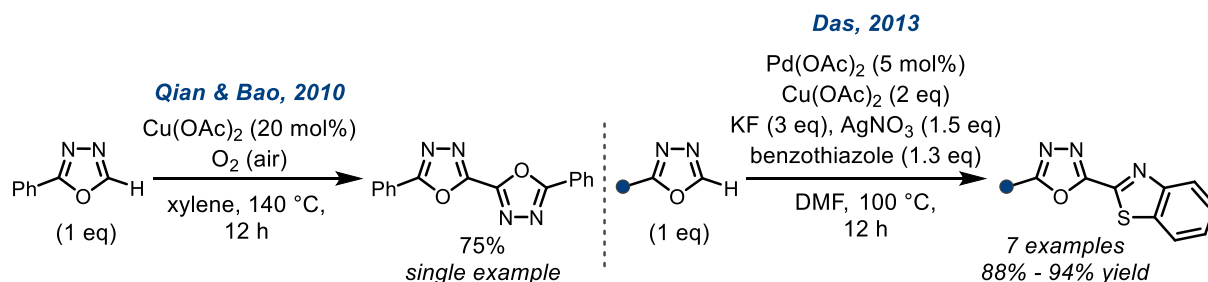
Since Miura's report, copper-catalysis in combination with aryl iodide coupling partners have been used for the C-H arylation of 2-substituted 1,3,4-oxadiazoles by the groups of Hong,¹⁰² Das,¹⁰³ Vidavalur,¹⁰⁴ and Ackermann.¹⁰⁵ Beyond aryl iodides, alternative coupling partners such as aryl boronic acids,¹⁰⁶⁻¹⁰⁸ trialkoxyl silanes,¹⁰⁹ sodium sulfonates,^{110, 111} *N*-methoxy amides,¹¹² sulfonhydrazides,¹¹³ mesylates,¹¹⁴ diaryl iodoniums,¹¹⁵ trimethylammonium triflates,¹¹⁶ disulfides,¹¹⁷ nitriles,¹¹⁸ bromides,^{119, 120} triazenes,¹²¹ acyl-glutamides,¹²² and C-H bonds (*via* (un)directed C-H activations) have been demonstrated to achieve the desired arylation (selected literature examples are shown in scheme 1.13).¹²³⁻¹²⁷ Among these reports copper catalysis is ubiquitous, however many also use palladium, or other transition metals, as co-

catalysts, possibly to undergo efficient oxidative addition into the aryl coupling partner, before further reactivity can occur with the 2-substituted 1,3,4-oxadiazole.



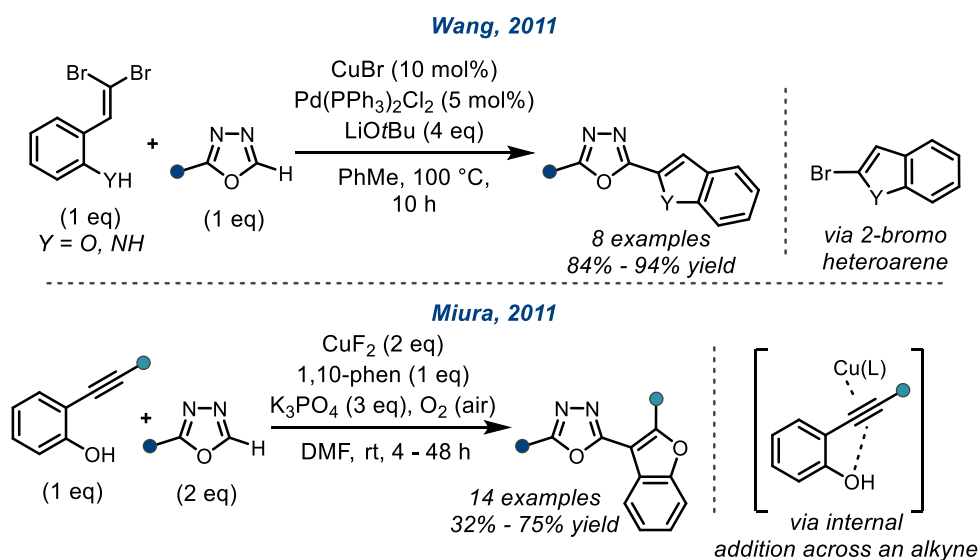
Scheme 1.13: Selected arylations of 2-substituted 1,3,4-oxadiazoles.

A subset of 1,3,4-oxadiazole arylations include oxidative couplings using heteroarenes, and dimerizations of 2-substituted 1,3,4-oxadiazoles. The dimerization of 2-phenyl 1,3,4-oxadiazole was described in 2010 by Qian and Bao using copper(II) acetate as the catalyst and with dioxygen as the terminal oxidant (scheme 1.14, left).¹²⁸ Subsequent reports have performed oxidative couplings using thiophene,¹²⁹ or benzothiazole,^{130, 131} as the coupling partner also under copper catalysis. A different tactic came from the Das group who utilized palladium(II) acetate as a catalyst with stoichiometric copper and silver oxidants for the oxidative coupling of 2-substituted 1,3,4-oxadiazoles with benzothiazole (scheme 1.14, right).¹⁰⁸



Scheme 1.14: Selected oxidative couplings of 2-substituted 1,3,4-oxadiazoles.

The arylation of 2-substituted 1,3,4-oxadiazoles can additionally be coupled to a metal-catalyzed cyclization event. The cyclization event can occur independently of the 2-substituted 1,3,4-oxadiazole arylation *via* coupling of an 1,1-dibromo alkene with an internal nucleophile to afford a 2-bromo heteroarene, ready to perform the arylation (scheme 1.15, top).^{132, 133} Alternatively, it can occur following addition of an internal nucleophile across an alkyne (scheme 1.15, bottom).^{134, 135} This addition is suggested by the authors to be assisted by the cuprated-1,3,4-oxadiazole acting as Lewis-acid for the alkyne and affords an sp^2 -metalated species from which reductive elimination gives the product. These cyclization methods provide difficult to access C-2, or C-3 arylated indoles, benzothiophenes, and benzofurans products depending on the starting materials used.

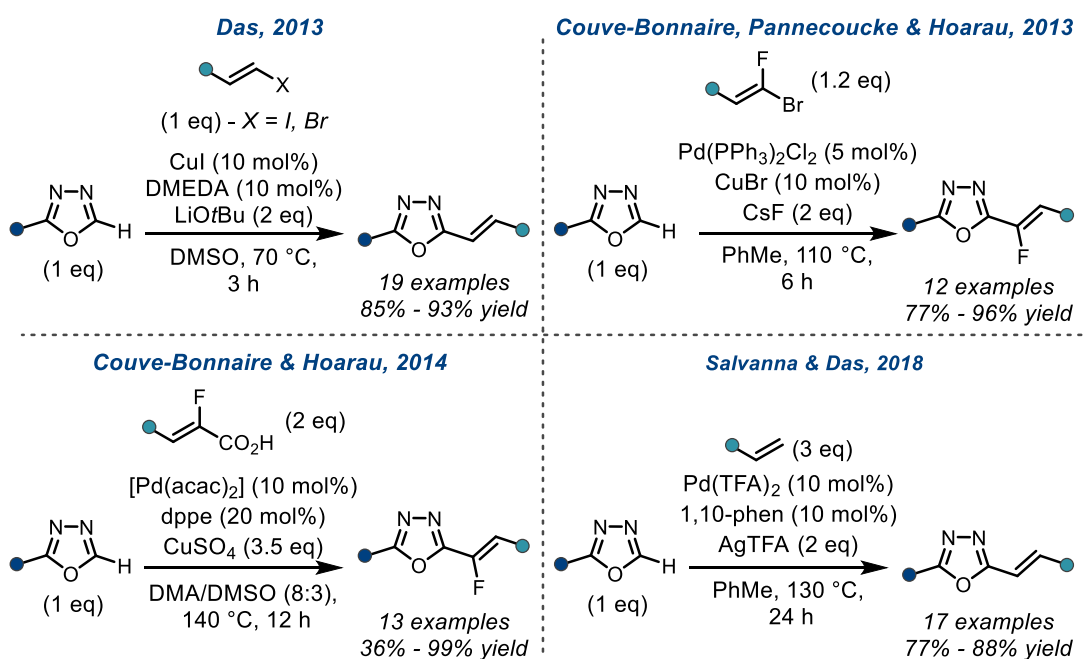


Scheme 1.15: Selected 1,3,4-oxadiazole C-H arylations involving cyclization events.

Alkenylations of 2-Substituted 1,3,4-Oxadiazoles

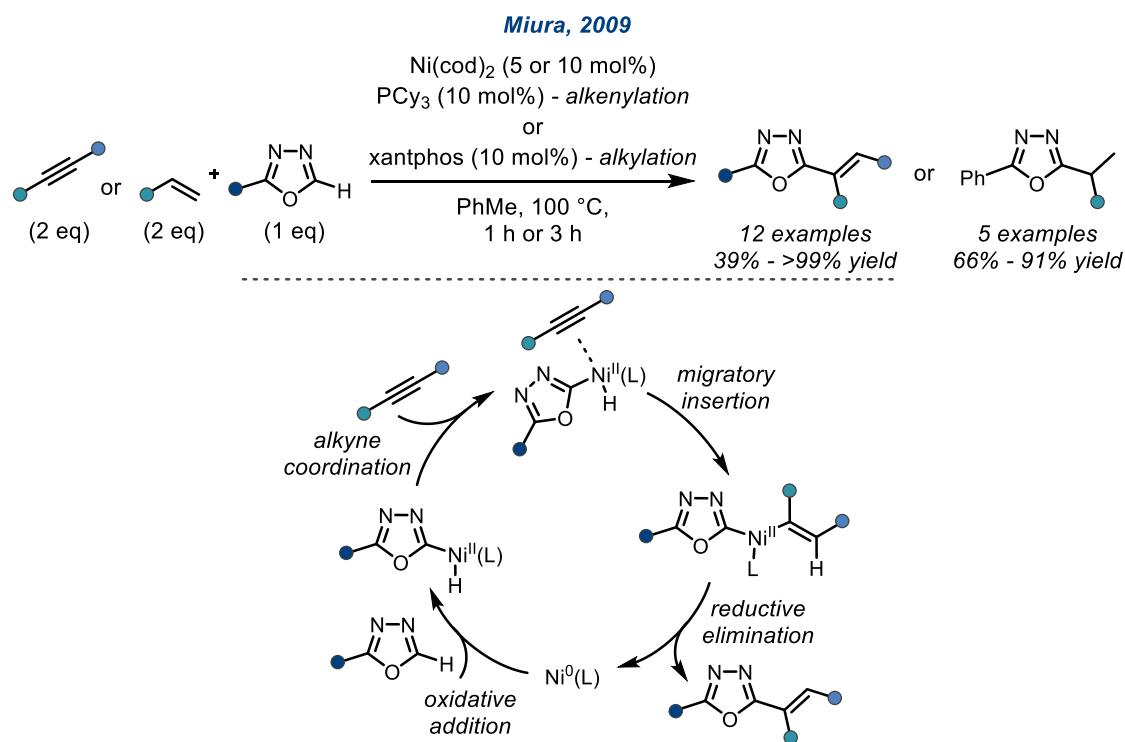
Access to 1,3,4-oxadiazole-bearing alkenes can be provided *via* the C-H alkenylation of 2-substituted 1,3,4-oxadiazoles using either alkene or alkyne coupling partners. An alkenyl bromide was first used as a coupling partner for a 1,3,4-oxadiazole C-H alkenylation in 2012, with a copper(I) iodide/DMEDA catalyst system efficiently providing the alkenylated product

(scheme 1.16, top left).¹³⁶ Following this, in 2013, Couve-Bonnaire, Pannecoucke and Hoarau demonstrated that 1-bromo-1-fluoro-alkenes could undergo a similar coupling reaction under palladium catalysis, with copper(I) bromide as a co-catalyst (scheme 1.16, top right).¹³⁷ Moreover, the C-H alkenylation of 1,3,4-oxadiazoles using a palladium and copper co-catalytic system was further explored by Couve-Bonnaire and Hoarau,¹³⁸ and Hoarau,¹³⁹ for the engagement of alkenyl carboxylic acids coupling partners in a decarboxylative variant of this transformation (scheme 1.16, bottom left). One disadvantage of these initial reports was the need for prefunctionalized alkenes as coupling partners, but this limitation was overcome in 2018 with a report of the first Heck-type reaction of 2-substituted 1,3,4-oxadiazoles with terminal alkene coupling partners (scheme 1.16, bottom right).¹⁴⁰ Critical to its success was the use of silver trifluoroacetate as an oxidant, with lower yields observed for alternative copper or silver oxidants.



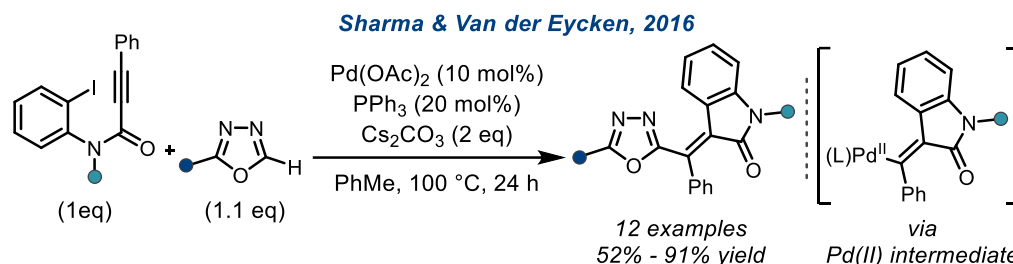
Scheme 1.16: Selected examples of 1,3,4-oxadiazole C-H alkenylations using alkene coupling partners.

The use of alkynes as coupling partners for the C-H alkenylation of 2-substituted 1,3,4-oxadiazoles is less investigated, nevertheless there have been two reports of their use.¹⁴¹⁻¹⁴⁴ The first came from the Miura group in 2009 using a nickel(0) catalyst with tricyclohexylphosphine as a ligand (scheme 1.17).¹⁴¹ The authors suggested a mechanism firstly involving an oxidative addition into the 1,3,4-oxadiazole C-H bond, without assistance by an external base, affording a nickel(II) hydride species. Then, migratory insertion across the alkyne occurs, and reductive elimination gives the alkenylated 1,3,4-oxadiazole product. Notably, in the same report a C-H alkylation was achieved using styrenes under an analogous mechanistic proposal. The second report came from the Yoshikai group in 2010 utilizing a cobalt-based catalytic system for a similar transformation, however this report only featured a single example using a 1,3,4-oxadiazole (2-phenyl 1,3,4-oxadiazole) as a substrate.¹⁴²



Scheme 1.17: C-H alkenylation, or alkylation, of 1,3,4-oxadiazoles using an alkyne, or alkene, coupling partner.

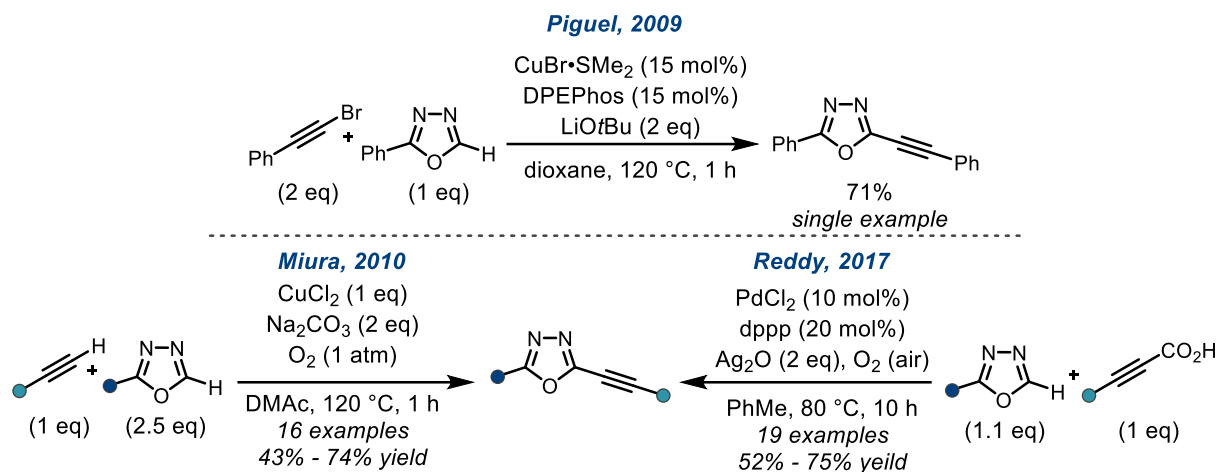
Furthermore, a domino carbopalladation/C-H alkenylation reaction featuring an alkyne-bearing aryl iodide as the starting material was disclosed in 2016 by Sharma and Van der Eycken, and provided rapid access to synthetically useful 3-alkylidene-oxindole structures (scheme 1.18).¹⁴³



Scheme 1.18: A domino C-H alkenylation reaction using 2-substituted 1,3,4-oxadiazoles.

Alkynylations of 2-Substituted 1,3,4-Oxadiazoles

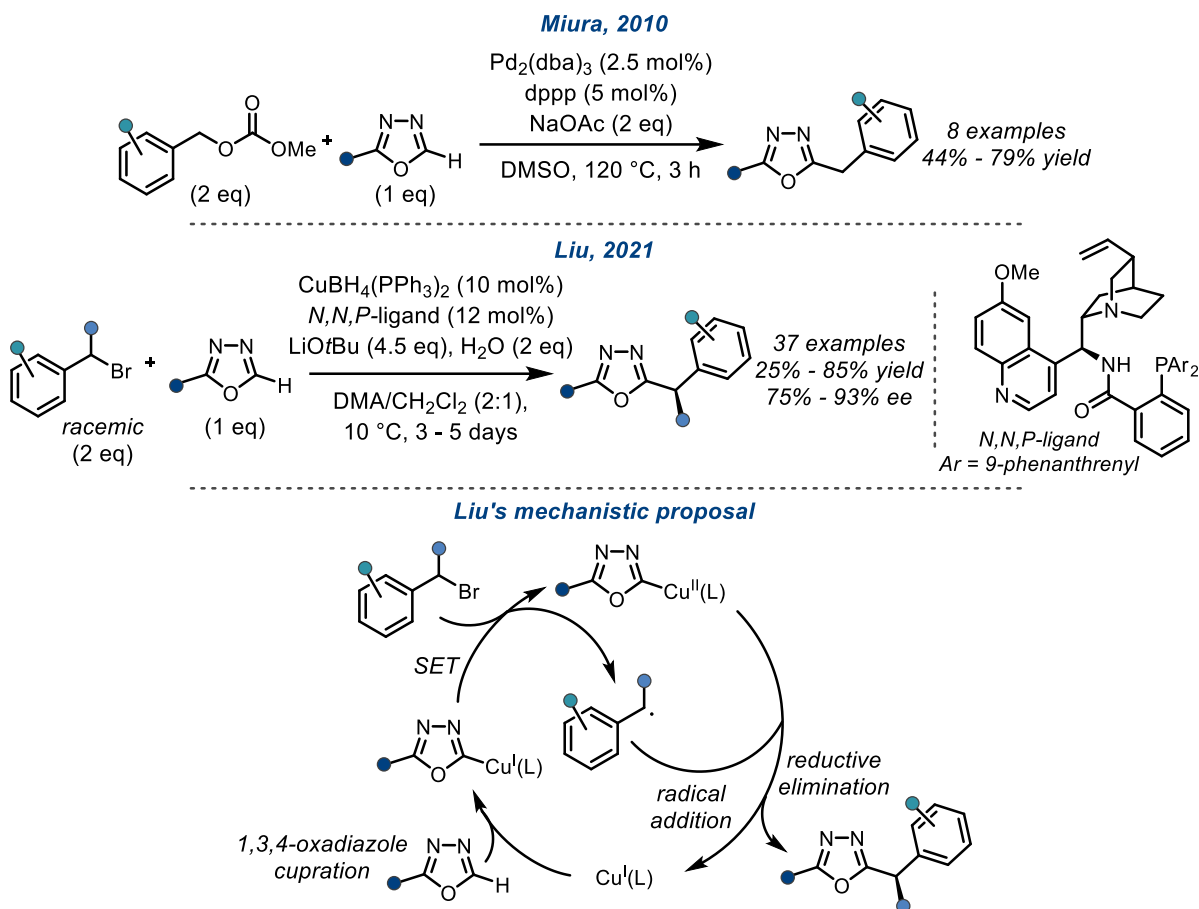
The Piguel group detailed the first alkynylation of a 2-substituted 1,3,4-oxadiazole using an alkynyl bromide coupling partner, as part of a study on the alkynylation of diverse azole structures in 2009 (scheme 1.19, top).¹⁴⁵ Mechanistically, Piguel *et al* suggest a reaction pathway analogous to the C-H arylation mechanism shown in scheme 1.12 where the first step is a base-assisted cupration of the 1,3,4-oxadiazole, giving a copper(I)-1,3,4-oxadiazole species. A subsequent oxidative addition into the bromoalkyne gives a copper(III) species from which reductive elimination affords the product. Following Piguel's report, the groups of Miura,¹⁴⁶ Das,¹⁴⁷ and Evano have reported comparable approaches to this transformation with greater effort dedicated to the exploration of the scope of compatible 1,3,4-oxadiazoles.¹⁴⁸ In 2010, it was found that alkynyl bromides can be replaced by terminal alkynes however the methodology was constrained by the use of 2.5 equivalents of the 1,3,4-oxadiazole coupling partner (scheme 1.19, bottom left).¹⁴⁹ Most recently, in 2017, the Reddy group disclosed the use of alkynyl carboxylic acids as coupling partners in the first report of a palladium-catalyzed decarboxylative reaction variant (scheme 1.19, bottom right).¹⁵⁰



Scheme 1.19: Selected examples of 1,3,4-oxadiazole C-H alkynylations.

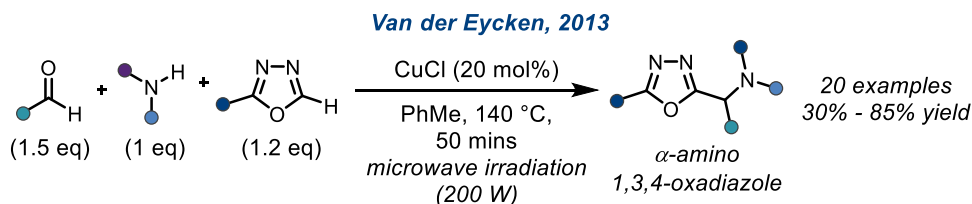
Alkylations of 2-Substituted 1,3,4-Oxadiazoles

The transition metal catalyzed C-H alkylation of a 1,3,4-oxadiazole was first described in 2010, using benzylic carbonates as coupling partners under palladium catalysis (scheme 1.20, top).¹⁵¹ Following this report, allylic phosphonate esters,¹⁵² benzyl chlorides,¹⁵³ benzylic trimethylammonium triflates,¹⁵⁴ isatins,¹⁵⁵ and *N*-tosylhydrazones¹⁵⁶ have been disclosed as effective coupling partners for this reaction class. Uniquely for 1,3,4-oxadiazole C-H alkylations, Liu's enantioselective report in 2021 invokes a single-electron transfer (SET) from a copper(I)-1,3,4-oxadiazole complex to a benzylic bromide to generate a radical intermediate and a copper(II)-1,3,4-oxadiazole complex (scheme 1.20, middle & bottom). The addition of the radical to the copper(II)-complex then gives a copper(III) intermediate, in a formal oxidative addition process, and subsequently the desired C-C bond is formed by reductive elimination.¹⁵⁷



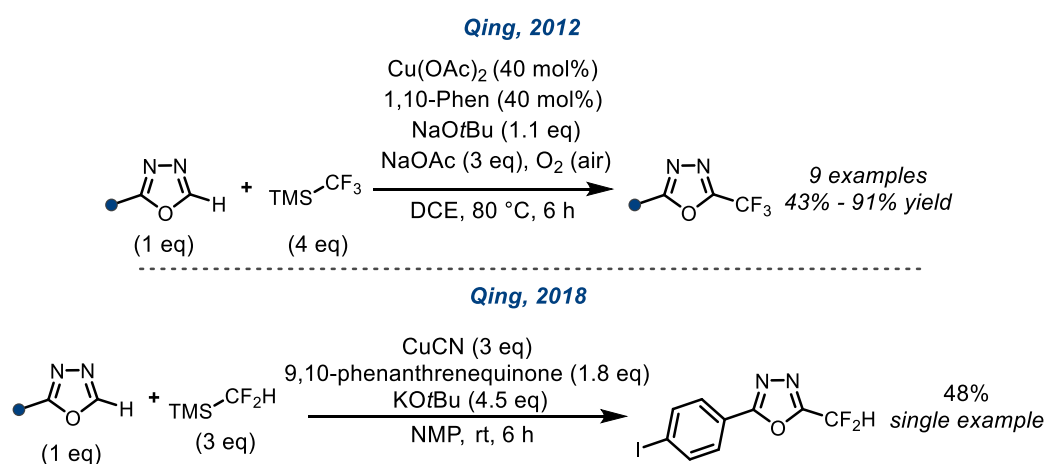
Scheme 1.20: Selected examples of 1,3,4-oxadiazole C-H alkylations.

In addition to the above-mentioned electrophilic species, positively-charged iminium ions have also been exploited as electrophilic species for the C-H alkylation of 2-substituted 1,3,4-oxadiazoles, and were shown to generate valuable α -amino 1,3,4-oxadiazole products in a multicomponent reaction (scheme 1.21).¹⁵⁸



Scheme 1.21: α -Amino 1,3,4-oxadiazole synthesis via a C-H alkylation reaction.

While the above alkylation methodologies allow access to diverse 2,5-disubstituted 1,3,4-oxadiazoles, they are unsuitable for the installation of fluoroalkyl groups, including the coveted trifluoromethyl moiety. A solution to this problem was disclosed by Qing in 2012 who reported that 1,3,4-oxadiazole trifluoromethylation could be achieved using a copper(II) acetate/1,10-phenanthroline catalyst system, with trifluoromethyltrimethylsilane as the trifluoromethylating reagent (scheme 1.22, top).¹⁵⁹ During this study the authors discovered that the addition of sodium acetate significantly slowed the dimerization of the 1,3,4-oxadiazole starting materials. Later, in 2018, their strategy was extended to allow for the difluoromethylation of azoles, including one example of a 1,3,4-oxadiazole (scheme 1.22, bottom). This methodology however required use of stoichiometric quantities of copper(I) cyanide and a 9,10-phenanthrenequinone oxidant with other oxidants tested including PIDA, DTBP, and silver carbonate failing to yield the desired product.¹⁶⁰

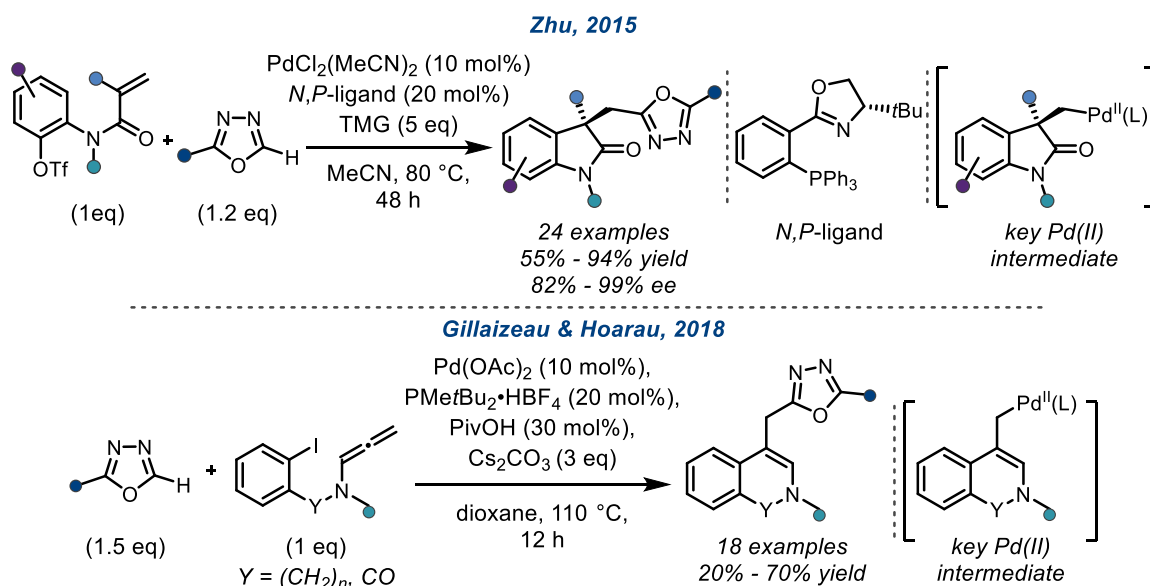


Scheme 1.22: Qing's 1,3,4-oxadiazole C-H trifluoromethylation and difluoromethylation methodologies.

Domino Reactions Involving 2-Substituted 1,3,4-Oxadiazoles

Transition metal catalyzed domino reactions provide methods for building molecular complexity in a programmed manner, and have been reviewed extensively in the literature.¹⁶¹⁻¹⁶⁵ 1,3,4-

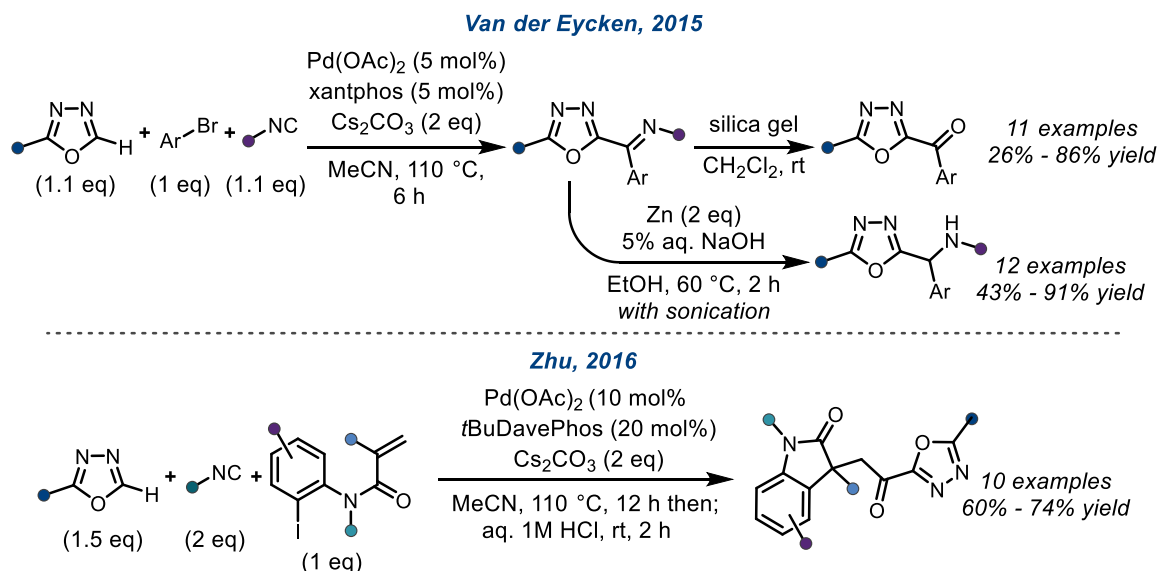
Oxadiazoles have been used in palladium-catalyzed domino reactions by the groups of Zhu,¹⁶⁶⁻¹⁶⁸ Sharma and Van der Eycken,¹⁴³ Gillaizeau and Hoarau,¹⁶⁹ and Kuram, as the 1,3,4-oxadiazoles can act as spectators in the reaction mixture until needed to react with a palladium(II) reactive intermediate (scheme 1.23).¹⁷⁰ One commonality to these reports is that following a palladium(0) oxidative addition, and a subsequent migratory insertion into a tethered alkene (or allene) a carbon-palladium(II) intermediate possessing no β -hydrogens is formed (scheme 1.23). This deliberate design prevents the palladium(II) species from undergoing a β -hydride elimination allowing it to be long-lived enough to react with the 1,3,4-oxadiazole and subsequently afford the desired products.



Scheme 1.23: Selected examples of palladium-catalyzed domino reactions using 1,3,4-oxadiazoles.

Independently, the groups of Van der Eycken and Zhu expanded upon the domino alkylations of 1,3,4-oxadiazoles by utilizing them in multicomponent palladium-catalyzed reactions involving the insertion of isocyanides into palladium(II) intermediates (scheme 1.24).^{171, 172} These reactions are similar to the domino reactions discussed above as any palladium(II)

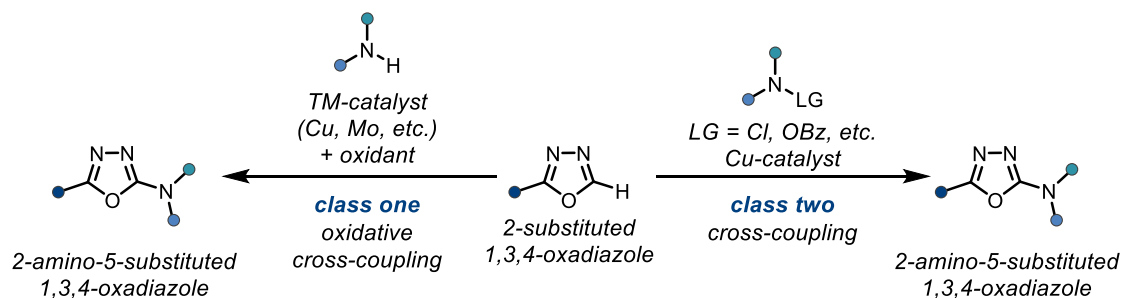
intermediates are prevented from undergoing β -hydride elimination. They additionally suggest that the critical carbon-palladium(II) intermediates undergo reactivity with isocyanides faster than with the 1,3,4-oxadiazoles present in the reaction mixture.¹⁷¹ Furthermore, Van der Eycken's report provided access to α -amino 1,3,4-oxadiazoles *via* reduction of the imine products using zinc dust in a one-pot procedure.¹⁷²



Scheme 1.24: Domino reactions of 1,3,4-oxadiazoles involving isocyanides.

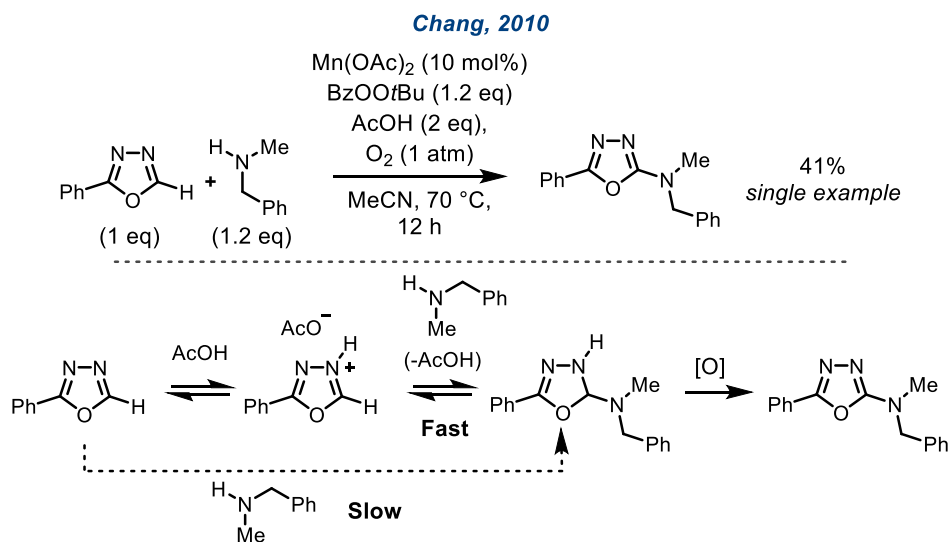
1.2.3.2 Carbon-Nitrogen Bond Forming Methodologies

The transition metal catalyzed amination of 2-substituted 1,3,4-oxadiazoles can occur *via* two reaction classes: firstly, a secondary (or primary) amine can be reacted with the 1,3,4-oxadiazole, usually in the presence of a transition metal catalyst, and an oxidant to give the desired 2-amino-5-substituted 1,3,4-oxadiazole (scheme 1.25, left); or, secondly, the amine can be pre-oxidized, for example as a *N*-chloroamine, making it an electrophilic reaction partner for the 1,3,4-oxadiazole when in the presence of a copper catalyst and a base (scheme 1.25, right).



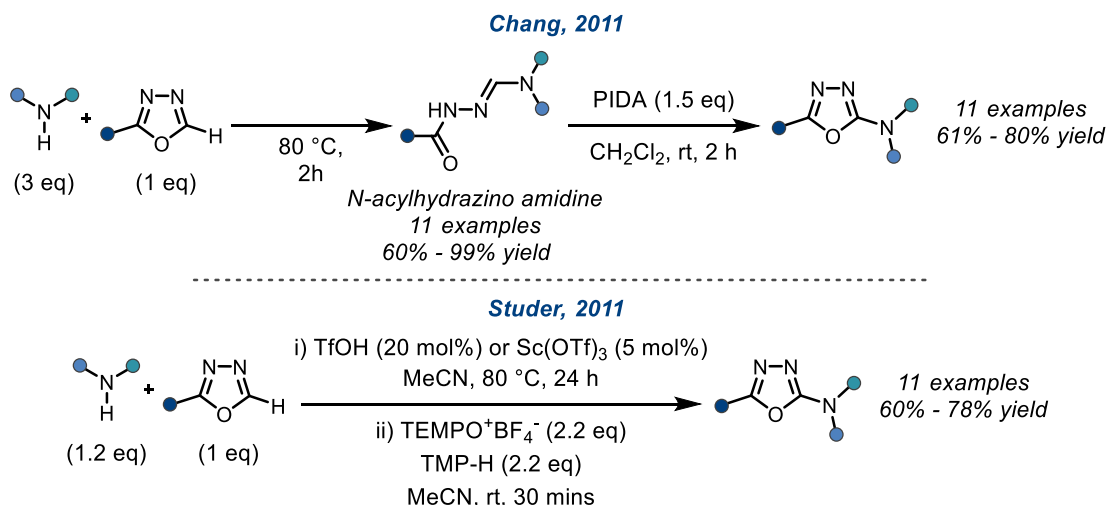
Scheme 1.25: Two reaction classes of 1,3,4-oxadiazole C-H amination.

The first report of class one came in 2010 from the Chang group, where 2-phenyl 1,3,4-oxadiazole was reacted with *N*-methylbenzylamine in the presence of manganese acetate, acetic acid, tert-butyl hydroperoxide, and dioxygen giving an aminated 1,3,4-oxadiazole in 41% yield (scheme 1.26, top).¹⁷³ The authors suggest a mechanism where the 1,3,4-oxadiazole is protonated by acetic acid, thus increasing its electrophilicity, and allowing for the reversible formation of an aminal which is oxidized *in situ* to give the product (scheme 1.26, bottom).¹⁷³⁻¹⁸¹ After this report, copper-catalyzed oxidative C-H aminations of 1,3,4-oxadiazoles using nucleophilic amine coupling partners and dioxygen as the terminal oxidant have been reported by the groups of Huang,¹⁷⁴ Bolm and Miura,¹⁷⁶ Miura,¹⁷⁹ and De Vos.¹⁸¹ Furthermore, in 2018 Ackermann *et al* disclosed an electrochemical C-H amination of 1,3,4-oxadiazoles that proceeded without the need for stoichiometric chemical oxidants.¹⁸⁰



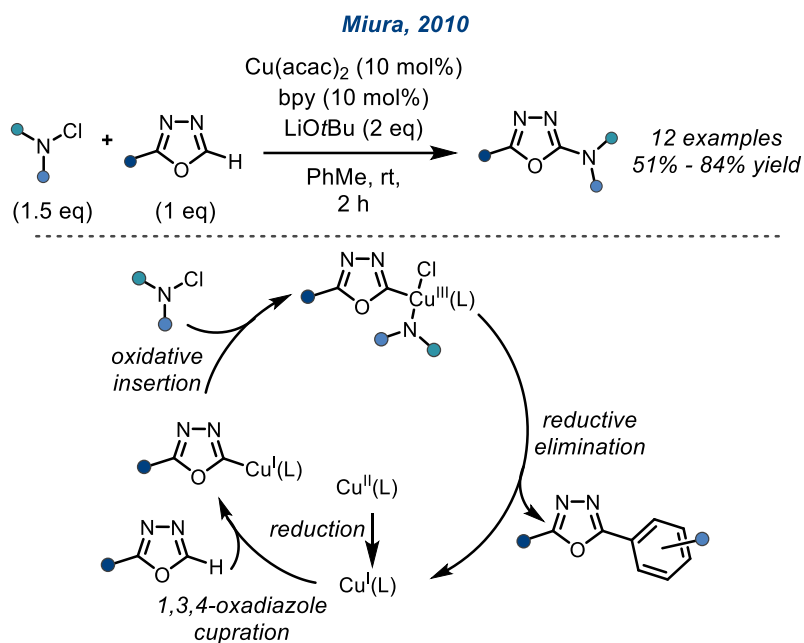
Scheme 1.26: Chang's report of an oxidative 2-amino-5-phenyl 1,3,4-oxadiazole synthesis and their proposed mechanism.

An alternative transition metal free approach relying on first opening the 1,3,4-oxadiazole ring using an amine and heat to afford an isolable *N*-acylhydrazone amidine, with an oxidative cyclization subsequently performed using PIDA, was detailed by the Chang group in 2011 (scheme 1.27, top).¹⁷⁵ Contemporaneously the Studer group described a one-pot protocol for this transformation which utilized a Brønsted- or Lewis-acid to promote the 1,3,4-oxadiazole ring opening using only a small excess of amine, with the subsequent oxidative cyclization being performed using $\text{TEMPO}^+\text{BF}_4^-$ (scheme 1.27, bottom).¹⁷⁸ These two methods are conceptually similar to the oxidative cyclization approaches discussed in section 1.2.2 as the *N*-acylhydrazone amidine intermediate can be seen as a specific type of *N*-acyl hydrazone.



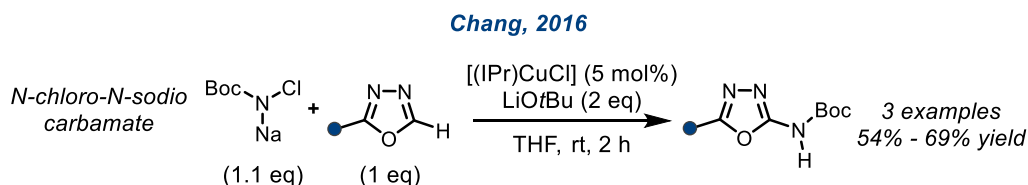
Scheme 1.27: Transition metal free 1,3,4-oxadiazole C-H amination reactions.

A 1,3,4-oxadiazole C-H amination using a pre-oxidized amine coupling partner was first reported by the Miura group in 2011. The authors employed *N*-chloroamines as electrophilic aminating reagents, for a copper-catalyzed amination of 2-substituted 1,3,4-oxadiazoles (scheme 1.28, top).¹⁸² Mechanistically, the authors proposed an initial reduction of a copper(II) species to a copper(I) species – for which the detailed mechanism remains unclear. This copper(I) species can then undergo a base-assisted cupration of the 1,3,4-oxadiazole, which is followed by oxidative addition into the *N*-chloroamine by the Cu(I)-1,3,4-oxadiazole intermediate. Finally, the product is afforded after reductive elimination from the generated Cu(III) complex (scheme 1.28, bottom).



Scheme 1.28: The first report of a 1,3,4-oxadiazole C-H amination using an electrophilic amine coupling partner, and the authors proposed mechanism.

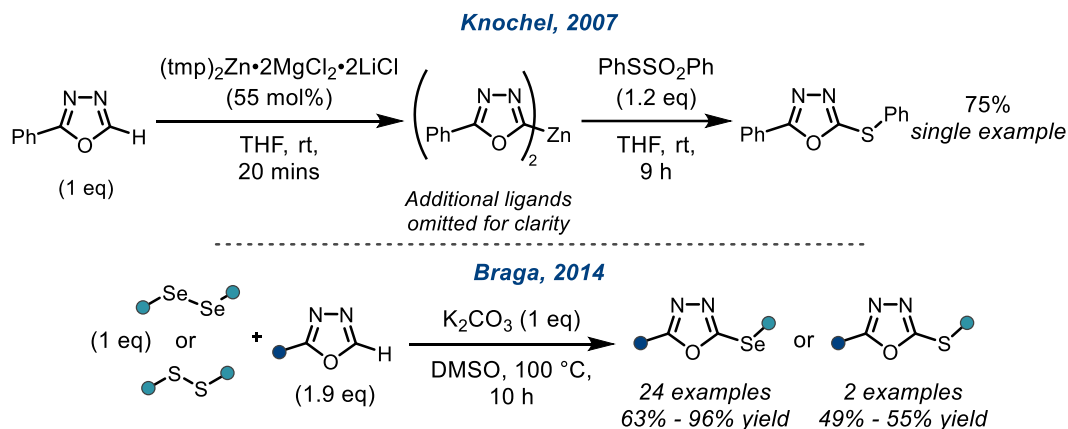
Subsequently, in 2011, it was demonstrated that *N*-benzoyloxy amines could be employed as an alternative electrophilic aminating reagent, improving upon and replacing the unstable *N*-chloroamines previously used.¹⁸³ Consequently, *N*-benzoyloxy amines and copper catalysts, have found prominent use as an amination system for stoichiometrically-deprotonated 1,3,4-oxadiazoles.⁹⁶⁻⁹⁸ Most recently, in 2016 the Chang group reported a copper-catalyzed C-H amination of 1,3,4-oxadiazoles using *N*-chloro-*N*-sodio-carbamates, yielding *N*-Boc protected 2-amino-5-substituted 1,3,4-oxadiazole products (scheme 1.29).¹⁸⁴



Scheme 1.29: Synthesis of *N*-Boc protected 2-amino-5-substituted 1,3,4-oxadiazoles.

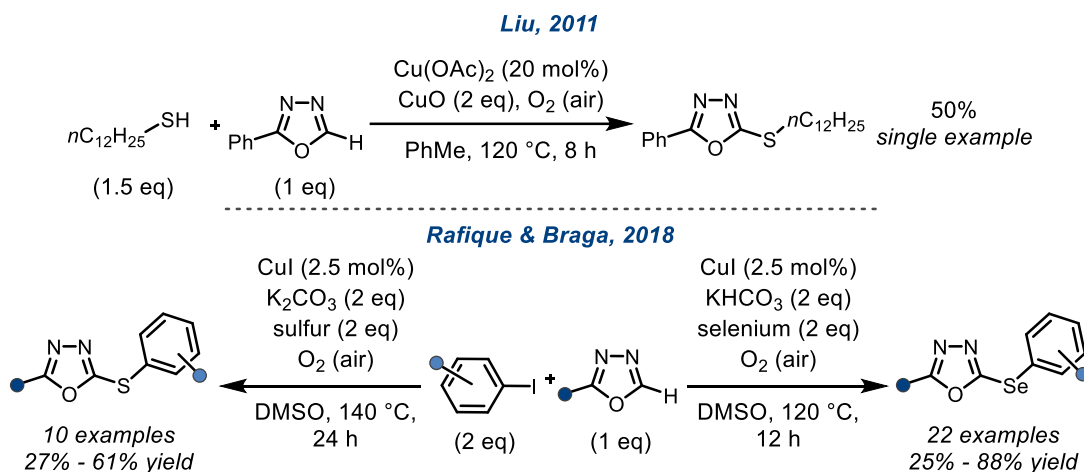
1.2.3.3 Carbon-Sulfur and Carbon-Selenium Bond Forming Methodologies

Transition metal catalyzed thiolations, and selenations, of 2-substituted 1,3,4-oxadiazoles are less studied than the corresponding C-C, and C-N bond formations, and additionally have been achieved using either stoichiometric (scheme 1.30, top),⁹⁹ or transition metal free approaches with disulfide or diselenide electrophiles (scheme 1.30, bottom).¹⁸⁵⁻¹⁸⁷



Scheme 1.30: Selected examples of transition metal free C-H chalcogenation of 2-substituted 1,3,4-oxadiazoles.

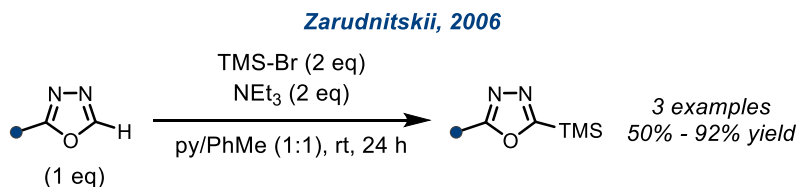
A transition metal catalyzed methodology was first disclosed by the Liu group in 2011, using thiols as coupling partners under oxidative reaction conditions (scheme 1.31, top).¹⁸⁸ Later, in 2018, a multicomponent approach to this class of 1,3,4-oxadiazoles was disclosed by Rafique and Braga, utilizing copper(I) iodide as a catalyst and aryl iodides and elemental sulfur (or selenium) as coupling partners (scheme 1.31, bottom).¹⁸⁹ Notably, this approach circumvented the requirement for the use and synthesis of potentially difficult to access, and handle, aromatic sulfur or selenium compounds. The mechanism for this transformation was not fully elucidated however the presence of radical intermediates was ruled out as the reaction proceeded in the presence of 5 equivalents of TEMPO with only a 12% reduction in yield. Additionally, in the absence of a 2-substituted 1,3,4-oxadiazole coupling partner, diphenyl diselenide was produced in 20% yield, indicating the possibility of its formation during the reaction.



Scheme 1.31: Selected examples of 1,3,4-oxadiazole C-H chalcogenations.

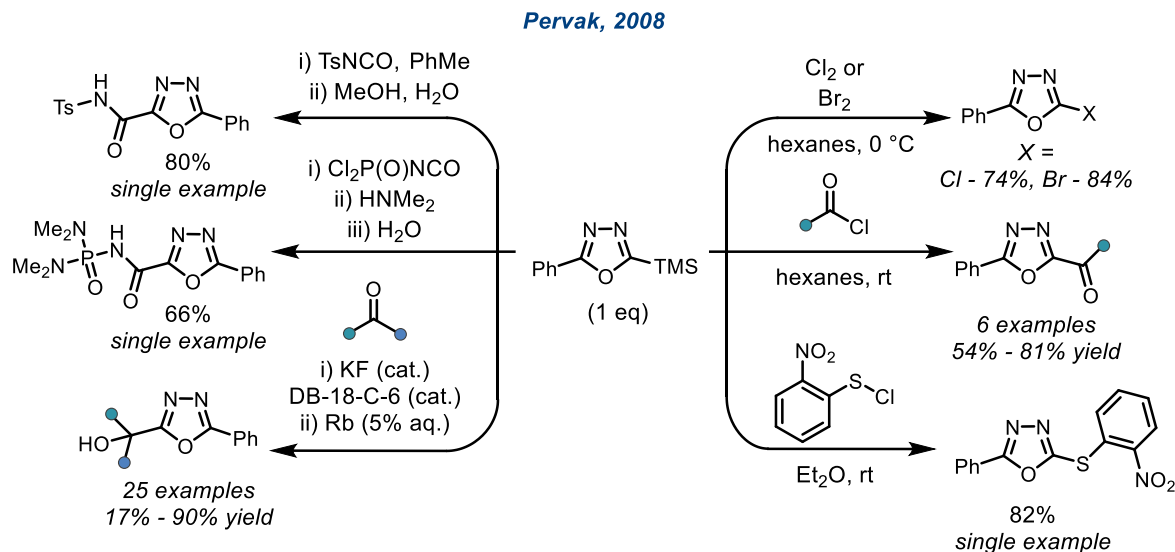
1.2.3.4 C-H Functionalizations of 2-Substituted 1,3,4-Oxadiazoles via C-H Silylation

A multistep 1,3,4-oxadiazole C-H functionalization strategy has been disclosed by Zarudnitskii, and Pervak. Firstly, Zarudnitskii utilized a reaction system of trimethylsilyl bromide and triethylamine for the synthesis of 2-aryl-5-trimethylsilyl 1,3,4-oxadiazoles in moderate to excellent yields (scheme 1.32).¹⁹⁰



Scheme 1.32: Zarudnitskii's synthesis of 2-aryl-5-trimethylsilyl 1,3,4-oxadiazoles.

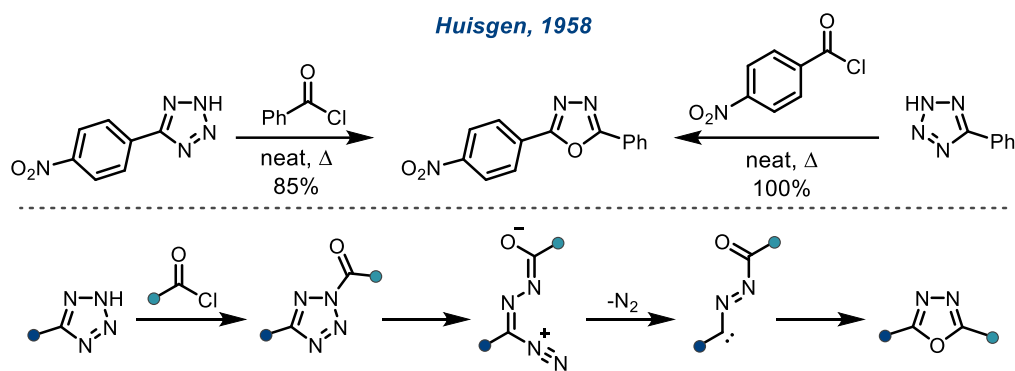
Pervak later demonstrated that these silylated 1,3,4-oxadiazoles can be reacted with electrophilic partners and undergo *ipso*-substitution at the trimethylsilylated position to yield 2,5-disubstituted 1,3,4-oxadiazoles under mild conditions (scheme 1.33).¹⁹¹ The scope of electrophiles included: isocyanates, elemental halogens, acyl chlorides, ketones, and aldehydes showcasing diverse substitutions of the 1,3,4-oxadiazole core in only two synthetic steps.



Scheme 1.33: Diverse functionalizations of 2-phenyl-5-trimethylsilyl 1,3,4-oxadiazole.

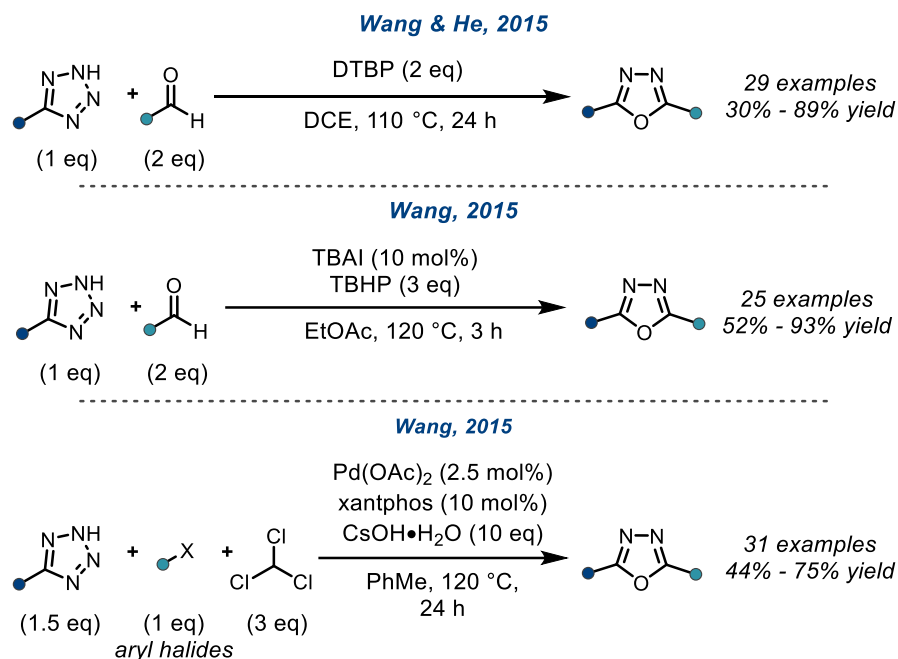
1.2.4 Synthesis of 1,3,4-Oxadiazoles via the Huisgen Tetrazole Rearrangement

In 1958, Huisgen hypothesized that when a 5-substituted 1*H*-tetrazole was reacted with an acyl chloride and subsequently heated, a 2,5-disubstituted 1,3,4-oxadiazole product should be obtained (scheme 1.34, top).¹⁹² This prediction was confirmed by synthesis of the same 1,3,4-oxadiazole, starting from two different 5-aryl 1*H*-tetrazoles and their complementary acyl chlorides. Mechanistically, the authors suggest the reaction proceeds through *N*-acylation of the tetrazole, and then *N-N* bond cleavage achieved by thermolysis. Subsequently, loss of nitrogen then affords a carbene species which reacts with the amide oxygen forming the 1,3,4-oxadiazole ring system (scheme 1.34, bottom). Since its discovery, this reaction has since been expanded to work using carboxylic acids (or acyl chlorides) in flow using ultraviolet radiation, instead of heating, to promote the reaction,¹⁹³ or in flow using high temperatures (>200 °C) but short reaction times, improving upon Huisgen's first reported conditions.¹⁹⁴



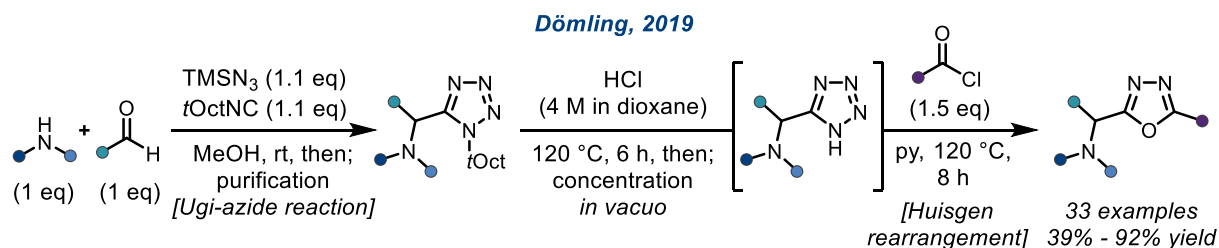
Scheme 1.34: Huisgen's report of a rearrangement of tetrazoles to 1,3,4-oxadiazoles, and the authors suggested mechanism.

Variations of the Huisgen rearrangement have emerged using alternative starting materials to expand the utility of the reaction. Two oxidative variations from Wang, and He, were disclosed in 2015 making use of aldehydes as reactive coupling partners (scheme 1.35).^{195, 196} A different mechanism is proposed in each report, with Wang and He's first report proposing a direct oxidation of the aldehyde by DTBP to its acyl cation, allowing for capture by the tetrazole to give the *N*-acyl tetrazole intermediate (scheme 1.35, top).¹⁹⁶ However, Wang's following report suggested that the tetrazole directly attacks the aldehyde, affording a hemiaminal intermediate, which is then oxidized to the *N*-acyl tetrazole by the TBAI and TBHP oxidative system (scheme 1.35, middle). In both reports, the *N*-acyl tetrazole affords the 1,3,4-oxadiazole products by a thermally promoted Huisgen rearrangement. Furthermore, Wang additionally reported a multicomponent and palladium-catalyzed synthesis of 1,3,4-oxadiazoles from aryl halides, 5-substituted 1*H*-tetrazoles, and chloroform in 2015 (scheme 1.35, bottom).¹⁹⁷ They proposed that chloroform in combination with cesium hydroxide generates carbon monoxide *in situ* providing the additional carbon atom needed for synthesis of the critical *N*-acyl tetrazole intermediate.



Scheme 1.35: Methodologies utilizing a Huisgen rearrangement for 1,3,4-oxadiazole synthesis.

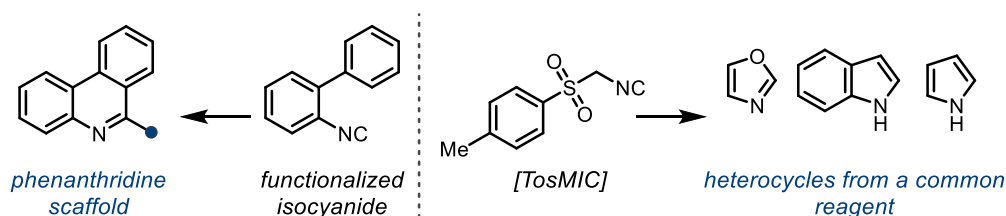
Multicomponent reactions (MCRs), such as the Ugi reaction, provide versatile methods for synthesis of diverse compounds in a single step.¹⁹⁸ Synthesis of tetrazoles *via* the Ugi-azide reaction is an example of an MCR.¹⁹⁹ Dömling has utilized a strategy involving a sequence comprised of an Ugi-azide reaction, and a Huisgen rearrangement, to yield 2,5-disubstituted 1,3,4-oxadiazoles (scheme 1.36).^{200, 201} Importantly, this strategy used *tert*-octyl isocyanide as a component in the Ugi-azide reaction, as it provided a *N*-protecting group that was shown to be cleaved under acidic conditions to give the 1*H*-tetrazoles needed for the Huisgen rearrangement. The exploitation of a multicomponent reaction as the first step in the reported sequences allowed for a wide variety of product structures to be rapidly synthesized.



Scheme 1.36: Selected example of the strategic use of an Ugi-azide reaction, and Huisgen rearrangement, for 2,5-disubstituted 1,3,4-oxadiazole synthesis.

1.2.5 Reactions using (*N*-Isocyanoimino)triphenylphosphorane (NIITP)

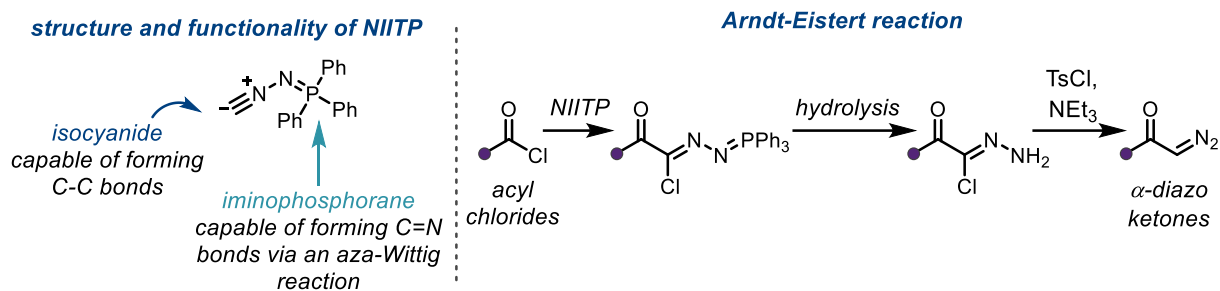
Functionalized isocyanide nucleophiles have historically been used to give rapid access to heterocycles, often *via* Ugi-type reactivity, in a range of synthetic contexts. For example, TosMIC undeniably remains an important isocyanide used for the synthesis of oxazoles, pyrroles, and other important heterocyclic scaffolds (scheme 1.37).²⁰²⁻²⁰⁴



Scheme 1.37: Heterocycle synthesis using functionalized isocyanides.

The functionalized isocyanide (*N*-isocyanoimino)triphenylphosphorane (NIITP) has been widely explored for its ability to act as a ligand for metal complexes, and for its ability to convert acyl chlorides into diazo ketones in a modified Arndt-Eistert reaction (also called the Aller reaction).²⁰⁵⁻²⁰⁷ Its structure features two functional handles capable of different bond-forming reactions: firstly an isocyanide, which readily forms C-C bonds with C=O and C=N electrophiles, and secondly, an iminophosphorane which can perform aza-Wittig reactions with carbonyl groups (scheme 1.38). The combination of these nucleophilic moieties has allowed NIITP to

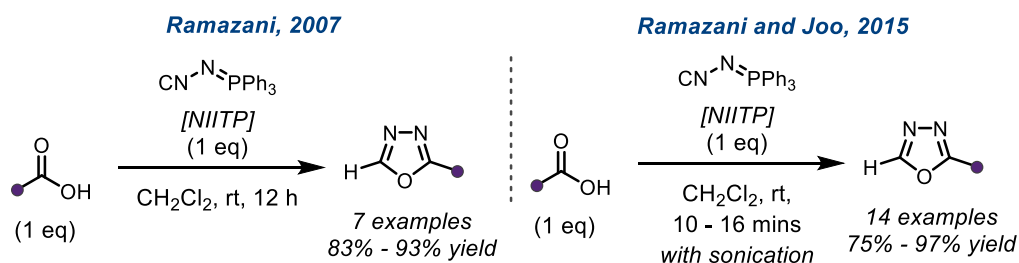
act as an efficient *CNN* source in the synthesis of 1,3,4-oxadiazoles, and related heterocycles.^{206, 207}



Scheme 1.38: Structure and functionality of NIITP, and its use for the modified Arndt-Eistert (or Aller) reaction.

1.2.5.1 Reactivity with Carboxylic Acids

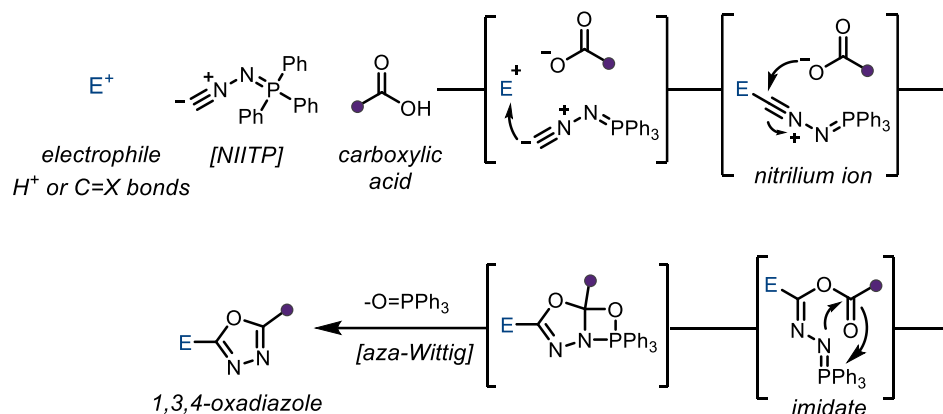
The use of NIITP for the synthesis of 1,3,4-oxadiazoles was first disclosed by Ramazani in 2007 who showed that benzoic acids treated with NIITP formed 2-aryl 1,3,4-oxadiazoles in good yields (scheme 1.39, left).²⁰⁸ Following this, Ramazani and Joo showed that this reaction could proceed with significantly shortened reaction times under ultrasonic radiation (scheme 1.39, right).²⁰⁹



Scheme 1.39: Synthesis of 2-aryl 1,3,4-oxadiazoles from carboxylic acids using NIITP, and improved conditions using ultrasonics.

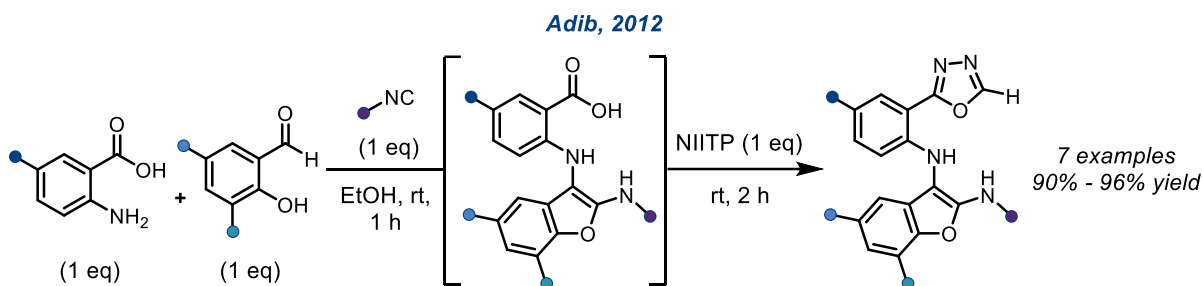
The generally accepted mechanism for this reaction, and the majority of 1,3,4-oxadiazole syntheses using NIITP, is depicted in scheme 1.40. Firstly, the isocyanide reacts with the

electrophile, most often a C=O, or C=N, bond, but in this case a proton from the carboxylic acid giving a nitrilium ion. Nucleophilic addition of the carboxylate anion into the nitrilium ion affords an imidate, and finally an intra-molecular aza-Wittig reaction generates the 1,3,4-oxadiazole product and eliminates triphenylphosphine oxide as the sole by-product.



Scheme 1.40: General reaction mechanism for 1,3,4-oxadiazole synthesis with NIITP.

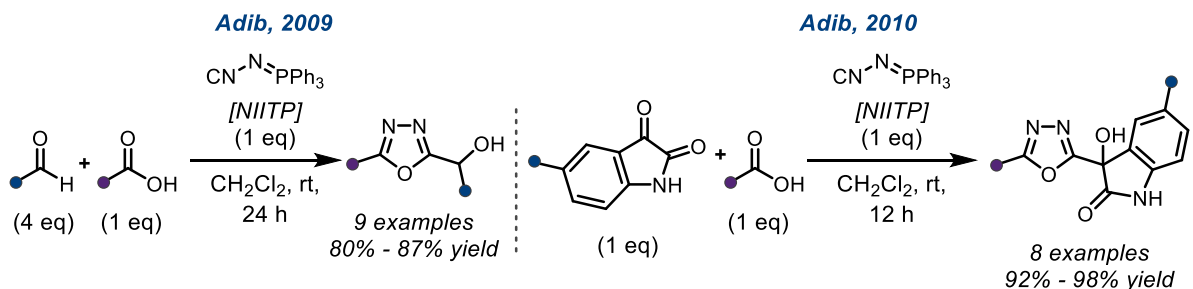
This reaction has been used to synthesis 2-substituted 1,3,4-oxadiazoles from a range of carboxylic acids²¹⁰⁻²¹⁴ – including one use for the synthesis of derivatives of the antiviral RO819.²¹⁵ Additionally, NIITP was employed in a tandem synthesis of benzofuran-1,3,4-oxadiazole hybrids in a report from Adib in 2012 (scheme 1.41).²¹⁶ This transformation was achieved by firstly, a MCR between an anthranilic acid, a hydroxybenzaldehyde, and an isocyanide affording an (isolable) benzofuran-containing carboxylic acid. A subsequent addition of NIITP then afforded the desired benzofuran-1,3,4-oxadiazole hybrids in excellent yield in a one-pot reaction.



Scheme 1.41: Tandem synthesis of benzofuran-1,3,4-oxadiazole hybrids.

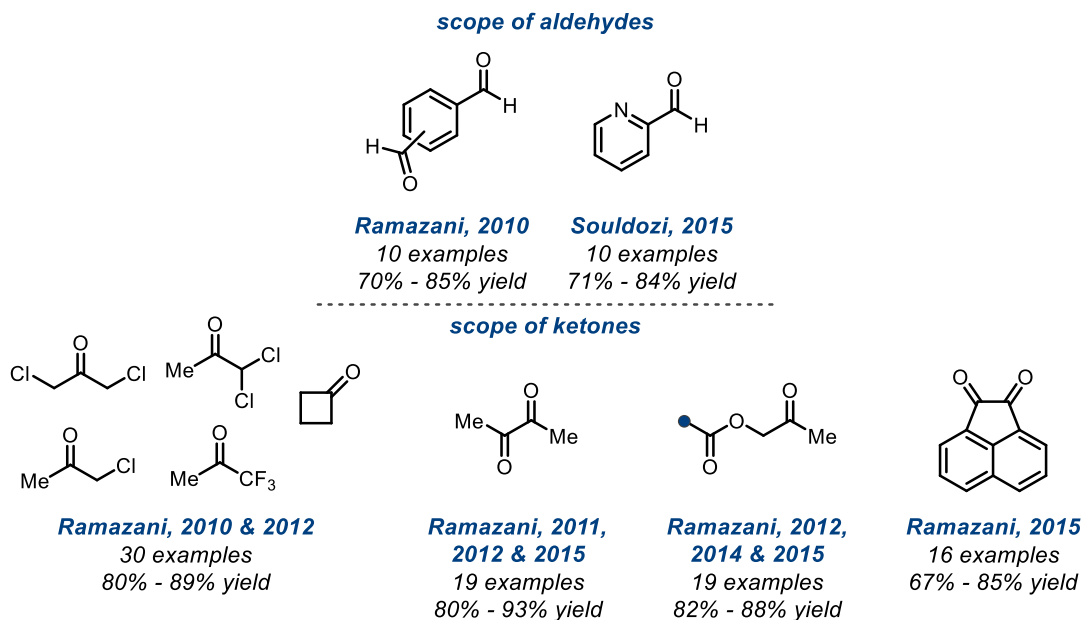
1.2.5.2 Reactivity with C=O Electrophiles

A Passerini-like MCR involving NIITP, a carboxylic acid, and a C=O electrophile was first disclosed in 2009 by Adib, using aldehydes as an electrophile for the synthesis of α -hydroxy 1,3,4-oxadiazole products (scheme 1.42, left).²¹⁷ Critical to the success of this reaction was the use of a large excess (4 equivalents) of the aldehyde component, to provide good yields of the α -hydroxy 1,3,4-oxadiazole products. Interestingly, when only 1 equivalent of aldehyde was used, the major product (>90%) was a 2-substituted 1,3,4-oxadiazole, formed by the competitive reaction of the carboxylic acid and NIITP as described by Ramazani.²⁰⁸ The reaction follows the general mechanism shown in scheme 1.40, where the aldehyde carbonyl is the electrophile for the reaction and presumably activated toward nucleophilic attack by reversible protonation from the carboxylic acid. An analogous reaction using isatins was described in 2010, however this time a 1:1:1 stoichiometry could be utilized likely due to the increased electrophilicity of isatins compared to aldehydes (scheme 1.42, right).²¹⁸



Scheme 1.42: First reports of NIITPs use in Passerini-like multicomponent reactions with C=O electrophiles.

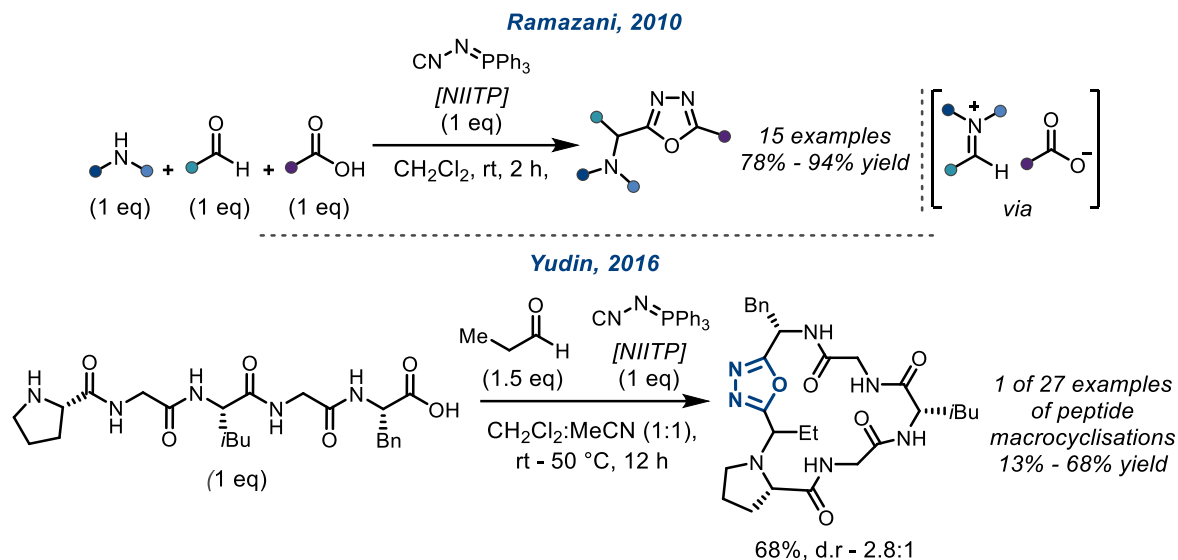
Since these initial reports, a wide range of both aldehydes and ketones have been shown to react efficiently with NIITP in the presence of carboxylic acids to afford α -hydroxy 1,3,4-oxadiazole products; these reactions are summarized in scheme 1.43.²¹⁷⁻²³⁴ One notable limitation is that when ketones are used they require activation by electron-withdrawing groups positioned alpha to the reactive ketone, or in one case by the ring strain imposed by a cyclobutene ring. This limitation likely stems from both the increased steric hindrance of ketones (compared to aldehydes), as well as limitations on the nucleophilicity of the isocyanide portion of NIITP, with the direct reaction of the carboxylic acid partner with NIITP being the major competitive side reaction. The iminophosphorane portion of NIITP could feasibly undergo an aza-Wittig reaction with both aldehydes and ketones reaction partners, however these side-reactions are likely out-competed by other reaction processes and were not discussed in any of the referenced literature.



Scheme 1.43: Scope of reactive C=O electrophiles reactive with NIITP.

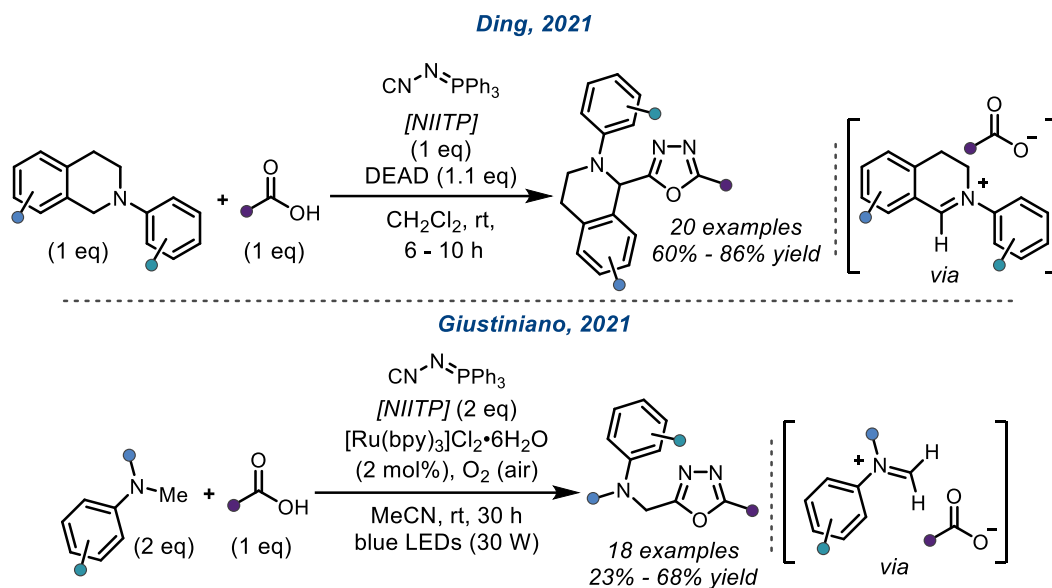
1.2.5.3 Reactivity with C=N Electrophiles

Ramazani in 2010 disclosed the first use of NIITP for the synthesis of α -amino 1,3,4-oxadiazoles, using a Ugi-type MCR with iminium ions (formed *in situ*) as the electrophilic partner for NIITP (scheme 1.44, top).²³⁵ Excellent yields were achieved using aromatic aldehydes and carboxylic acids, with nucleophilic secondary amine coupling partners; however, the functional group tolerance of this method was not explored beyond halogen substitutions at various positions of the aldehyde's, and carboxylic acid's, benzene rings. In future reports, a wide range of aldehydes and ketones, and primary and secondary amines were demonstrated to be amenable to this MCR.²³⁶⁻²⁵⁸ The effectiveness of this reaction was exemplified by the Yudin group, who used the methodology for the synthesis of 27 peptide macrocycles (scheme 1.44, bottom).⁴⁵ They suggested that efficiency of the macrocyclization is in part due to zwitterionic control, as observed in aziridine-aldehyde-based cyclizations, with the pendant triphenylphosphonium ion augmenting an electrostatic attraction between the two termini.²⁵⁹⁻²⁶¹



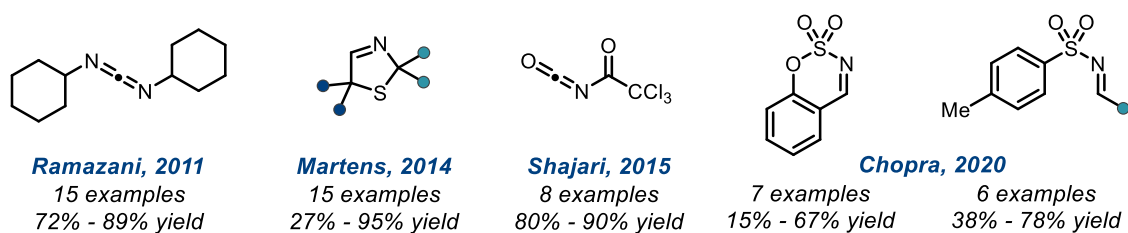
Scheme 1.44: Ramazani's multicomponent α -amino 1,3,4-oxadiazole synthesis, and its application to peptide macrocyclizations by the Yudin group.

In 2021, NIITP was shown by the groups of Ding,²⁶² and Giustiniano,²⁶³ to be reactive with iminium ions generated under oxidative reaction conditions (scheme 1.45). Ding's methodology utilized DEAD as an effective oxidant for *N*-aryl 1,2,3,4-tetrahydroisoquinolines, however its reactivity with other classes of amines was unexplored (scheme 1.45, top). In comparison, Giustiniano *et al*/ applied photoredox catalysis, using dioxygen as the terminal oxidant, for the oxidation of *N*-methyl anilines to their corresponding methylene iminium ions, generating methylene-bridged α -amino 1,3,4-oxadiazole products (scheme 1.45, bottom).



Scheme 1.45: α -Amino 1,3,4-oxadiazole synthesis via oxidatively-generated iminium ions.

Aside from iminium ions NIITP has been revealed to be reactive with other classes of C=N electrophiles including: carbodiimides,²⁶⁴ 3-thiazolines,²⁶⁵ isocyanates,²⁶⁶ and sulfamidates and *N*-sulfonyl imines (scheme 1.46).²⁶⁷ The reaction of NIITP with *N*-sulfonyl imines, is of particular interest as the products could potentially yield primary α -amino 1,3,4-oxadiazoles after *N*-sulfonyl deprotection, however this possibility has remained unexplored.

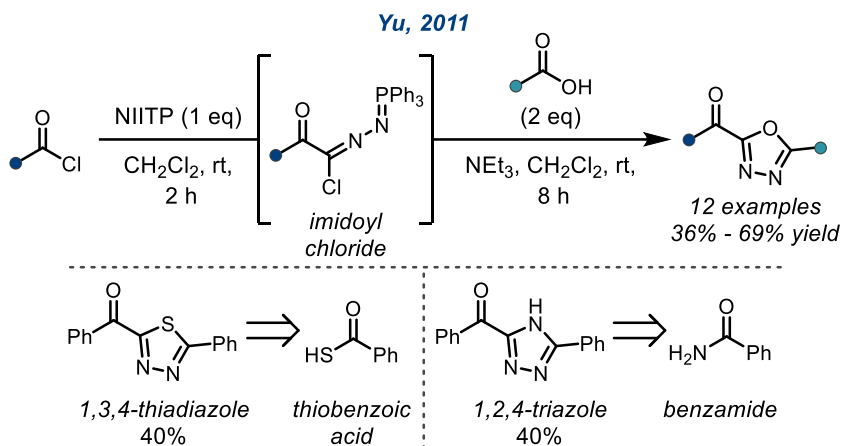


Scheme 1.46: Scope of C=N electrophiles reactive with NIITP.

1.2.5.4 Reactivity with Acyl Chlorides

Beyond C=O and C=N electrophiles NIITP has also been shown to be reactive with acyl chlorides in the Arndt-Eistert reaction (scheme 1.38). The imidoyl chloride intermediate formed has been shown by Yu to be reactive towards carboxylic acids, and to form α -keto 1,3,4-

oxadiazoles in an interrupted Arndt-Eistert reaction (scheme 1.47, top).²⁶⁸ The mechanism for the second step likely proceeds by carboxylate anion addition into the imidoyl chloride, followed by chloride elimination to give an imidate which can undergo an intramolecular aza-Wittig reaction to forge the 1,3,4-oxadiazole ring, as shown in scheme 1.40. A benefit of this two-stage methodology was the ability to access both a 1,3,4-thiadiazole, and a 1,2,4-triazole product by exchanging the carboxylic acid for thiobenzoic acid, or benzamide, respectively, although only moderate yields and singular examples were shown for these transformations (scheme 1.47, bottom).



Scheme 1.47: Yu's interrupted Arndt-Eistert reaction for the synthesis of α -keto 1,3,4-oxadiazoles from acyl chlorides and NIIP, and its use for heterodiazole synthesis.

1.3 Limitations of Current 1,3,4-Oxadiazole Syntheses

As demonstrated above, the synthesis of 1,3,4-oxadiazoles have been achieved using many approaches. However, there are still significant limitations to the strategies thus far presented. The limitations of dehydrative or oxidative strategies come from their need for functionalized starting materials, requiring multiple synthetic steps before the construction of the 1,3,4-oxadiazole ring; as well as the use of dehydrating or oxidizing reagents that can limit the functional group tolerance of these methods.

The C-H functionalization of 2-substituted 1,3,4-oxadiazoles presents an excellent way of providing diverse products from a single precursor, however the reaction scopes of these methods are frequently limited to only 2-aryl 1,3,4-oxadiazoles due to their ease of access, with 2-alkyl 1,3,4-oxadiazole rarely appearing. Furthermore, these methods still require multistep synthesis for construction of the 2-substituted 1,3,4-oxadiazole starting materials with the most common routes being based on the above dehydrative approaches.

1,3,4-Oxadiazole synthesis *via* the Huisgen-tetrazole rearrangement is inherently limited by the high temperatures used, and the expulsion of nitrogen which would pose potential safety concerns for larger scale reactions. Although the use of feedstock acyl chloride or carboxylic acid reaction partners is beneficial, the requirement for a 1*H*-tetrazole starting material means that in practice the products could often be more efficiently synthesized using a dehydrative method and two carboxylic acids as starting materials, while avoiding the use of potentially energetic 1*H*-tetrazoles.

Lastly, approaches using NIITP as a *CNN* source for 1,3,4-oxadiazole synthesis have been developing rapidly within the last decade. Of note is that NIITP allows the synthesis of 2-substituted 1,3,4-oxadiazoles from carboxylic acids using a single reagent. Moreover, its ability to act in Passerini- or Ugi-type multicomponent reactions due to its isocyanide functionality, makes it an excellent choice for synthesis of 2,5-disubstituted 1,3,4-oxadiazoles where the retrosynthetic route can be traced back to arrive at a C=O, or C=N electrophile. However, multicomponent reactions using NIITP are limited in scope with respect to the carboxylic acid component where Coro and Rivera *et al* have noted that “The scope of the carboxylic component is currently limited to aromatic, cinnamic, and amino acids”.²⁰⁶

1.4 Conclusion and Thesis Aims

In conclusion, the discussed limitations to existing 1,3,4-oxadiazole syntheses have meant that dehydrative methods remain the method of choice in complex synthetic contexts, where this approach benefits from feedstock carboxylic acid starting materials and a wide variety of conditions that allow ready tuning of the reaction to specific substrates. However, as NIITP has been shown to be an excellent precursor for 1,3,4-oxadiazoles in multicomponent reactions, the development of new multicomponent reactions utilizing NIITP's efficient coupling with electrophiles to streamline access to complex 1,3,4-oxadiazoles was targeted and pursued.

To this end, **Chapter 2** focuses on expanding our group's work on the reductive functionalization of tertiary amides and lactams, using NIITP and carboxylic acids to provide a multicomponent synthesis of α -amino 1,3,4-oxadiazoles. The key aim of this project was to investigate if this approach could achieve the late-stage functionalization of complex amide (or lactam), and carboxylic acid containing molecules. Also examined was an extension of method to α -amino heterodiazole synthesis using NIITP and *S*-, *N*-, and *C*-centered Brønsted acids.

The project disclosed in **Chapter 3** aimed to expand the scope of neutrally-charged C=N electrophiles reactive with NIITP. Finding *N*-carbamoyl imines compatible in a multicomponent Ugi-type reaction with NIITP and carboxylic acids, the scope of the reaction with respect to both reaction partners was investigated. The synthetic utility of the *N*-carbamoyl α -amino 1,3,4-oxadiazole products was additionally examined. Furthermore, a preliminary study into an enantioselective reaction variant, and the use of *N*-acyl iminium ion electrophiles was explored.

Changing focus from α -amino 1,3,4-oxadiazole synthesis, **Chapter 4** discusses an investigation into a streamlined, and multicomponent, approach to 2,5-disubstituted 1,3,4-oxadiazoles that targeted the merger of two modern approaches for 1,3,4-oxadiazole synthesis – synthesis of 2-substituted 1,3,4-oxadiazole using NIITP, and the C-H functionalization of 2-

substituted 1,3,4-oxadiazoles. Additionally, the multicomponent synthesis of synthesis of 2-amino-5-substituted 1,3,4-oxadiazoles from carboxylic acids, NIITP, and secondary amine reaction partners was studied.

Detailed experimental procedures and spectroscopic data for synthesized compounds is reported in **Chapter 5**.

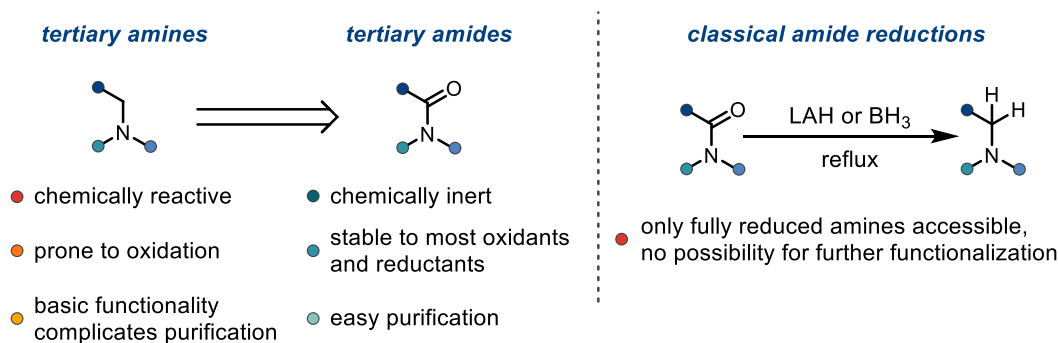
Collated references from all chapters are presented in **Chapter 6**.

Chapter 2: Catalytic Reductive Amide Functionalization for Late-Stage α -Amino 1,3,4-Oxadiazole Synthesis

2.1 Introduction to Reductive Amide Functionalization

2.1.1 General Concept and First Reports

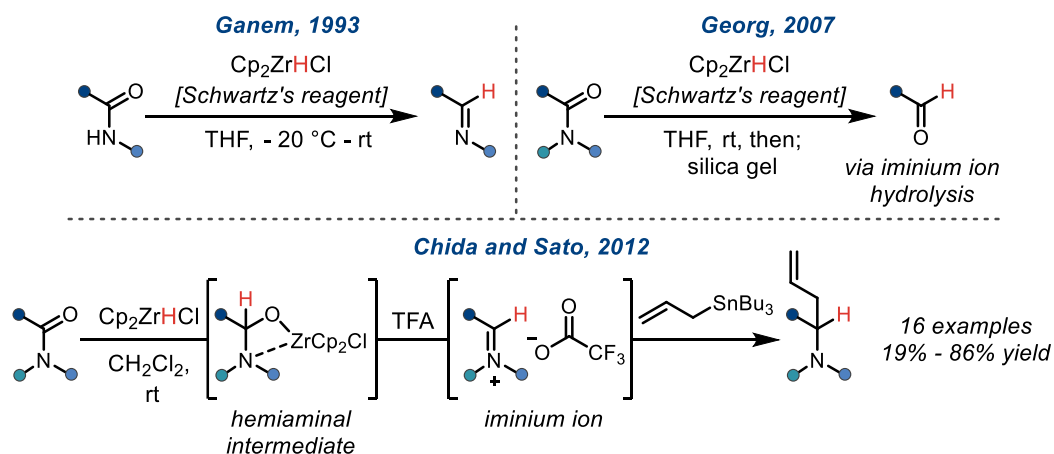
Synthesis of tertiary amines from amides is a widely exploited strategy, particularly in total synthesis where unprotected tertiary amines pose chemoselectivity, reactivity, and purification challenges (scheme 2.1, left).^{269, 270} The benefit of this strategy is that the problematic tertiary amine can remain protected as the tertiary amide until the end of the synthetic sequence, or until needed for further transformations. While modern methods can achieve chemoselective amide reductions, common laboratory reagents such as LAH, or boranes, are still routinely used to accomplish the complete reduction of amides, to tertiary amine functionalities, when chemoselectivity is not an issue (scheme 2.1, right).²⁷¹⁻²⁷⁴



Scheme 2.1: Advantages of tertiary amides as a protecting group for tertiary amines, and classic amide reductions.

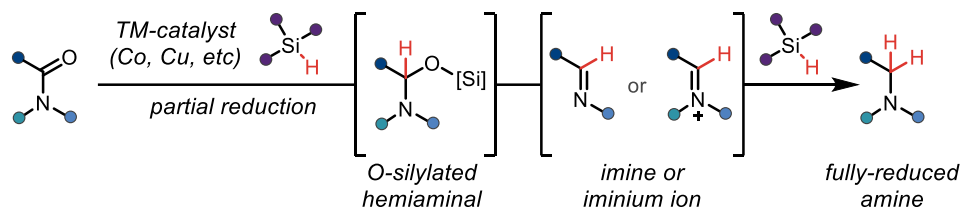
While traditional borane, and alane, reductants only provide access to fully-reduced tertiary amine compounds, in 1993 it emerged that a chemoselective mono-reduction of secondary amides to imines could be achieved using Schwartz's reagent (Cp_2ZrHCl) (scheme 2.2, top left).²⁷⁵ Later, in 2007 the reactivity of this reagent was further exploited by Georg who

demonstrated that tertiary amides can be selectively mono-reduced, giving aldehyde reaction products after hydrolysis of an iminium ion intermediate (scheme 2.2, top right).²⁷⁶ Importantly Georg's reported transformation took place even in the presence of potentially-reducible esters, nitriles, and carbamates. These methods demonstrated that the partial reduction of amides was possible using stoichiometric organometallic reagents, however it took a further five years before Chida and Sato reported the first reductive functionalization of tertiary amides (scheme 2.2, bottom).²⁷⁷ Their methodology employed an initial mono-reduction of a tertiary amide using Schwartz's reagent as reported by Georg; however the hemiaminal intermediate generated was subsequently ionized to form an iminium ion *in situ* using TFA. This reactive intermediate was intercepted by allyl tributyltin as a carbon-centered nucleophile, generating α -allylated tertiary amine products. The scope of this methodology showed that both tertiary and secondary amides were amenable to the reductive functionalization protocol. Furthermore, the method was shown to be tolerant of ester and nitro groups without any observable reduction of these functionalities by Schwartz's reagent.



Scheme 2.2: Stoichiometric amide mono-reductions (top), and the first report of the reductive functionalization of tertiary amides using Schwartz's reagent (bottom).

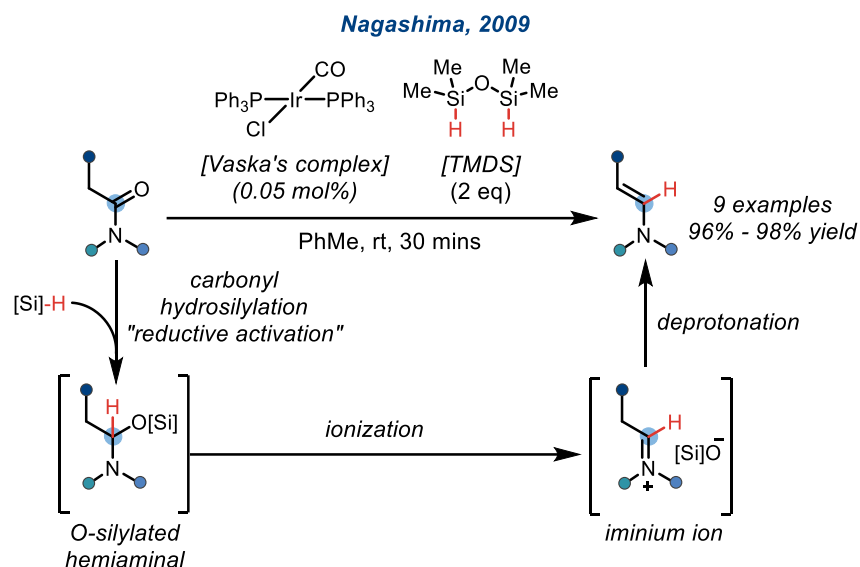
Schwartz's reagent remains widely-used for chemoselective amide reductions, yet these protocols have drawbacks such as the use of stoichiometric zirconium organometallics, and the required preparation of the reagent which is an air-, moisture-, and light-sensitive solid.²⁷⁸ At the time, transition metal catalyzed amide reductions, using silanes as reductants, were well explored using Co, Cu, Fe, Mo, Rh, Ru, and Zn species,²⁷⁹⁻²⁸⁸ however these all afforded the fully-reduced tertiary amine products – without access to key hemiaminal intermediates as provided by Schwartz's reagent (scheme 2.3). This limitation has led to the use of these catalysts for reductive amide functionalization remaining evasive.



Scheme 2.3: Amide reduction via transition metal catalyzed hydrosilylation.

A catalytic partial reduction of tertiary amides to aldenamines by carbonyl hydrosilylation was first realized by the Nagashima group using Vaska's complex ($\text{IrCl}(\text{CO})(\text{PPh}_3)_2$)²⁸⁹ with 1,1,3,3-tetramethyldisiloxane (TMDS) as the silane reductant (scheme 2.4).²⁹⁰ Vaska's complex stood out among those catalysts investigated by Nagashima for its high selectivity for tertiary amides in the presence of esters, ketones, and alkenes, and for its ability to reductively activate the amide at room temperature without a further undesired reduction to a tertiary amine occurring. Their proposed mechanism for this transformation proceeds through an initial amide hydrosilylation affording an *O*-silylated hemiaminal, subsequent elimination of a siloxide gives an iminium ion which – upon proton loss - forms the enamine product. This report critically shows Vaska's complex as able to access an *O*-silylated hemiaminal intermediate from a tertiary amide without undergoing over reduction; a prominent pathway using other transition

metal catalysts as the high reaction temperatures often required encourages ionization of the O-silylated hemiaminal intermediate to a readily-reduced iminium ion.

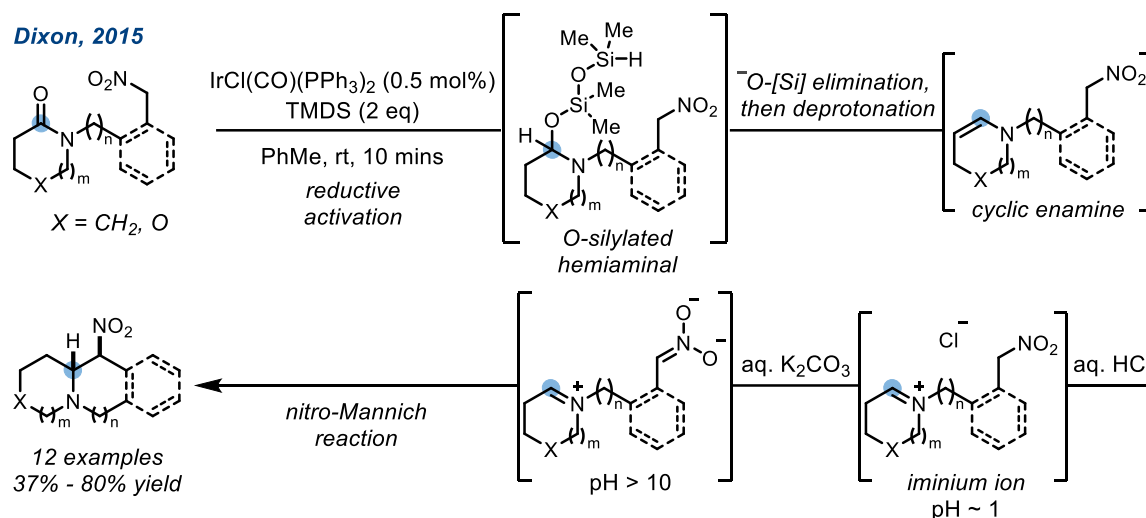


Scheme 2.4: Nagashima's report of aldenamine synthesis from tertiary amides using Vaska's complex and their proposed mechanism.

2.1.2 Catalytic Reductive Amide Functionalization using Vaska's Complex

The ability of Vaska's complex to access metastable O-silylated hemiaminal species has been effectively leveraged for the catalytic reductive functionalization of tertiary amides since Nagashima's initial report.²⁹¹⁻²⁹³ The first reports of the catalytic reductive functionalization of amides using Vaska's complex came from the Dixon (scheme 2.5),²⁹⁴ and Chida and Sato groups in 2015 (scheme 2.6).²⁹⁵ The Dixon group reported a reductive intramolecular nitro-Mannich reaction of tertiary lactams with internal nitro-alkanes. Mechanistically, based on evidence provided by ¹H NMR analysis, they suggest the starting lactam undergoes reductive activation by Vaska's complex and TMDS to afford an enamine, as per Nagashima's report.²⁹⁰ After this, a workup involving 1M HCl addition – generating an iminium ion – and following basification with potassium carbonate, affords the nitro-Mannich products. This methodology

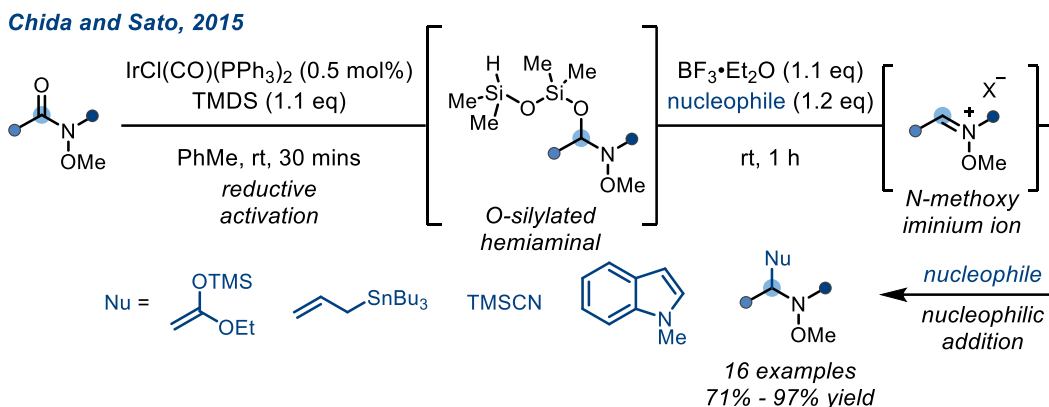
afforded a range of bicyclic amine systems, and its utility was demonstrated by the synthesis of (±)-*epi-epiquinamide* in four steps.



Scheme 2.5: Dixon's first report of the catalytic reduction functionalization of lactams using Vaska's complex.

Chida and Sato's report concerned the reductive functionalization of *N*-methoxy amides, using Vaska's complex and TMDS as the catalytic reductive system, in combination with carbon-based nucleophiles in a catalytic version of their previous methodology (schemes 2.2 & 2.6).²⁹⁶ In agreement with Dixon,²⁹⁴ and Nagashima,²⁹⁰ Chida and Sato's mechanistic proposal begins with the initial reaction of the *N*-methoxy amide with Vaska's complex and TMDS, affording an *O*-silylated hemiaminal. They suggest this *O*-silylated hemiaminal is stable until treated with a Lewis acid ($\text{BF}_3 \cdot \text{OEt}_2$) which promotes its collapse to form an *N*-methoxy iminium ion *in situ* which can then react with a carbon-based nucleophile affording the α -functionalized *N*-methoxy amine products. The absence of enamine formation in their proposed mechanism was supported by subjection of an *N*-methoxyamide bearing an enantioenriched α -stereocentre

(94% ee) to the reaction conditions, which yielded two product diastereomers each with an 100% es² measured.



Scheme 2.6: Chida and Sato's first report of the catalytic reduction functionalization of *N*-methoxy amides using Vaska's complex.

Following Dixon's,²⁹⁴ and Chida and Sato's reports,²⁹⁶ reductive amide functionalization methodologies have utilised the mild and chemoselective activation provided by Vaska's complex for a broad range of reactions involving tertiary amides as sources for reactive intermediates, as shown by the example product structures in scheme 2.7.^{294, 295, 297-313} Additionally, the area of reductive amide functionalization has been the subject of recent reviews by the Dixon,²⁹¹ Furman,²⁹² and Nagashima groups.²⁹³

For example, Huang in 2016 reported a reductive A³ coupling reaction using an iridium/copper co-catalytic system.²⁹⁷ In their report the amide was first hydrosilylated with Vaska's complex and TMDS to afford the *O*-silylated hemiaminal intermediate common to all the reactions in scheme 2.7. After this, addition of an alkyne coupling partner and copper(I) bromide afforded the propargylic amine products. The authors suggest that the *O*-silylated hemiaminal intermediate is collapsed *in situ* to the iminium ion by protonation from the alkyne (acidified by

² es = enantiospecificity = (% ee of starting materials / % ee of products) * 100

coordination to a copper species) and subsequent elimination of the silanol moiety. This methodology was later expanded in 2020 to allow for lactam substrates to be used,³⁰⁷ and further still in 2021 with an enantioselective variant using a bis-phosphine ligand to provide enantiocontrol of the alkyne addition into the iminium ion.³¹¹

The Chida and Sato group discovered that *N*-hydroxy amides – upon treatment with Vaska's complex and TMDS – yielded nitrones with complete regiocontrol, determined by the starting position of the amide carbonyl group in the substrate.²⁹⁸ This reaction is reported to proceed *via* a reductive activation of the *N*-hydroxy amide, along with concomitant *O*-silylation of the *N*-hydroxy group. A following addition of either TBAF, or PPTS, affords the nitrone after elimination of the silanol group and *N*-hydroxy deprotection.

In 2017, the Dixon group reported two reductive functionalization reactions, starting with a reductive Strecker reaction.²⁹⁹ In this work it was found that TMSCN acted efficiently as a Lewis-acid, and formally a TMS⁺ source, causing collapse of the *O*-silylated hemiaminal to the desired iminium ion electrophile which could subsequently react with the cyanide nucleophile present in the reaction mixture. Later in 2017, the Dixon group disclosed a reductive coupling of tertiary amides, and lactams, with Grignard nucleophiles,³⁰⁰ and demonstrated the methodology on 100 mmol scale using only 0.05 mol% of Vaska's complex in 2019.³⁰¹ Furthermore, an umpolung synthesis of α -alkylated tertiary amines was achieved by the Dixon group in 2020 using a dual-iridium catalyzed hydrosilylation and photoredox strategy – with access to reactive α -amino radicals provided by single-electron reductions of reductively-generated iminium ions.³¹³

The use of isocyanides as nucleophiles for reductive amide functionalization was first described by the Dixon group in 2018 in an Ugi-type reaction affording α -amino secondary (thio)amides, and α -amino tetrazoles.³⁰³ The use of isocyanide nucleophiles was further explored by the

Huang group in 2018, using methyl 2-isocyano-2-phenyl-acetate for the synthesis of 5-methoxy oxazoles.³⁰² An additional discussion of these methodologies will be presented in section 2.1.3.

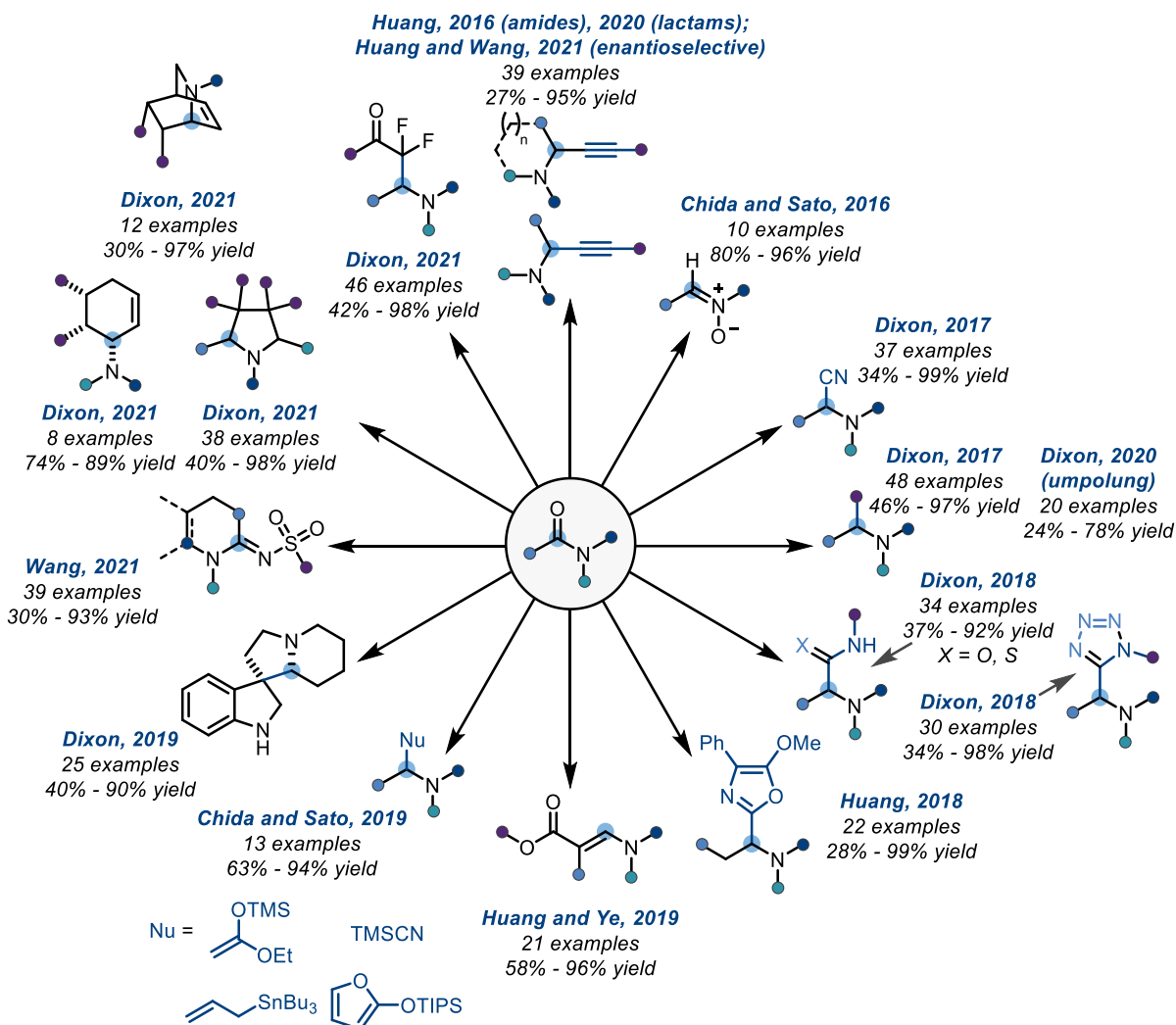
Aside from C-C bond forming methodologies, the Vaska's/TMDS catalytic system has attracted interest for the synthesis of complex enamines within total synthesis efforts.³¹⁴⁻³¹⁷ A standalone synthesis method applying the Vaska's complex and TMDS system for enamine synthesis came from Huang and Ye in 2019,³⁰⁶ exploiting the catalytic system for the reduction of β -enamido esters to β -enamino esters – a functional group seen in alkaloids and antibacterial agents.³¹⁸

The scope of carbon-based nucleophiles employed in reductive amide functionalizations was expanded in 2019 by the groups' of Chida and Sato,³⁰⁵ and Dixon.³⁰⁴ Chida and Sato demonstrated use of allyl stannanes, and silyl ketene acetals including 2-silyloxy furans, in good yields when using mild Brønsted- (PPTS or TFA) or Lewis-acids ($\text{BF}_3 \cdot \text{Et}_2\text{O}$ or $\text{Sc}(\text{OTf})_3$) to promote the ionization of the *O*-silylated hemiaminal and subsequent nucleophilic addition into the iminium ion.³⁰⁵ In the same year the Dixon group reported an interrupted Pictet-Spengler reaction with a tethered indole acting as a nucleophile for the iminium ion, and resulting in the formation of spirocyclic indoline products.³⁰⁴

The synthesis of *N*-sulfonylformamidines routinely uses difficult to access enamine intermediates, formed oxidatively from an amine *via* dehydrogenation – leading to site- and chemo-selectivity challenges when a tertiary amine with multiple α -CH bonds is employed. An approach to cyclic *N*-sulfonylformamidines with complete site-selectivity was developed in 2021 by Wang using lactams as dormant enamine precursors – unveiled by reductive activation with the Vaska's/TMDS catalytic system – which then reacted with sulfonyl azides to afford the desired products.³¹⁰ The usefulness of the presented method was exemplified by application to the late-stage functionalization of lactam containing drugs and natural products.

The above reports have shown the excellent utility of the Vaska's/TMDS catalytic system for accessing reactive enamine and iminium ion intermediates. The Dixon group in 2021 showed that this catalytic system could be used to access dienamine, and azomethine imine intermediates from β,γ -unsaturated amides,³⁰⁹ and tertiary amides containing a suitably positioned electron-withdrawing, or trimethylsilyl group.³¹² These works demonstrated that carefully designed amides can undergo fundamental [4+2] or dipolar-[3+2] cycloadditions generating polycyclic structures, and decorated pyrrolidines under a reductive amide functionalization protocol. Furthermore, the shortest synthesis (five steps) of catharanthine to date was accomplished through the synthesis of the elusive biosynthetic precursor and dienamine dehydrosecodine and a subsequent intramolecular [4+2] cycloaddition reaction.³⁰⁹

The introduction of *gem*-difluoromethylene ($-\text{CF}_2-$) groups into molecules has gained attention in both pharmaceuticals and agrochemicals – as an oxygen bioisostere –³¹⁹ and in materials science due to physical and chemical properties imparted by the fluorine atoms.^{320, 321} In 2021 the Dixon group reported a method for the synthesis of β,β -difluoro- α -amino motifs *via* a reductive Reformatsky reaction.³⁰⁸ Utilizing reductively generated iminium ions as electrophiles reactive with nucleophilic difluoro-Reformatsky reagents ($\text{BrZnCF}_2\text{COR}$), the reaction proceeded smoothly giving high yields of the desired products, which could be further transformed into valuable β,β -difluoro- α -amino containing molecules.



Scheme 2.7: Overview of reductive amide functionalization methodologies using Vaska's complex since Dixon's, and Chida and Sato's first reports.

2.1.3 Catalytic Reductive Amide Functionalizations Involving Isocyanide Nucleophiles

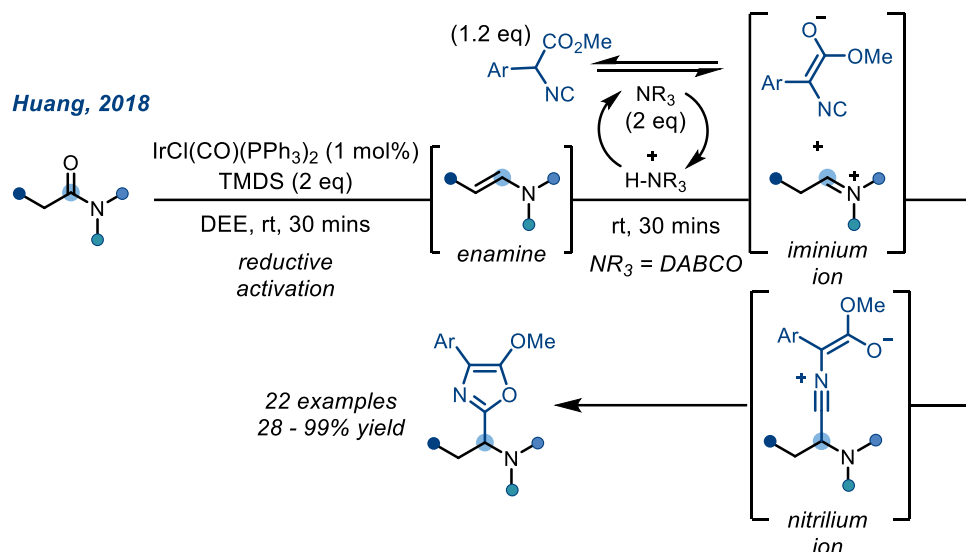
Reductive amide functionalization methodologies involving isocyanides as carbon-based nucleophiles have been reported by both the Huang,³⁰² and Dixon groups.³⁰³ Firstly, the Dixon group in 2017 reported a reductive and multicomponent Ugi and Ugi-azide reaction involving tertiary amides and lactams, an isocyanide nucleophile and either (thio)acetic acid, or trimethylsilyl azide (scheme 2.8). The mechanism for this reaction follows that of an Ugi reaction with the isocyanide undergoing addition into the reductively-generated iminium ion to afford a

nitrilium ion intermediate. Then addition of the (thio)acetate anion into the nitrilium ion affords a (thio)imidate which can then undergo an acyl transfer to release the desired product (scheme 2.8). The reported Ugi-azide reaction likely proceeds *via* a similar mechanism however with an azide anion (N_3^-), released by TMS azide *in situ*, undergoing a (formal) dipolar cycloaddition with the nitrilium ion intermediate to afford the α -amino tetrazole product.



Scheme 2.8: Dixon's reductive Ugi and Ugi-azide reactions and their proposed reaction mechanism.

The mechanism of Huang's report describing the reaction of isocyanacetate nucleophiles is similar, however they propose that the acid that allows for the iminium ion to form from the O-silylated hemiaminal, or enamine, is a trialkylammonium ion generated by deprotonation of the isocyanacetate by its conjugate base – in this case DABCO – (scheme 2.9). Following iminium ion generation the isocyanide moiety undergoes addition into the iminium ion to give a nitrilium ion intermediate which is then attacked in an intramolecular fashion by an oxy-anion to give the 5-methoxy oxazole products.



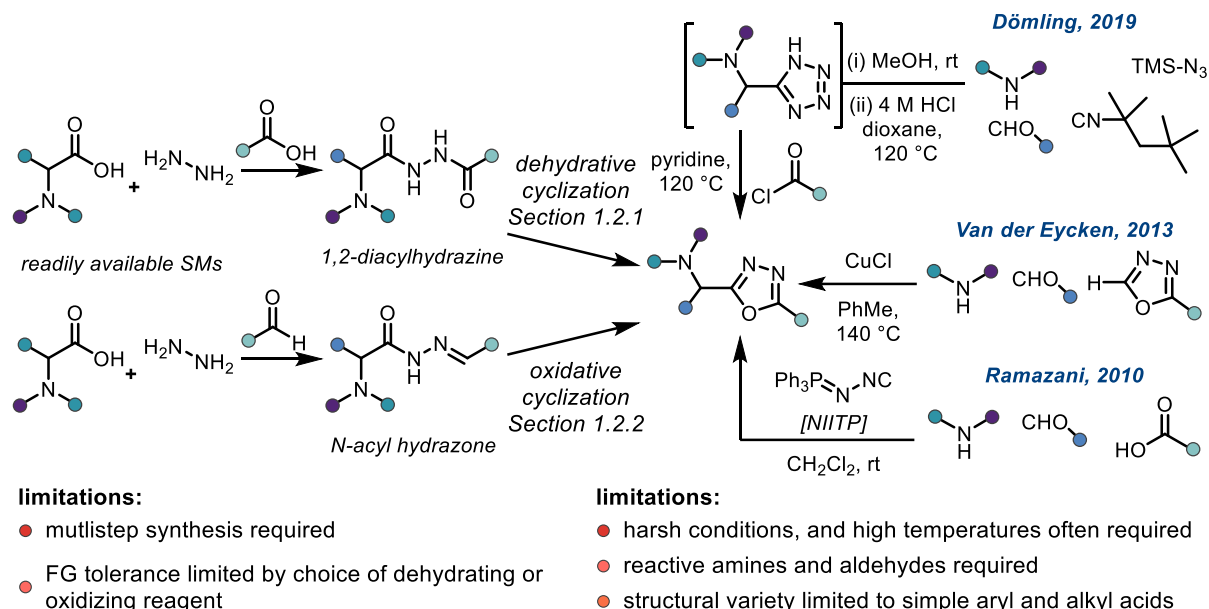
Scheme 2.9: Huang's reaction of isocyanoacetate esters with reductively-generated iminium ions and their proposed reaction mechanism.

2.2 Current Approaches to α -Amino 1,3,4-Oxadiazole Synthesis

Current approaches to α -amino 1,3,4-oxadiazoles are largely dependent on the dehydrative or oxidative approaches to 1,3,4-oxadiazole synthesis as discussed in sections 1.2.1 and 1.2.2 and use α -amino acids as key building blocks (scheme 2.10, left). However, in recent years developments by the groups of Ramazani,²³⁵ Van der Eycken,¹⁵⁸ and Dömling,²⁰⁰ have provided direct methodologies for α -amino 1,3,4-oxadiazole synthesis (scheme 2.10, right). Prevalent in these direct methods is the condensation of secondary amines and aldehydes to generate iminium ion intermediates. Reliance on these highly-reactive starting materials has resulted in limitations including: i) restricted use of reaction partners bearing electrophilic functional groups (such as Michael acceptors, alkyl halides, etc.); ii) anilines affording low yields of the desired products due to inefficient condensations with aldehydes; iii) limited structural variety focused on simple aryl and alkyl carboxylic acids and aldehydes due to their reliable reactivity.

indirect synthesis of α -amino 1,3,4-oxadiazoles

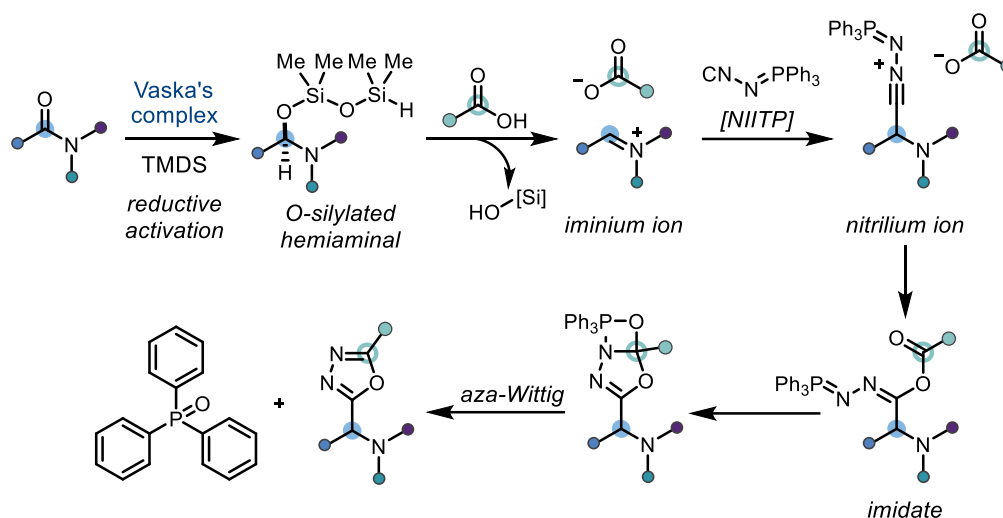
direct synthesis - recent developments



Scheme 2.10: Indirect and direct approaches to α -amino 1,3,4-oxadiazole synthesis.

2.3 Project Concept

The success of reductive amide functionalization methodologies involving simple isocyanides and isocyanoacetates, combined with Ramazani's report of a multicomponent α -amino 1,3,4-oxadiazole synthesis using NIITP led us to hypothesize that a reductively-generated iminium ion in combination with NIITP and a suitable carboxylic acid would form the desired α -amino 1,3,4-oxadiazole product, following the reaction mechanism shown in scheme 2.11. The reaction mechanism would start with the reductive activation of the tertiary amide to afford an O-silylated hemiaminal, which upon treatment with a carboxylic acid would generate an electrophilic iminium ion intermediate. Following this, the reaction pathway would likely follow the same general mechanism as other 1,3,4-oxadiazole syntheses involving NIITP, as shown in scheme 1.40, liberating triphenylphosphine oxide as the major by-product.



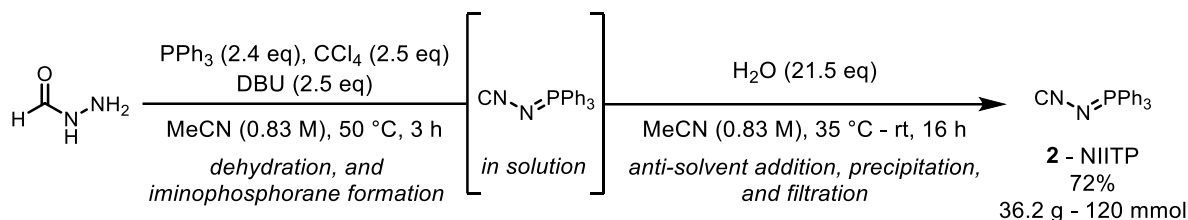
Scheme 2.11: Reaction proposal and mechanism for the reductive synthesis of α -amino 1,3,4-oxadiazoles from tertiary amides.

Inspired by these recent direct approaches for α -amino 1,3,4-oxadiazole synthesis, we reasoned that pursuing a strategy replacing reactive secondary amines and aldehydes in favour of tertiary amides – reductively activated by the Vaska’s/TMDS catalytic system – would circumvent the limitations associated with the existing synthetic approaches. This would include providing reliable access to cyclic- and aniline-based iminium ions, permitting synthesis of α -amino 1,3,4-oxadiazoles with significantly enhanced structural and chemical diversity. Furthermore, this strategy would allow the late-stage functionalization of both amide and carboxylic acid containing drug-like molecules, as has been shown to be a significant advantage of previous reductive amide functionalization methodologies.²⁷⁻⁴²

2.4 Reaction Discovery and Optimization

This project commenced using *N*-benzyl lactam **1** as the model substrate, chosen as piperidines, and related nitrogen heterocycles, are key components of many pharmaceutical compounds and synthesis of functionalized counterparts from chemically robust lactams continues to be highly desirable.³²²⁻³²⁵ Although NIITP (**2**) is commercially available its high

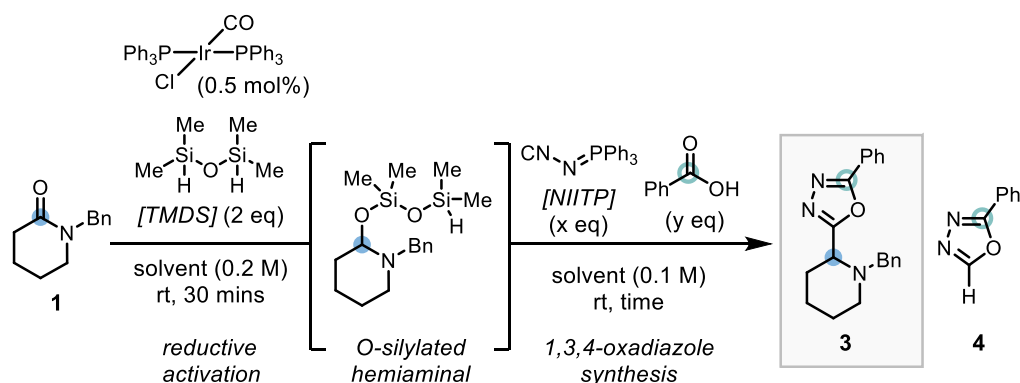
price led us to synthesize it *via* dehydration of formyl hydrazine with concomitant iminophosphorane formation, following Bio's procedure (scheme 2.12).²⁰⁵ This procedure proved reliable for synthesis of NIITP (**2**) in batches of up to 36.2 g (120 mmol) with isolation accomplished by precipitation from the reaction mixture and filtration.



Scheme 2.12: Synthesis of NIITP on decagram scale following Bio's procedure.²⁰⁵

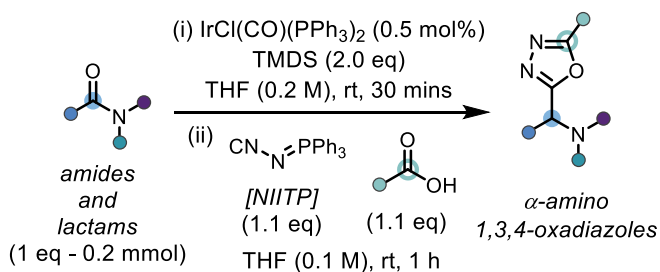
With starting material synthesis complete, we observed that upon treatment of **1** with 0.5 mol% of Vaska's complex and 2 equivalents of TMDS in THF at room temperature, complete consumption was achieved within 30 mins, presumably forming the desired O-silylated hemiaminal intermediate. Then, NIITP (2 equivalents) and benzoic acid (2 equivalents) were added into the reaction mixture and the reaction was allowed to stir overnight. After this time, we were delighted to find that the desired α -amino 1,3,4-oxadiazole (**3**) could be isolated *via* FCC in a 78% yield (scheme 2.13, entry 1). However, a mono-substituted 1,3,4-oxadiazole side-product (**4**) presumably formed from the excesses of NIITP and benzoic acid present in the reaction mixture was observed in significant quantities and complicated isolation of **3**. The formation of **4** was eliminated by reducing the amounts of both NIITP and benzoic acid to 1.1 equivalents and the reaction time after NIITP and benzoic acid addition to 1 hour. These changes allowed for isolation of **3** in a 87% isolated yield (entry 2), without significant formation of side-product **4** being observed. A small solvent screen revealed THF to be optimal for this transformation, with dichloromethane (entry 3) and toluene (entry 4) – solvents regularly used for reductive amide functionalizations – giving lower yields of the desired product **3**. The optimal conditions, and standard conditions used for the reaction scope are shown in scheme 2.13.B.

A | reaction optimization



entry	solvent	x (eq)	y (eq)	time (h)	3 (%) ^a
1	THF	2	2	16	(78)
2	THF	1.1	1.1	1	96 (87)
3	CH_2Cl_2	1.1	1.1	1	72
4	PhMe	1.1	1.1	1	76

B | standard conditions for reaction scope



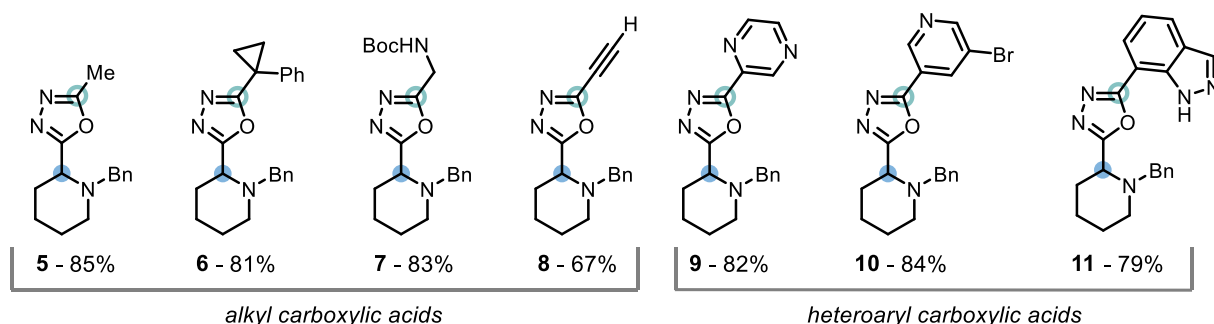
Scheme 2.13: A) Optimization of the reductive synthesis of α -amino 1,3,4-oxadiazole **3**. General conditions: **1** (0.2 mmol), $\text{IrCl}(\text{CO})(\text{PPh}_3)_2$ (0.5 mol%), 1,1,3,3-tetramethyldisiloxane (2 eq), solvent (1 mL), 30 mins; then NIITP (x eq), BzOH (y eq), solvent (2 mL). ^a NMR yield using 1,3,5-trimethoxybenzene as internal standard, isolated yields in parentheses. B)

Standard conditions used for the reaction scope.

2.5 Reaction Scope

2.5.1 Carboxylic Acid Scope

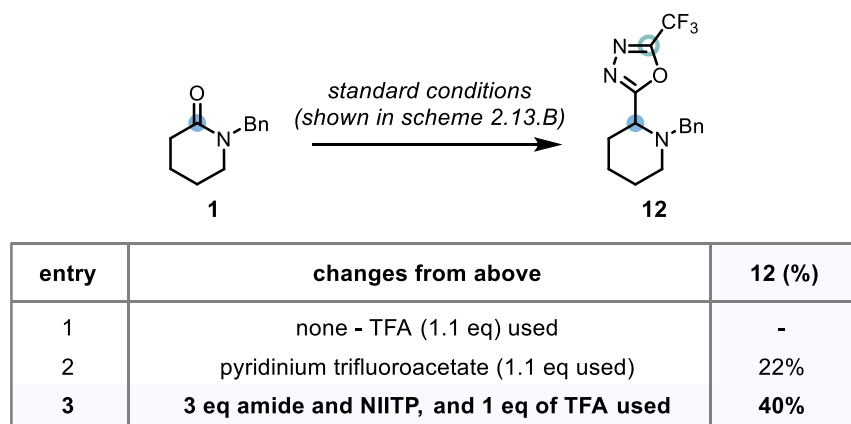
With optimal conditions established we first looked to investigate the reaction scope with respect to the carboxylic acid component. As we hoped to broaden the range of acids beyond the simple aromatic acids typically tolerated in reactions using NIITP we started our investigation using a range of alkyl and heteroaryl carboxylic acids (scheme 2.14). We were pleased to find that acetic acid (**5**) and 1-phenyl-1-cyclopropanecarboxylic acid (**6**) gave excellent yields of the desired α -amino 1,3,4-oxadiazoles. The functionalized alkyl carboxylic acids *N*-Boc glycine (**7**) and propiolic acid (**8**) additionally gave products with either a protected amine (**7**) or an alkyne (**8**) poised for further derivatization, in good yields. When exploring the tolerance of this methodology to Lewis-basic functionalities, three heteroaryl carboxylic acids were employed and readily gave the products **9** – **11** in 79% – 82% yield.



Scheme 2.14: Reaction scope of alkyl and heteroaryl carboxylic acids.

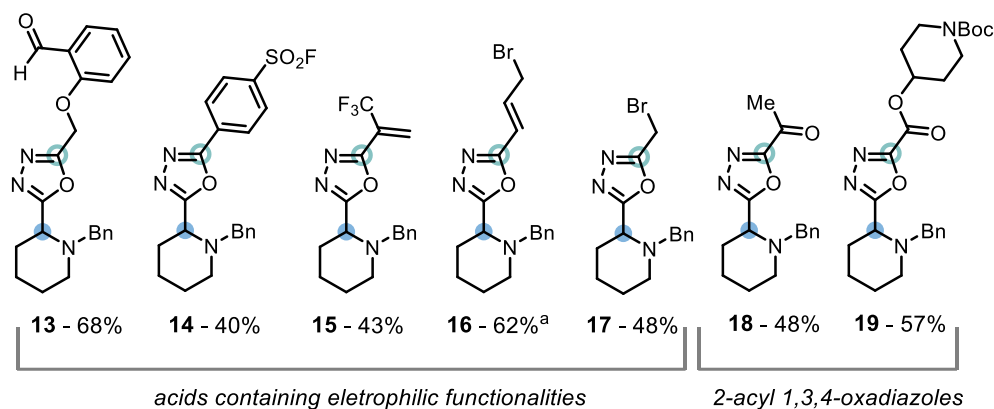
Continuing the investigation into the scope of carboxylic acids, the synthesis of trifluoromethyl 1,3,4-oxadiazole **12** was targeted (scheme 2.15). Unfortunately, use of TFA as the carboxylic acid component under our standard conditions gave no formation of α -amino 1,3,4-oxadiazole **12** (scheme 2.15, entry 1). Hypothesizing that the increased acidity of TFA, compared to other alkyl carboxylic acids, was unfavourable for the reaction its pyridinium salt was used and pleasingly led to the desired product (**12**) being isolated in 22% yield (entry 2). Further work

revealed that using an excess of both *N*-benzyl lactam (**1**) and NIITP and only 1 equivalent of TFA afforded the product (**12**) in a modest 40% isolated yield (entry 3).



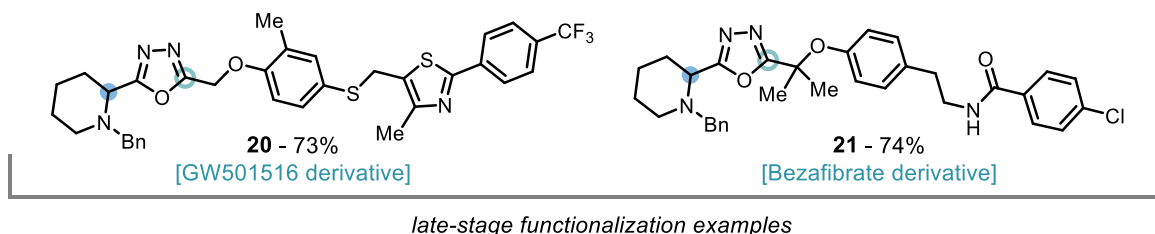
Scheme 2.15: Investigation into the synthesis of trifluoromethyl 1,3,4-oxadiazole **12**.

Next, the tolerance of the reaction with respect to electrophilic functionalities was explored, as these would provide handles for further functionalization and would be difficult to synthesize by the existing direct approaches using nucleophilic secondary amines as starting materials (scheme 2.16). Under the standard conditions carboxylic acids containing aldehydes (**13**), sulfonyl fluorides (**14**), trifluoromethyl alkenes (**15**), allylic bromides (**16**), and alkyl bromides (**17**) were all tolerated giving the α -amino 1,3,4-oxadiazole products **13** – **17** in good yields. Additionally, pyruvic acid (**18**) and an oxalic acid half ester (**19**) could be successfully reacted to provide 1,3,4-oxadiazoles containing useful carbonyl functionalities.



Scheme 2.16: Reaction scope of carboxylic acids containing electrophilic functionalities, and synthesis of 2-acyl 1,3,4-oxadiazoles. ^a 2 eq of acid used.

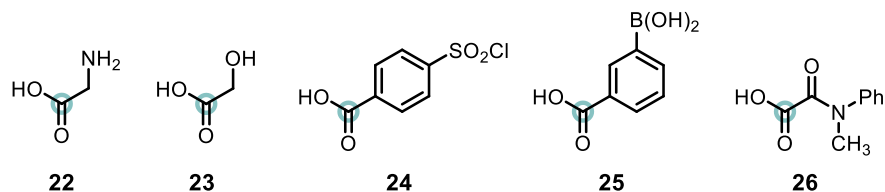
The potential for the method to be applied in drug discovery programs was demonstrated by the successful late-stage functionalization of two carboxylic acid containing APIs GW501516 (**20**) and bezafibrate (**21**) in 73% and 74% yield respectively (scheme 2.17).



Scheme 2.17: Examples of the late-stage functionalization of carboxylic acid containing APIs.

Although the method was tolerant of many different functional groups some carboxylic acids could not be tolerated and gave no yield of the desired α -amino 1,3,4-oxadiazole (scheme 2.18). The first two of these compounds glycine (**22**) and glycolic acid (**23**) contain unprotected heteroatoms which are likely the cause of their failed reactions. A reaction involving 4-(chlorosulfonyl)benzoic acid (**24**) led to product formation being observed in the crude reaction mixture, however the instability of the sulfonyl chloride group meant that the desired product underwent decomposition upon isolation necessitating a switch to the more stable sulfonyl fluoride (as in compound **14**). When employed under the standard reaction conditions, *m*-

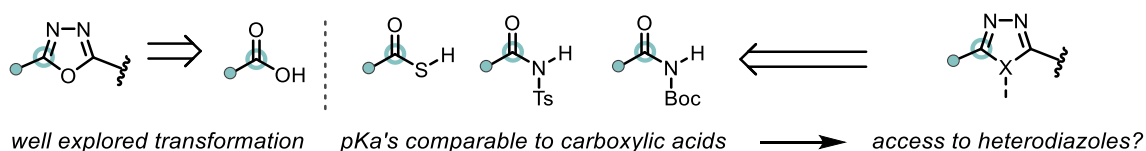
carboxyphenylboronic acid (**25**) and oxalic acid half amide (**26**) gave no observable product formation in the crude reaction mixture.



Scheme 2.18: Failed carboxylic acid substrates.

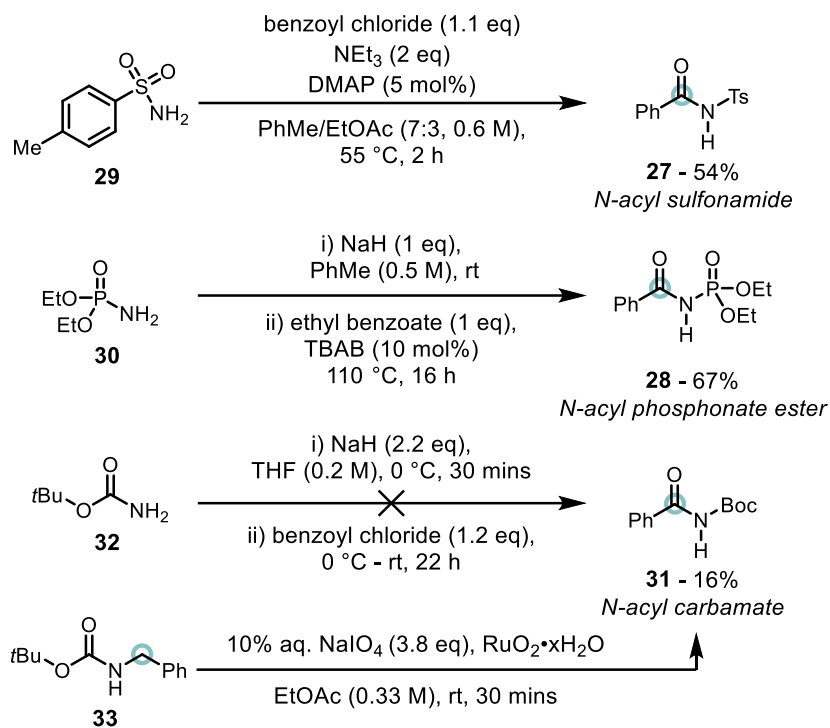
2.5.2 Extension to α -Amino Heterodiazole Synthesis

Having established a broad scope of reactivity with respect to carboxylic acids the possibility for the synthesis of α -amino heterodiazoles in the methodology was next investigated. Literature reports of heterodiazole synthesis using NIITP were limited but we hypothesized this could be achieved by exchanging the carboxylic acid reaction component for a *S*-, or *N*-substituted carbonyl derivative of comparable Brønsted acidity (scheme 2.19).^{268, 326, 327}



Scheme 2.19: Potential access to heterodiazoles from *S*-, and *N*-Brønsted acids.

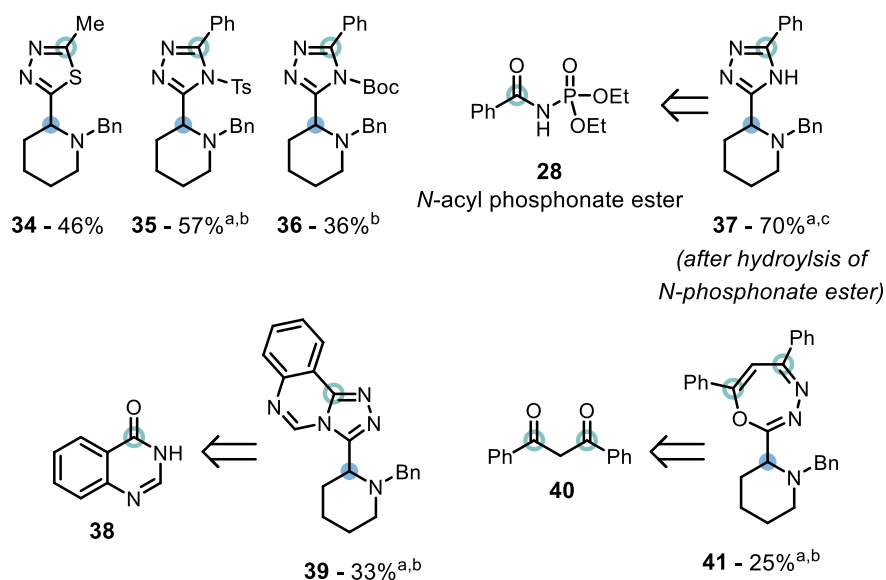
Thioacids, *N*-acyl sulfonamides, *N*-acyl carbamates, and *N*-acyl phosphonate esters suggested themselves as suitable candidates for investigation of α -amino heterodiazole synthesis. Simple thioacids such as thioacetic acid are commercially available, however the *N*-acyl Brønsted acids **27** and **28** were not but were readily synthesized by acylation of the corresponding primary sulfonamide (**29**), and phosphoramidate (**30**) (scheme 2.20). Although *N*-acyl carbamate **31** was not available through direct acylation of *tert*-butyl carbamate (**32**), its synthesis was achieved, albeit in low yields, by oxidation of *N*-Boc benzylamine (**33**) as reported by Yoshifuji.³²⁸



Scheme 2.20: Synthesis of *N*-Brønsted acids **27**, **28**, and **31**.

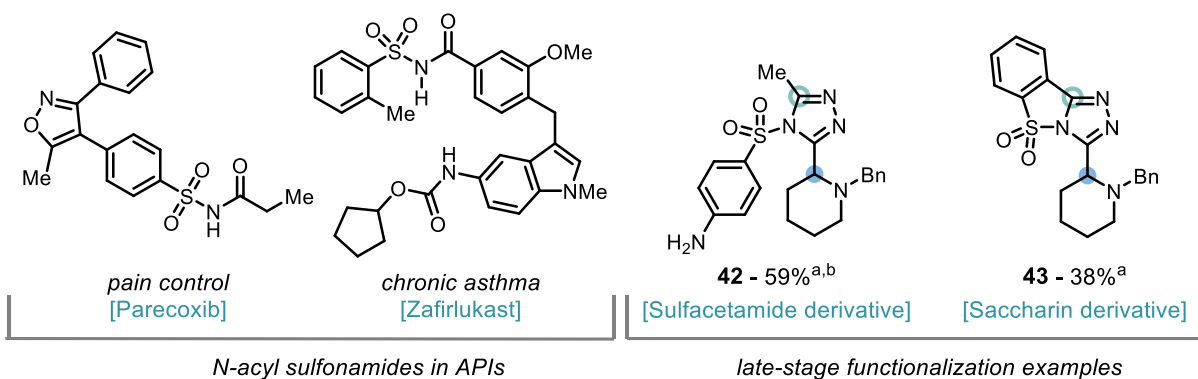
Starting with thioacetic acid we were pleased to find the desired α -amino 1,3,4-thiadiazole (**34**) could be isolated in moderate yield, providing a single-atom modification of the parent 1,3,4-oxadiazole (**5**) (scheme 2.21).²⁶⁸ Following this, use of a *N*-acyl sulfonamide (**27**) and a *N*-acyl carbamate (**31**) successfully afforded α -amino 1,2,4-triazoles **35** and **36**, representing the first application of these protected amides as *N*-Brønsted acids for α -amino 1,2,4-triazole synthesis using NIITP. When *N*-acyl phosphonate ester **28** was used as an *N*-Brønsted acid we noticed that partial hydrolysis of the product to the α -amino *N*-H 1,2,4-triazole **37** had occurred. Exploiting this discovery, the addition of lithium hydroxide to the reaction mixture after completion of the 1,2,4-triazole forming step gave full *N*-phosphonate ester hydrolysis after 1 hour and an excellent isolated yield of the α -amino *N*-H triazole **37** in a one-pot procedure. Furthermore, use of 4-hydroxyquinazoline (**38**) as a *N*-Brønsted acid afforded an α -amino [1,2,4]triazolo[4,3-*c*]quinazoline (**39**) in 33 % yield.³²⁷ Finally, based on work from Ramazani,

we utilized 1,3-diphenyl-1,3-propanedione (**40**) as a carbon-based Brønsted acid to yield an unusual α -amino 1,3,4-oxadiazepine scaffold (**41**).³²⁶



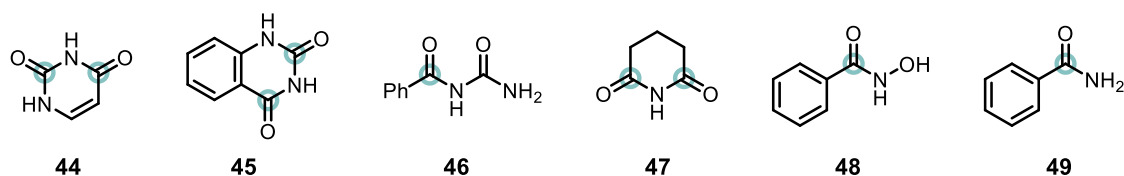
Scheme 2.21: Scope of α -amino heterodiazoles. ^a 2 eq acid and NIITP used, and 2nd step stirred for 16 h. ^b 1 mol% IrCl(CO)(PPh₃)₂ used. ^c 0.1 mmol scale, after reaction completion LiOH (25.2 mg, 0.6 mmol, 6 eq) was added to the reaction mixture and stirred for 1 h.

N-Acyl sulfonamides are becoming increasingly common in medicinal chemistry, as carboxylic acid bioisosteres, and are components of APIs such as parecoxib, zafirlukast, and sulfacetamide (scheme 2.22).³²⁹ Consequently, the developed methodology was applied for the late-stage functionalization of sulfacetamide (**42**) and saccharin (**43**), giving novel α -amino 1,2,4-triazoles **42** and **43** in 59% and 38% yield respectively. To the best of our knowledge these results represent the first use of this valuable, and desirable, functional group for late-stage functionalization.



Scheme 2.22: Examples of the late-stage functionalization of *N*-acyl sulfonamides. ^a 2 eq acid and NIITP used, and 2nd step stirred for 16 h. ^b 1 mol% IrCl(CO)(PPh₃)₂ used.

Although success was found using the above *C*-, *S*-, and *N*-Brønsted acids as carboxylic acid replacements, we found that other potential replacements such as; pyrimidinedione (**44**), quinazolidinedione (**45**), benzoyl urea (**46**), glutarimide (**47**), *N*-hydroxy benzamide (**48**) all gave complex reaction mixtures from which no desired α -amino 1,2,4-triazole products were identified or isolated (scheme 2.23). Furthermore, although benzamide (**49**) has been successfully used by Yu for *N*-H 1,2,4-triazole synthesis with NIITP (schemes 1.47, bottom),²⁶⁸ it was found to be unproductive under the standard reaction conditions (scheme 2.23).



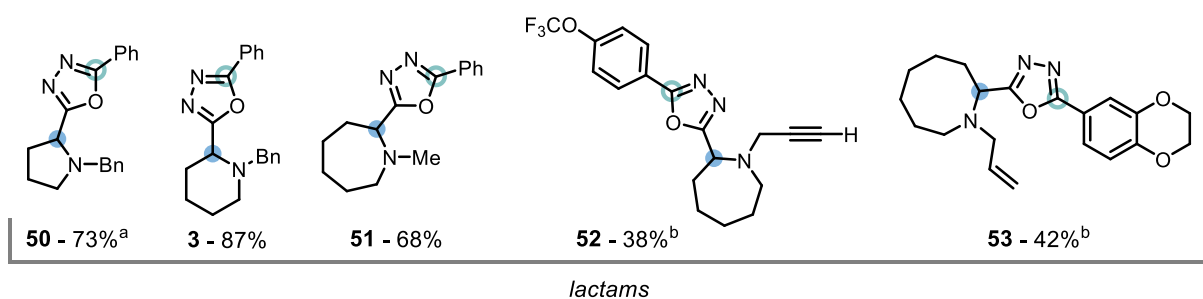
Scheme 2.23: Failed α -amino 1,2,4-triazole precursors.

2.5.3 Amide and Lactam Scope

With the reaction scopes of both carboxylic acids, and alternative *C*-, *S*-, and *N*-Brønsted acids scrutinized, next explored was the reaction scope with respect to the amide, or lactam, component. To fully exemplify the flexibility of the methodology the carboxylic acid was

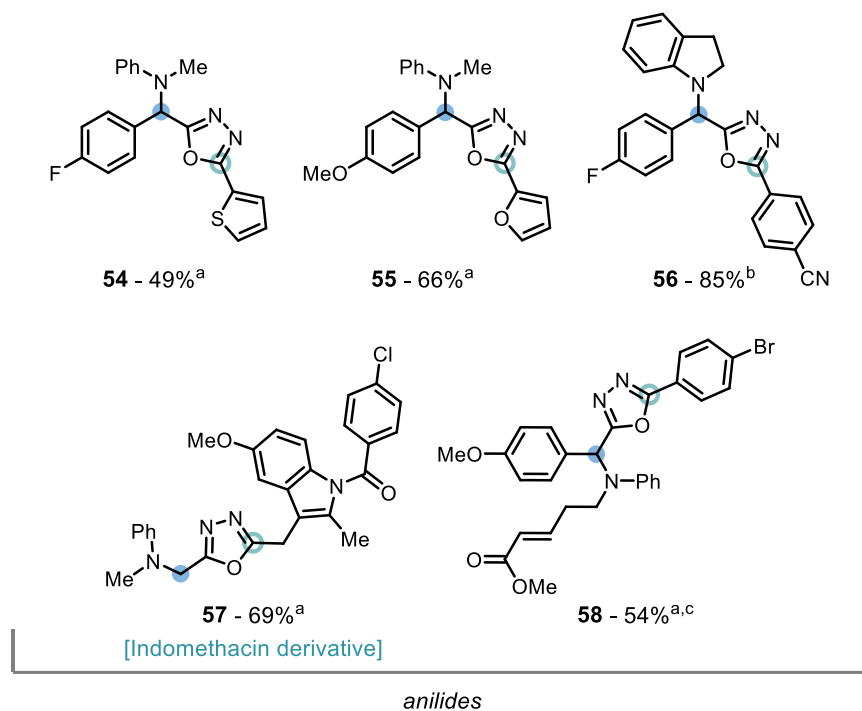
changed throughout the amide scope to maximize the diversity of the α -amino 1,3,4-oxadiazole structures generated.

Starting with lactams we discovered that lactams of ring sizes 5 – 8 (**3**, **50** – **53**) were all well-tolerated, with functional groups such as terminal alkynes (**52**) and alkenes (**53**) being untouched by the mild amide reductive activation supplied by Vaska's complex and TMSD (scheme 2.24). Notably, synthesis of **50** (from 1-benzylpyrrolidin-2-one) required use of 3 equivalents of carboxylic acid and NIITP, and an elongated reaction time. This was due to a propensity to form an enamine which was the only product identified in the crude ^1H NMR when the standard reaction conditions were employed.



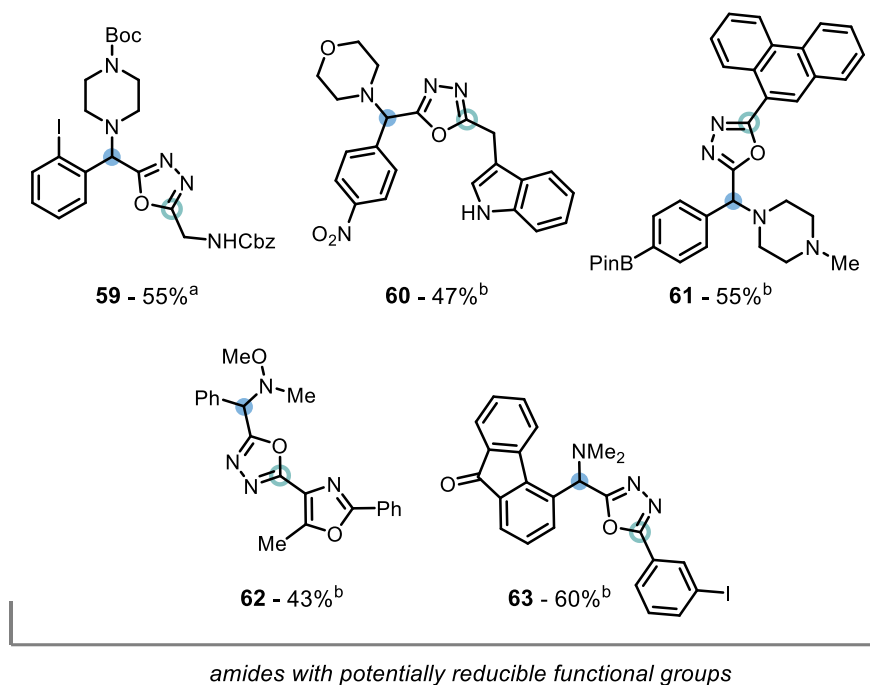
Scheme 2.24: Scope of lactams with ring sizes from 5 – 8. ^a 3 eq acid and NIITP used, and 2nd step stirred for 16 h. ^b 1 mol% $\text{IrCl}(\text{CO})(\text{PPh}_3)_2$ used.

Simple anilides (**54** – **56**) were next investigated for their reactivity, and we found that while they reacted productively affording products **54** – **56** in 49% – 85% yield, higher loadings of Vaska's complex (up to 5 mol%) were required for the reductive activation step to reach completion within 30 mins (scheme 2.25). We can attribute this to the lower Lewis-basicity of anilides when compared to *N,N*-dialkyl tertiary amides.³³⁰⁻³³² *N*-Methylformanilide was successfully coupled with API indomethacin to afford the complex α -amino 1,3,4-oxadiazole **57** in 69% yield, and an anilide containing an α,β -unsaturated ester could be chemoselectively activated at the amide carbonyl to afford **58** in good yield.



Scheme 2.25: Scope of anilides. ^a 5 mol% $\text{IrCl}(\text{CO})(\text{PPh}_3)_2$ used. ^b 1st step using 3 mol% $\text{IrCl}(\text{CO})(\text{PPh}_3)_2$ in PhMe . ^c 0.1 mmol scale.

One key advantage of the Vaska's complex and TMS system for the reductive activation of tertiary amides is the high chemoselectivity observed in the presence of other potentially reducible functional groups.²⁹¹ This attribute was demonstrated with tertiary amides containing aryl iodides and carbamates (**59**), nitro groups (**60**), boronic esters (**61**), *N*-O bonds (**62**), and ketones (**63**) all generating the desired α -amino 1,3,4-oxadiazoles **59** – **63** without any concomitant reduction of these sensitive, and synthetically useful, functionalities observed (scheme 2.26).

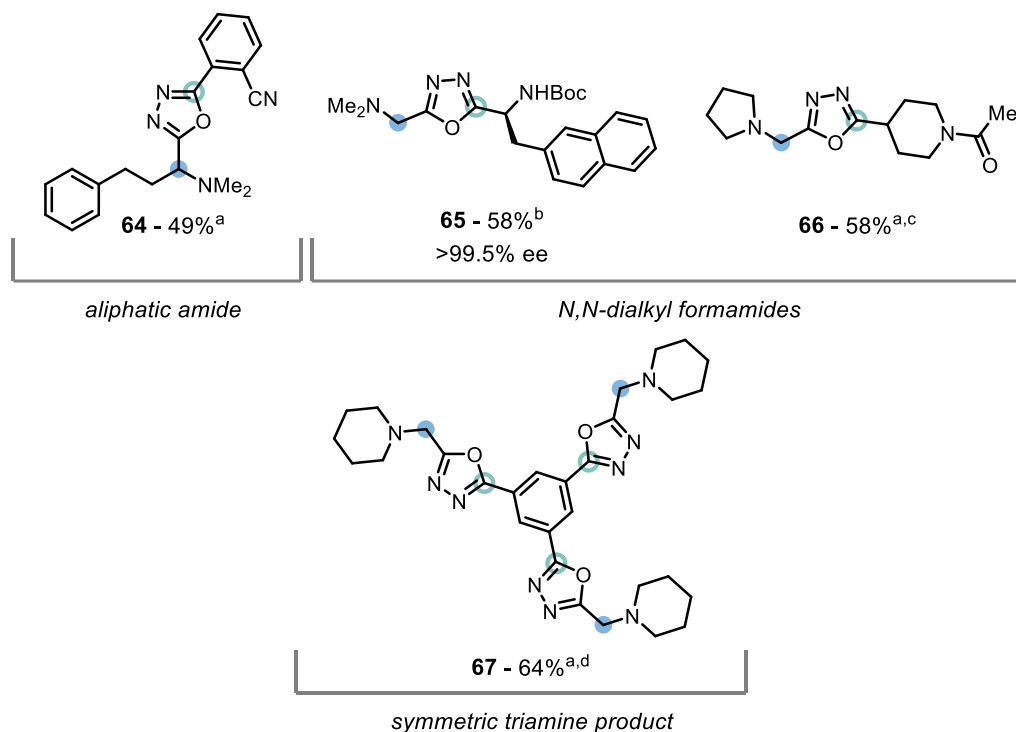


Scheme 2.26: Scope of amides with potentially reducible functional groups. ^a 5 mol%

*IrCl(CO)(PPh₃)₂ used. ^b 1 mol% *IrCl(CO)(PPh₃)₂ used.**

Next, an aliphatic amide was successfully reacted giving the α -amino 1,3,4-oxadiazole **64** in 49% yield (scheme 2.27). This, along with synthesis of **50**, shows that, if formed, enamine intermediates are likely turned into their electrophilic iminium ion counterparts by the slight excess of carboxylic acid employed in the reaction. The commercially available formamides, *N,N*-dimethyl formamide and 1-formylpyrrolidine were next subjected to the standard reaction conditions affording methylene bridged α -amino 1,3,4-oxadiazoles structures **65** and **66**, both in 58% yield. Furthermore, the use of a single enantiomer α -amino acid when synthesizing **65** gave the final compound in enantiopure form. This shows that any racemization of the α -amino acid stereocenter is negligible under the standard conditions. The successful synthesis of **66**, which contains a tertiary amide, suggests that when NIITP and a carboxylic acid are added to the reaction mixture the activity of Vaska's for amide hydrosilylation is passivated. Subsequently, the symmetric triamine **67** was synthesized in 64% yield, utilizing an excess 1-

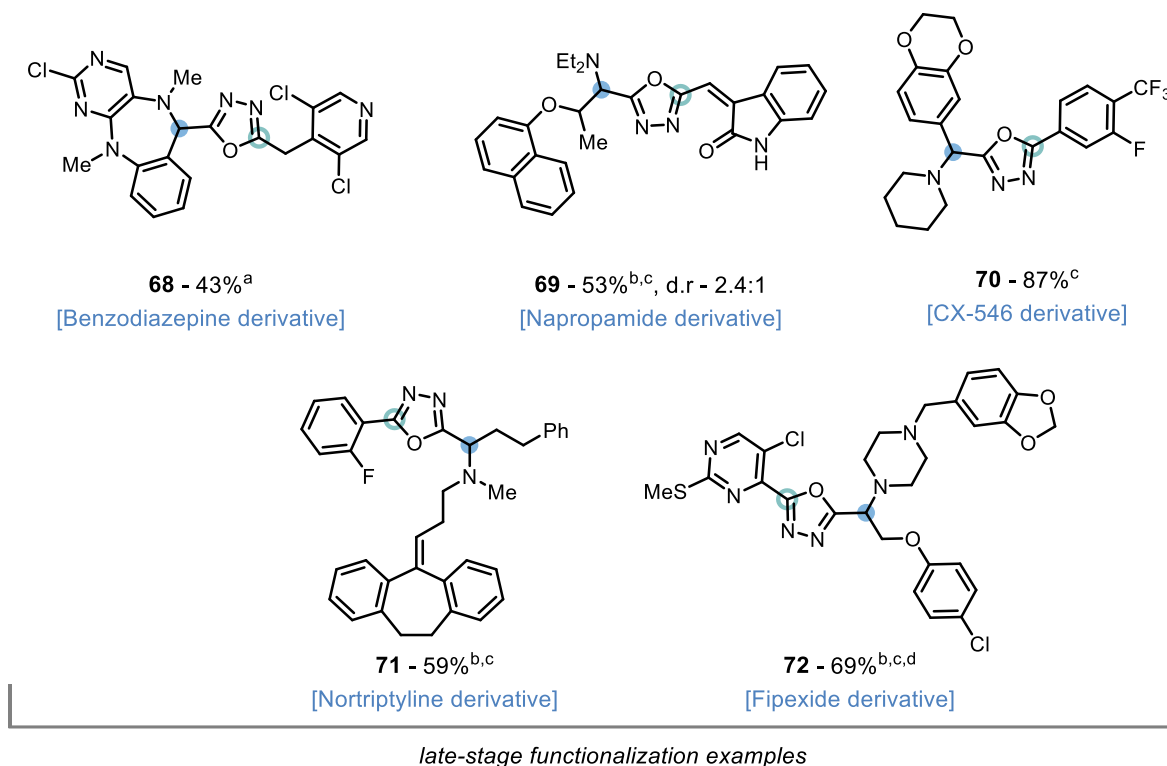
formylpiperidine and NIITP, with 1,3,5-benzenetricarboxylic acid as the limiting reagent, highlighting the robustness of the established methodology.



Scheme 2.27: Scope of aliphatic amides, *N,N*-dialkyl formamides, and synthesis of a symmetric triamine. ^a 1 mol% $\text{IrCl}(\text{CO})(\text{PPh}_3)_2$ used. ^b ee of **65** determined by HPLC analysis. ^c 2 mmol scale. ^d 6 eq of amide and NIITP, and 1 eq of carboxylic acid used, see section 5.2.3 for full experimental details.

The scope of amides was concluded with the application of drug-like molecules, and APIs, containing tertiary amides to our methodology (scheme 2.28). These included a benzodiazepine scaffold (**68**), the herbicide napropamide (**69**), the experimental drug CX-546 (**70**), a derivative of nortriptyline (**71**), and the psychoactive drug fipexide (**72**), which together gave yields of the desired α -amino 1,3,4-oxadiazoles **68** – **72** ranging from 43% - 87%. The success of these examples serves to demonstrate the exquisite chemoselectivity of Vaska's

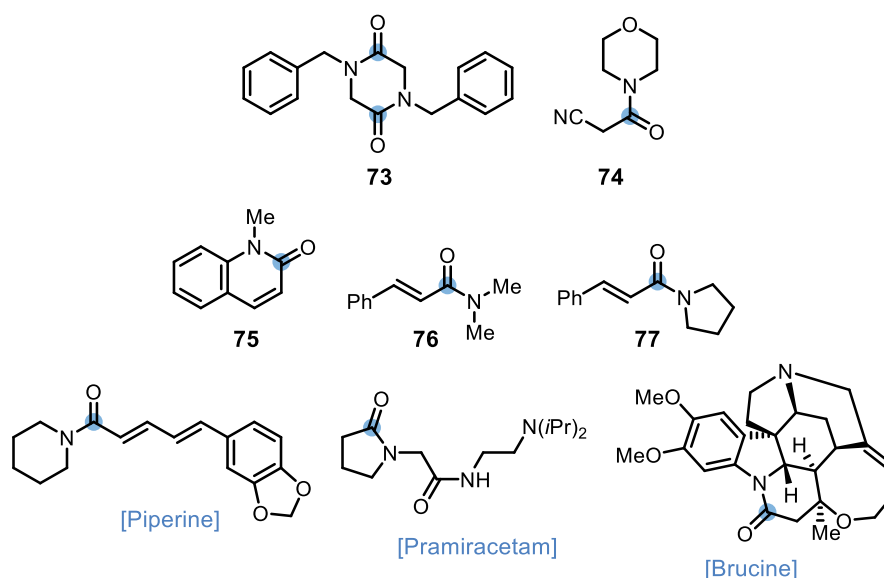
complex and TMDS and why it has become the catalyst system of choice for the reductive functionalization of tertiary amides and lactams.



Scheme 2.28: Examples of the late-stage functionalization of amide containing APIs, and drug-like molecules. ^a 0.07 mmol scale, 5 mol% $\text{IrCl}(\text{CO})(\text{PPh}_3)_2$, and 2 eq of acid and NIITP used. ^b 2 eq of acid and NIITP used, and the 2nd step stirred for 16 h. ^c 1 mol% $\text{IrCl}(\text{CO})(\text{PPh}_3)_2$ used. ^d 0.19 mmol scale.

Although the developed methodology was tolerant of substrates containing many different functionalities, and structures, there were amides and lactams which failed to yield the desired α -amino 1,3,4-oxadiazole products (scheme 2.29). The examples in scheme 2.29 failed for a variety of reasons. For example, although it was apparent by crude ^1H NMR that diketopiperazine **73**, after reductive activation, underwent reaction with carboxylic acids and NIITP, it proved challenging to ascertain if the desired double-reductive activation, and subsequently double-1,3,4-oxadiazole formation, had occurred. Furthermore, all attempts to

isolate related α -amino 1,3,4-oxadiazole products were without merit. After subjecting amides **74** – **77** to our standard reaction conditions no product formation was observed by crude ^1H NMR analysis, with the major observed peaks for **74** – **77** relating to the over-reduced tertiary amine side-products. The failure of examples **75** – **77**, and additionally of the API piperine, highlights the incompatibility of the method with α,β -unsaturated amides as a major limitation, in contrast with the successful use of α,β -unsaturated amides in previous Vaska's complex catalyzed reductive amide functionalization methodologies.^{299, 300} Unfortunately, the reductive functionalization of pramiracetam proved unprofitable as even using 5 mol% of Vaska's did not induce pramiracetam to form the critical *O*-silylated hemiaminal intermediate. Furthermore, the reductive functionalization of brucine was fruitless after multiple attempts, in contrast to a previous report from our group on the reductive cyanation of tertiary amides.²⁹⁹

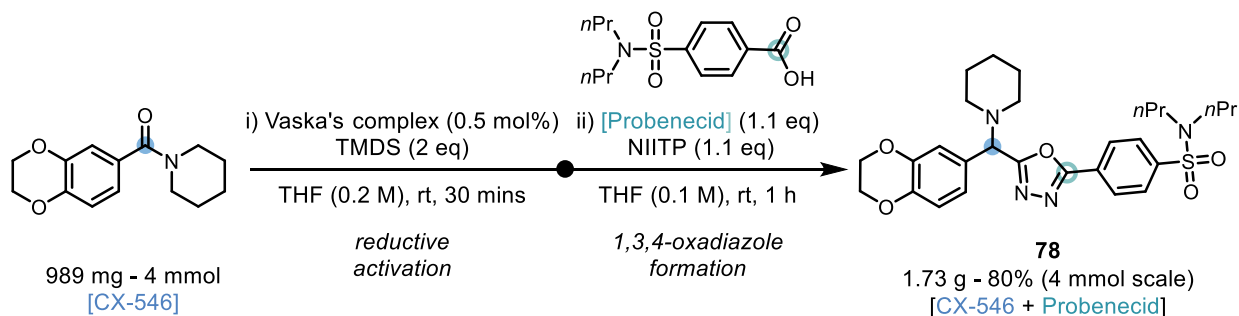


Scheme 2.29: Failed amide and lactam substrates.

2.6 Scale-up and Product Derivatization

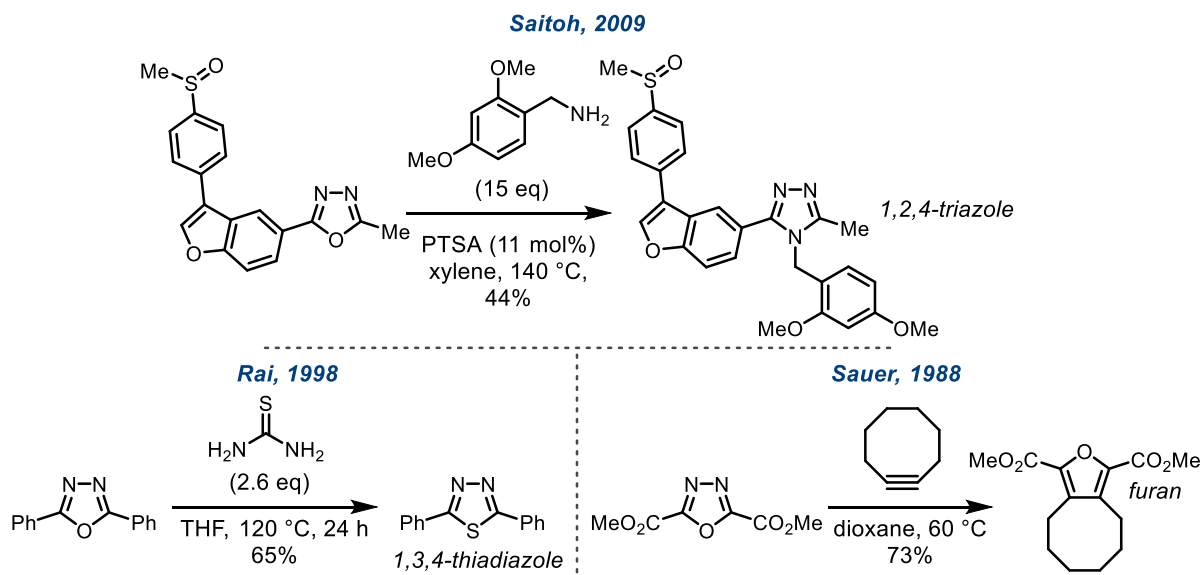
To further demonstrate the utility of this newly developed method, a gram-scale example was performed using two API coupling partners – the amide containing experimental drug CX-546

and the carboxylic acid containing API probenecid – to synthesise the 1,3,4-oxadiazole-fused drug-drug conjugate **78** (scheme 2.30). Proceeding smoothly, this afforded 1.73 g of the 1,3,4-oxadiazole-fused drug-drug conjugate **78** without needing any adjustments of the standard reaction conditions (scheme 2.13.B).



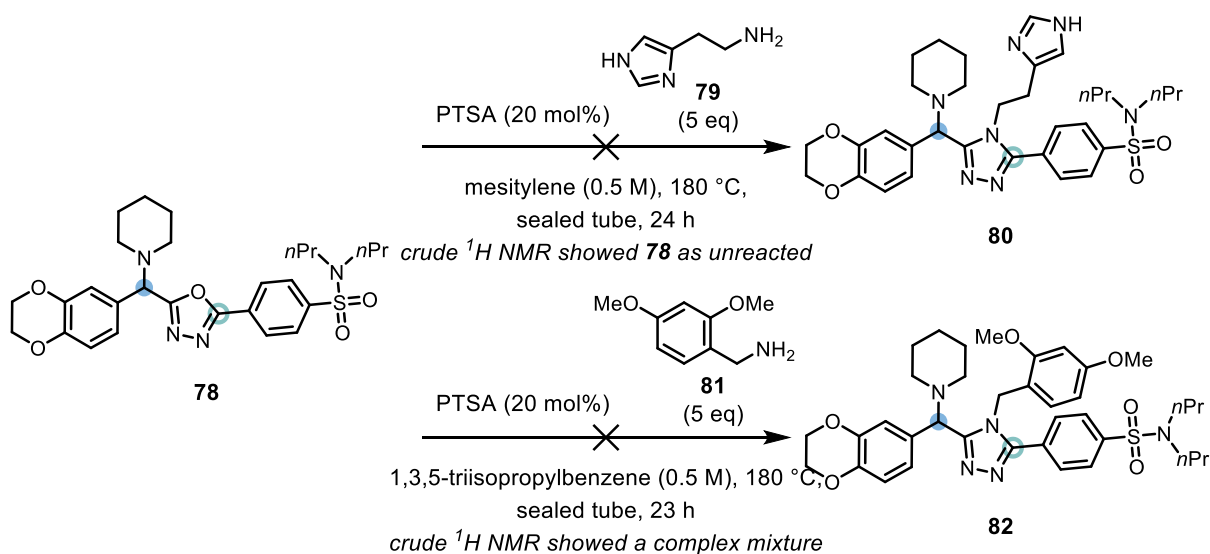
Scheme 2.30: Gram scale synthesis of the 1,3,4-oxadiazole-fused drug-drug conjugate **78**.

With plentiful quantities of **78** in hand derivatization of the 1,3,4-oxadiazole moiety into a 1,2,4-triazole (scheme 2.31, top),³³³ 1,3,4-thiadiazole (scheme 2.31, bottom left),³³⁴ or furan (scheme 2.31, bottom right),³³⁵ as precedented in the literature, was examined.



Scheme 2.31: Literature precedent for transformation of a 1,3,4-oxadiazole into a 1,2,4-triazole, 1,3,4-thiadiazole, or furan.

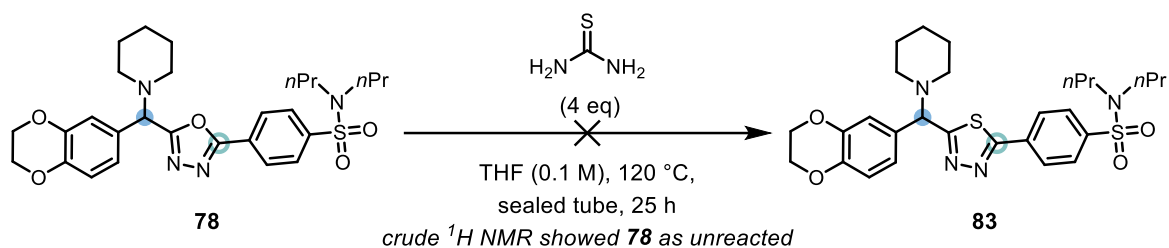
Starting with 1,2,4-triazole synthesis, the incorporation of a drug-like amine into **78**, generating a tri-drug conjugate, was targeted. For this, we chose histamine (**79**) due to its structure containing a sterically unhindered primary amine. Unfortunately, when **78** was reacted with a large excess of histamine in the presence of PTSA as a catalyst none of the desired 1,2,4-triazole **80** could be observed by crude ^1H NMR (scheme 2.32). Exchanging histamine for 2,4-dimethoxybenzylamine (**81**), in line with precedent from Saitoh,³³³ and mesitylene for 1,3,5-triisopropylbenzene in favour of its higher boiling point (232 °C vs. 165 °C) to prevent concentration of the reaction mixture at the high temperature employed was next investigated. Similarly, the attempted substitution failed and ^1H NMR analysis of the crude reaction mixture showed a complex mixture from which no product (**82**) or remaining starting material (**78**) could be identified.



Scheme 2.32: Exploration of the synthesis of 1,2,4-triazoles **80**, and **81**, from 1,3,4-oxadiazole **78**.

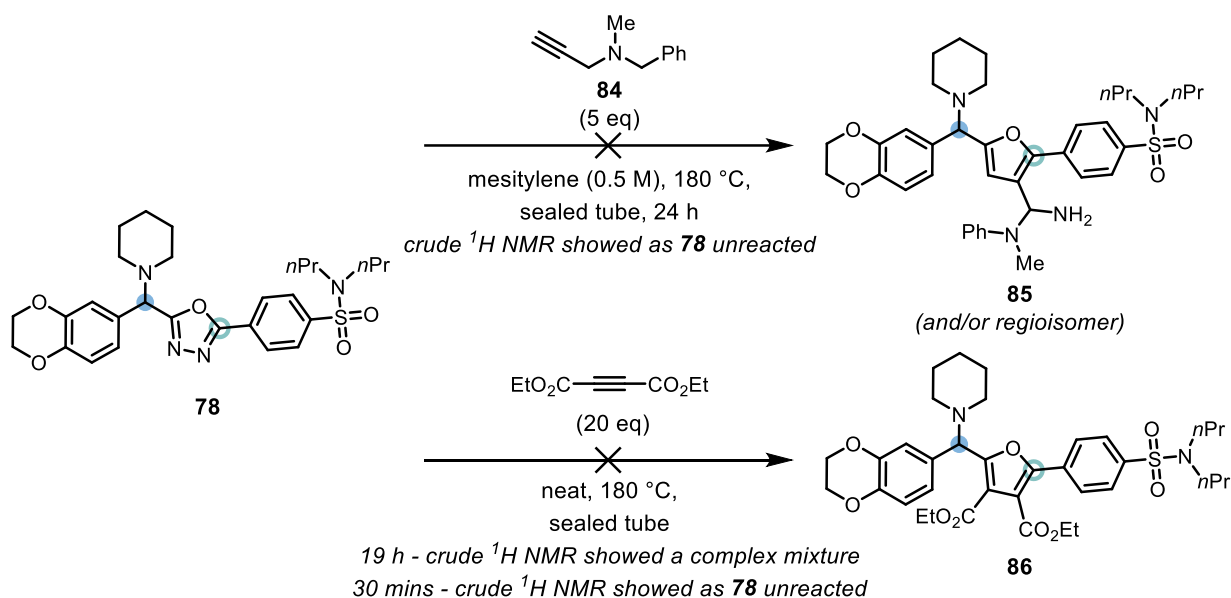
Due to the failure of the above reactions, next examined was the synthesis of 1,3,4-thiadiazole **83** from the 1,3,4-oxadiazole **78** using thiourea as a nucleophilic source of sulfur. In agreement with the results in scheme 2.32 we found **78** resistant to nucleophilic addition and no reaction

between **78** and thiourea was realized even at the elevated temperatures reported for the reaction (scheme 2.33).³³⁴ We believe that the disappointing reactivity observed between **78** and primary amine, and thiourea, nucleophiles is likely due to either the hindered nature of the 1,3,4-oxadiazole in **78** preventing nucleophilic addition, or the favoured regeneration of **78** from collapse of the tetrahedral intermediate generated after an initial nucleophile addition into the 1,3,4-oxadiazole C=N bond rather than opening of the 1,3,4-oxadiazole ring as desired.



Scheme 2.33: Failed synthesis of 1,3,4-thiadiazole **83** from 1,3,4-oxadiazole **78**.

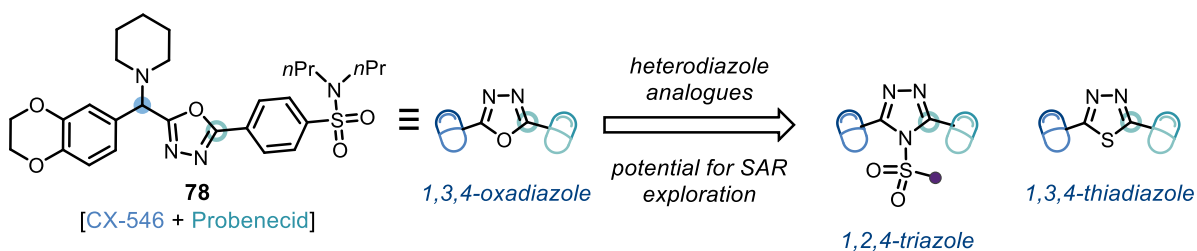
An exploration of furan synthesis from **78** by reaction with both an electron-rich alkyne (paryline, **84**), and the electron-poor diethyl acetylenedicarboxylate proved unfruitful, even with large excesses of reagents and high reaction temperatures (scheme 2.34). This suggests that to perform the [4+2], retro-[4+2] cycloaddition sequence required for furan formation from a 1,3,4-oxadiazole, and an alkyne, activation of the 1,3,4-oxadiazole with electron-withdrawing groups, as in scheme 2.31, is essential. Alternatively, work by the Boger group has shown that an intramolecular reaction between a tethered alkyne and a 1,3,4-oxadiazole is favourable.³³⁶



Scheme 2.34: Attempted investigation into synthesis of furans **85** and **86** by [4+2], retro-[4+2] cycloadditions of alkynes with 1,3,4-oxadiazole **78**.

2.7 Synthesis of Heterodiazole-Fused Drug-Drug Conjugates

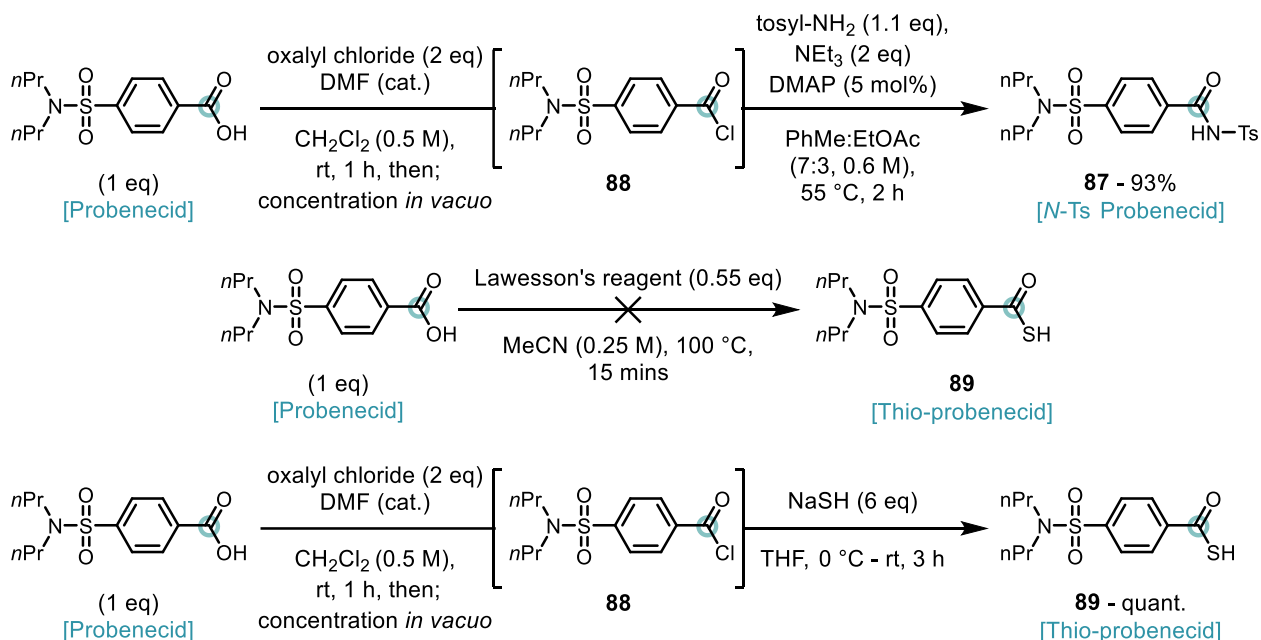
As a result of the successful synthesis of α -amino heterodiazoles (section 2.5.2), and of 1,3,4-oxadiazole-fused drug-drug conjugate **78** (scheme 2.30), the method was applied to show the possible investigation of heterodiazole structure-activity relationships (SAR) using **78** as the scaffold molecule (scheme 2.35).



Scheme 2.35: Potential for SAR exploration by synthesis of α -amino heterodiazole analogues.

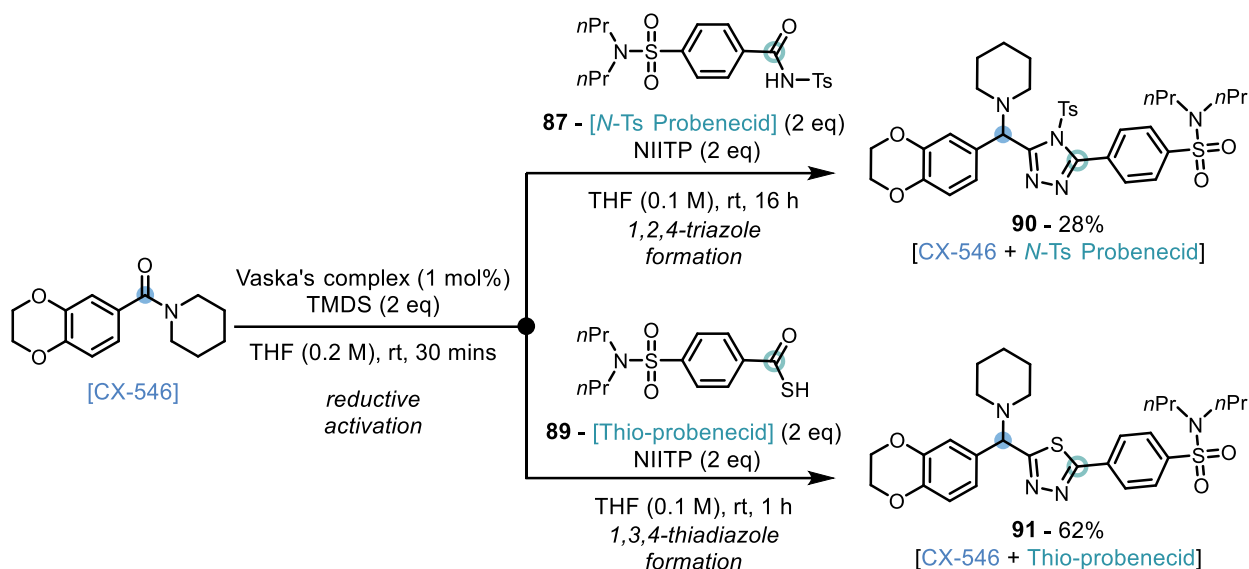
The synthesis of heterodiazole analogues of **78** firstly required the synthesis of an *N*-Brønsted acid and thioacid analogue of the chosen carboxylic acid API probenecid (scheme 2.36).

Synthesis of its *N*-Ts analogue **87** was readily achieved in 93% yield using a two-step one-pot approach where firstly probenecid was transformed into acyl chloride **88** and secondly aminated using *p*-toluenesulfonamide. Next, the use of Lawesson's reagent for the conversion of a carboxylic acid to a thioacid as preceded by Danishefsky was first studied,³³⁸ however synthesis of thio-probenecid **89** failed yielding only recovered probenecid starting material in 64% after isolation. The desired transformation was later achieved by treatment of acyl chloride **88** with NaSH in THF which, after an acidic aqueous workup, afforded thio-probenecid **89** in quantitative yield and sufficient purity to use without further purification.



Scheme 2.36: Synthesis of *N*-Ts probenecid **87** and thio-probenecid **89**.

With *S*- and *N*-Brønsted acid analogues of probenecid in hand, they were then applied to the developed methodology for synthesis of 1,2,4-triazole (**90**), and 1,3,4-thiadiazole (**91**), analogues of **78** (scheme 2.37). These reactions proceeded smoothly affording the heterodiazole-fused drug-drug conjugates **90** and **91** in 28% and 62% yield respectively, demonstrating the successful synthesis of three distinct diazole heterocycles (**78**, **90**, and **91**) from the carboxylic acid API probenecid.



Scheme 2.37: Synthesis of heterodiazole-fused drug-drug conjugates **90** and **91**.

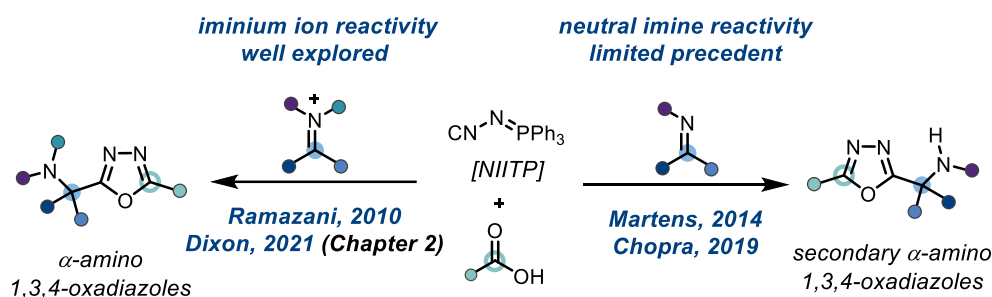
2.8 Conclusions

In conclusion a novel three-component coupling reaction for the synthesis of α -amino 1,3,4-oxadiazoles from tertiary amides and lactams, feedstock carboxylic acids, and *N*-isocyanoiminotriphenylphosphorane (NIITP) has been developed. This reaction takes advantage of the mild and chemoselective reductive activation of tertiary amides provided by the combination of Vaska's complex and TMDS, to provide chemically complex products structures as demonstrated by the late-stage functionalization of ten drug-like amides and carboxylic acids. Furthermore, the method was utilized for the synthesis of difficult to access α -amino heterodiazoles, from easily accessible *C*-, *S*-, and *N*-Brønsted acids, culminating in the synthesis of three heterodiazole-fused drug-drug conjugates from experimental drug CX-546 and API probenecid (and its thioacid and *N*-acyl sulfonamide analogues).

Chapter 3: Primary α -Amino 1,3,4-Oxadiazole Synthesis via an Ugi-Type Reaction of *N*-Carbamoyl Imines with NIITP³

3.1 Introduction – Project Concept

The reactivity of NIITP with iminium ions and neutral C=O electrophiles is well explored (sections 1.2.5.2 & 1.2.5.3);^{235, 339} however, at the start of this project the use of neutral C=N imines as electrophiles for 1,3,4-oxadiazole synthesis with NIITP had limited precedent, with key reports from Martens, and Chopra (schemes 1.46 & 3.1).^{265, 267}

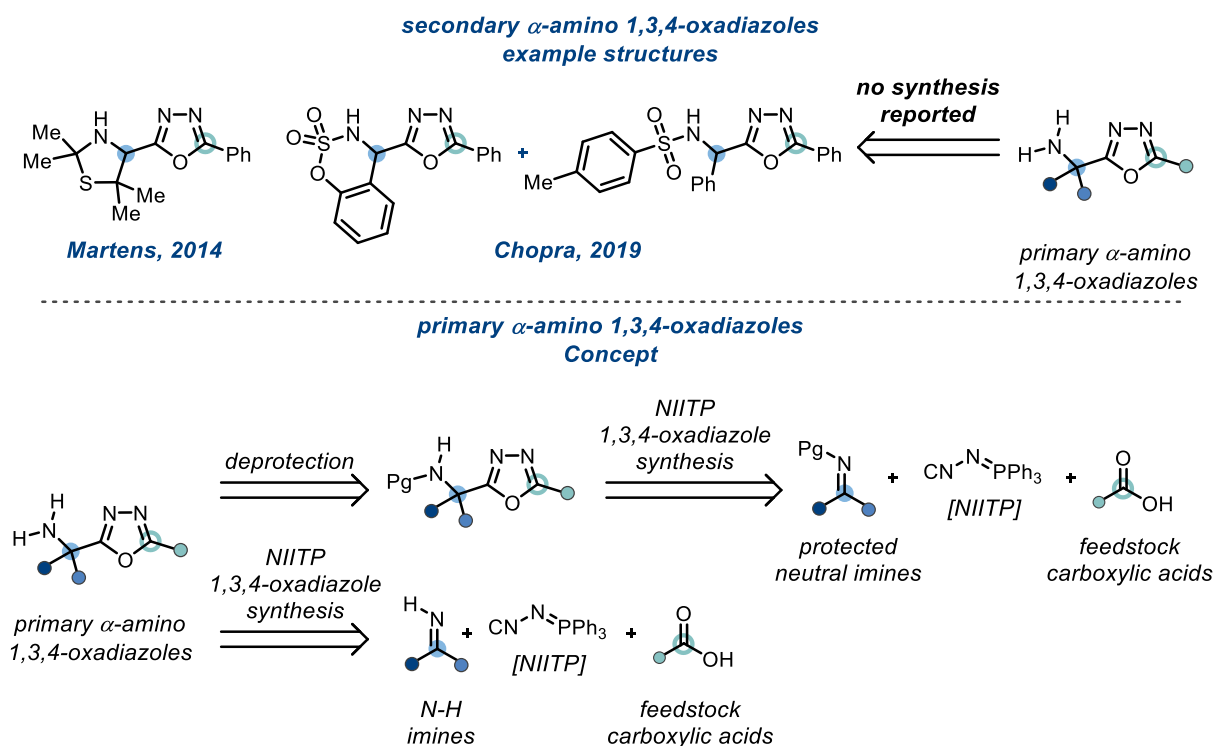


Scheme 3.1: Reactivity of NIITP with various C=N electrophiles.

Although Martens²⁶⁵ and Chopra²⁶⁷ had reported the use of 3-thiazolines, and sulfamidates and *N*-sulfonyl imines of aryl aldehydes, respectively, for 1,3,4-oxadiazole synthesis using NIITP, these reactions afforded only secondary α -amino 1,3,4-oxadiazoles (scheme 3.2, top). Additionally, only a limited reaction scope and no investigation into *N*-sulfonyl deprotection was reported by Chopra; as such, primary α -amino 1,3,4-oxadiazoles remained a class of compounds unexplored by these approaches. Therefore, an investigation into primary α -amino 1,3,4-oxadiazole synthesis would advance the known chemistry of NIITP into an unexplored area. Retrosynthetically, primary α -amino 1,3,4-oxadiazoles would be available from two types

³ The work disclosed in this chapter was performed in conjunction with Elizabeth Boulter, a Part II student, and Tatiana Rogova, a DPhil student, under the supervision of D.M.R. and all results have been included in this chapter for completeness.

of imine precursors (scheme 3.2, bottom): firstly, a suitably protected neutral imine, which would give the required primary amine after deprotection; and secondly, an *N*-H imine from which a 1,3,4-oxadiazole synthesis using NIITP would directly afford the primary amine product.



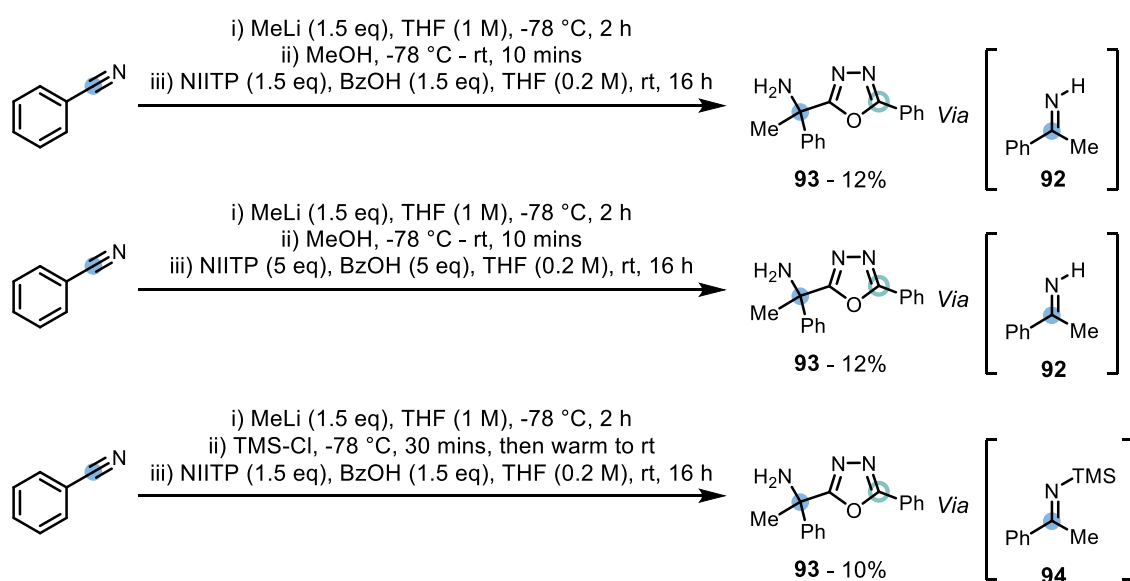
Scheme 3.2: Secondary α -amino 1,3,4-oxadiazole structures, and retrosynthetic analysis of a primary α -amino 1,3,4-oxadiazole synthesis.

3.2 Reaction Discovery

3.2.1 Investigation into the Reactivity of *N*-H Imines with NIITP

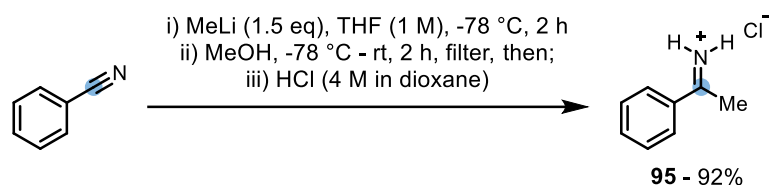
In the first instance, investigation of a one-pot synthesis of primary α -amino 1,3,4-oxadiazoles from *N*-H ketimines was targeted. These imines can be synthesized from readily available benzonitriles and organometallics, with a subsequent quench giving the desired imines *in situ* (scheme 3.3). Our first attempt at this three-step one-pot procedure started with addition of methyl lithium into benzonitrile with a subsequent MeOH quench to yield the *N*-H ketimine **92**. Finally, a 1,3,4-oxadiazole synthesis using NIITP and benzoic acid, pleasingly yielded the

primary α -amino 1,3,4-oxadiazole **93** in 12% yield (scheme 3.3, top). An increase in the equivalents of both benzoic acid and NIITP employed in the final step (to five equivalents each) failed to improve the yield of **93** (scheme 3.3, middle). Hypothesizing that the potentially nucleophilic lithium methoxide formed from the methanolic quench might be damaging to the 1,3,4-oxadiazole formation from *N*-H imine **92**, an alternative quench using trimethylsilyl chloride to generate *N*-TMS imine **94** and lithium chloride was examined. Unfortunately, this change provided no uplift in the yield of **93** formed (scheme 3.3, bottom).



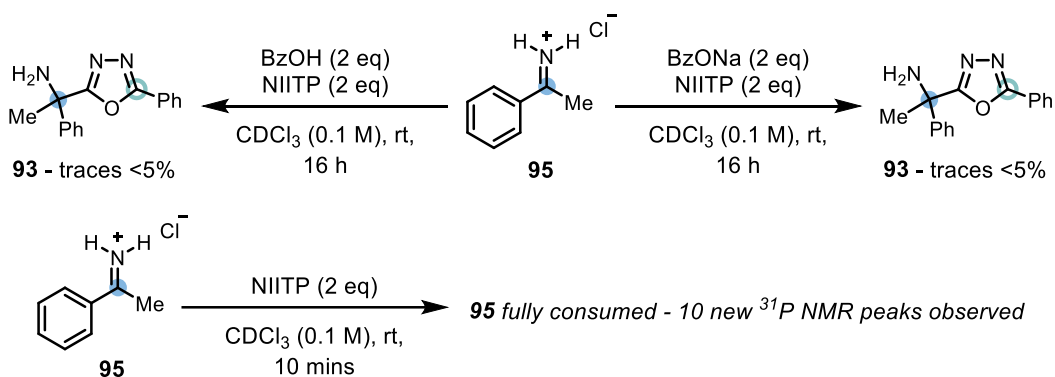
Scheme 3.3: Three-step, one-pot synthesis of primary α -amino 1,3,4-oxadiazole **93** from benzonitrile via ketimines **92** and **94**.

Due to the low yields of the one-pot procedure, and the difficult synthetic tractability for optimization presented by using a multi-stage process, we decided to isolate *N*-H ketimine hydrochloride salt **95** as a model substrate for further investigation. This was achieved in excellent yield by addition of methyl lithium into benzonitrile, followed by a MeOH quench as above, and finally precipitation of the hydrochloride salt using hydrogen chloride in dioxane (scheme 3.4).



Scheme 3.4: Synthesis of *N*-H ketimine **95**.

The reaction of NIITP with **95** was next investigated, using both benzoic acid and sodium benzoate as the carboxylate reaction component (scheme 3.5). Unlike the one-pot procedure, these reactions only yielded trace amounts of primary α -amino 1,3,4-oxadiazole **93**. Further investigation showed that without addition of a carboxylate reaction partner, NIITP reacted with **95** and showed complete consumption of **95** and significant decomposition of NIITP, with 10 new peaks observed by ^{31}P NMR analysis, in only 10 mins.

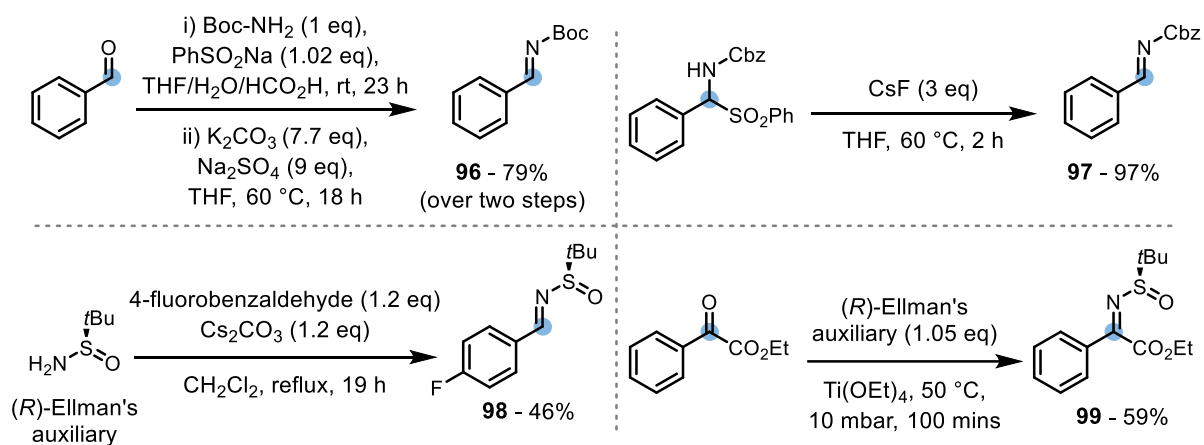


Scheme 3.5: Investigation into synthesis of **93** from **95**, and the reaction of NIITP and **95** in the absence of a carboxylate reaction partner.

3.2.2 Investigation into the Reactivity of Neutral C=N Electrophiles with NIITP

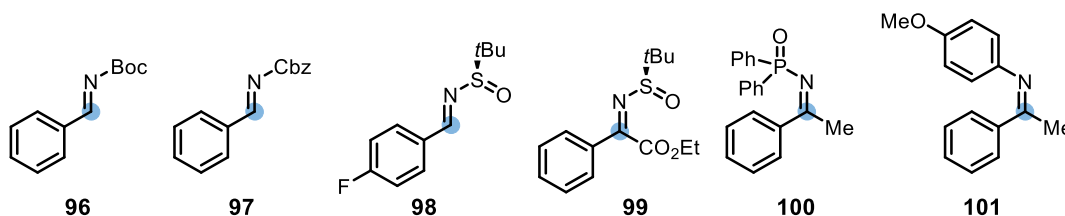
Finding a strategy using *N*-H ketimines problematic, the next target was an approach to primary α -amino 1,3,4-oxadiazoles *via* *N*-protected secondary α -amino 1,3,4-oxadiazoles, as presented in scheme 3.2. To this end, a selection of neutral imines with readily removable protecting groups were synthesized (scheme 3.6). *N*-Carbamoyl imines **96** and **97** were synthesized through a similar approach; firstly, the synthesis of an α -amino sulfone from a

primary carbamate and an aldehyde in the presence of sodium benzenesulfinate. Secondly, elimination of the sulfonyl group under basic conditions, using either potassium carbonate (scheme 3.6, top left) or cesium fluoride (scheme 3.6, top right) to give the desired imines **96** and **97**. *N*-Sulfinyl imines **98** and **99** were available from direct condensation of (*R*)-Ellman's auxiliary with the corresponding aldehyde under basic conditions (scheme 3.6, bottom left), or with the corresponding ketone under Lewis-acidic and dehydrative conditions (scheme 3.6, bottom right).



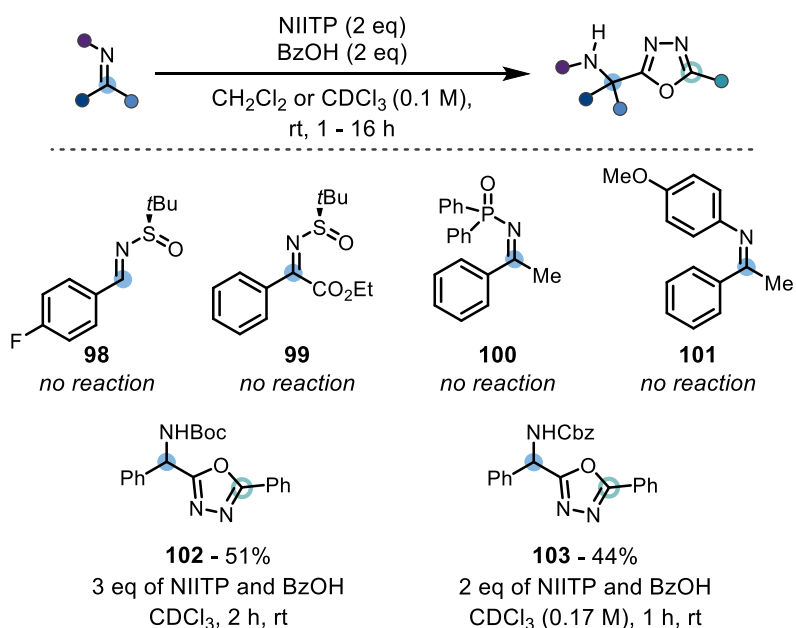
Scheme 3.6: Synthesis of *N*-carbamoyl and *N*-sulfinyl protected imines.

These four imines (**96** – **99**) combined with two protected ketimines (**100** & **101**) sourced from our laboratory database gave a selection of 6 protected imines to be investigated, with both aldimines and ketimines represented (scheme 3.7). Importantly, the choice of *N*-sulfinyl imines **98** and **99** was informed by the potential for the auxiliary to provide stereochemical induction and form diastereomerically, and enantiomerically, pure products.



Scheme 3.7: *N*-Protected imines used during reaction discovery.

Unfortunately, four of the chosen imines (**98** – **101**) showed no reactivity towards NIITP in the presence of benzoic acid, and only a side-product from the direct reaction of benzoic acid with NIITP (2-phenyl-1,3,4-oxadiazole, **4**), as reported by Ramazani,²⁰⁸ was observed. This showed that these imines are presumably not electrophilic enough to react with NIITP, even under the potentially activating acidic conditions provided by the carboxylic acid coupling partner (scheme 3.8). Fortunately, product formation was observed using *N*-carbamoyl imines **96** and **97** and the desired α -amino 1,3,4-oxadiazole products **102** and **103** were isolated in 51% and 44% yield respectively.

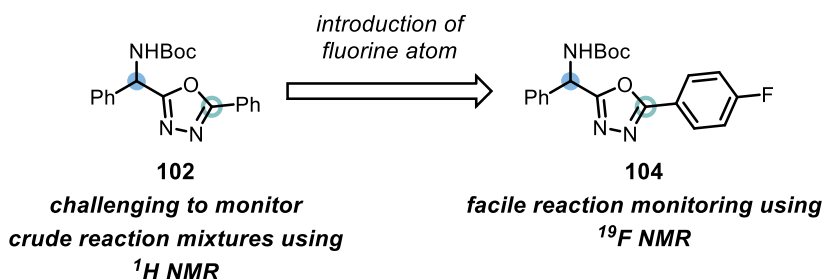


Scheme 3.8: Screen of *N*-protected imine electrophiles **96** – **101**.

Interestingly, to the best of our knowledge, these results represent the first use of *N*-carbamoyl imines **96** and **97** in a multicomponent Ugi-type reaction, despite their wide-reaching applications in C–C bond forming methodologies.^{340, 341} Potentially, this is due to their relatively low electrophilicity ($E = -14.2$, on Mayr's electrophilicity scale)³⁴²⁻³⁴⁴ when compared to iminium ions ($E = -9.4$)³⁴⁵, which inhibits nucleophilic addition by typical unfunctionalized isocyanides. Moreover, the presence of the electron-donating iminophosphorane group in NIITP may provide increased nucleophilicity compared to unfunctionalized isocyanides. Two key advantages of using *N*-carbamoyl imines as electrophiles presented themselves: firstly, their synthesis is readily achieved from commercially available aldehydes and primary carbamates in only two steps; and secondly, when *N*-Boc imines are used, subsequent *N*-Boc removal is trivial under acidic conditions, positioning *N*-Boc imines especially as excellent electrophiles for primary α -amino 1,3,4-oxadiazole synthesis.

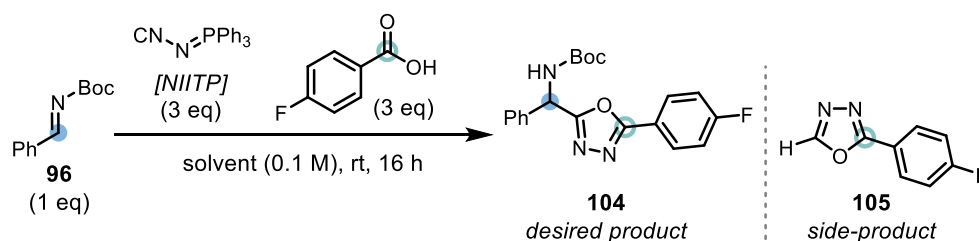
3.3 Reaction Optimization

Having identified a promising hit using *N*-carbamoyl imine electrophiles, *N*-Boc imine **96**, favoured for its ease of *N*-deprotection compared to *N*-Cbz imine **97**, was chosen as a model electrophile for optimization. Initially, observing the reaction yield and tracking side-product formation by crude ¹H NMR proved challenging due to the *N*-Boc group causing broadening of the single aliphatic C-H ¹H resonance in **102**, with most of the aromatic resonances overlapping and being unsuitable for reaction analysis. To overcome this problem, we swapped to using 4-fluorobenzoic acid-derived **104** as a model substrate, allowing us to use ¹⁹F NMR to monitor the reaction and thereby permitting facile reaction analysis, including tracking of any unidentified fluorinated side-products (scheme 3.9).



Scheme 3.9: Evolution of model substrate **102** into **104** for facile reaction monitoring with ^{19}F NMR.

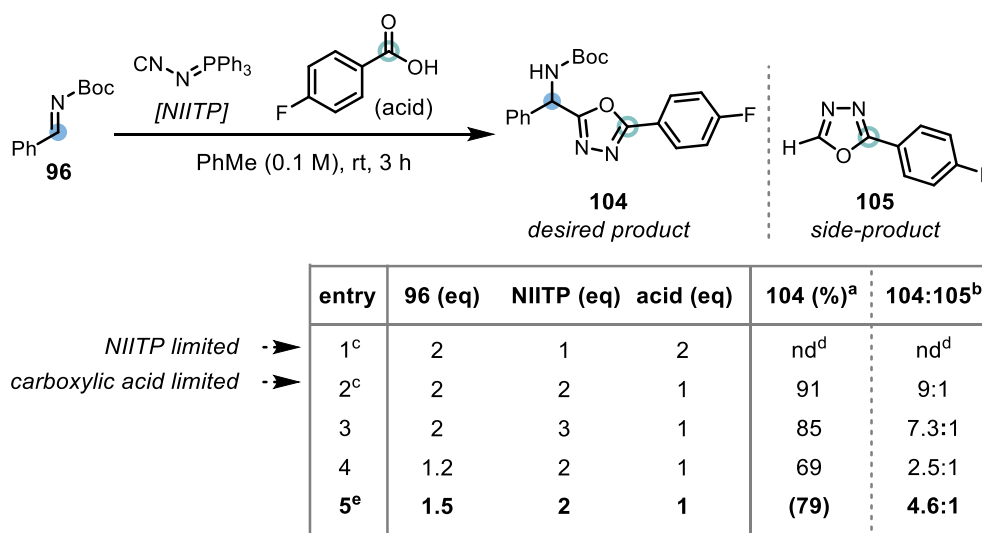
With **104** chosen as the model substrate, reaction optimization commenced with a solvent screen (scheme 3.10), which revealed ethyl acetate (entry 4) and toluene (entry 5) to be the optimal solvents, of those evaluated, for this reaction. During the solvent screen, the use of 3 equivalents of carboxylic acid and NIITP was observed to promote the formation of side-product **105** in quantities exceeding those of the desired product **104**, complicating its purification – in agreement with our previous observations discussed in section 2.4.



entry	solvent	104 (%) ^a	104:105 ^b
1	CH ₂ Cl ₂	45	1:2.3
2	THF	63	1:3.2
3	MeCN	41	1:1.6
4	EtOAc	75	1:2.7
5	PhMe	86	1:2.2

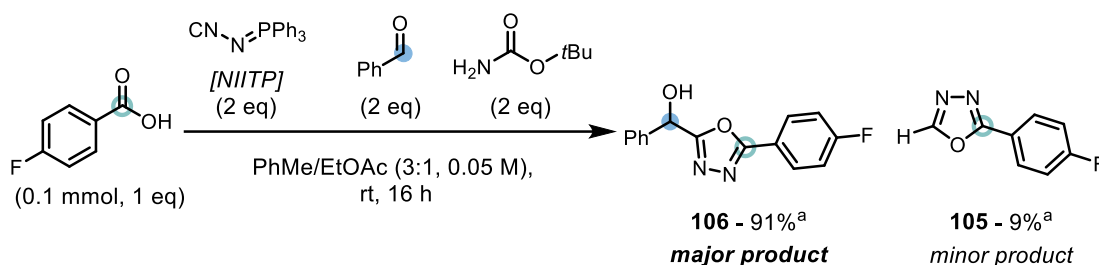
Scheme 3.10: Solvent screen (0.1 mmol scale). ^a ^{19}F NMR yield using α,α,α -trifluorotoluene as an internal standard. ^b Ratios of **104:105** determined by ^{19}F NMR.

An optimization to minimize the formation of side-product **105** was next investigated by evaluating the effect of the reaction stoichiometry on the formation of both **104** and **105** (scheme 3.11). This revealed that when limited by NIITP the reaction gave an intractable mixture of products by ^{19}F NMR (entry 1). However, when the carboxylic acid was the limiting reagent, we observed a clean reaction profile with an excellent 91% ^{19}F NMR yield of **104** and minimal formation of **105** (entry 2). Additionally, increasing the equivalents of NIITP led to a lower reaction yield and increased formation of **105** (entry 3). Decreasing the amount of *N*-Boc imine **96** used to a small excess of only 1.2 equivalents showed a significant reduction in yield with a concomitant rise in the amount of side-product **105** produced (entry 4). A compromise between an excess amount of *N*-Boc imine **96** and the reaction yield was finally achieved with 1.5 equivalents of **96** giving an excellent 79% isolated yield of the *N*-Boc α -amino 1,3,4-oxadiazole **104**, with only minor formation of side-product **105** detected (entry 5).



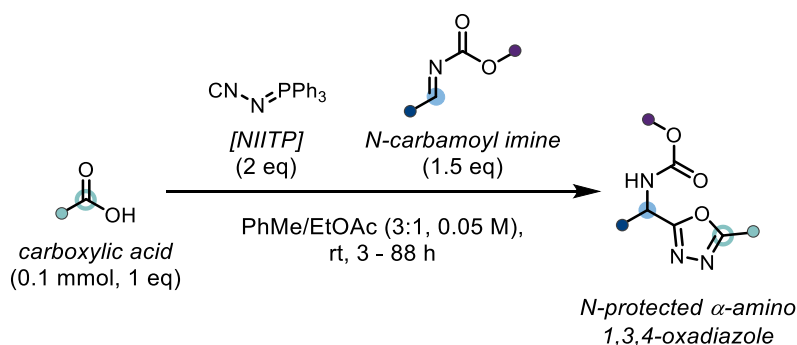
Scheme 3.11: Stoichiometry screen (0.1 mmol scale). ^a ^{19}F NMR yield using α,α,α -trifluorotoluene as an internal standard. ^b Ratios of **104:105** determined by ^{19}F NMR. ^c Reaction time = 23 h. ^d Not determined due to overlapping ^{19}F peaks. ^e **96** added as PhMe solution, acid added as EtOAc solution, 0.05 M reaction concentration.

With optimal conditions using preformed *N*-Boc imine **96** established, next examined was the possibility of forming **96** *in situ* from *tert*-butyl carbamate and benzaldehyde (scheme 3.12). Disappointingly, ^{19}F NMR analysis of crude reaction mixture showed only a 9% yield of mono-substituted 1,3,4-oxadiazole **105** and a 91% yield of **106** – derived from the three-component reaction of benzaldehyde, NIITP, and 4-fluorobenzoic acid as reported by Adib –²¹⁷ without any of the desired product **104** being observed (scheme 3.12).



Scheme 3.12: Examination of *in situ* *N*-carbamoyl imine formation. ^a $^{19}\text{F}\{^1\text{H}\}$ NMR yields determined by comparison of starting carboxylic acid, **105**, and **106** peaks.

This established that condensation of benzaldehyde with *tert*-butyl carbamate was outcompeted by the reactivity of NIITP with benzaldehyde and 4-fluorobenzoic acid.²¹⁷ Ultimately, this experiment concluded the reaction optimization and gave the standard conditions for the reaction scope as those shown in scheme 3.13.

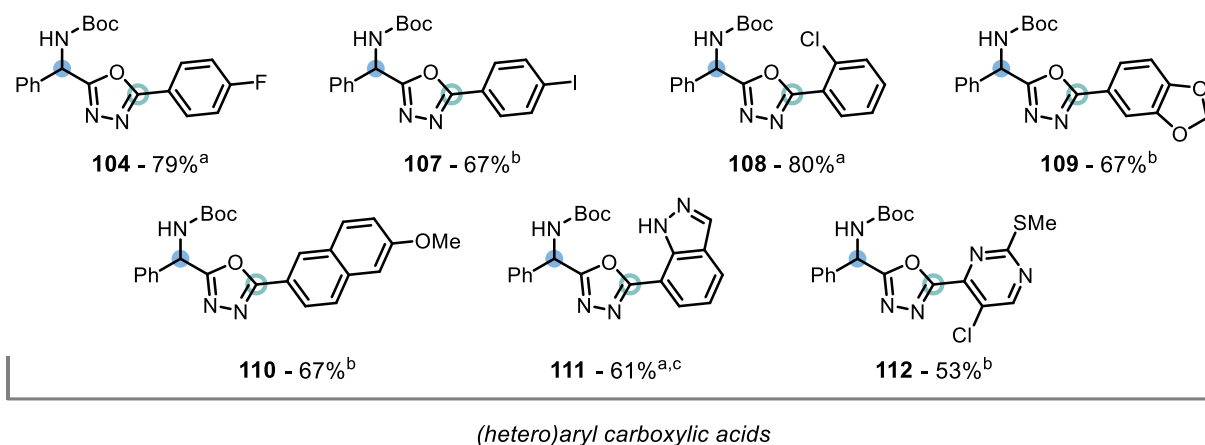


Scheme 3.13: Standard conditions used for the reaction scope.

3.4 Reaction Scope

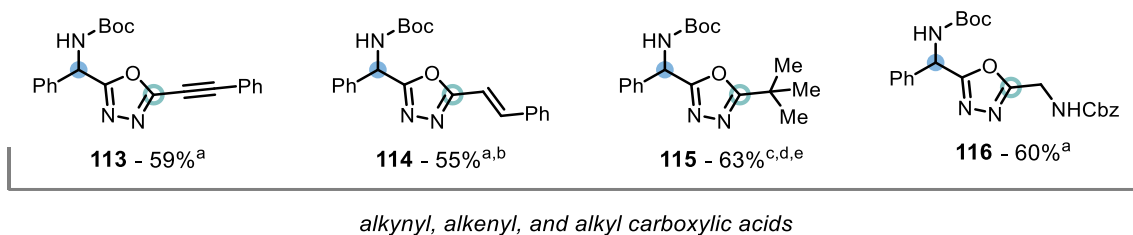
3.4.1 Scope of Carboxylic Acids

With optimal reaction conditions identified, the reaction scope with respect to the carboxylic acid component was first investigated. The aryl carboxylic acids 4-iodobenzoic acid (**107**), 2-chlorobenzoic acid (**108**), piperonylic acid (**109**), and 6-methoxy-2-naphthoic acid (**110**) gave the desired *N*-Boc α -amino 1,3,4-oxadiazoles in good (67%) to excellent (80%) yields (scheme 3.14). Additionally, the heteroaromatic acids 1*H*-indazole-7-carboxylic acid (**111**) and 5-chloro-2-(methylthio)pyrimidine-4-carboxylic acid (**112**) were successfully employed in the reaction, demonstrating a tolerance of Lewis-basic nitrogen atoms.



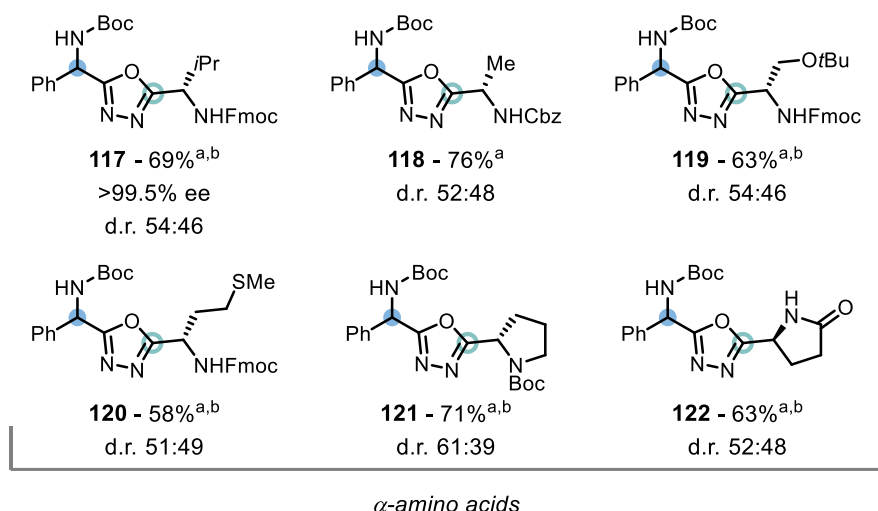
Scheme 3.14: Scope of (hetero)aryl carboxylic acids. ^a Reaction time = 16 h. ^b Reaction time = 3 h. ^c 3 eq of *N*-carbamoyl imine used.

Next, alkynyl (**113**) and alkenyl (**114**) carboxylic acids were utilized to generate *N*-Boc α -amino 1,3,4-oxadiazole structures bearing unsaturated C–C bonds (scheme 3.15). Furthermore, use of pivalic acid (**115**) and *N*-Cbz glycine (**116**) demonstrated the application of both hindered carboxylic acids and *N*-protected α -amino acids to the developed methodology.



Scheme 3.15: Scope of alkynyl, alkenyl, and alkyl carboxylic acids. ^a Reaction time = 3 h. ^b 1.2 eq of imine used. ^c 0.3 mmol scale. ^d 2 eq of *N*-carbamoyl imine used. ^e Reaction time = 48 h.

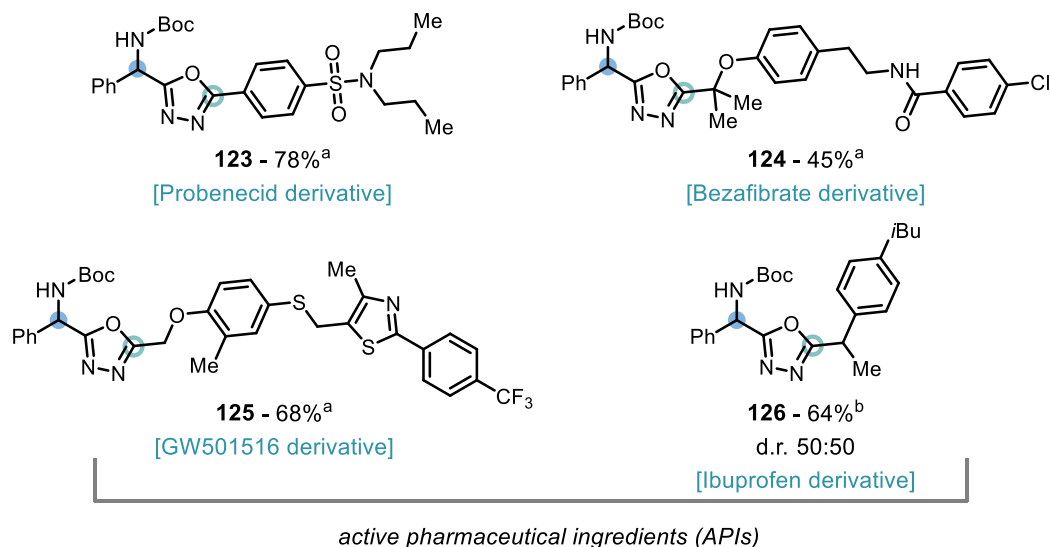
Encouraged by the successful application of glycine (**116**), a range of α -amino acids (**117** – **122**) were reacted to give the complex peptidomimetic structures **117** – **122** in 58% – 76% yield (scheme 3.16). This demonstrated tolerance of *N*-Fmoc (**117** & **120**), *N*-Cbz (**118**), *O*-*t*Bu (**119**), and *N*-Boc (**121**) amino acid protecting groups, as well as a secondary amide functional group (**122**). In the cases of **117** – **120**, this afforded orthogonally protected heteroatoms in the *N*-Boc α -amino 1,3,4-oxadiazole products. Interestingly, chiral HPLC analysis of an appropriate scalemic mixture of **117** identified that both diastereomers of **117** were synthesized in enantiopure form when the corresponding enantiopure Fmoc-valine was used as the carboxylic acid coupling partner. This highlighted that no epimerization of the α -amino acid stereocentre was occurring under the reaction conditions – in line with a similar observation in section 2.5.3 during analysis of **65**. By analogy, compounds **118** – **122** are similarly enantiopure diastereomeric pairs. We postulate that the deviation of the diastereomeric ratios observed from a purely statistical (i.e., 50:50) ratio is likely due to the *in situ* formation of a chiral ion pair, from *N*-Boc imine **96** and the α -amino acid partner, delivering a weak directing effect on the addition of NIITP into this electrophilic imine species.



Scheme 3.16: Scope of *α*-amino acids, ee of **117** determined by chiral HPLC analysis. ^a

Reaction time = 3 h. ^b 0.2 mmol scale.

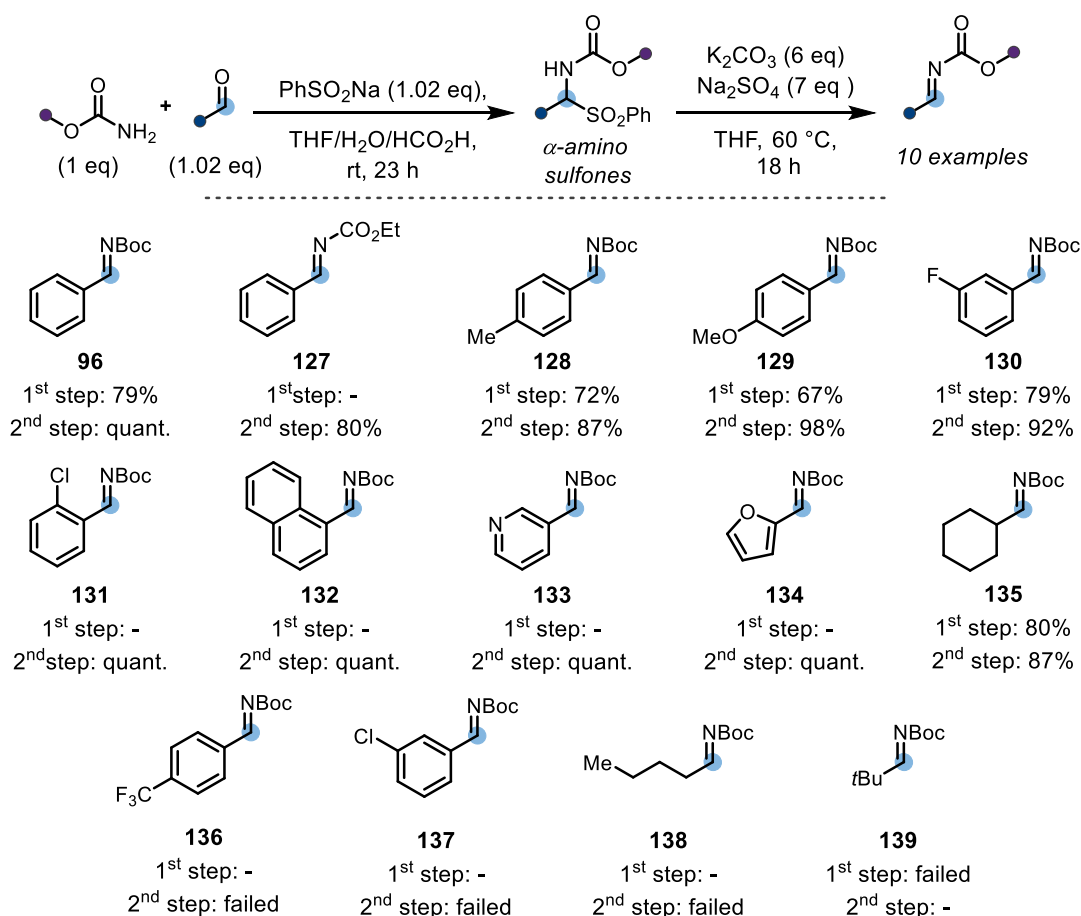
The application of carboxylic acid containing APIs and drug-like molecules to the developed procedure was next surveyed (scheme 3.17). This led to the successful synthesis of *N*-Boc *α*-amino 1,3,4-oxadiazoles **123** – **126** from probenecid (**123**), bezafibrate (**124**), GW501516 (**125**), and ibuprofen (**126**), highlighting the applicability of the method for the late-stage functionalization of complex carboxylic acids.



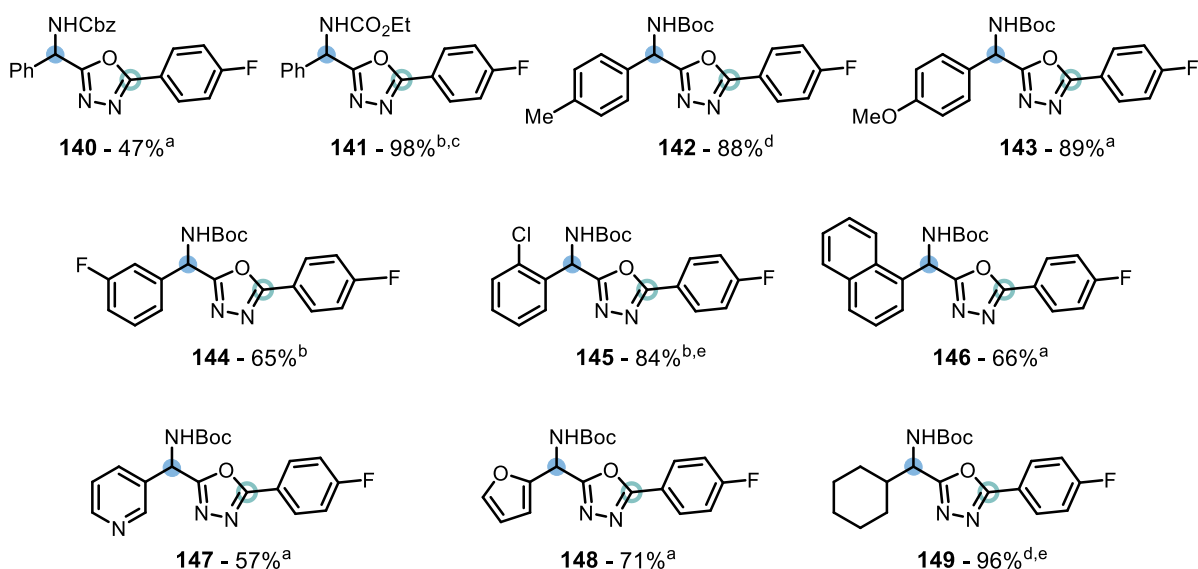
Scheme 3.17: Scope of APIs. ^a Reaction time = 3 h. ^b Reaction = 16 h.

3.4.2 Scope of *N*-Carbamoyl Imines

With the scope of the carboxylic acid component revealed, the scope of the *N*-carbamoyl imine component was next explored. This commenced with the synthesis of a range of *N*-carbamoyl imines by condensation of primary carbamates with aldehydes and sodium benzenesulfinate, and a subsequent basic elimination from their α -amino sulfones, following the general procedure for **96**. Applying this procedure afforded the successful synthesis of ten *N*-carbamoyl imines (**96**, **127** – **135**) with four substrates of interest (**136** – **139**), including primary and tertiary alkyl *N*-Boc imines (**138** & **139**), failing to be synthesized (scheme 3.18). The substrates **97** and **127** – **135** were then subjected to the developed method.

Scheme 3.18: Synthesis of *N*-carbamoyl imines.

With a range of *N*-carbamoyl imines synthesized, the exploration of the reaction scope began with exchanging the imine **96**'s *N*-Boc group for an *N*-Cbz (**97**) or an *N*-ethyl carbamate (**127**) protecting group and gave the desired α -amino 1,3,4-oxadiazoles **140** and **141** in 47% and 98% yield respectively (scheme 3.19). Secondly, electron-rich *para*-methyl (**128**) and *para*-methoxy (**129**) group containing *N*-carbamoyl imines were subjected and found to be well tolerated with excellent yields of the desired products (**142** & **143**) obtained. Next, an exploration of *N*-Boc imines bearing *meta*-fluoro (**130**), *ortho*-chloro (**131**), and 1-naphthyl (**132**) substituents uncovered the reaction's insensitivity towards steric bulk with the synthesis of **144** – **146**. Lastly, *N*-Boc imines containing heteroaromatic groups (**133** & **134**), and a cyclohexyl group (**135**) were applied successfully, yielding diverse *N*-Boc α -amino 1,3,4-oxadiazole products **147** – **149** in moderate (57%) to excellent (96%) yields.

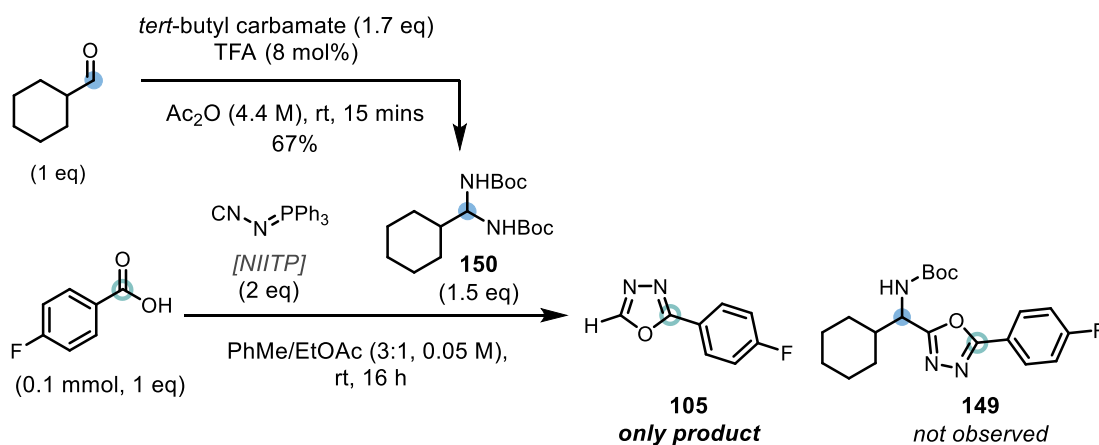


Scheme 3.19: Scope of *N*-carbamoyl imines. ^a reaction time = 3 h. ^b reaction time = 16 h. ^c

0.12 mmol scale. ^d reaction time = 88 h. ^e 2 eq imine used.

Due to the present limitations of *N*-carbamoyl imine synthesis (scheme 3.18), and the failure of an *in situ* *N*-Boc imine synthesis (scheme 3.12), *N*-Boc amins were additionally targeted as precursors to *N*-Boc imine electrophiles – as reported by Maruoka under acidic conditions.³⁴⁶

This was investigated using *cyclo*-hexyl aminal **150**, which when applied to the standard reaction conditions gave no observable formation of the desired product **149** (scheme 3.20). Instead, only the mono-substituted 1,3,4-oxadiazole **105** was detected. Hypothetically, this is due to the pKa of 4-fluorobenzoic acid not being low enough to protonate aminal **105** and cause ionization to the reactive *N*-Boc imine **135** in sufficient quantities for the reaction to afford a reasonable yield of **149**. Maruoka's original report of *N*-Boc aminals showed that the use of TFA, copper(II) triflate, or BINOL-phosphoric acids as catalysts was essential for further transformation of aminal **150** into its corresponding *N*-Boc imine, corroborating this hypothesis.³⁴⁶

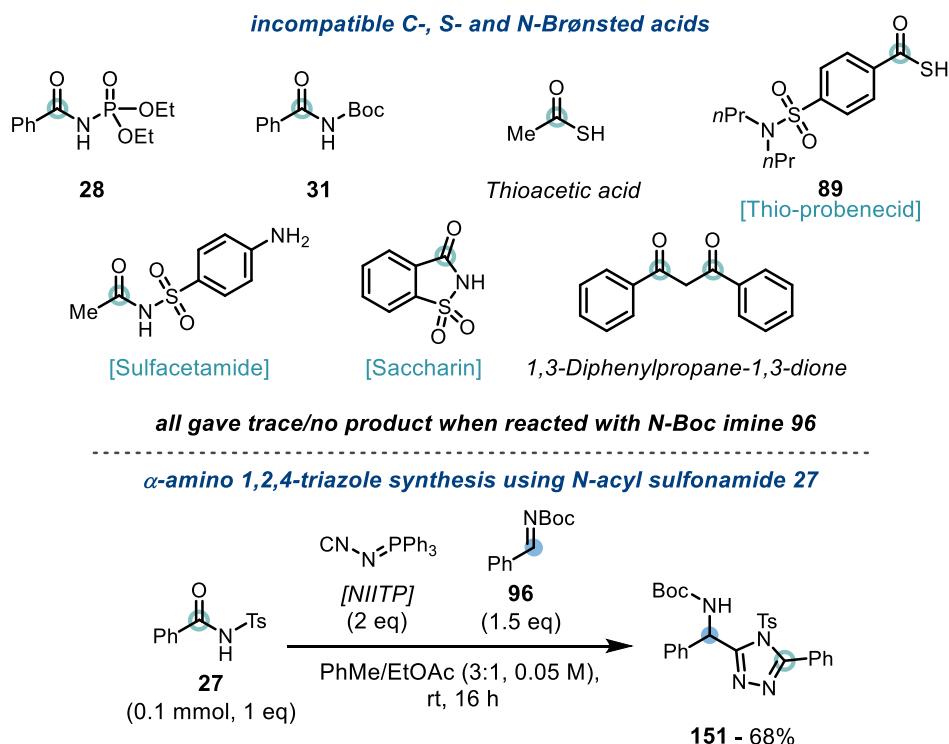


Scheme 3.20: An examination into the application of *N*-Boc aminal **150** as an *N*-Boc imine precursor.

3.4.3 Extension to *N*-Boc α -Amino Heterodiazole Synthesis

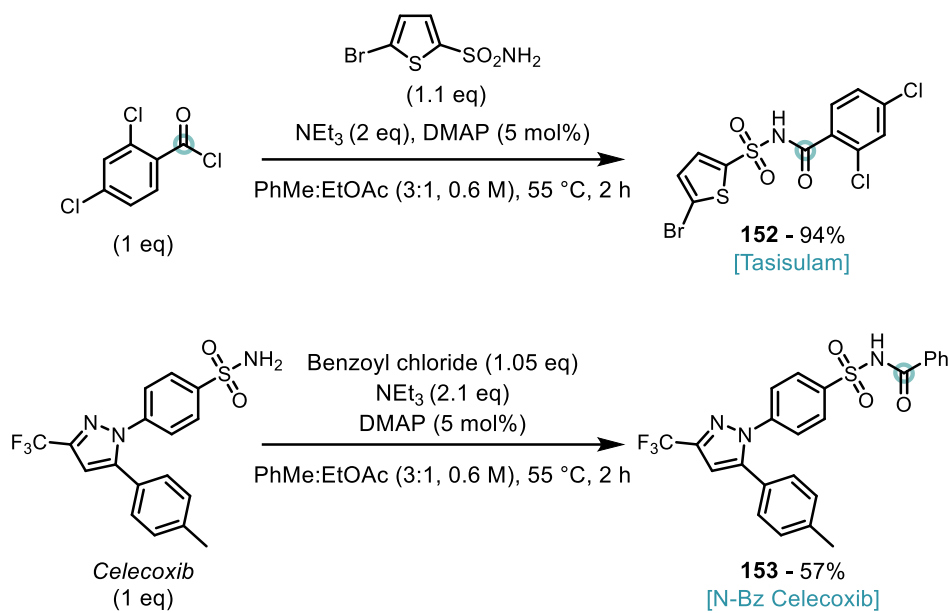
With the reaction scope of both carboxylic acid and *N*-carbamoyl imine reaction components having been scrutinized, next explored was the synthesis of *N*-Boc α -amino heterodiazoles by substituting the carboxylic acid reaction partner for a *C*-, *S*- or *N*-Brønsted acid – a strategy previously used with success in section 2.5.2. Regrettably, this revealed that the majority of *C*-, *S*-, and *N*-Brønsted acids that were previously successful for reductive α -amino heterodiazole synthesis in section 2.5.2 were incompatible with this methodology and gave only trace, or

negligible, yield of the desired *N*-Boc α -amino heterodiazole products (scheme 3.21, top). However, the *N*-acyl sulfonamide **27** acted as an appropriate carboxylic acid replacement and yielded the *N*-Boc α -amino 1,2,4-triazole **151** in 68% isolated yield without any change to the standard reaction conditions (scheme 3.21, bottom).



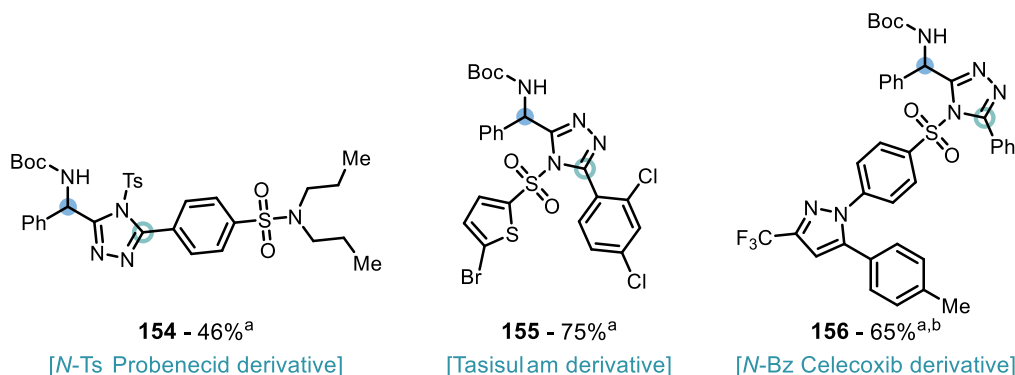
Scheme 3.21: Incompatible C-, S- and N-Brønsted acids, and synthesis of α -Amino 1,2,4-triazole **151** using *N*-acyl sulfonamide **27**.

To capitalize on the successful synthesis of **151**, the *N*-acyl sulfonamide containing API tasisulam (**152**), and an *N*-acyl derivative of sulfonamide containing API celecoxib (**153**) were synthesized by acylation of the corresponding sulfonamides, an approach previously successfully used for the synthesis of **27** (schemes 2.20 & 3.22).



Scheme 3.22 Synthesis of tasisulam **152** and N-Bz celecoxib **153**.

Application of the previously synthesized *N*-Ts derivative of probenecid (**87**), tasisulam (**152**), and *N*-Bz celecoxib (**153**) to the developed methodology, using *N*-Boc imine **96** as a coupling partner, afforded the three *N*-Boc α -amino 1,2,4-triazoles **154** – **156** in 46% to 75% yield (scheme 3.23). This showed that APIs natively containing an *N*-acyl sulfonamide group (tasisulam), as well as readily accessible derivatives of sulfonamide containing (celecoxib), or carboxylic acid containing (probenecid) APIs can undergo late-stage functionalization using the developed methodology.

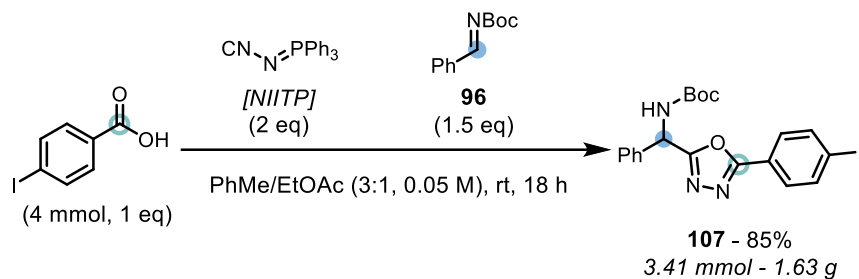


Scheme 3.23: Synthesis of *N*-Boc α -amino 1,2,4-triazoles **154** – **156**. ^a Reaction time = 16 h.

^b 3 eq of *N*-carbamoyl imine **96** used.

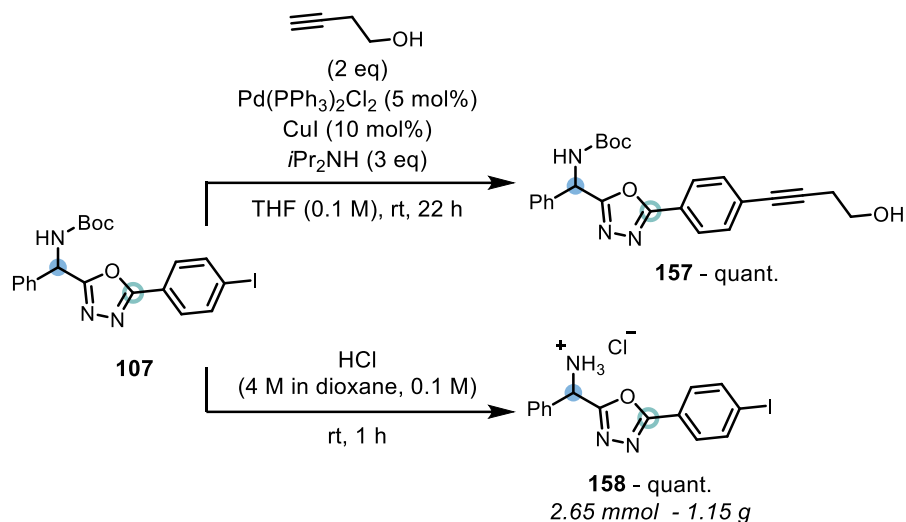
3.5 Scale-up and Product Derivatization

The standard reaction conditions were scaled-up to afford over a gram of *N*-Boc α -amino 1,3,4-oxadiazole **107** (scheme 3.24). Notably, the reaction yield for **107** improved from 67%, on 0.1 mmol scale, to 85% at 4 mmol scale.



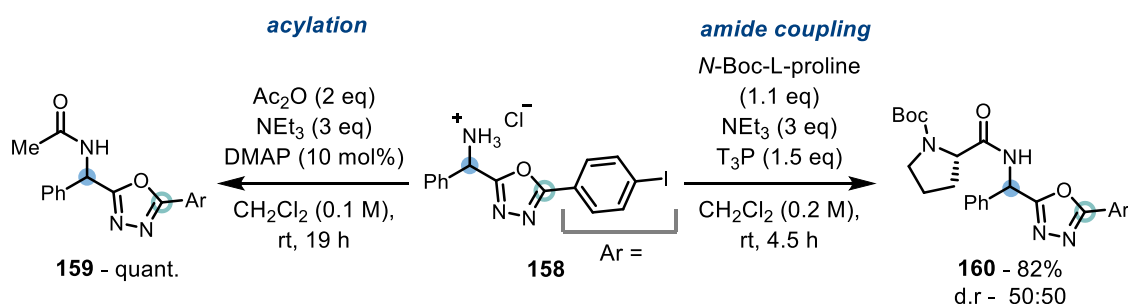
Scheme 3.24: Reaction scale-up for synthesis of **107**.

Having ample quantities of **107** in hand allowed for the performance of derivatization reactions, starting with a Sonogashira reaction to afford **157**, which demonstrates the value of the aryl iodide functional group handle of **107** (scheme 3.25, top). Secondly, *N*-Boc deprotection was achieved on gram-scale using 4 M HCl in dioxane, and afforded the primary α -amino 1,3,4-oxadiazole **158** directly as its hydrochloride salt without requiring additional purification (scheme 3.25, bottom).



Scheme 3.25: Sonogashira reaction, and N-Boc deprotection of **107**.

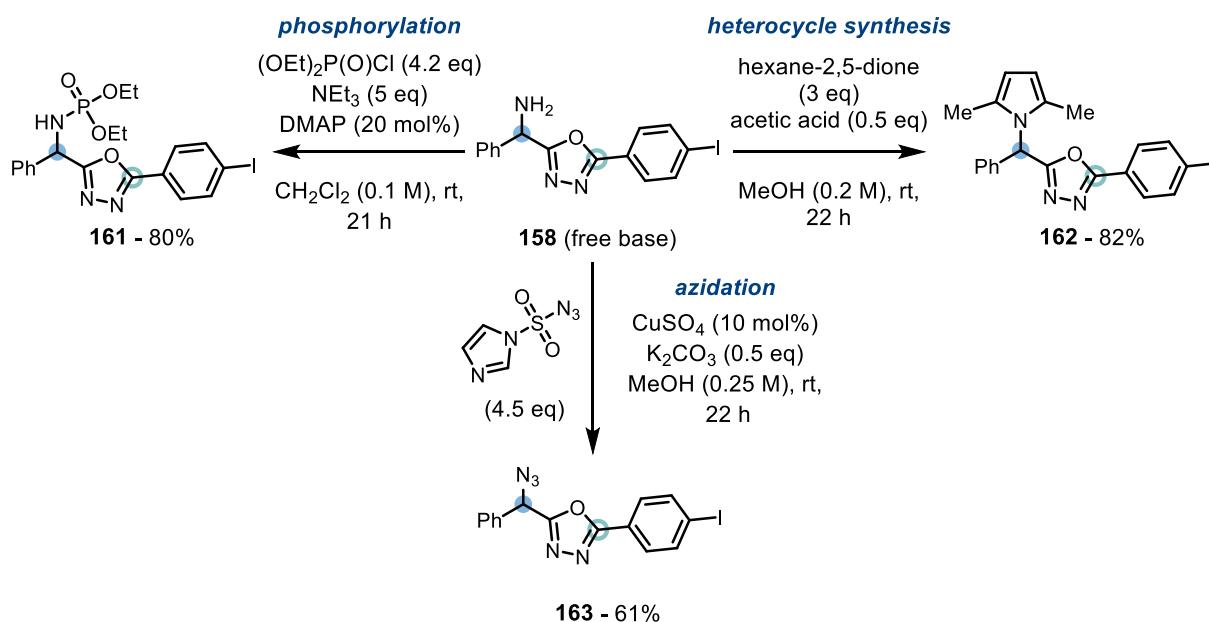
To demonstrate the value of the methodology in providing access to primary amine **158**, we evaluated its synthetic potential by performing a range of derivatizations. Firstly, **158** was directly used in amidations, either with acetic anhydride in the case of **159** (scheme 3.26, left), or with Boc-L-proline using T₃P as a coupling agent in the case of **160** (scheme 3.26, right). This gave secondary amide products in excellent yields, using **158** directly as its hydrochloride salt.



Scheme 3.26: Amidations of **158**.

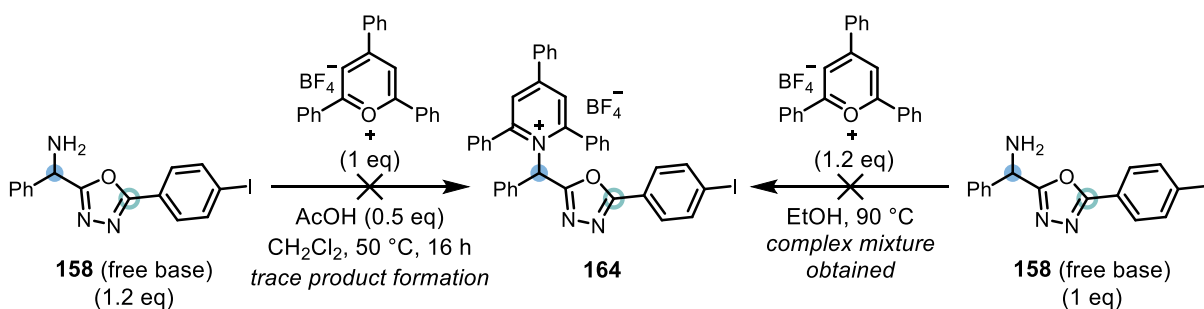
Although the use of **158** as its hydrochloride salt is potentially beneficial, further derivatizations required the use of **158** as a free base, which was readily acquired after a basic aqueous workup. Using **158**'s free base, *N*-phosphorylation was achieved using diethyl chlorophosphate,

giving **161** in 80% yield (scheme 3.27, top left). Furthermore, the primary amine of **158** was incorporated into a pyrrole (**162**) using a Paal-Knorr synthesis (scheme 3.27, top right),^{347, 348} and into an azide (**163**) following Shen and Wang's procedure,^{349, 350} after initially finding 4-acetamidobenzenesulfonyl azide ineffective as a diazo transfer reagent (scheme 3.27, bottom). The synthesis of **159** – **163** highlights the versatility of **158** for the synthesis of functionalized 1,3,4-oxadiazole containing molecules.



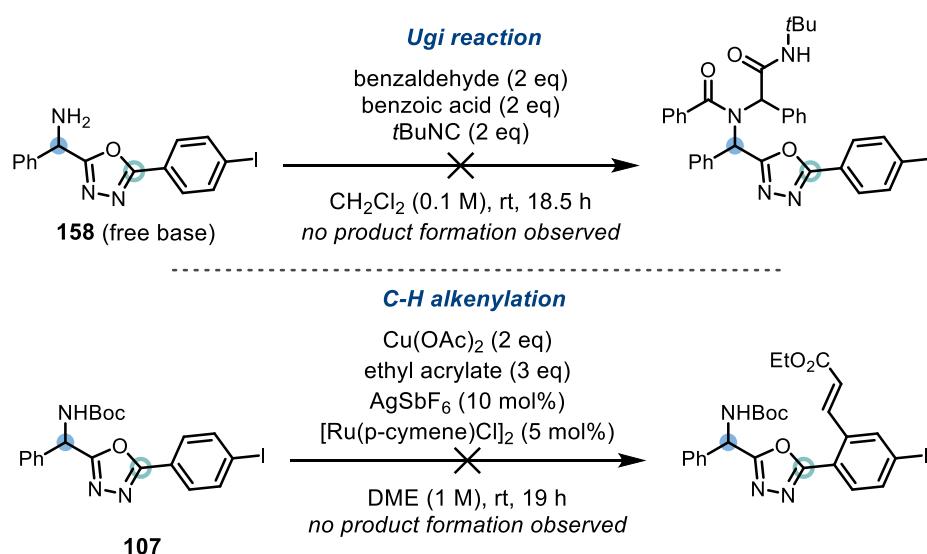
Scheme 3.27: Further derivatizations of **158**.

To further demonstrate the usefulness of primary amine **158** for the installation of diverse functionalities, the synthesis of its Katritzky salt **164** from 2,4,6-triphenylpyrylium tetrafluoroborate was targeted.^{351, 352} Unfortunately, due to the hindered nature of **158**, attempts at this transformation proved fruitless, with mild conditions giving only trace (<5%) product formation (scheme 3.28, left), and more forcing conditions yielding decomposition of **158** (scheme 3.28, right).³⁵³



Scheme 3.28: Exploration of the synthesis of Katritzky salt **164** from **158**.

The sterically-congested nature of **158** also led to attempts to utilize it in an Ugi reaction being unsuccessful (scheme 3.29, top).³⁵⁴ Additionally, the 1,3,4-oxadiazole motif of **107** proved unsuitable for use as a directing group in a ruthenium-catalyzed C–H alkenylation, with no product formation being observed (scheme 3.29, bottom).^{355, 356}



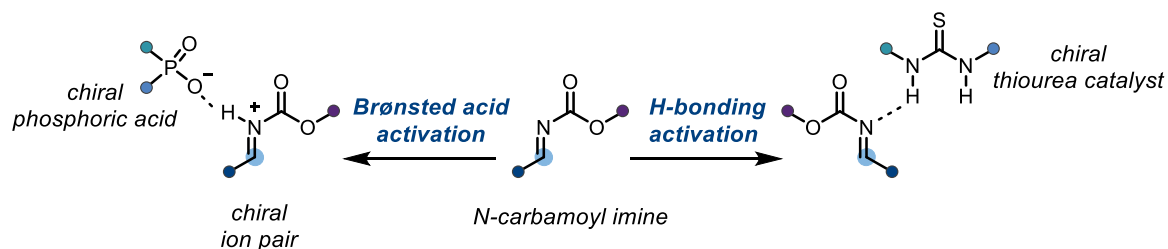
Scheme 3.29: Unsuccessful use of **158** in an Ugi reaction and **107** for a 1,3,4-oxadiazole directed C–H alkenylation.

3.6 Future work – Investigations into an Enantioselective Reaction Variant and the Use of *N*-Acyl Iminium Ion Electrophiles

Presented in this section are results arising from the discovery phase of this project, which were shelved in favour of the *N*-carbamoyl imine work presented above, either due to time constraints (section 3.6.1), or lack of promising lead results during the brief period of investigation (sections 3.6.2).

3.6.1 Investigation into an Enantioselective Reaction Variant

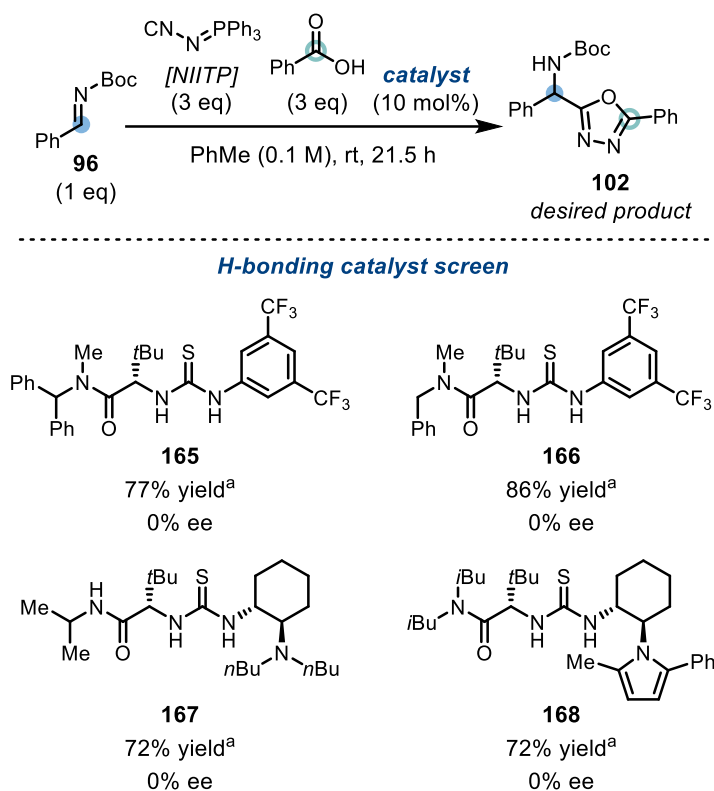
Enantioselective C–C bond forming reactions of *N*-carbamoyl imines have been realized under a variety of catalytic modes, including organocatalytic Brønsted acidic and hydrogen bonding modes (scheme 3.30).^{340, 357-359} The partial or full protonation of the *N*-carbamoyl imine provided under these catalytic modes serves to activate this electrophilic species and bind the chiral catalyst and electrophile together allowing for the induction of enantioselectivity to occur.



Scheme 3.30: *N*-Carbamoyl imine activation under Brønsted acid and hydrogen bonding conditions.

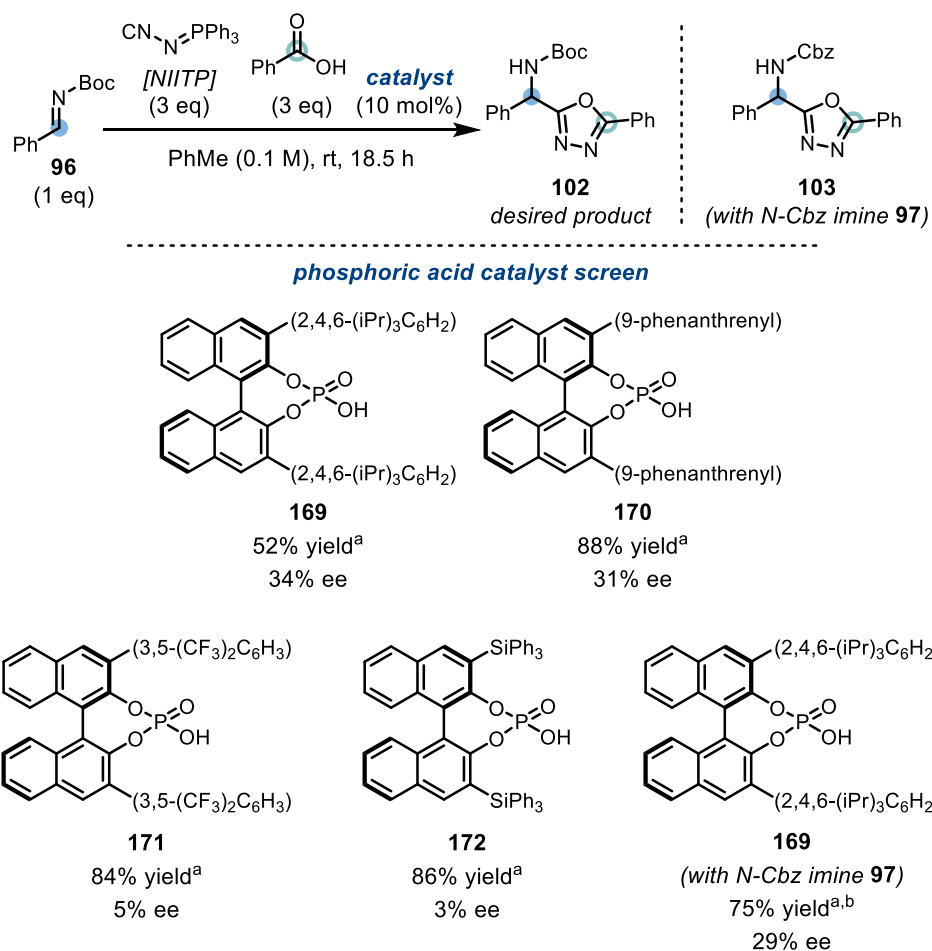
At the outset of the project, before the reaction was fully optimized, an exploration to understand if either of these activation modes was applicable to the developed methodology was carried out. Firstly, a screen of hydrogen bonding catalysts (**165** – **168**) quickly revealed that hydrogen bonding was unsuitable for the induction of enantioselectivity, giving α -amino 1,3,4-oxadiazole product **102** in racemic form, albeit in good yields (scheme 3.31). Furthermore, reducing the

reaction temperature from room temperature to either $-20\text{ }^{\circ}\text{C}$ or $-78\text{ }^{\circ}\text{C}$, and employing catalyst **165**, did not change the observed lack of enantioselectivity.



Scheme 3.31: H-bonding catalyst screen, ee of **102** determined by chiral HPLC analysis. ^a ¹H NMR yield determined using 1,3,5-trimethoxybenzene as an internal standard.

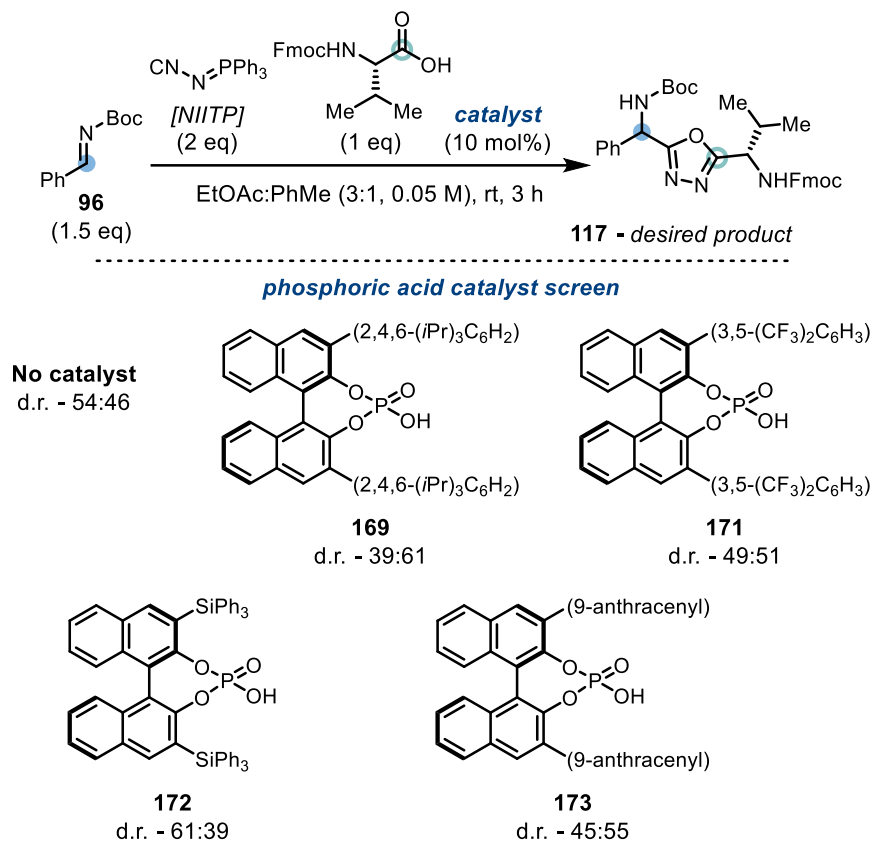
Chiral phosphoric acids were next targeted as sources of enantioinduction (scheme 3.32). Encouragingly, the use of (*R*)-TRIP (**169**) gave the desired product **102** in 52% yield with a 34% enantiomeric excess (ee). The reaction's ee was slightly diminished when using a 9-phenanthrenyl substituted BINOL-phosphoric acid (**170**), giving **102** with a 30% ee. In contrast, use of catalysts **171** & **172** gave the product **102** in excellent yields but without ees exceeding 5%. Replacing *N*-Boc imine **96** with the *N*-Cbz protected imine **97** and using (*R*)-TRIP (**168**) as the catalyst gave the α -amino 1,3,4-oxadiazole product **103** in increased yield, but with a reduced ee (34% ee for **102**, vs 29% ee for **103**).



Scheme 3.32: Chiral phosphoric acid screen, ee of **102** and **103** determined by chiral HPLC analysis. ^a ¹H NMR yield determined using 1,3,5-trimethoxybenzene as an internal standard. ^b *N*-Cbz imine **97** used as starting material generating **103** as the product.

Due to time-constraints imposed by COVID-19 restrictions within the CRL, the investigation into an enantioselective reaction variant was suspended in favor of pursuing a full optimization and scope of the racemic reaction (sections 3.3 – 3.5). However, later in the project these preliminary results of a chiral phosphoric acid catalyst controlling the stereoselectivity of the reaction were corroborated when investigating if a diastereoselective synthesis of **117** could be achieved (scheme 3.33). This showed that addition of chiral phosphoric acids **169**, and **171** – **173** altered the diastereoselectivity observed in the synthesis of **117** from the 54:46 d.r.

obtained in the absence of a catalyst, with the observed d.r.s ranging from 61:39 to 39:61. The catalysts **169** and **173** showed the strongest diastereocontrol reversing the uncatalyzed d.r. to give **117** with d.r.s of 39:61 and 45:55 respectively, providing a promising proof-of-concept for use of chiral phosphoric acids to control the enantioselectivity or diastereoselectivity of the developed reaction.

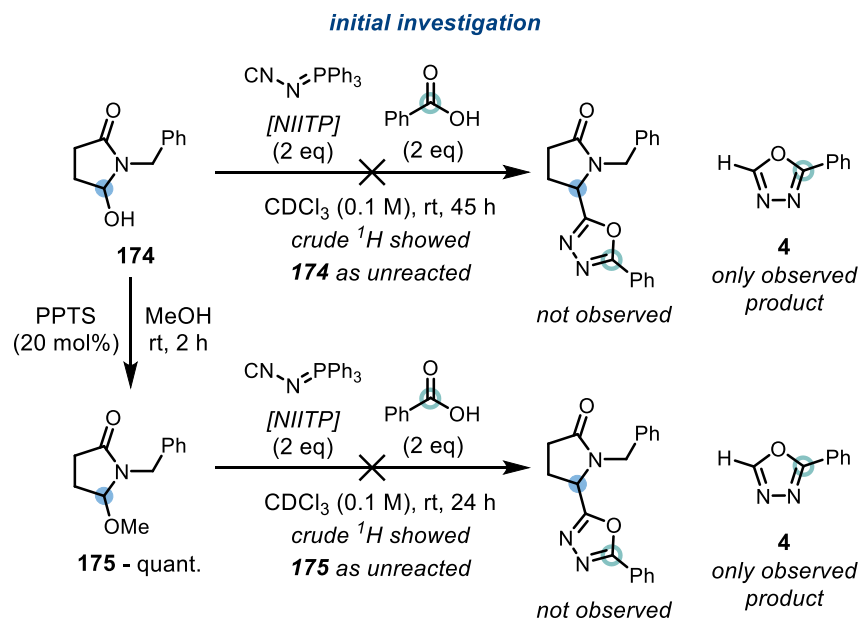
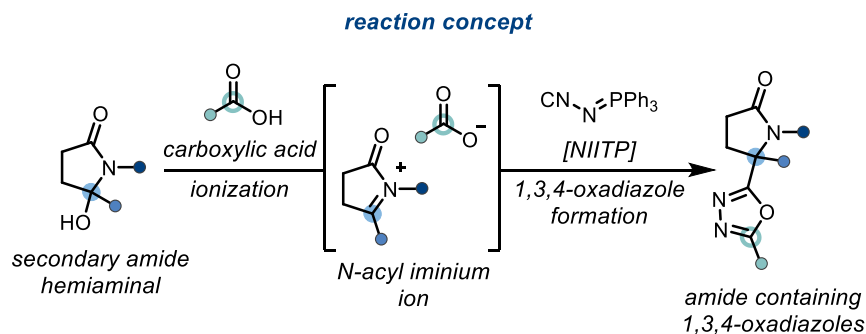


Scheme 3.33: A preliminary investigation into the control of diastereoselectivity in the synthesis of **117**, d.r. of **117** determined by HPLC analysis.

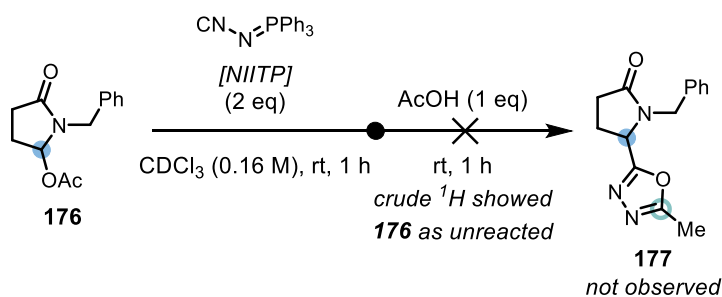
Future work on an enantioselective, or diastereoselective, reaction variant would require a further screen of chiral phosphoric acids catalysts, and alternative chiral Brønsted acid catalysts.^{357, 358, 360} Moreover, an in-depth evaluation of the *N*-carbamoyl group of the imine component would be essential to maximize the reaction's ee.

3.6.2 Investigation into the Use of *N*-Acyl Iminium Ion Electrophiles

Alongside *N*-carbamoyl imines, *N*-acyl iminium ions were a class of electrophiles with unknown reactivity with NIITP and therefore untapped potential. These reactive ions are often generated *in situ* from secondary amide hemiaminals (scheme 3.34, top). During the discovery phase of this project, their use was also targeted. However, preliminary investigations demonstrated unsuccessful use of hydroxy hemiaminal **174**, or *O*-methoxy hemiaminal **175**, with NIITP and benzoic acid, yielding the side-product **4** as the only observed product with **174** and **175** remaining unreacted (scheme 3.34, middle). Further examination with *O*-acetoxy hemiaminal **176**, chosen for its lower pKa leaving group conceivably promoting ionization to the desired *N*-acyl iminium ion, and without a carboxylic acid coupling partner, proved fruitless, even when encouraged to undergo ionization with an equivalent of acetic acid none of the desired product (**177**) was detected (scheme 3.34, bottom). Critical to future work employing this class of electrophiles would be the discovery of a method of hemiaminal activation that efficiently afforded the desired *N*-acyl iminium ion intermediate in the presence of NIITP and a carboxylic acid, allowing the desired reaction to proceed and outcompete formation of any mono-substituted 1,3,4-oxadiazole side-products such as **4**.



reactivity of O-acetoxy hemiaminal 176



Scheme 3.34: Reaction concept of *N*-acyl iminium ions and NIITP and initial investigations using *N*-acyl iminium precursors **174** – **176**.

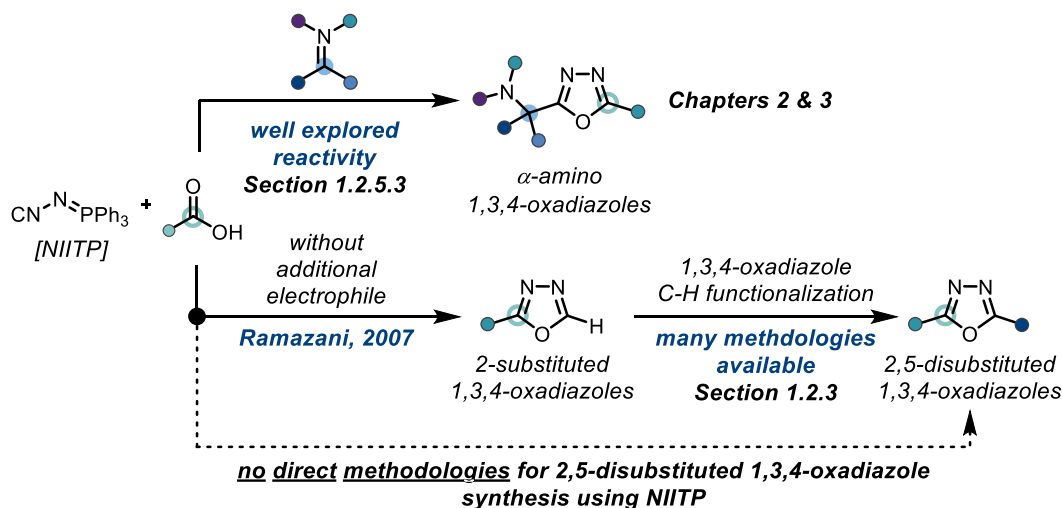
3.7 Conclusion

In conclusion, *N*-carbamoyl imines have been shown to react with NIITP and a carboxylic acid (or *N*-acyl sulfonamide) coupling partner to afford desirable *N*-protected α -amino 1,3,4-oxadiazoles (or 1,2,4-triazoles) in a three-component Ugi-type reaction of these prominent electrophiles. The reaction scope was tolerant of alkyl, alkenyl, alkynyl, and (hetero)aryl carboxylic acids, including suitably protected α -amino acids, and of (hetero)aryl *N*-carbamoyl aldimine reaction partners. The synthesis of *N*-Boc α -amino 1,2,4-triazoles was achieved by an exchange of the carboxylic acid partner for an *N*-Brønsted acidic *N*-acyl sulfonamide and demonstrated using three API derivatives. A gram-scale example, and derivatization (including facile *N*-Boc deprotection), of the α -amino 1,3,4-oxadiazole products highlighted the synthetic utility of the developed methodology. Additionally, investigations into an enantioselective reaction variant, and use of *N*-acyl iminium ions as reactive intermediates present avenues for future explorations and further expansion of this project.

Chapter 4: 2,5-Disubstituted 1,3,4-Oxadiazole Synthesis via a One-pot Construction-Functionalization Strategy

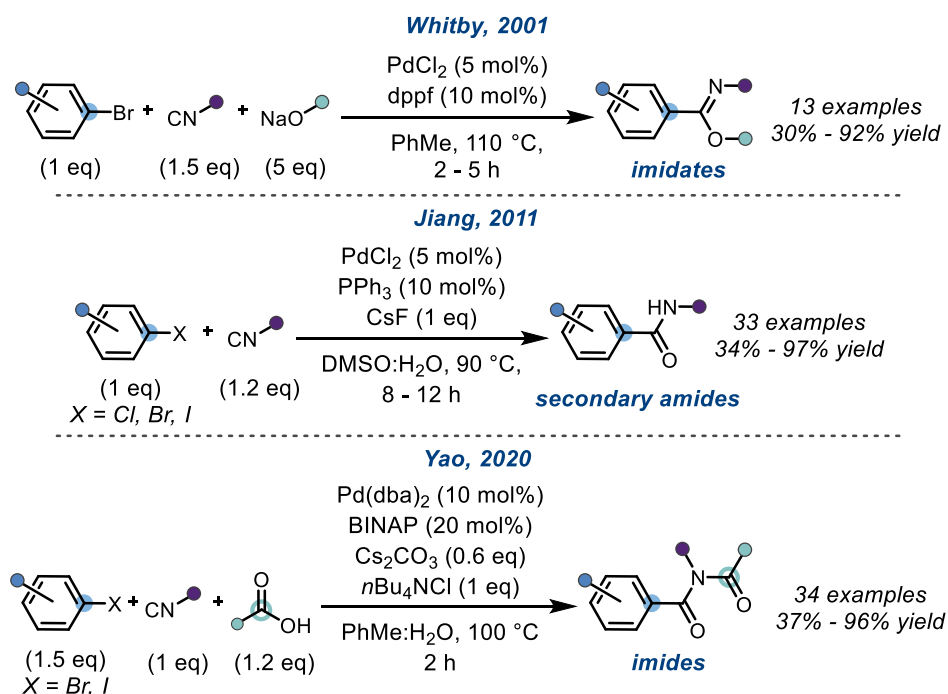
4.1 Introduction – Project Concept

Throughout chapters 2 and 3 the reactivity of NIITP with C=N electrophiles has been explored and expanded with a focus on new ways to access electrophilic intermediates (amide reductive functionalization, chapter 2),³³⁹ and new classes of C=N electrophiles (*N*-carbamoyl imines, chapter 3)³⁶¹ for α -amino 1,3,4-oxadiazole synthesis. In addition to C=N electrophiles (section 1.2.5.3), C=O electrophiles are known to exhibit Passerini-type reactivity with NIITP (section 1.2.5.2); and, Ramazani has reported synthesis of 2-substituted 1,3,4-oxadiazoles with NIITP in the absence of an additional electrophile (section 1.2.5.1).^{208, 209} However, no reports of the utilization of NIITP for general a 2,5-disubstituted 1,3,4-oxadiazole synthesis exist despite plentiful methodologies for C-H functionalization of 2-substituted 1,3,4-oxadiazoles (as discussed in section 1.2.3).



Scheme 4.1: The known and unexplored reactivity of NIITP.

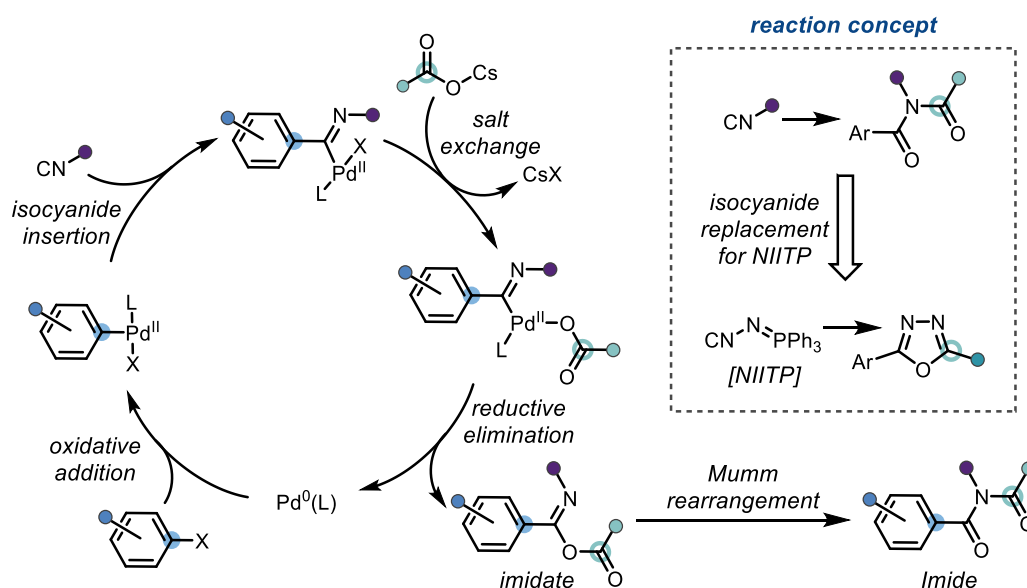
Taking 2,5-diaryl 1,3,4-oxadiazoles as an example, existing syntheses are reliant on the multi-step approaches previously discussed in chapter 1, such as the C-H arylation of 2-substituted 1,3,4-oxadiazoles (section 1.2.3.1), or dehydrative and oxidative, cyclizations (sections 1.2.1 & 1.2.2). As such, it was envisioned that a streamlined and multicomponent approach to 2,5-diaryl 1,3,4-oxadiazoles using NIITP, a carboxylic acid, and a complementary arene coupling partner would provide improved synthetic access to these molecules. Palladium-catalyzed arylations using aryl iodides in combination with isocyanides, where NIITP could act as a suitable replacement, have been reported by Whitby (scheme 4.2, top),³⁶² Jiang (scheme 4.2, middle),³⁶³ and Yao for the synthesis of imidates, secondary amides, and imides, respectively (scheme 4.2, bottom).³⁶⁴



Scheme 4.2: Selected palladium-catalyzed couplings using isocyanides.

In closer detail, Yao's proposed mechanism is initiated by an oxidative addition of a palladium(0) species into the aryl halide electrophile, then the isocyanide coupling partner coordinates to the palladium and undergoes a 1,1-migratory insertion (scheme 4.3). A

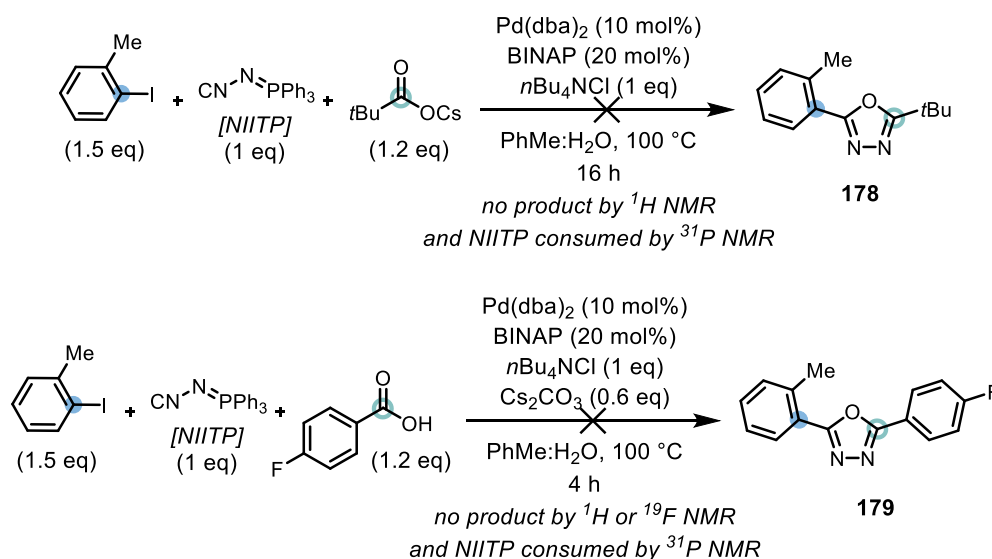
subsequent salt exchange with a cesium carboxylate (formed *in situ* from the carboxylic acid and cesium carbonate) and reductive elimination gives an imidate and the active palladium(0) catalyst. A Mumm rearrangement then affords the imide product. We postulated that the isocyanide in Yao's methodology could be replaced by NIITP to afford an imidate (after reductive elimination) which was poised to form an 1,3,4-oxadiazole ring *via* an aza-Wittig reaction (as shown in scheme 1.40). This would generate a 2,5-diaryl 1,3,4-oxadiazole in a multicomponent and one-pot fashion from an aryl halide, a carboxylic acid, and NIITP. The success of this strategy would rely on the *in situ* formation of a palladium-ligand complex that would escape potential complexation from either the iminophosphorane group of NIITP, or from triphenylphosphine oxide – generated from the 1,3,4-oxadiazole constructing aza-Wittig reaction – in favour of productive complexation to the isocyanide group.



4.1.1 Initial Investigations

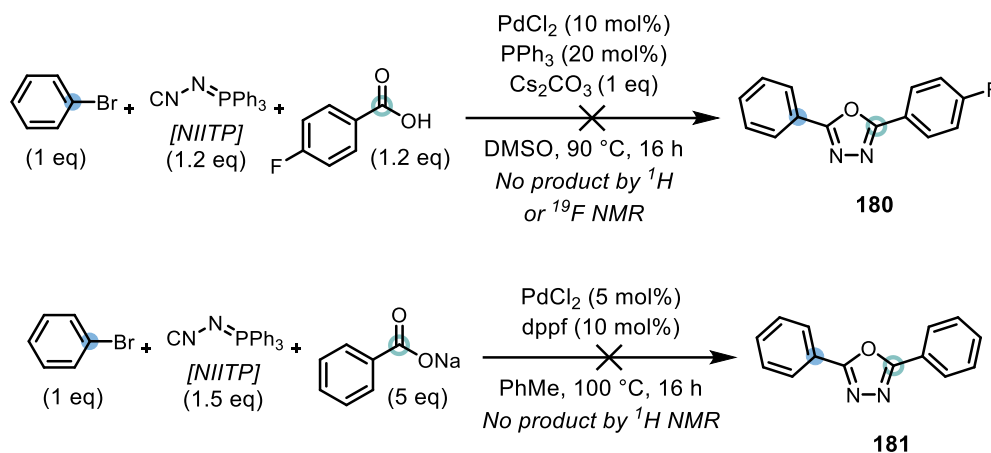
The initial investigation was started with the use of NIITP as a replacement for the aryl isocyanides in Yao's methodology; with the application of 1-iodo-2-methylbenzene as the aryl

iodide, and cesium pivalate as the carboxylate component, targeting synthesis of 2,5-disubstituted 1,3,4-oxadiazole **178** (scheme 4.4). Unfortunately, product **178** was not observed despite the complete consumption of NIITP (as confirmed by ^{31}P NMR). Moreover, substituting cesium pivalate with 4-fluorobenzoic acid and cesium carbonate similarly led to no formation of product **179**, as revealed by ^1H and ^{19}F NMR, despite also providing complete consumption of NIITP.



Scheme 4.4: Investigation into 2,5-disubstituted 1,3,4-oxadiazole synthesis using Yao's conditions.

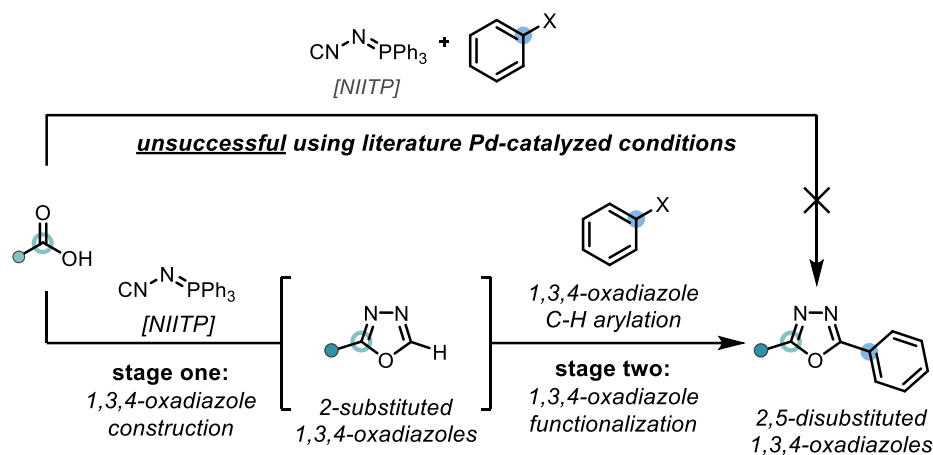
Next, reaction conditions disclosed by Jiang,³⁶³ and Whitby,³⁶² for palladium-catalyzed isocyanide insertions into aryl halides were investigated (scheme 4.5). Unfortunately, and in line with the results in scheme 4.4, employing NIITP in combination with a carboxylic acid (or sodium carboxylate), under their reported conditions gave no formation of the 2,5-disubstituted 1,3,4-oxadiazole products **180** or **181**.



Scheme 4.5: Evaluation of NIITP under Jiang's (top), and Whitby's (bottom) reported conditions.

4.2 Pursuit of a One-Pot 1,3,4-Oxadiazole Construction-Functionalization Protocol

The failure of NIITP as an isocyanide replacement in palladium-catalyzed arylations led to a re-evaluation of the project strategy (scheme 4.6). Instead of a one-stage reaction, pursuit of a practical two-stage and one-pot approach was proposed. Hypothetically, this would be achievable by firstly constructing a 2-substituted 1,3,4-oxadiazole using NIITP and a carboxylic acid;²⁰⁸ with a C-H functionalization performed subsequently to install the second 1,3,4-oxadiazole substituent, giving a 2,5-disubstituted 1,3,4-oxadiazole product. Importantly, this strategy would allow the utilization of 1,3,4-oxadiazole C-H functionalization reactions beyond the arylations originally targeted above, to provide a one-pot and multicomponent synthesis of diverse 1,3,4-oxadiazoles. Nevertheless, as 1,3,4-oxadiazole C-H arylations are amongst the most precedented 1,3,4-oxadiazole C-H functionalizations (section 1.2.3.1), a 1,3,4-oxadiazole construction-arylation protocol was first pursued.

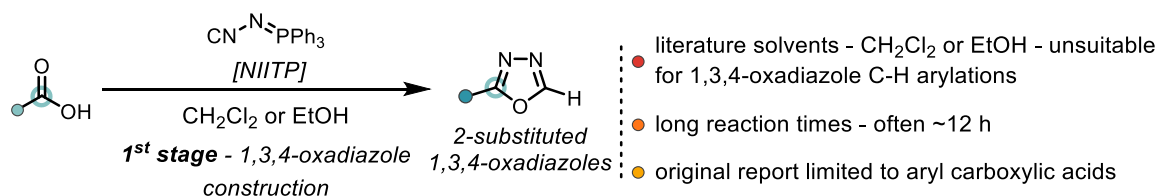


Scheme 4.6: Project overview – pursuing a one-pot 1,3,4-oxadiazole construction-functionalization strategy.

4.3 Development of a One-Pot 1,3,4-Oxadiazole Construction-Arylation

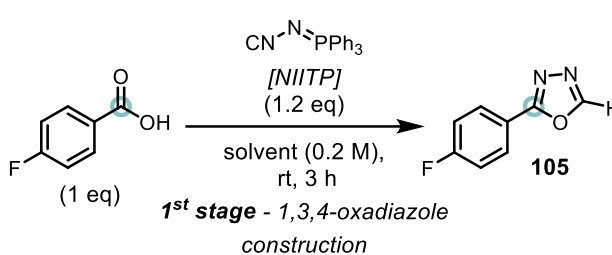
4.3.1 Optimization of the 2-Substituted 1,3,4-Oxadiazole Synthesis

First, the optimization of the 1,3,4-oxadiazole construction using NIITP (stage one) was targeted (scheme 4.7). A survey of the literature revealed that the only solvents previously used for this reaction were dichloromethane,^{208, 209} and ethanol;²¹⁶ both of which are incompatible with reaction conditions typically used for 1,3,4-oxadiazole C-H arylations, which generally involve high temperatures (section 1.2.3.1). Long reaction times of ~12 hours were also routine in these transformations and were considered to be impractical and undesirable in an efficient one-pot two-stage protocol.²⁰⁸ Furthermore, the search revealed that aryl carboxylic acid coupling partners were most investigated for this reaction; only two examples of alkenyl carboxylic acids and no examples of alkyl carboxylic acids were found.^{209, 212}



Scheme 4.7: Stage one optimization considerations.

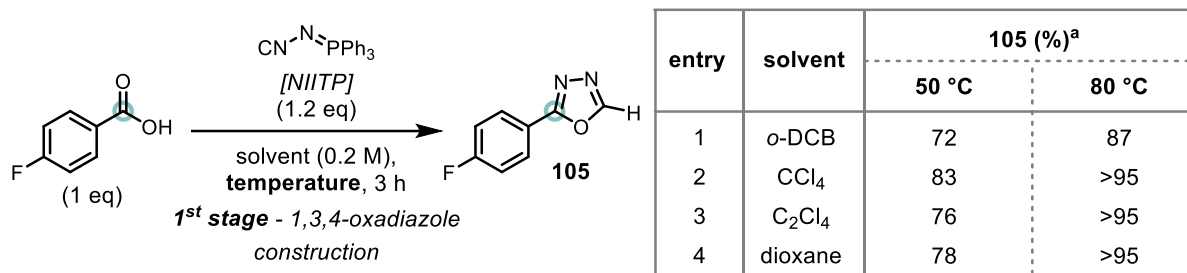
The optimization was initiated by an extensive solvent screen, using 4-fluorobenzoic acid as our model substrate yielding 2-substituted 1,3,4-oxadiazole **105** as the product, and allowing for facile reaction monitoring by ^{19}F NMR. The evaluation of the reactions after only 3 hours allowed the assessment of the comparative speeds of 1,3,4-oxadiazole construction (scheme 4.8). This revealed that the best solvents for the reaction were 1,2-dichlorobenzene (entry 1), dichloromethane (entry 3), and tetrachloromethane (entry 4) as they gave clean reaction profiles and yields of **105** above 30%. Toluene gave a high reaction yield (40%) however, a complex reaction profile with multiple peaks not corresponding to either 4-fluorobenzoic acid or **105** was observed by ^{19}F NMR (entry 2); moreover, 1,2-dichloroethane (entry 5), ethanol (entry 6), and acetonitrile (entry 13), gave similarly complex reaction profiles. Tetrachloroethene furnished **105** in 26% yield with a clean reaction profile (entry 7). The ethereal solvents dioxane (entry 8) and tetrahydrofuran (entry 9) gave poor yields of **105**, however in these solvents it was observed that NIITP was insoluble potentially hindering its reactivity. Furthermore, although polar aprotic solvents DMF (entry 10) and DMSO (entry 11) gave homogenous reaction mixtures, low yields (<10%) were witnessed. 2,2,2-Trifluoroethanol gave trace yields of **105** (entry 12), indicating that its increased polarity compared to ethanol (entry 6) is detrimental to the 1,3,4-oxadiazole construction.



entry	solvent	105 (%) ^a
1	o-DCB	45
2	PhMe	40 (complex reaction profile)
3	CH ₂ Cl ₂	37
4	CCl ₄	34
5	DCE	34 (complex reaction profile)
6	EtOH	< 30 (complex reaction profile)
7	C ₂ Cl ₄	26
8	dioxane	13
9	THF	12
10	DMF	9
11	DMSO	6
12	TFE	trace
13	MeCN	>6 ¹⁹ F peaks observed

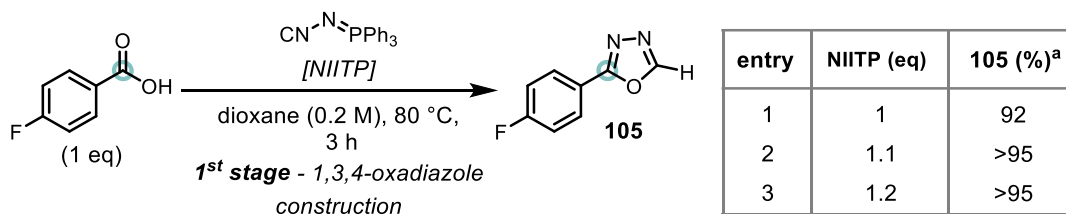
Scheme 4.8: Solvent screen (0.1 mmol scale) in descending order by NMR yields. ^a ¹⁹F{¹H} NMR yield determined by comparing the starting material, **105**, and side-products' peaks.

As none of the above solvents provided full conversion to **105** during the limited 3 hour reaction time, a second solvent screen at 50 °C was conducted (scheme 4.9). For this, a range of solvents consisting of chlorinated solvents that performed well at rt, and dioxane (due to its prevalence in 1,3,4-oxadiazole C-H functionalization) were evaluated (entries 1 – 4). All the solvents chosen achieved high yields of **105** (>70%) within the 3 hour reaction time. Moreover, this revealed dioxane as an excellent reaction solvent giving **105** in 78% yield (entry 4), and a homogenous reaction mixture at the temperature used. A further screening round conducted at 80 °C, using the same solvents, revealed that three of the four solvents chosen now gave quantitative NMR yields of **105** during the 3 hour reaction time (scheme 4.9).



Scheme 4.9: Solvent screen at 50 °C and 80 °C (0.1 mmol scale). ^a ¹⁹F{¹H} NMR yield determined by comparing the starting material, **105**, and side-products' peaks.

Dioxane, being frequently used in 1,3,4-oxadiazole C-H functionalizations (section 1.2.3), was chosen for further optimization which showed a small excess (1.1 equivalents) of NIITP to be optimal – giving >95% NMR yield of **105** after the 3 hour reaction time (scheme 4.10).

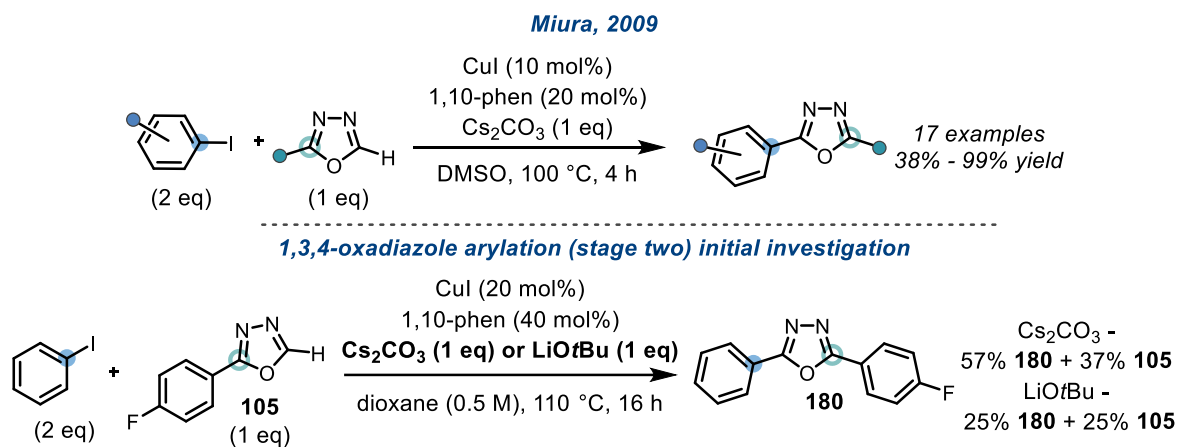


Scheme 4.10: NIITP stoichiometry screen (0.1 mmol scale). ^a ¹⁹F{¹H} NMR yields were determined by comparing the starting material, **105**, and side-products' peaks.

4.3.2 Optimization of the One-Pot 1,3,4-Oxadiazole Construction-Arylation Protocol

With an effective method for the synthesis of **105** established, combining the optimized conditions with a 1,3,4-oxadiazole C-H arylation methodology was next investigated. Evaluating the literature, a copper-catalyzed 1,3,4-oxadiazole C-H arylation with aryl iodides, reported by Muira,¹⁰¹ was chosen for examination (schemes 1.12 & 4.11, top). Its use of an abundant copper(I) iodide/1,10-phenanthroline catalytic system and feedstock aryl iodide electrophiles was seen as advantageous. The reported methodology utilizes DMSO as a reaction medium, however firstly dioxane was evaluated as a replacement solvent, using both cesium carbonate and lithium *tert*-butoxide as bases (scheme 4.11, bottom). Satisfyingly, this

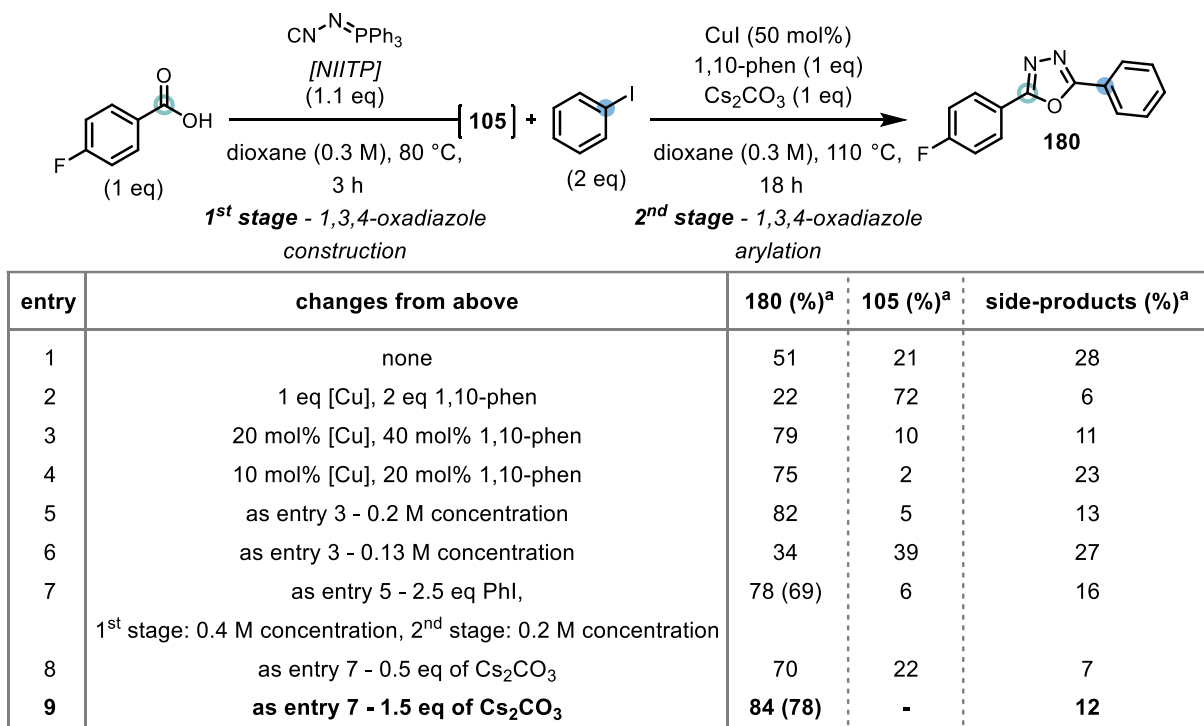
showed dioxane as a suitable solvent for the reaction giving a 57% yield of product **180**, with a remaining 37% of **105** unconsumed using cesium carbonate as a base. Lithium *tert*-butoxide provided low a low yield of both **180** and **105**, showing that ~ 50% of **105** had decomposed into unidentified side-products.



Scheme 4.11: Investigation of dioxane as a reaction solvent for 1,3,4-oxadiazole C-H arylation (0.1 mmol scale). $^{19}\text{F}\{^1\text{H}\}$ NMR yields were determined by comparing **105**, **180**, and side-products' peaks.

With dioxane proven as a suitable reaction medium, optimization of a one-pot 1,3,4-oxadiazole construction-arylation protocol was performed (scheme 4.12). This commenced with use of 50 mol% copper(I) iodide as a catalyst and 1 equivalent of 1,10-phenanthroline as a ligand for the 1,3,4-oxadiazole arylation, which gave the desired product **180** in 51% yield (entry 1). Increased catalyst and ligand loading led to lower conversion (entry 2), and a loading of 20 mol% copper(I) iodide with 40 mol% 1,10-phenanthroline was found to be optimal (entry 3). Lower catalyst, and ligand, loadings resulted in diminished yields of **180** and increased quantities of side-products (entry 4). Varying the reaction concentration revealed that a concentration of 0.2 M was beneficial (entry 5), with a lower reaction yield observed at a reaction concentration of 0.13 M (entry 6). For practicality, dilution of the reaction mixture to the optimal concentration of 0.2 M after the completion of the reaction's first stage – ensuring full transfer of the reagents added

for the second stage into the reaction mixture – was assessed and gave a 69% isolated yield of **180** (entry 7). Finally, scrutiny of the amount of cesium carbonate used showed 1.5 equivalents to be optimal, and gave the desired 2,5-disubstituted 1,3,4-oxadiazole **180** in an excellent 78% isolated yield in a single-pot protocol (entries 8 & 9). This gave the standard conditions for the reaction scope to be those shown at the top of scheme 4.13.



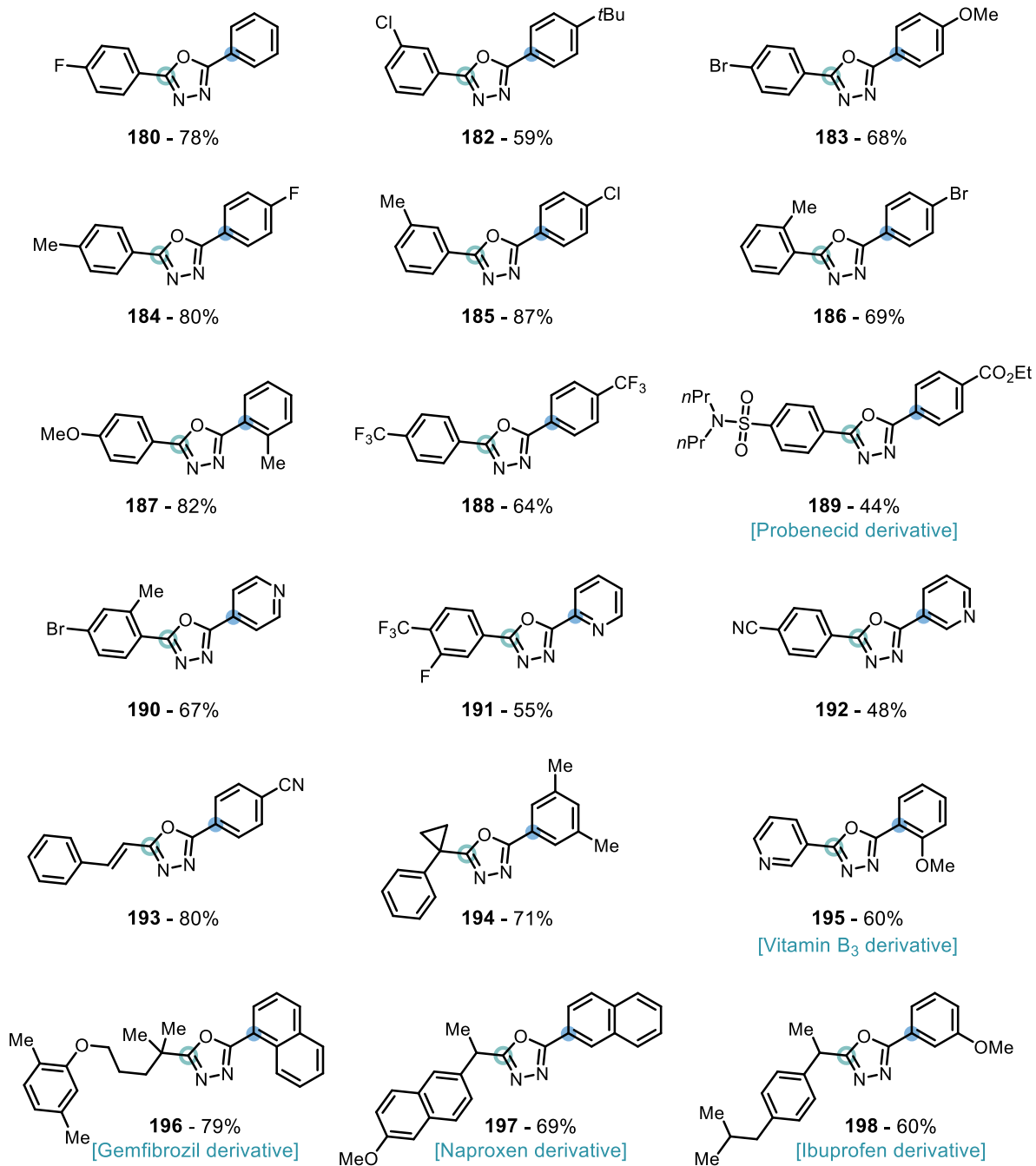
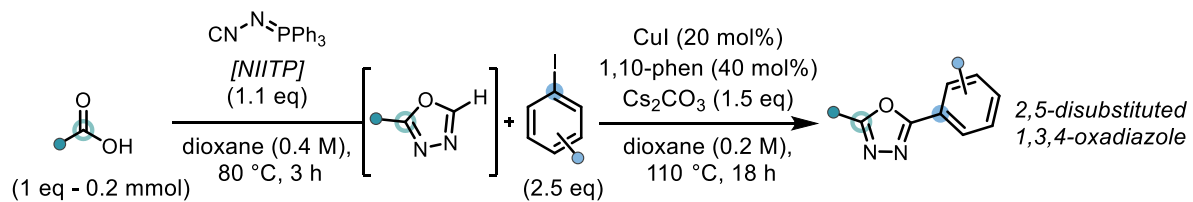
Scheme 4.12: 1,3,4-Oxadiazole construction-arylation reaction optimization (0.1 mmol scale).

^a ¹⁹F{¹H} NMR yields were determined by comparing **105**, **180**, and side-products' peaks, isolated yields in parentheses.

4.3.3 Reaction Scope of the 1,3,4-Oxadiazole Construction-Arylation Protocol

With the one-pot 1,3,4-oxadiazole construction-arylation protocol optimized, the reaction scope was explored (scheme 4.13). The aryl iodide and carboxylic acid coupling partners were varied concurrently to maximize the diversity of the 2,5-disubstituted 1,3,4-oxadiazole products obtained from this multicomponent approach (scheme 4.13).

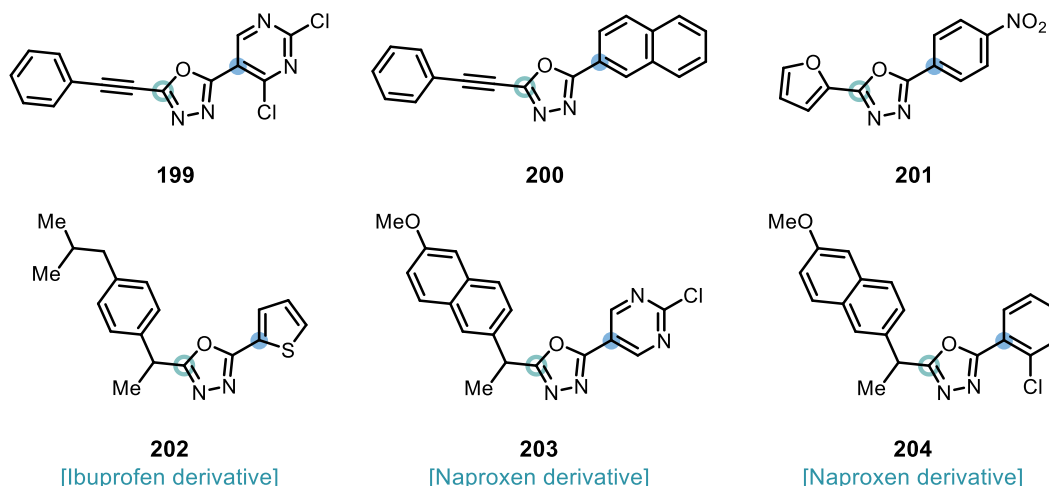
Firstly, analyzing the scope of the carboxylic acid reaction partner, it was found that, along with the 4-fluorobenzoic acid (**180**) used in the model reaction, 3-chlorobenzoic acid (**182**), and 4-bromobenzoic acid (**183**) were tolerated and gave the 1,3,4-oxadiazole products **182** and **183** without undergoing any potential dehalogenative side-reactions being observed. The successful use of 4-methylbenzoic acid (**184**), 3-methylbenzoic acid (**185**), and 2-methylbenzoic acid (**186**) proved the reaction's insensitivity towards steric effects. Electron-rich 4-methoxybenzoic acid (**187**), and electron-poor 4-(trifluoromethyl)benzoic acid (**188**) and probenecid (**189**) afforded the desired 1,3,4-oxadiazole products **187**, **188**, and **189** in 82%, 64%, and 44% yield, respectively. Utilization of disubstituted benzoic acids 4-bromo-2-methylbenzoic acid (**190**) and 3-fluoro-4-(trifluoromethyl)benzoic acid (**191**) revealed the reactions ability to yield complex 2,5-disubstituted 1,3,4-oxadiazole structures in a single synthetic step. The scope of benzoic acids was concluded with use of 4-cyanobenzoic acid furnishing **192** in 48% yield. Advancing forwards, alkenyl (**193**) and alkyl (**194**) carboxylic acids were used and pleasingly gave excellent yields of the alkenyl and alkyl substituted 1,3,4-oxadiazole products **193** and **194**. Additionally, the application of APIs vitamin B₃ (**195**), gemfibrozil (**196**), naproxen (**197**), and ibuprofen (**198**) to the developed methodology demonstrated its capability for the late-stage functionalization of carboxylic acids – key components of numerous biologically active molecules.³⁶⁻⁴⁰



Scheme 4.13: 1,3,4-Oxadiazole construction-arylation reaction scope (0.2 mmol scale).

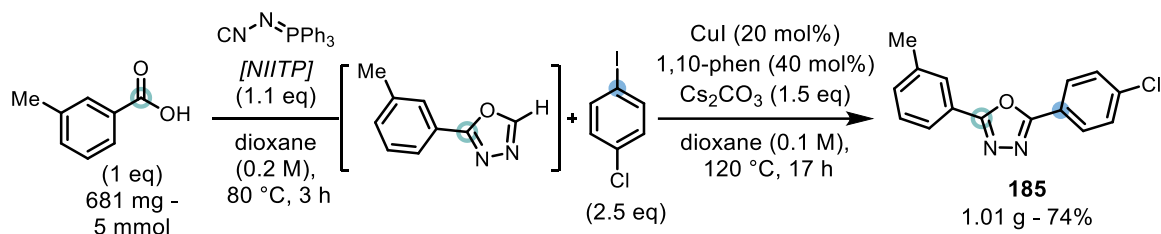
Reviewing the scope of the aryl iodide component, it was found that electron rich coupling partners 1-(tert-butyl)-4-iodobenzene (**182**) and 1-iodo-4-methoxybenzene (**183**) gave 1,3,4-oxadiazole products **182** and **183** in 59% and 68% yield respectively. A series of halogen containing aryl iodides was next evaluated and this showed that 4-fluoro (**184**), 4-chloro (**185**), and 4-bromo (**186**) substituents were well tolerated and provided products **184** – **186**, once again without the formation of dehalogenated side-products. The reaction's sensitivity to sterics was tested with 1-iodo-2-methylbenzene (**187**) which afforded **187** in an excellent 82% yield. Coupling partners bearing electron-withdrawing trifluoromethyl (**188**), and ethyl ester (**189**) groups were tolerated giving good yields of the 1,3,4-oxadiazole products **188** and **189**. Next, employing all possible regioisomers of iodopyridine (**190** – **192**) identified the reaction's tolerance to heteroaryl moieties. Furthermore, a varied set of aryl iodides including 4-iodobenzonitrile (**193**), 1-iodo-3,5-dimethylbenzene (**194**), 1-iodo-2-methoxybenzene (**195**), 1-iodonaphthalene (**196**), 2-iodonaphthalene (**197**), and 1-iodo-3-methoxybenzene (**198**) were all successfully utilized and afforded diverse 2,5-disubstituted 1,3,4-oxadiazole structures **193** – **198** in good (60%) to excellent (80%) yields.

During exploration of the reaction scope there were a number of reactions that failed to yield the desired 2,5-disubstituted 1,3,4-oxadiazole products – shown in scheme 4.14. Attempts to synthesize compounds **199** and **200** failed, probably due to the use of 3-phenylpropionic acid as the carboxylic acid component, as the aryl iodide component for **200** (2-iodonaphthalene) was used successfully for the synthesis of **197** (scheme 4.13). Unfortunately, as neither the carboxylic acid nor the aryl iodide coupling partner for **201** were utilized successfully in the reaction scope, it could not be determined which component was the cause of the reaction's failure. Presumably, intolerance of the aryl iodide coupling partners led to undesirable results during synthesis of compounds **202** – **204** as both naproxen and ibuprofen were later used successfully for the synthesis of **197** and **198** (scheme 4.13).



Scheme 4.14: Failed examples (0.2 mmol scale).

Despite this, to further exemplify the effectiveness of the developed method, a 5 mmol scale reaction was performed and yielded 1.01 g of **185** in a one-pot reaction using only commercially available materials (scheme 4.15).



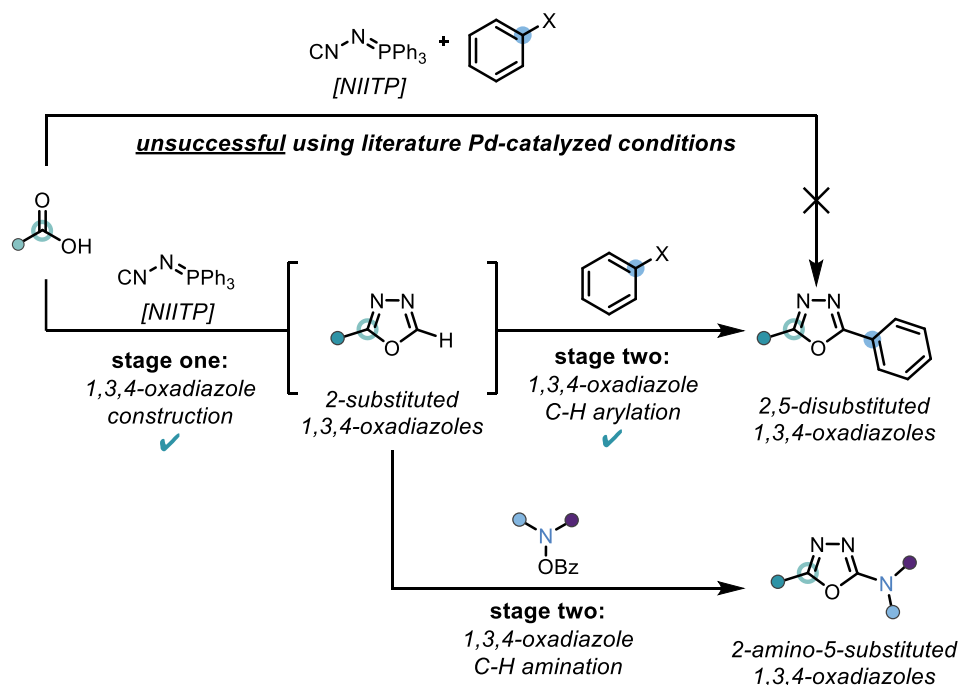
Scheme 4.15: A 5 mmol scale 1,3,4-oxadiazole construction-arylation example.

4.4 Development of a 1,3,4-Oxadiazole Construction-Amination Using Electrophilic Amine Coupling Partners

4.4.1 Concept

Having successfully identified an effective strategy for the one-pot synthesis of 2,5-disubstituted 1,3,4-oxadiazoles, exploring alternative C-H functionalizations for the second stage of the protocol was next prioritized. To this end, a C-H amination using electrophilic amine coupling partners – mirroring the aryl iodides previously used, and as preceded in section

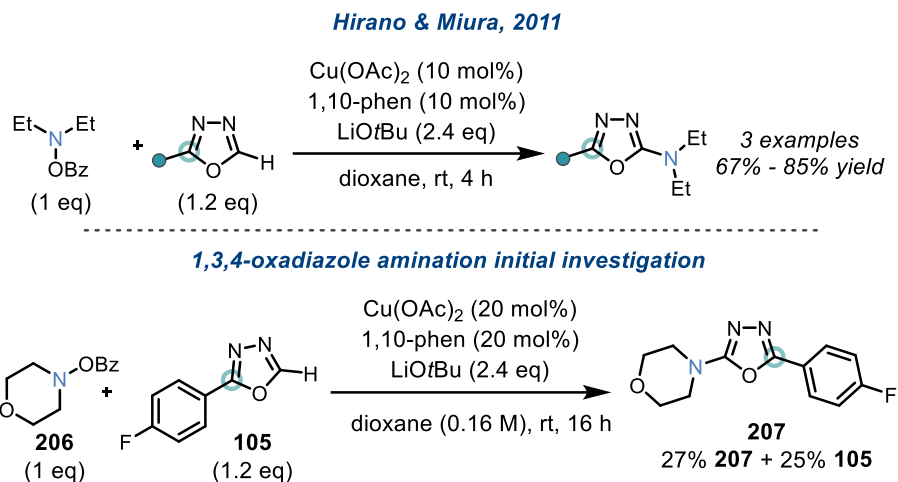
1.2.3.2 – was chosen to explore the possibility of installing C-N bonds using the strategy, thus increasing the diversity of 1,3,4-oxadiazoles available from a single carboxylic acid precursor (scheme 4.16).



Scheme 4.16: Extension of the 1,3,4-oxadiazole construction-functionalization strategy for the synthesis of 2-amino-5-substituted 1,3,4-oxadiazoles using electrophilic amine coupling partners.

4.4.2 Initial Experiments and Optimization

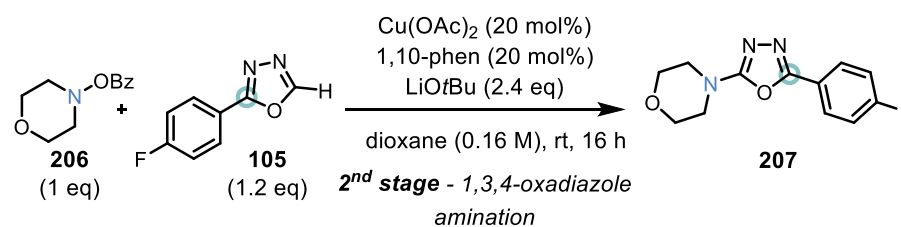
First, encouraged by previous successes with a copper catalyst in the 1,3,4-oxadiazole construction-arylation protocol, a copper(II) acetate-catalyzed C-H amination using *N*-benzoyloxy amines as coupling partners was investigated (scheme 4.17, top).¹⁸³ Morpholino benzoate (**206**) as a prevalent electrophilic aminating reagent was chosen as the model substrate, and when reacted with 2-substituted 1,3,4-oxadiazole **105** using conditions reported by Hirano and Miura it afforded a 27% conversion to the desired 2-amino-5-substituted 1,3,4-oxadiazole **207**, with an additional 25% of **105** observed by ¹⁹F NMR (scheme 4.17, bottom).



Scheme 4.17: Investigation into a 1,3,4-oxadiazole C-H amination with N-benzoyloxy amine coupling partners (0.1 mmol scale). $^{19}\text{F}\{^1\text{H}\}$ NMR yields were determined by comparing **105**, **207**, and side-products' peaks.

With a successful hit confirmed, the optimization of the synthesis of **207** was conducted (scheme 4.18). Attempts to substitute lithium *tert*-butoxide with cesium carbonate provided low conversions at room temperature and at 50 °C (entries 2 & 3). Furthermore, the use of elevated temperatures (110 °C) led to significant decomposition of **105** without an increase in conversion to **207** (entry 4). Concentration of the reaction mixture led to lower conversion (entry 5); however, an increased conversion was obtained upon dilution of the reaction mixture (entry 6). Subsequent experiments revealed that a lower catalyst loading gave increased conversion to **207** (entry 7) and although a similar conversion was noted in the absence of 1,10-phenanthroline, this result was accompanied by an increase in side-product formation (entry 8). The use of copper(I) acetate gave none of the desired product **207**, illustrating that use of copper(II) acetate is critical (entry 9). Disappointingly, an increase in the catalyst and ligand loading to 50 mol% afforded no increase in conversion to **207** (entry 10), and removal of the 1,10-phenanthroline ligand proved beneficial again (entry 11). A breakthrough finally occurred when using triphenylphosphine as the ligand, giving 66% conversion to **207**, with 32% of **105**

and only 2% of side-products observed (entry 12). An increase (entry 13), or decrease (entry 14), in the loading of copper(II) acetate and triphenylphosphine proved to be detrimental to the conversion, even at slightly elevated temperatures (entry 15). Finally, optimal conditions were found using 50 mol% of copper(II) acetate with 1 equivalent of triphenylphosphine as the ligand with a reaction temperature of 40 °C giving an excellent 78% conversion to **207**, and almost complete consumption of **105** (entry 16).



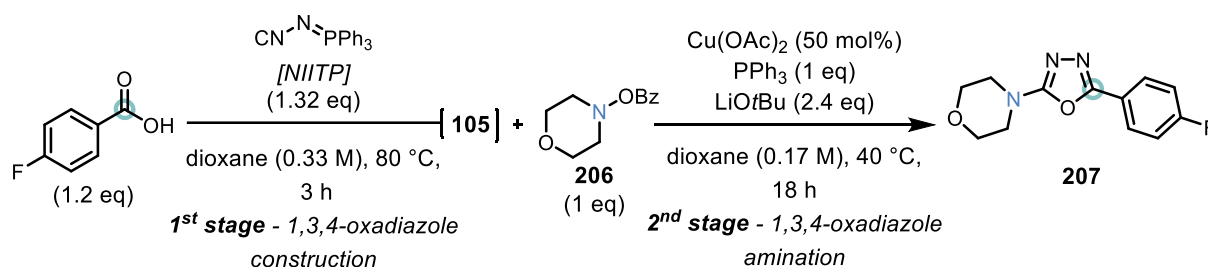
entry	changes from above	207 (%) ^a	105 (%) ^a	side-products (%) ^a
1	none	27	25	48
2	Cs ₂ CO ₃ (2.4 eq) as base, rt	7	93	-
3	as entry 2 - 50 °C	19	81	-
4	as entry 2 - 110 °C	19	33	48
5	0.33 M concentration	10	60	30
6	0.083 M concentration	42	24	34
7	Cu(OAc) ₂ (10 mol%), 1,10-phen (10 mol%),	41	41	18
8	Cu(OAc) ₂ (10 mol%), no 1,10-phen	41	27	32
9	CuOAc (10 mol%), 1,10-phen (10 mol%)	-	50	50
10	Cu(OAc) ₂ (50 mol%), 1,10-phen (50 mol%)	40	40	20
11	Cu(OAc) ₂ (50 mol%), no 1,10-phen	54	19	27
12	Cu(OAc)₂ (50 mol%), PPh₃ (1 eq) as ligand	66	32	2
13	Cu(OAc) ₂ (1 eq), PPh ₃ (2 eq) as ligand	57	6	37
14	Cu(OAc) ₂ (10 mol%), PPh ₃ (20 mol%) as ligand	47	37	16
15	as entry 14 - 50 °C	52	12	36
16	as entry 12 - 40 °C	78	4	18

Scheme 4.18: 1,3,4-Oxadiazole C-H amination reaction optimization (0.1 mmol scale).^a

¹⁹F{¹H} NMR yields were determined by comparing **105**, **207**, and side-products' peaks.

With an optimal set of conditions for the 1,3,4-oxadiazole C-H amination established, these conditions were then translated into a one-pot synthesis of 2-amino-5-substituted 1,3,4-

oxadiazole **207**, starting from 4-fluorobenzoic acid (scheme 4.19). This revealed that under the optimized conditions a reduced conversion of 61% to **207** was obtained. Fortunately, an increase in the loading of copper(II) acetate and triphenylphosphine effectively recovered the conversion to that previously seen in scheme 4.18, entry 16 and gave a 64% isolated yield of the desired product **207**. This gave the standard reaction conditions used for the investigation of the scope and limitations of a one-pot 1,3,4-oxadiazole construction-amination as those shown at the top of scheme 4.20.



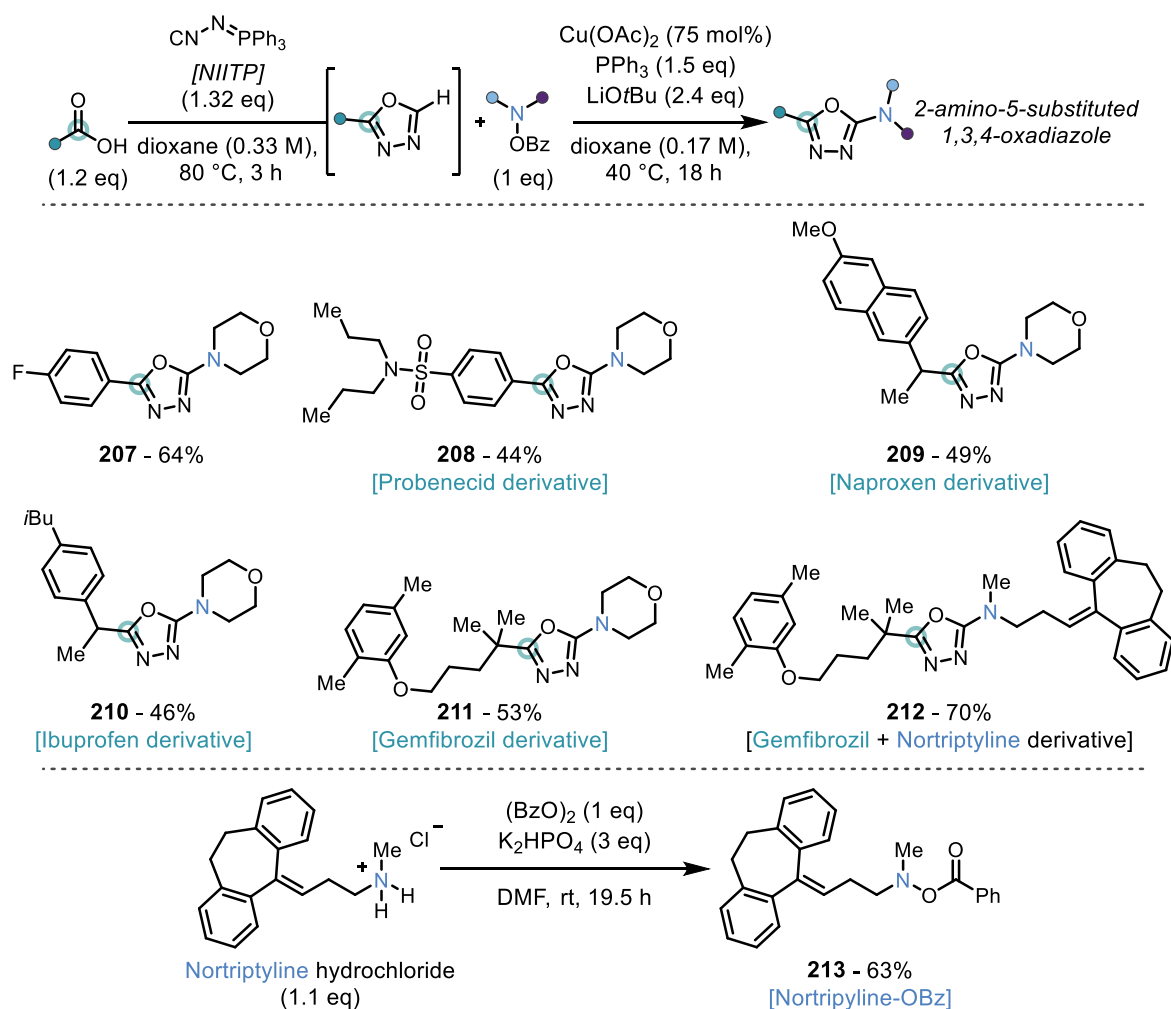
entry	changes from above	207 (%) ^a	105 (%) ^a	side-products (%) ^a
1	None	61	31	8
2	Cu(OAc)₂ (75 mol%), PPh₃ (1.5 eq)	76 (64)	13	11

Scheme 4.19: 1,3,4-Oxadiazole construction-amination reaction optimization (0.17 mmol scale). ^a ¹⁹F{¹H} NMR yields were determined by comparing **105**, **207**, and side-products' peaks, isolated yields in parentheses.

4.4.3 Reaction Scope of the 1,3,4-Oxadiazole Construction-Amination Protocol

A one-pot 1,3,4-oxadiazole construction-amination protocol established, the scope with respect to the carboxylic acid component was explored with **206** as the coupling partner (scheme 4.20, middle). This involved the application of four carboxylic acid containing APIs, probenecid (**208**), naproxen (**209**), ibuprofen (**210**), and gemfibrozil (**211** & **212**), to the developed methodology. A choice made to highlight the potential of the methodology for late-stage functionalization of carboxylic acids. This afforded the corresponding 2-amino-5-substituted 1,3,4-oxadiazoles **208**

– **211** in yields ranging from 44% to 53%. To demonstrate how the method could be applied for the late-stage functionalization of secondary amine containing APIs, an *N*-benzoyloxy derivative of nortriptyline (**213**) was synthesized in a single step using dibenzoyl peroxide as an electrophilic benzyloxy source (scheme 4.20, bottom).³⁶⁵ When **213** was applied in the developed method, with gemfibrozil as the carboxylic acid coupling partner, it afforded the 1,3,4-oxadiazole-fused drug-drug conjugate **212** in an excellent 70% isolated yield.

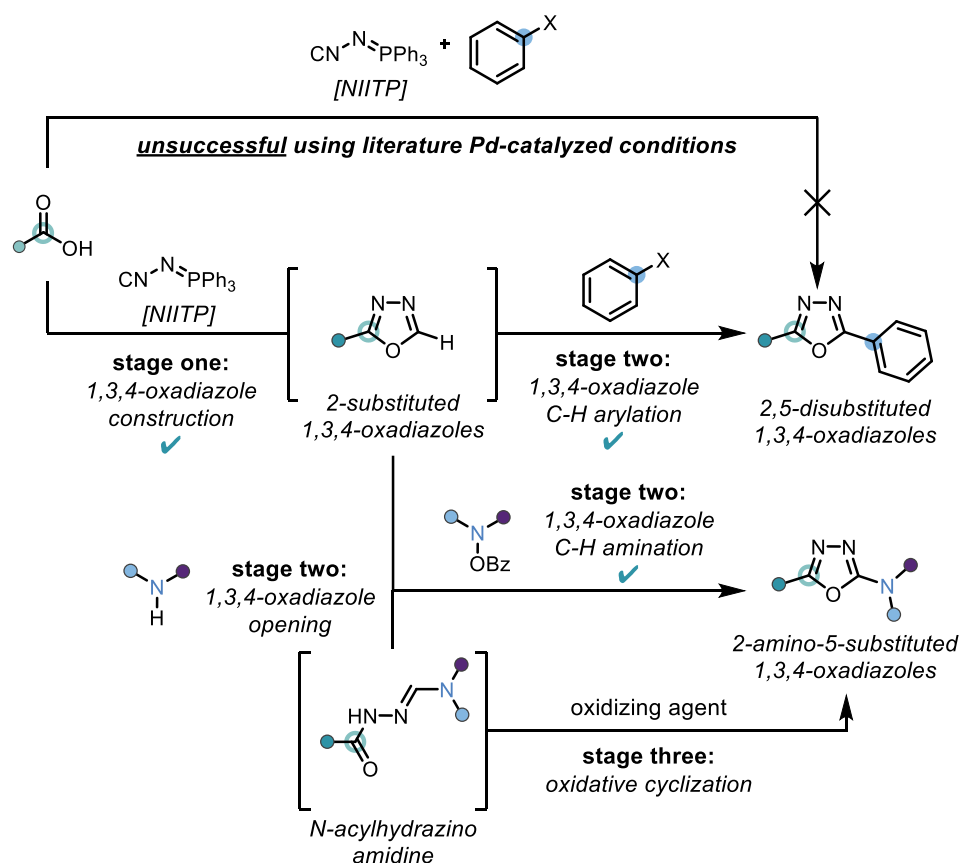


Scheme 4.20: 1,3,4-Oxadiazole construction-amination reaction scope (0.17 mmol scale), and synthesis of nortriptyline-OBz **213**.

4.5 Development of a 1,3,4-Oxadiazole Construction-Amination Using Nucleophilic Amine Coupling Partners

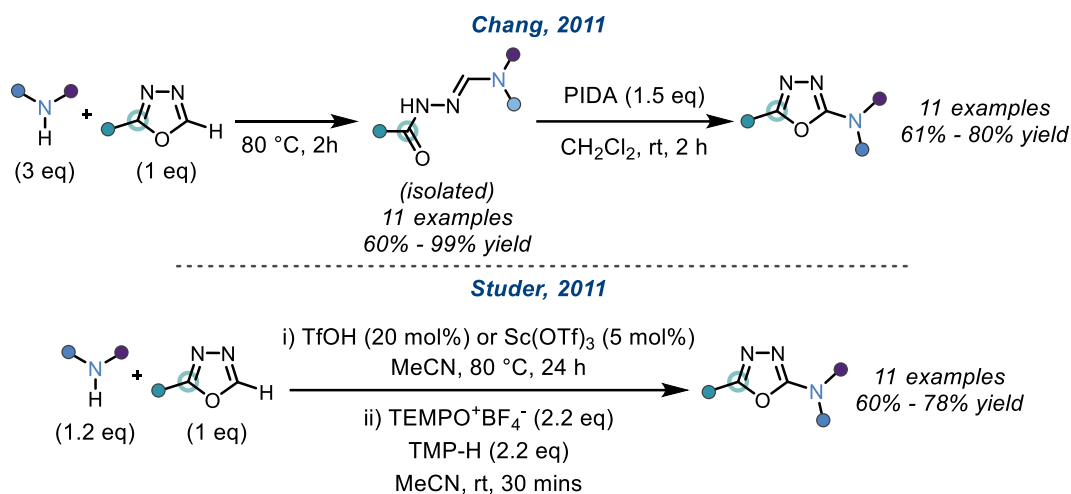
4.5.1 Concept

Finding electrophilic amine coupling partners amenable to our one-pot 1,3,4-oxadiazole construction-functionalization strategy, an extension focusing on the use of nucleophilic amine coupling partners was a logical next step (scheme 4.21, for relevant precedence see section 1.2.3.2). Crucially, the use of secondary amine coupling partners would eliminate the need for any functionalization of the starting materials providing a desirable and practical protocol using only feedstock chemicals as starting materials.



Scheme 4.21: Extension of the 1,3,4-oxadiazole construction-functionalization strategy for synthesis of 2-amino-5-substituted 1,3,4-oxadiazoles using nucleophilic amines.

After evaluating the relevant literature precedent for 2-substituted 1,3,4-oxadiazole amination using secondary amine reaction partners, reports from the Chang,¹⁷⁵ and Studer groups stood out as promising starting points for the optimization of the strategy (scheme 4.22).¹⁷⁸ Chang's report utilizes thermal activation, a high concentration (i.e., neat), and an excess of the secondary amine partner to open the 1,3,4-oxadiazole ring and afford an *N*-acylhydrazino amidine; which, after isolation, could be oxidized to the desired 2-amino-5-substituted 1,3,4-oxadiazole products using PIDA (scheme 4.22, top).¹⁷⁵ The Studer group has disclosed a one-pot approach to this transformation using a Brønsted- or Lewis-acid to promote the ring-opening of the 2-substituted 1,3,4-oxadiazole by a small excess of a secondary amine. Subsequently, the addition of TEMPO⁺BF₄⁻ promotes an oxidative ring-closure to afford the 2-amino-5-substituted 1,3,4-oxadiazole product in a one-pot reaction (scheme 4.22, bottom).

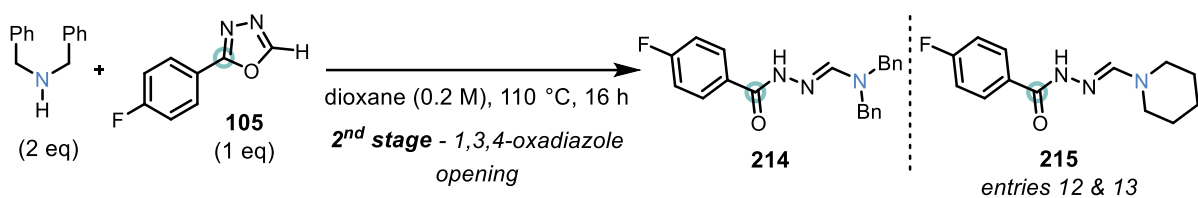


Scheme 4.22: Precedent for 2-amino-5-substituted 1,3,4-oxadiazole synthesis from secondary amines and 2-substituted 1,3,4-oxadiazoles.

4.5.2 Optimization of the Nucleophilic 1,3,4-Oxadiazole Ring-Opening

Studer's reported conditions served as a starting point for our investigation, however it was previously observed that acetonitrile was a poor solvent for the 1,3,4-oxadiazole construction using NIITP (scheme 4.8). As such, an optimization of the opening of 2-substituted 1,3,4-

oxadiazole **105** using dioxane as the reaction solvent – being optimal for 1,3,4-oxadiazole construction using NIITP (section 4.3.1) – was conducted with dibenzylamine as a model secondary amine (scheme 4.23). No reaction was observed in the absence of an acid catalyst (entry 1), and low conversions were obtained in the presence of catalytic quantities of either scandium(III) triflate (entry 2), or *para*-toluene sulfonic acid (entry 3). Agreeably, the use of a phosphoric acid (diphenyl phosphate, entry 4) or a disulfonimide (Ts₂NH, entry 5) Brønsted-acidic catalyst gave promising 46% and 56% yields of **214**, respectively. An increase in the loading of the disulfonimide catalyst to 1 equivalent (entry 6), or a decrease to 20 mol% delivered lower yields of **214** (entry 7). An increased amount of dibenzylamine failed to provide a significant uplift in conversion (entry 8). Moreover, the reaction concentration was found to have a significant effect, with higher concentrations giving increased yields of **214** (entries 9 & 10), with use of a 0.4 M reaction concentration being chosen for further optimization (entry 9). A 1.5x increase in reaction time (16 h to 24 h) failed to improve the yield of **214** obtained (entry 11). Gratifyingly, exchanging dibenzylamine for piperidine, together with an exchange of disulfonimide Ts₂NH for the commercially available disulfonimide (PhSO₂)₂NH, gave a substantial uplift in yield with 88% of **215** observed (entry 12). Finally, increasing the reaction concentration from 0.2 M to 0.4 M gave an excellent 93% NMR yield of **215** with only 3% of **105** remaining (entry 13).



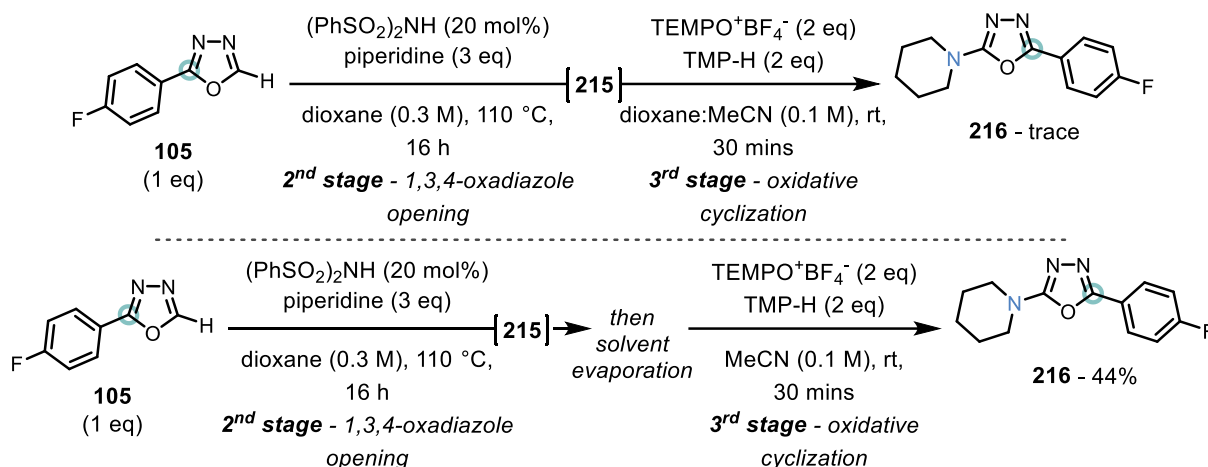
entry	changes from above	product (%) ^a	105 (%) ^a
1	none - no catalyst	-	100
2	Sc(OTf) ₃ (20 mol%)	8	90
3	PTSA (50 mol%)	8	86
4	(PhO) ₂ P(O)OH (50 mol%)	46	44
5	Ts ₂ NH (50 mol%)	56	36
6	Ts ₂ NH (1 eq)	33	50
7	Ts ₂ NH (20 mol%)	52	45
8	as entry 3 - Bn ₂ NH (3 eq)	64	25
9	as entry 4 - 0.4 M concentration	68	23
10	as entry 4 - 0.8 M concentration	78	14
11	as entry 8 - 24 h reaction time	64	24
12	piperidine (2 eq) as nucleophile, (PhSO ₂) ₂ NH (20 mol%), 0.2 M concentration ^b	88	9
13	as entry 12 - 0.4 M concentration ^b	93	3

Scheme 4.23: Optimization of nucleophilic ring opening of **105** in dioxane (0.1 mmol scale).^a

¹⁹F{¹H} NMR yields were determined by comparing **105**, **214** (or **215**), and side-products' peaks. ^b **215** produced as product.

4.5.3 Investigations into the Oxidative Ring-Closure

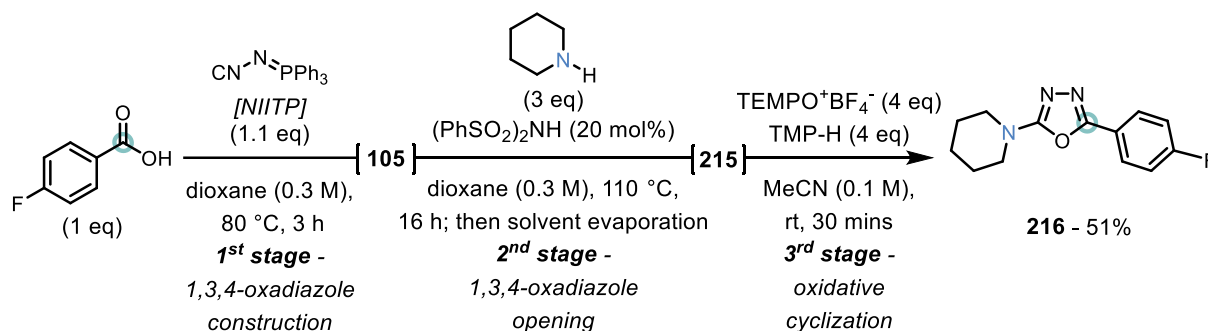
With a reliable method for the opening of 2-substituted 1,3,4-oxadiazole **105** with piperidine found, the integration of this method into a one-pot synthesis of 2-amino-5-substituted 1,3,4-oxadiazole **216** from **105** was attempted (scheme 4.24). Our initial investigations of a two-stage process found a solvent mixture of dioxane and acetonitrile was unsuitable for an oxidative cyclization using TEMPO⁺BF₄⁻, yielding only trace quantities of **216** (scheme 4.24, top). However, performing a full solvent switch to acetonitrile after the 1,3,4-oxadiazole ring opening pleasingly afforded the desired 1,3,4-oxadiazole **216** in 44% isolated yield over the two-steps (scheme 4.24, bottom).



Scheme 4.24: Investigations into a two-stage synthesis of 2-amino-5-substituted 1,3,4-oxadiazole **216** from **105**.

4.5.4 Proof-of-Concept of a Three-Stage One-Pot Protocol

These separate investigations were then assembled into a one-pot protocol (scheme 4.25). This proved to be successful, furnishing 2-amino-5-substituted 1,3,4-oxadiazole **216** in 51% isolated yield over three steps (an average of 80% per step). This result provides an excellent proof-of-concept for a potential future project, and an exemplar of the practicality, and flexibility, of the developed 1,3,4-oxadiazole construction-functionalization strategy.



Scheme 4.25: A three-stage one-pot synthesis of 2-amino-5-substituted 1,3,4-oxadiazole

216.

4.6 Conclusion and Future Work

In conclusion, a one-pot, and multicomponent, 1,3,4-oxadiazole construction-functionalization strategy has been established for the synthesis of 2,5-disubstituted (or 2-amino-5-substituted) 1,3,4-oxadiazoles from feedstock carboxylic acids, NIITP, and aryl iodides (or *N*-benzoyloxy amines). Alkyl and aryl carboxylic acid coupling partners were successfully utilized in both methodologies and the arylative method was tolerant of (hetero)aryl iodides, including iodopyridines. The aminative method was successfully utilized for the late-stage functionalization of the secondary amine API nortriptyline *via* its *N*-benzoyloxy derivative. An extension of the aminative protocol to include the use of nucleophilic secondary amine reaction partners was investigated, and proof-of-concept obtained for a three-stage one-pot synthesis of the 2-amino-5-substituted 1,3,4-oxadiazole **216** in a promising 51% yield.

Future work based on this project, and in particular the results discussed in section 4.5, would be three-fold: firstly, a screen of oxidants used for the oxidative cyclization would be essential to find a reagent that is compatible with dioxane as a solvent to avoid an undesirable, and inefficient, late-stage solvent switch. Secondly, further investigation of the 1,3,4-oxadiazole ring opening with a range of secondary amines would be required with the target of developing of a general methodology. Finally, beyond arylations and aminations, there are still many existing 2-substituted 1,3,4-oxadiazole C-H functionalization methodologies (see section 1.2.3), that could find application to the developed 1,3,4-oxadiazole construction-functionalization strategy, and streamline the synthesis of complex 1,3,4-oxadiazole containing molecules.

Chapter 5: Experimental Section

5.1 General Experimental Details

General Techniques: Reactions were carried out under a nitrogen atmosphere unless stated otherwise. Glassware was oven-dried and cooled under vacuum then purged with nitrogen before use. Room temperature refers to 22 ± 2 °C. Inert atmosphere techniques, such as Schlenk technique, were used for the handling of air/moisture sensitive reagents. Reactions carried out at 0 °C were cooled using an ice bath. Reactions carried out at high temperatures were heated using an oil bath or, preferably, using DrySyn® heating blocks. Reaction temperatures refer to external temperatures, for example of a heating block or oil bath, not of internal reaction temperatures unless stated otherwise.

Nomenclature and Numbering: Compounds are named following IUPAC nomenclature as generated by ChemDraw. Compounds are numbered arbitrarily, and not according to the IUPAC system, to allow for comparison between series of like-compounds.

Solvents and Reagents: Where solvent dryness was important, CH_2Cl_2 , 1,4-dioxane, Et_2O , MeOH, THF, and PhMe were either obtained from Sure/Seal™ bottles purchased from Sigma-Aldrich, an MBRAUN-SPS solvent purification system in which solvent is passed through an activated alumina column under nitrogen, or by standing over 3 Å molecular sieves under an atmosphere of nitrogen. Reagents were used as obtained without further purification unless stated otherwise. Chromatography: Thin layer chromatography (TLC) was carried out using Merck aluminium backed DC60 F254 plates (particle size 0.2 mm). TLC sheets were visualised by UV light, then developed by staining with potassium permanganate, anisaldehyde, cerium ammonium molybdate, vanillin, or iodine on silica. Purification by flash column chromatography (FCC) was carried out using Merck silicagel 60 F254 (particle size 43–60 µm).

Characterisation: Proton (^1H) and carbon (^{13}C) spectra were recorded on Bruker AVANCE NEO600 (600/151 MHz), Bruker AVG400 (400/101 MHz), Bruker AVH400 (400/101 MHz), Bruker AVF400 (400/101 MHz), Bruker AVB500 (500/126 MHz), Bruker AVC500 (500/126 MHz), and Bruker DPX200 (200 MHz) NMR spectrometers. Spectra are referenced to the residual solvent peak. Chemical shifts (δ) are given in parts per million (ppm, ± 0.01) and coupling constants (J) are given in Hertz (Hz, ± 0.1 as measured on Mestrenova, without rounding). The following convention is used to report chemical shifts: δ (multiplicity, coupling constant(s), number of protons, assignment (if possible)), with chemical shifts reported in descending order. Peak multiplicities are described as observed and as singlets (s), doublets (d), triplets (t), quartets (q), pentets (p), heptets (h), nonuplets (n), and in combination e.g. doublet of doublets (dd), or as a multiplet (m) over a peak range. Additionally, peaks may be described as broad (br), or apparent (app).

Infrared spectra were recorded using a Bruker Tensor 27 FT-IR spectrometer. Selected diagnostic absorption maxima (ν_{max}) are reported in wavenumbers (cm^{-1}). High resolution mass spectra were recorded by Chemistry Research Laboratory staff using a Bruker Daltronics MicroTOF spectrometer (ESI). Mass to charge ratios (m/z) are reported in Daltons. Melting points were recorded using a Leica Galen III hot-stage microscope apparatus and are reported uncorrected in degrees Celcius ($^{\circ}\text{C}$). Optical rotations were recorded using a Perkin Elmer 241 optical activity polarimeter at 25°C . The enantiomeric excesses were determined by HPLC analysis on an Agilent 1200 Series instrument employing a chiral stationary phase column specified in the individual experiment and by comparing the samples with the appropriate racemic, or scalemic, mixtures. Optical rotations were recorded using a Perkin Elmer 341 polarimeter; $[\alpha]_{\text{D}}^{\text{T}}$ values are reported in $10^{-1}\text{deg}\cdot\text{cm}^2\text{g}^{-1}$; concentrations (c) are quoted in g/100 mL; D refers to the D-line of sodium (589 nm); temperatures (T) are given in degrees Celsius ($^{\circ}\text{C}$). (+) and (–) compound number prefixes indicate the sign of the optical rotation.

Synthesis of known compounds: For compounds previously reported in the literature two relevant pieces of characterization data are given, unless the compound was used without purification or made by another group member and available in the laboratory. References are given for experimental procedures and data.

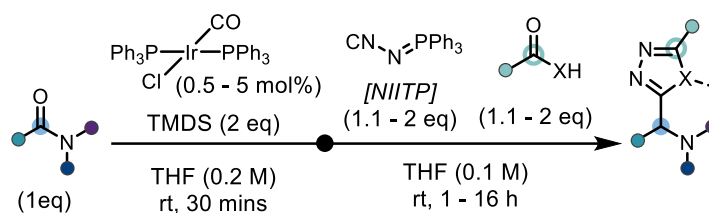
Starting materials: Carboxylic acids were obtained from commercial chemical suppliers and used as received unless stated otherwise.

Chapter 2: Tertiary amides and lactams were obtained from commercial chemical suppliers, or sourced from our group's, and others within the Chemical Research Laboratories' (CRL), internal chemical database, and used without analysis or purification unless stated otherwise.

Chapter 3: Compounds **127 – 135** were synthesized according to the procedure for compound **96**, and **150** according to Maruoka's procedure,³⁴⁶ by Tatiana Rogova and used without further analysis or purification. Compounds **109, 110, 112 – 123, 140, 147** and **148** were synthesized according to **General procedure B** by Elizabeth Boulter and full characterization data can be found within the cited references.^{361, 366}

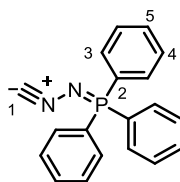
Chapter 4: Aryl iodides were obtained from commercial chemical suppliers and used as received. Copper(I) iodide (43153, Puratronic®, 99.998% metal basis), and copper(II) acetate (44355, 99.999% metal basis) were purchased from Alfa Aesar and used as received.

5.2 Experimental Details for Chapter 2

5.2.1 General Procedure A: Reductive Synthesis of α -Amino Heterodiazoles

To an oven-dried screw cap vial, equipped with magnetic stirrer, the amide (0.20 mmol, 1.0 eq) and IrCl(CO)(PPh₃)₂ (Vaska's complex, 0.5 – 5.0 mol%) were added. The vial was evacuated and backfilled with nitrogen (x3). Anhydrous THF (1.0 mL, 0.20 M) was added followed in quick succession by TMDS (71 μ L, 0.40 mmol, 2.0 eq), and the vial capped and stirred at rt. After 30 mins, the vial was opened and a suspension of NIITP (1.1 – 2.0 eq) in THF (1.0 mL, 0.10 M total) was added, followed by the appropriate O-, C-, S-, or N-Brønsted acid (1.1 – 2.0 eq) as a single portion. The vial was recapped and stirred at rt for 1 - 16 h. After this time CH₂Cl₂ (10 mL) was added and the reaction washed with saturated aqueous NaHCO₃ (20 mL), then the aqueous extracted with CH₂Cl₂ (3 x 10 mL). The combined organics were dried (MgSO₄), filtered, and concentrated *in vacuo* to afford the crude product. The crude was then purified by FCC, and subsequent PTLC when required, to afford the pure α -amino heterodiazole products.

5.2.2 Synthesis of Starting Materials

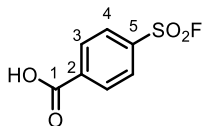
N-Isocyanoiminotriphenylphosphorane – NIITP – 2

To an over-dried flask was added formyl hydrazide (10 g, 167 mmol, 1.0 eq), triphenylphosphine (105 g, 400 mmol, 2.4 eq), DBU (62.3 mL, 416 mmol, 2.5 eq), and anhydrous MeCN (200 mL, 0.84 M). The reaction mixture was then warmed to 50 °C, and carbon tetrachloride (40.3 mL, 416 mmol, 2.5 eq) added dropwise over 1 h maintaining the reaction temperature at 50 °C. After complete addition, the reaction was allowed to stir at 50 °C for a further 2 h, and then cooled to 35 °C. Water (200 mL) was then added over 30 mins maintaining the reaction temperature at 35 °C, and after complete addition the reaction was allowed to cool to rt over 16 h. The reaction was then cooled to 0 °C for 30 mins and the precipitate isolated by filtration and washed with cold water:MeCN (1:1, 2 x 100 mL) to afford the *title compound* (36.2 g, 72%) as a beige powder. Data was consistent with that found in the literature.²⁰⁵

¹H NMR (400 MHz, CDCl₃) δ 7.74 – 7.61 (m, 9H), 7.57 – 7.49 (m, 6H).

³¹P NMR (162 MHz, CDCl₃) δ 28.6.

¹³C NMR (101 MHz, CDCl₃) δ 133.4 (d, *J* = 2.8, C₅), 132.9 (d, *J* = 9.4, C₄), 129.2 (d, *J* = 12.2, C₃), 125.3 (d, *J* = 97.9, C₂), 112.0 (d, *J* = 4.5, C₁).

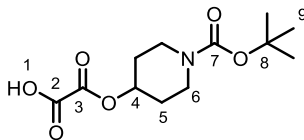
4-(fluorosulfonyl)benzoic acid – S1

To a rbf was added 4-(chlorosulfonyl)benzoic acid (500 mg, 2.3 mmol, 1.0 eq), potassium hydrogenfluoride (1.95 g, 25.0 mmol, 11 eq), MeCN (12.5 mL, 0.18 M), and water (12.5 mL, 0.18 M). The reaction mixture was allowed to stir at rt for 2 h before being diluted with water (150 mL) and extracted with EtOAc (3 x 50 mL). The combined organics were dried (MgSO₄), filtered, and concentrated *in vacuo* to afford the *title compound* (366 mg, 79%) as a beige powder. Data was consistent with that found in the literature.³⁶⁷

¹H NMR (400 MHz, DMSO) δ 13.81 (br, s, 1H, OH), 8.26 (s, 4H, C₃ & C₄).

¹⁹F NMR (376 MHz, DMSO) δ 66.0.

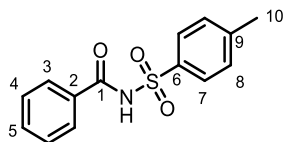
¹³C NMR (101 MHz, DMSO) δ 166.0 (C₁), 138.2 (C₂), 135.4 (d, *J* = 24.0, C₅), 131.4 (ArCH), 129.3 (ArCH).

2-((1-(*tert*-butoxycarbonyl)piperidin-4-yl)oxy)-2-oxoacetic acid – S2

To an oven-dried rbf was added 1-Boc-4-hydroxypiperidine (503 mg, 2.5 mmol, 1.0 eq), anhydrous CH_2Cl_2 (4.0 mL, 1.6 M), and anhydrous Et_2O (12.5 mL, 0.20 M). The reaction mixture was cooled to 0 °C and oxalyl chloride (420 μL , 5.0 mmol, 2.0 eq) was added dropwise. The reaction was then allowed to stir and reach rt over 24 h, before being cooled to 0 °C and quenched by the addition of water (50 mL). The aqueous was extracted with Et_2O (3 x 25 mL), and the combined organic dried (MgSO_4), filtered, and concentrated *in vacuo* to afford the *title compound* (682 mg, quant.) as a white solid. Data was consistent with that found in the literature.³⁶⁸

^1H NMR (400 MHz, CDCl_3) δ 11.05 (s, 1H, O₁), 5.09 (tt, $J = 7.8, 3.7$, 1H, C₄), 3.73 (ddd, $J = 13.6, 7.0, 4.0$, 2H, C₆), 3.30 (ddd, $J = 13.7, 8.3, 3.7$, 2H, C₆), 1.93 (ddt, $J = 14.2, 7.4, 3.8$, 2H, C₅), 1.82 – 1.70 (m, 2H, C₅), 1.45 (s, 9H, C₉).

^{13}C NMR (101 MHz, CDCl_3) δ 158.3 (C), 157.8 (C), 155.4 (C), 81.1 (C₈), 73.1 (C₄), 40.8 (C₆), 30.1 (C₅), 28.4 (C₉).

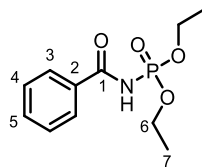
N-tosylbenzamide – 27

To an oven-dried rbf was added *p*-toluenesulfonamide (**29**) (856 mg, 5.0 mmol, 1.0 eq), triethylamine (1.4 mL, 10.0 mmol, 2.0 eq), DMAP (31 mg, 0.25 mmol, 5 mol%), anhydrous PhMe (6.25 mL, 0.80 M), and anhydrous EtOAc (2.5 mL, 2.0 M). To the reaction mixture was added benzoyl chloride (640 μ L, 5.5 mmol, 1.1 eq) as a single portion and the reaction was heated to 55 °C for 2 h. After this time the reaction was cooled to rt and aqueous HCl (2.0 M, 100 mL) added, and the reaction extracted with EtOAc (3 x 100 mL). The combined organics were then dried (MgSO₄), filtered, and concentrated *in vacuo* to afford the crude product. The crude was purified by recrystallization from EtOH to afford the *title compound* (740 mg, 54%) as a beige solid. Data was consistent with that found in the literature.³⁶⁹

¹H NMR (400 MHz, CDCl₃) δ 9.55 (s, 1H, NH), 8.10 – 8.04 (m, 2H, C₇), 7.89 – 7.83 (m, 2H, C₃), 7.61 – 7.52 (m, 1H, C₅), 7.46 – 7.40 (m, 2H, C₄), 7.39 – 7.34 (m, 2H, C₈), 2.45 (s, 3H, C₁₀).

¹³C NMR (101 MHz, CDCl₃) δ 164.5 (C₁), 145.3 (ArC), 135.5 (ArC), 133.5 (C₅), 131.2 (ArC), 129.7 (C₈), 128.9 (C₄), 128.7 (C₇), 127.9 (C₃), 21.7 (C₁₀).

diethyl benzoylphosphoramidate – 28

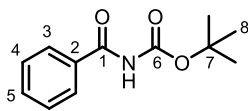


To an oven-dried rbf was added diethyl phosphoramidate (**30**) (766 mg, 5.0 mmol, 1.0 eq), anhydrous PhMe (10 mL, 0.50 M), and sodium hydride (60% wt., 200 mg, 5.0 mmol, 1.0 eq). The reaction was allowed to stir at rt for 30 mins before the addition of TBAB (161 mg, 0.50 mmol, 0.1 eq), and ethyl benzoate (718 μ L, 5.0 mmol, 1.0 eq). The reaction was heated to 110 $^{\circ}$ C for 16 h, before being cooled to rt. Aqueous HCl (2.0 M, 100 mL) was added, and the reaction extracted with EtOAc (3 x 100 mL). The combined organics were then dried (MgSO_4), filtered, and concentrated *in vacuo* to afford the crude product. The crude was purified by FCC (85% EtOAc/pentane) to afford the *title compound* (863 mg, 67%) as a beige solid. Data was consistent with that found in the literature.³⁷⁰

^1H NMR (400 MHz, CDCl_3) δ 9.41 (s, 1H, NH), 8.07 – 7.99 (m, 2H, C₃), 7.53 – 7.44 (m, 1H, C₅), 7.42 – 7.33 (m, 2H, C₄), 4.29 – 4.08 (m, 4H, C₆), 1.29 (td, $J = 7.1, 1.0$, 6H, C₇).

^{31}P NMR (162 MHz, CDCl_3) δ -1.6.

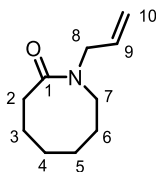
^{13}C NMR (101 MHz, CDCl_3) δ 168.0 (d, $J = 2.8$, C₁), 132.7 (C₅), 132.6 (d, $J = 10.6$, C₂), 128.5 (C₄), 128.4 (C₃), 64.2 (d, $J = 5.9$, C₆), 16.1 (d, $J = 6.8$, C₇).

tert-butyl benzoylcarbamate – 31

To an rbf containing *tert*-butyl benzoylcarbamate (**33**) (1.04 g, 5.0 mmol, 1.0 eq), 10% aqueous sodium periodate (40 mL, 4 g NaIO₄, 19.0 mmol, 3.8 eq), and EtOAc (15 mL, 0.33 M) was added ruthenium(IV) oxide hydrate (75 mg). After stirring at rt for 30 mins, water (100 mL) was added, and the reaction extracted with EtOAc (3 x 50 mL). The combined organics were washed with saturated aqueous sodium thiosulfate (100 mL), then dried (MgSO₄), filtered, and concentrated *in vacuo* to afford the crude product. The crude was purified by FCC (30% EtOAc/pentane) to afford the *title compound* (182 mg, 16%) as a white solid. Data was consistent with that found in the literature.³²⁸

¹H NMR (400 MHz, CDCl₃) δ 8.02 (s, 1H, NH), 7.85 – 7.75 (m, 2H, C₃), 7.58 – 7.51 (m, 1H, C₅), 7.50 – 7.41 (m, 2H, C₃), 1.53 (s, 9H, C₈).

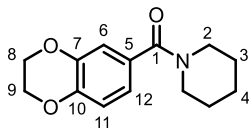
¹³C NMR (101 MHz, CDCl₃) δ 165.3 (C₁), 149.7 (C₆), 133.5 (C₅), 132.7 (C₂), 128.8 (C₄), 127.5 (C₃), 82.8 (C₇), 28.0 (C₈).

1-allylazocan-2-one – S3

To an oven-dried rbf was added 1-aza-2-cyclooctanone (636 mg, 5.0 mmol, 1.0 eq), and anhydrous THF (50 mL, 0.10 M). The reaction was then cooled to 0 °C and sodium hydride (60% in mineral oil, 300 mg, 7.5 mmol, 1.5 eq) was added. After stirring at 0 °C for 30 mins, allyl bromide (650 μ L, 7.5 mmol, 1.5 eq) was added as a single portion and the reaction allowed to stir and reach rt over 20 h. After this time saturated aqueous NH_4Cl (50 mL) was added, and the reaction extracted with EtOAc (3 x 75 mL). The combined organics were dried (MgSO_4), filtered, and concentrated *in vacuo* to afford the crude product. The crude was purified by FCC (60% EtOAc/pentane) to afford the *title compound* (794 mg, 95%) as a colourless oil. Data was consistent with that found in the literature.³⁷¹

^1H NMR (400 MHz, CDCl_3) δ 5.66 (ddt, $J = 17.2, 10.1, 6.1$, 1H, C_9), 5.07 – 4.97 (m, 2H, C_{10}), 3.85 (dt, $J = 6.2, 1.5$, 2H, C_8), 3.36 – 3.30 (m, 2H, C_1), 2.43 – 2.35 (m, 2H, C_7), 1.67 (ddd, $J = 9.5, 7.4, 4.4$, 2H, C_6), 1.51 (m, 2H, C_3), 1.45 – 1.39 (m, 2H, C_5), 1.39 – 1.30 (m, 2H, C_4).

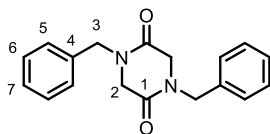
^{13}C NMR (101 MHz, CDCl_3) δ 174.5 (C_1), 133.7 (C_9), 117.0 (C_{10}), 47.3 (C_8), 46.1 (C_1), 33.7 (C_7), 28.9 (C_3), 28.7 (C_6), 26.1 (C_5), 24.3 (C_4).

(2,3-dihydrobenzo[b][1,4]dioxin-6-yl)(piperidin-1-yl)methanone – CX-546 – S4

To an oven dried rbf was added 2,3-dihydrobenzo[b][1,4]dioxine-6-carboxylic acid (1.44 g, 8.0 mmol, 1.0 eq), piperidine (1.2 mL, 12 mmol, 1.5 eq), triethylamine (3.3 mL, 24 mmol, 3.0 eq), and CH₂Cl₂ (40 mL, 0.20 M). The reaction mixture was cooled to 0 °C and propylphosphonic anhydride solution (50% in EtOAc, 9.4 mL, 16 mmol, 2.0 eq) was added as a single portion, then the reaction allowed to stir and reach rt over 23 h. The reaction mixture was then washed with aqueous HCl (2.0 M, 2 x 100 mL), saturated aqueous NaHCO₃ (100 mL), and brine (100 mL), then dried (MgSO₄), filtered, and concentrated *in vacuo* to afford the *title compound* (1.72 g, 87%) as a beige powder. Data was consistent with that found in the literature.³⁷²

¹H NMR (400 MHz, CDCl₃) δ 6.91 (d, *J* = 1.6, 1H, C₆), 6.89 – 6.81 (m, 2H, C₁₁ & C₁₂), 4.24 (s, 4H, C₈ & C₉), 3.81 – 3.22 (m, 4H, C₂), 1.64 (br, 2H, C₄), 1.55 (br, 4H, C₃).

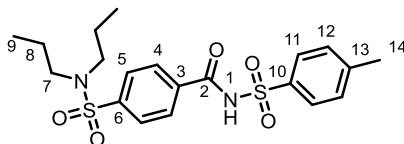
¹³C NMR (101 MHz, CDCl₃) δ 169.8 (C₁), 144.6 (ArC), 143.3 (ArC), 129.6 (ArC), 120.4 (C₁₂), 117.1 (C₁₁), 116.5 (C₆), 64.4 (C₈ or C₉), 64.3 (C₈ or C₉), 49.0 (C₂), 43.3 (C₂), 26.0 (C₃), 24.6 (C₄).

1,4-dibenzylpiperazine-2,5-dione – 73

To an oven-dried rbf was added piperazine-2,5-dione (571 mg, 5.0 mmol, 1.0 eq), and anhydrous THF (50 mL, 0.10 M). The reaction was then cooled to 0 °C and sodium hydride (60% in mineral oil, 600 mg, 15 mmol, 3.0 eq) was added. After stirring at 0 °C for 30 mins, benzyl bromide (1.8 mL, 15 mmol, 3.0 eq) was added as a single portion and the reaction allowed to stir and reach rt over 18 h. After this time saturated aqueous NH₄Cl (50 mL) was added, and the reaction extracted with EtOAc (3 x 75 mL). The combined organics were dried (MgSO₄), filtered, and concentrated *in vacuo* to afford the crude product. The crude was purified by FCC (65% → 80% EtOAc/pentane) to afford the *title compound* (221 mg, 15%) as a white solid. Data was consistent with that found in the literature.³⁷³

¹H NMR (400 MHz, CDCl₃) δ 7.38 – 7.31 (m, 6H), 7.31 – 7.23 (m, 4H), 4.59 (s, 4H, C₂), 3.94 (s, 4H, C₃).

¹³C NMR (101 MHz, CDCl₃) δ 163.3 (C₁), 135.0 (C₄), 129.0 (ArCH), 128.6 (ArCH), 128.2 (C₇), 49.33 (C₂), 49.26 (C₁).

4-(*N,N*-dipropylsulfamoyl)-*N*-tosylbenzamide – 87

In an oven-dried rbf 4-(*N,N*-dipropylsulfamoyl)benzoic acid (probenecid) (571 mg, 2.0 mmol, 1.0 eq) was suspended in CH_2Cl_2 (4.0 mL, 0.50 M), then oxalyl chloride (340 μL , 4.0 mmol, 2.0 eq) and DMF (3 drops) were added. After stirring at rt for 1 h the reaction was concentrated *in vacuo*, and the residue uptaken into a mixture of PhMe:EtOAc (2.5 mL:1.0 mL, 0.57 M). To reaction was added triethylamine (560 μL , 4.0 mmol, 2.0 eq), DMAP (12.2 mg, 0.10 mmol, 5 mol%), and *p*-toluenesulfonamide (377 mg, 2.2 mmol, 1.1 eq), then the reaction was heated to 55 °C for 2 h. The reaction was quenched by addition of aqueous HCl (2.0 M, 50 mL), then extracted with EtOAc (3 x 25 mL), and the combined organics dried (MgSO_4), filtered, and concentrated *in vacuo* to afford the crude product. The crude was purified by FCC (EtOAc), and the product fractions concentrated *in vacuo* then washed with aqueous HCl (2.0 M, 50 mL), extracted with CH_2Cl_2 (3 x 25 mL), and the combined organics dried (MgSO_4), filtered, and concentrated *in vacuo* to afford the *title compound* (814 mg, 93%) as a white powder.

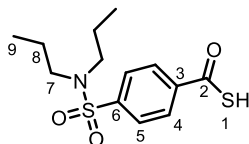
m.p.: 138 – 140 °C

^1H NMR (400 MHz, CDCl_3) δ 9.58 (s, 1H, N_1), 8.03 (d, $J = 8.4$, 2H), 7.93 (d, $J = 8.5$, 2H), 7.80 (d, $J = 8.5$, 2H), 7.39 – 7.34 (m, 2H), 3.09 – 3.02 (m, 4H, C_7), 2.44 (s, 3H, C_{14}), 1.57 – 1.45 (m, 4H, C_8), 0.84 (t, $J = 7.4$, 6H, C_9).

^{13}C NMR (101 MHz, CDCl_3) δ 163.3 (C_2), 145.6 (ArC), 144.6 (ArC), 135.2 (ArC), 134.6 (ArC), 129.7 (ArCH), 128.7 (ArCH x 2), 127.4 (ArCH), 49.9 (C_7), 21.9 (C_8), 21.7 (C_{14}), 11.1 (C_9).

FT-IR(thin film): $\nu_{\text{max}}(\text{cm}^{-1}) = 3238, 2965, 2922, 1700, 1636, 1436, 1344, 1324, 1298, 1184, 1151, 1116, 1073, 991, 889, 852, 829, 754, 662$.

(ESI): m/z calculated for $C_{20}H_{27}O_5N_2S_2$ requires 439.1356 for $[M+H]^+$, found 439.1360.

4-(*N,N*-dipropylsulfamoyl)benzothioic S-acid – 89

In an oven-dried rbf probenecid (570 mg, 2.0 mmol, 1.0 eq) was suspended in CH₂Cl₂ (4.0 mL, 0.50 M), then oxalyl chloride (340 μ L, 4.0 mmol, 2.0 eq) and DMF (3 drops) were added. After stirring at rt for 1 h the reaction was concentrated *in vacuo*, then uptaken into THF (5.0 mL). In a separate rbf a suspension of sodium hydrosulfide hydrate (673 mg, 12 mmol, 6.0 eq) in THF (5.0 mL) was cooled to 0 °C, then the above THF solution of acyl chloride added dropwise over 5 mins. After complete addition the reaction was stirred at 0 °C for 1 h, then warmed to rt and stirred for a further 2 h. The reaction was quenched by addition of aqueous HCl (2.0 M, 50 mL), extracted with EtOAc (3 x 25 mL), and the combined organics dried (MgSO₄), filtered, and concentrated *in vacuo* to afford the *title compound* (660 mg, quant.) as a yellow oil which was used without further purification.

¹H NMR (400 MHz, CDCl₃) δ 8.00 (d, *J* = 8.5, 2H, C₄), 7.89 (d, *J* = 8.5, 2H, C₅), 4.83 (s, 1H, S₁), 3.14 – 3.05 (m, 4H, C₇), 1.61 – 1.48 (m, 4H, C₈), 0.86 (t, *J* = 7.4, 6H, C₉).

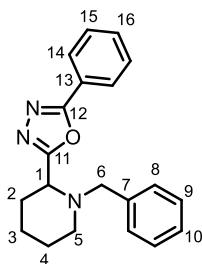
¹³C NMR (101 MHz, CDCl₃) δ 189.1 (C₂), 145.1 (ArC), 139.2 (ArC), 128.4 (C₅), 127.4 (C₄), 50.0 (C₇), 22.0 (C₈), 11.1 (C₉).

FT-IR(thin film): $\nu_{\max}(\text{cm}^{-1})$ = 3656, 2979, 2880, 1695, 1466, 1396, 1341, 1291, 1265, 1198, 1178, 1156, 1088, 993, 888, 844, 797, 775, 732, 702, 609.

(ESI): *m/z* calculated for C₁₃H₂₀O₃N₁S₂ requires 302.0879 for [M+H]⁺, found 302.0881.

5.2.3 Synthesis of α -Amino Heterodiazole Products

2-(1-benzylpiperidin-2-yl)-5-phenyl-1,3,4-oxadiazole – 3



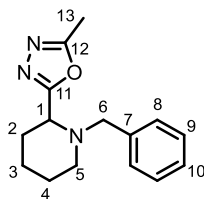
Following **general procedure A** (using 1-benzylpiperidin-2-one (**1**) (37.9 mg, 0.20 mmol, 1.0 eq) and Vaska's complex (0.8 mg, 1.0 μ mol, 0.5 mol%), and stirring for 1 h after addition of benzoic acid (26.9 mg, 0.22 mmol, 1.1 eq) and NIITP (66.5 mg, 0.22 mmol, 1.1 eq)): after FCC (30% Et₂O/pentane), **3** (55.8 mg, 87%) was afforded as a colourless oil.

¹H NMR (400 MHz, CDCl₃) δ 8.05 – 8.00 (m, 2H, C₁₄), 7.53 – 7.43 (m, 3H, C₁₅ & C₁₆), 7.30 – 7.20 (m, 4H, C₈ & C₉), 7.14 (d, J = 7.1, 1H, C₁₀), 3.97 (dd, J = 7.3, 4.7, 1H, C₁), 3.63 (d, J = 13.6, 1H, C₆), 3.42 (d, J = 13.7, 1H, C₆), 2.95 (dt, J = 11.7, 5.1, 1H, C₅), 2.33 – 2.23 (m, 1H, C₅), 2.03 – 1.90 (m, 2H, C₂), 1.86 – 1.73 (m, 1H, C₃), 1.69 – 1.59 (m, 2H, C₄), 1.52 – 1.42 (m, 1H, C₃).

¹³C NMR (101 MHz, CDCl₃) δ 167.3 (ArC), 164.8 (ArC), 138.1(C₇), 131.6 (C₁₆), 129.0 (C₁₅), 128.9 (ArCH), 128.2 (ArCH), 127.04 (C₁₀), 126.97 (C₁₄), 124.0 (C₁₃), 60.4 (C₆), 57.5 (C₁), 51.1 (C₅), 30.6 (C₂), 25.4 (C₄), 22.4 (C₃).

FT-IR(thin film): ν_{\max} (cm⁻¹) = 2980, 2889, 1533, 1473, 1450, 1251, 1069, 1028, 1007, 957, 732, 690.

(ESI): m/z calculated for C₂₀H₂₂ON₃ requires 320.1757 for [M+H]⁺, found 320.1754.

2-(1-benzylpiperidin-2-yl)-5-methyl-1,3,4-oxadiazole – 5

Following **general procedure A** (using 1-benzylpiperidin-2-one (**1**) (37.9 mg, 0.20 mmol, 1.0 eq) and Vaska's complex (0.8 mg, 1.0 μ mol, 0.5 mol%), and stirring for 1 h after addition of acetic acid (13 μ L, 0.22 mmol, 1.1 eq) and NIITP (66.5 mg, 0.22 mmol, 1.1 eq): after FCC (60% Et₂O/pentane), **5** (44.0 mg, 85%) was afforded as a tan semi-solid.

m.p.: 46 – 48 °C

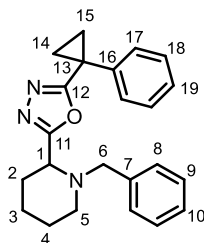
¹H NMR (400 MHz, CDCl₃) δ 7.18 – 7.02 (m, 5H, C₈ & C₉ & C₁₀), 3.69 (t, J = 6.2, 1H, C₁), 3.43 (d, J = 13.7, 1H, C₆), 3.23 (d, J = 13.7, 1H, C₆), 2.79 (dt, J = 11.6, 4.6, 1H, C₅), 2.32 (s, 3H, C₁₃), 2.15 – 2.04 (m, 1H, C₅), 1.79 – 1.71 (m, 2H, C₂), 1.69 – 1.56 (m, 1H, C₃), 1.54 – 1.43 (m, 2H, C₄), 1.33 – 1.20 (m, 1H, C₃).

¹³C NMR (101 MHz, CDCl₃) δ 167.5 (ArC), 163.8 (ArC), 137.9 (C₇), 129.0 (ArCH), 128.2 (ArCH), 127.0 (C₁₀), 60.4 (C₆), 57.7 (C₁), 51.5 (C₅), 30.6 (C₂), 25.3 (C₄), 22.6 (C₃), 11.0 (C₁₃).

FT-IR(thin film): ν_{\max} (cm⁻¹) = 2980, 2888, 1714, 1591, 1472, 1383, 1251, 1154, 1071, 955, 735, 698.

(ESI): m/z calculated for C₁₅H₂₀ON₃ requires 258.1601 for [M+H]⁺, found 258.1601.

2-(1-benzylpiperidin-2-yl)-5-(1-phenylcyclopropyl)-1,3,4-oxadiazole – 6



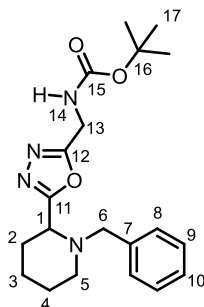
Following **general procedure A** (using 1-benzylpiperidin-2-one (**1**) (37.9 mg, 0.20 mmol, 1.0 eq) and Vaska's complex (0.8 mg, 1.0 μmol , 0.5 mol%), and stirring for 1 h after addition of 1-phenyl-1-cyclopropanecarboxylic acid (35.7 mg, 0.22 mmol, 1.1 eq) and NIITP (66.5 mg, 0.22 mmol, 1.1 eq)): after FCC (30% Et₂O/pentane), **6** (57.9 mg, 81%) was afforded as a yellow oil.

¹H NMR (400 MHz, CDCl₃) δ 7.29 – 7.23 (m, 2H), 7.22 – 7.14 (m, 3H), 7.14 – 7.05 (m, 3H), 7.03 (dd, $J = 7.8, 1.8, 2\text{H}$), 3.68 (dd, $J = 7.1, 4.9, 1\text{H}, C_1$), 3.37 (d, $J = 13.6, 1\text{H}, C_6$), 3.15 (d, $J = 13.6, 1\text{H}, C_6$), 2.69 (dt, $J = 11.6, 4.9, 1\text{H}, C_5$), 2.09 (dt, $J = 11.9, 6.4, 1\text{H}, C_5$), 1.75 – 1.66 (m, 2H, C₂), 1.66 – 1.56 (m, 1H, C₃), 1.55 – 1.47 (m, 2H, C₁₄ or C₁₅), 1.44 (m, 2H, C₄), 1.33 – 1.23 (m, 3H, C₃ & C₁₄ or C₁₅).

¹³C NMR (101 MHz, CDCl₃) δ 169.7 (ArC), 167.2 (ArC), 138.8 (ArC), 138.3 (ArC), 129.5 (ArCH), 128.9 (ArCH), 128.6 (ArCH), 128.2 (ArCH), 127.7 (ArCH), 127.0 (ArCH), 60.2 (C₆), 57.3 (C₁), 51.1 (C₅), 30.4 (C₂), 25.3 (C₄), 22.4 (C₁₃), 22.3 (C₃), 16.09 (C₁₄ or C₁₅), 16.07 (C₁₄ or C₁₅).

FT-IR(thin film): $\nu_{\text{max}}(\text{cm}^{-1}) = 2980, 2888, 1601, 1557, 1472, 1382, 1151, 1069, 1027, 965, 836, 737, 697, 636$.

(ESI): m/z calculated for C₂₃H₂₆ON₃ requires 360.2070 for [M+H]⁺, found 360.2067.

tert-butyl ((5-(1-benzylpiperidin-2-yl)-1,3,4-oxadiazol-2-yl)methyl)carbamate – 7

Following **general procedure A** (using 1-benzylpiperidin-2-one (**1**) (37.9 mg, 0.20 mmol, 1.0 eq) and Vaska's complex (0.8 mg, 1.0 μ mol, 0.5 mol%), and stirring for 1 h after addition of Boc-Gly-OH (38.5 mg, 0.22 mmol, 1.1 eq) and NIITP (66.5 mg, 0.22 mmol, 1.1 eq)): after FCC (60% Et₂O/pentane), **7** (61.5 mg, 83%) was afforded as a tan powder.

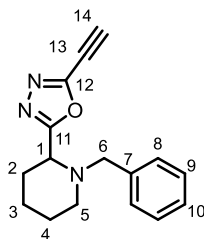
m.p.: 80 – 82 °C

¹H NMR (400 MHz, CDCl₃) δ 7.18 – 7.03 (m, 5H, C₈ & C₉ & C₁₀), 5.01 (s, 1H, N₁₄), 4.39 – 4.26 (m, 2H, C₁₃), 3.74 (t, J = 6.1, 1H, C₁), 3.42 (d, J = 13.6, 1H, C₆), 3.27 (d, J = 13.7, 1H, C₆), 2.79 (dt, J = 11.6, 4.8, 1H, C₅), 2.16 (dt, J = 12.0, 6.3, 1H, C₅), 1.75 (td, J = 6.6, 4.7, 2H, C₂), 1.62 (dt, J = 13.1, 5.2, 1H, C₃), 1.54 – 1.45 (m, 2H, C₄), 1.31 (s, 10H, C₃ & C₁₇).

¹³C NMR (101 MHz, CDCl₃) δ 167.9 (ArC), 163.9 (ArC), 155.4 (C₁₅), 138.0 (C₇), 128.9 (ArCH), 128.1 (ArCH), 127.0 (C₁₀), 80.5 (C₁₆), 60.4 (C₆), 57.5 (C₁), 51.4 (C₅), 35.9 (C₁₃), 30.4 (C₂), 28.3 (C₁₇), 25.3 (C₄), 22.3 (C₃).

FT-IR(thin film): $\nu_{\max}(\text{cm}^{-1})$ = 2980, 1715, 1584, 1507, 1453, 1391, 1366, 1250, 1163, 970, 937, 735, 698.

(ESI): m/z calculated for C₂₀H₂₉O₃N₄ requires 373.2234 for [M+H]⁺, found 373.2227.

2-(1-benzylpiperidin-2-yl)-5-ethynyl-1,3,4-oxadiazole – 8

Following **general procedure A** (using 1-benzylpiperidin-2-one (**1**) (37.9 mg, 0.20 mmol, 1.0 eq) and Vaska's complex (0.8 mg, 1.0 μ mol, 0.5 mol%), and stirring for 1 h after addition of propiolic acid (14 μ L, 0.22 mmol, 1.1 eq) and NIITP (66.5 mg, 0.22 mmol, 1.1 eq)): after FCC (20% Et₂O/pentane), **8** (36.0 mg, 67%) was afforded as a colourless oil.

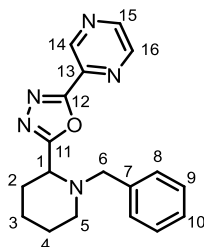
¹H NMR (400 MHz, CDCl₃) δ 7.32 – 7.20 (m, 5H), 3.97 (t, J = 5.9, 1H, C₁), 3.59 (d, J = 13.6, 1H, C₆), 3.53 (s, 1H, C₁₄), 3.43 (d, J = 13.6, 1H, C₆), 2.92 (dt, J = 11.7, 5.1, 1H, C₅), 2.32 (dt, J = 11.8, 5.8, 1H, C₅), 1.99 – 1.85 (m, 2H, C₂), 1.75 (dq, J = 16.5, 5.5, 1H, C₃), 1.71 – 1.55 (m, 2H, C₄), 1.56 – 1.39 (m, 1H, C₃).

¹³C NMR (101 MHz, CDCl₃) δ 168.0 (C₁₁), 149.9 (C₁₂), 137.8 (C₇), 128.9 (ArCH), 128.3 (ArCH), 127.2 (C₁₀), 85.7 (C₁₄), 67.6 (C₁₃), 60.3 (C₆), 57.3 (C₁), 50.7 (C₅), 30.4 (C₂), 25.2 (C₄), 22.0 (C₃).

FT-IR(thin film): $\nu_{\max}(\text{cm}^{-1})$ = 2939, 2855, 2134, 1595, 1518, 1494, 1452, 1371, 1345, 1319, 1261, 1209, 1178, 1156, 1128, 1105, 1068, 1049, 1027, 988, 910, 881, 836, 802, 777, 735, 697.

(ESI): m/z calculated for C₁₆H₁₈ON₃ requires 268.1444 for [M+H]⁺, found 268.1445.

2-(1-benzylpiperidin-2-yl)-5-(pyrazin-2-yl)-1,3,4-oxadiazole – 9



Following **general procedure A** (using 1-benzylpiperidin-2-one (**1**) (37.9 mg, 0.20 mmol, 1.0 eq) and Vaska's complex (0.8 mg, 1.0 μ mol, 0.5 mol%), and stirring for 1 h after addition of pyrazine-2-carboxylic acid (27.3 mg, 0.22 mmol, 1.1 eq) and NIITP (66.5 mg, 0.22 mmol, 1.1 eq)): after FCC (65% Et₂O/pentane), **9** (53.0 mg, 82%) was afforded as a yellow oil.

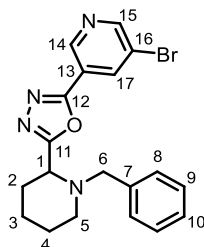
¹H NMR (400 MHz, CDCl₃) δ 9.25 (d, J = 1.4 Hz, 1H, C₁₄), 8.59 – 8.55 (m, 2H, C₁₅ & C₁₆), 7.15 – 7.10 (m, 2H, C₈), 7.10 – 7.04 (m, 2H, C₉), 7.01 – 6.95 (m, 1H, C₁₀), 3.91 (dd, J = 7.6, 4.2, 1H, C₁), 3.50 (d, J = 13.7, 1H, C₆), 3.34 (d, J = 13.7, 1H, C₆), 2.90 – 2.80 (m, 1H, C₅), 2.25 – 2.16 (m, 1H, C₅), 1.95 – 1.78 (m, 2H, C₂), 1.71 – 1.59 (m, 1H, C₃), 1.59 – 1.44 (m, 2H, C₄), 1.40 – 1.29 (m, 1H, C₃).

¹³C NMR (101 MHz, CDCl₃) δ 168.8 (ArC), 162.2 (ArC), 146.4 (ArCH), 144.6 (ArCH), 144.2 (C₁₄), 139.8 (C₁₃), 138.1 (C₇), 128.8 (C₈), 128.1 (C₉), 127.0 (C₁₀), 60.5 (C₆), 57.5 (C₁), 51.1 (C₅), 30.5 (C₂), 25.3 (C₄), 22.2 (C₃).

FT-IR(thin film): $\nu_{\max}(\text{cm}^{-1})$ = 2981, 2889, 1568, 1454, 1420, 1382, 1251, 1161, 1106, 1016, 965, 856, 734, 698.

(ESI): m/z calculated for C₁₈H₂₀ON₅ requires 322.1662 for [M+H]⁺, found 322.1663.

2-(1-benzylpiperidin-2-yl)-5-(5-bromopyridin-3-yl)-1,3,4-oxadiazole – 10



Following **general procedure A** (using 1-benzylpiperidin-2-one (**1**) (37.9 mg, 0.20 mmol, 1.0 eq) and Vaska's complex (0.8 mg, 1.0 μmol , 0.5 mol%), and stirring for 1 h after addition of 5-bromonicotinic acid (44.4 mg, 0.22 mmol, 1.1 eq) and NIITP (66.5 mg, 0.22 mmol, 1.1 eq)): after FCC (30% Et₂O/pentane), **10** (67.1 mg, 84%) was afforded as a brown powder.

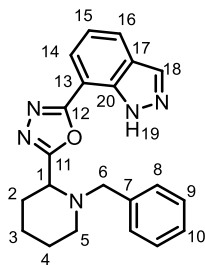
m.p.: 96 – 98 °C

¹H NMR (400 MHz, CDCl₃) δ 9.06 (d, $J = 1.8$, 1H), 8.74 (d, $J = 2.2$, 1H), 8.34 (t, $J = 2.1$, 1H, C₁₇), 7.21 – 7.13 (m, 4H, C₈ & C₉), 7.10 – 7.04 (m, 1H, C₁₀), 3.93 (t, $J = 6.1$, 1H, C₁), 3.55 (d, $J = 13.7$, 1H, C₆), 3.41 (d, $J = 13.8$, 1H, C₆), 2.93 (dt, $J = 11.7$, 4.9, 1H, C₅), 2.30 (ddd, $J = 12.0$, 7.3, 5.3, 1H, C₅), 1.94 – 1.86 (m, 2H, C₂), 1.79 – 1.70 (m, 1H, C₃), 1.67 – 1.58 (m, 2H, C₄), 1.49 – 1.37 (m, 1H, C₃).

¹³C NMR (101 MHz, CDCl₃) δ 168.2 (ArC), 161.5 (ArC), 153.4 (ArCH), 145.9 (ArCH), 137.9 (C₇), 136.4 (C₁₇), 128.8 (ArCH), 128.2 (ArCH), 127.1 (C₁₀), 121.7 (ArC), 121.0 (ArC), 60.6 (C₆), 57.7 (C₁), 51.7 (C₅), 30.6 (C₂), 25.3 (C₄), 22.4 (C₃).

FT-IR(thin film): $\nu_{\text{max}}(\text{cm}^{-1}) = 2980, 2889, 1600, 1537, 1472, 1451, 1382, 1302, 1263, 1153, 1099, 1078, 969, 890, 784, 733, 694$.

(ESI): m/z calculated for C₁₉H₂₀ON₄⁷⁹Br requires 399.0815 for [M+H]⁺, found 399.0816.

2-(1-benzylpiperidin-2-yl)-5-(1*H*-indazol-7-yl)-1,3,4-oxadiazole – 11

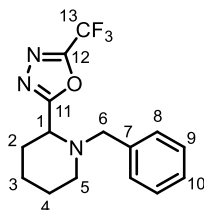
Following **general procedure A** (using 1-benzylpiperidin-2-one (**1**) (37.9 mg, 0.20 mmol, 1.0 eq) and Vaska's complex (0.8 mg, 1.0 μmol , 0.5 mol%), and stirring for 1 h after addition of 1*H*-indazole-7-carboxylic acid (35.7 mg, 0.22 mmol, 1.1 eq) and NIITP (66.5 mg, 0.22 mmol, 1.1 eq)): after FCC (60% Et₂O/pentane), **11** (56.9 mg, 79%) was afforded as a yellow oil.

¹H NMR (400 MHz, CDCl₃) δ 11.48 (br, s, 1H, N₁₉), 8.02 (s, 1H, C₁₈), 7.81 – 7.76 (m, 2H), 7.17 – 7.11 (m, 3H), 7.10 – 7.05 (m, 2H), 7.01 – 6.95 (m, 1H, C₁₀), 3.89 (dd, $J = 7.4, 4.6$, 1H, C₁), 3.52 (d, $J = 13.6$, 1H, C₆), 3.33 (d, $J = 13.7$, 1H, C₆), 2.89 – 2.80 (m, 1H, C₅), 2.26 – 2.17 (m, 1H, C₅), 1.93 – 1.80 (m, 2H, C₂), 1.74 – 1.62 (m, 1H, C₃), 1.58 – 1.47 (m, 2H, C₄), 1.43 – 1.30 (m, 1H, C₃).

¹³C NMR (101 MHz, CDCl₃) δ 166.8 (ArC), 163.3 (ArC), 137.9 (ArC), 136.7 (ArC), 135.3 (C₁₈), 128.9 (ArCH), 128.2 (ArCH), 127.1 (C₁₀), 125.1 (ArCH), 125.0 (ArCH), 124.1 (ArC), 120.7 (ArCH), 106.4 (ArC), 60.5 (C₆), 57.4 (C₁), 51.1 (C₅), 30.6 (C₂), 25.3 (C₄), 22.3 (C₃).

FT-IR(thin film): $\nu_{\text{max}}(\text{cm}^{-1}) = 3201, 2980, 1609, 1550, 1495, 1452, 1319, 1198, 1068, 946, 839, 734, 698$.

(ESI): m/z calculated for C₂₁H₂₂ON₅ requires 360.1819 for [M+H]⁺, found 360.1817.

2-(1-benzylpiperidin-2-yl)-5-(trifluoromethyl)-1,3,4-oxadiazole – 12

To an oven-dried screw cap vial equipped with magnetic stirrer, 1-benzylpiperidin-2-one (**1**) (56.8 mg, 0.30 mmol, 3.0 eq), and Vaska's complex (1.2 mg, 1.5 μ mol, 0.5 mol% with respect to the amide) were added. The vial was evacuated and backfilled with nitrogen (x3). Anhydrous THF (1.0 mL) was added followed in quick succession by TMDS (108 μ L, 0.60 mmol, 6.0 eq), and the vial capped and stirred at rt. After 30 mins, the vial was opened and NIITP (90.9 mg, 0.30 mmol, 3.0 eq) added, the vial was then sealed with a Suba-Seal™ and a solution of trifluoroacetic acid (7.7 μ L, 0.10 mmol, 1.0 eq) in THF (1.0 mL) added over 30 mins. After complete addition the reaction was stirred at rt for a further 1 h. After this time, CH₂Cl₂ (10 mL) was added and the reaction washed with saturated aqueous NaHCO₃ (20 mL), then the aqueous was extracted with CH₂Cl₂ (3 x 10 mL). The combined organics were dried (MgSO₄), filtered, and then concentrated *in vacuo* to afford the crude product: The crude was purified by FCC (10% Et₂O/pentane), to afford the *title compound* (12.5 mg, 40%) as a colourless oil.

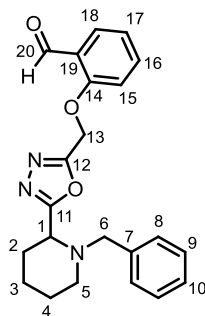
¹H NMR (400 MHz, CDCl₃) δ 7.35 – 7.03 (m, 5H), 3.97 (dd, *J* = 6.7, 4.9, 1H, C₁), 3.52 (d, *J* = 13.7, 1H, C₆), 3.41 (d, *J* = 13.6, 1H, C₆), 2.87 (dt, *J* = 11.9, 5.3, 1H, C₅), 2.33 (dt, *J* = 11.7, 5.8, 1H, C₅), 1.94 – 1.83 (m, 2H, C₂), 1.76 – 1.64 (m, 1H, C₃), 1.64 – 1.56 (m, 2H, C₄), 1.50 – 1.40 (m, 1H, C₃).

¹⁹F NMR (377 MHz, CDCl₃) δ -65.1

¹³C NMR (101 MHz, CDCl₃) δ 169.5 (C₁₁), 137.6 (C₇), 128.7 (ArCH), 128.3 (ArCH), 127.3 (C₁₀), 60.5 (C₆), 57.1 (C₁), 50.8 (C₅), 30.2 (C₂), 25.2 (C₄), 21.8 (C₃).

FT-IR(thin film): $\nu_{\max}(\text{cm}^{-1}) = 2980, 1586, 1453, 1406, 1322, 1259, 1207, 1164, 1128, 1048, 909, 754, 736, 698.$

(ESI): m/z calculated for $\text{C}_{15}\text{H}_{17}\text{ON}_3\text{F}_3$ requires 312.1318 for $[\text{M}+\text{H}]^+$, found 312.1316.

2-((5-(1-benzylpiperidin-2-yl)-1,3,4-oxadiazol-2-yl)methoxy)benzaldehyde – 13

Following **general procedure A** (using 1-benzylpiperidin-2-one (**1**) (37.9 mg, 0.20 mmol, 1.0 eq) and Vaska's complex (0.8 mg, 1.0 μmol , 0.5 mol%), and stirring for 1 h after addition of 2-(2-formylphenoxy)acetic acid (39.6 mg, 0.22 mmol, 1.1 eq) and NIITP (66.5 mg, 0.22 mmol, 1.1 eq): after FCC (55% Et₂O/pentane), **13** (51.1 mg, 68%) was afforded as a white crystalline solid.

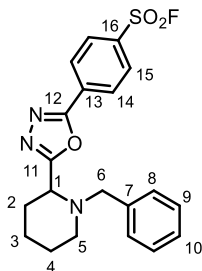
m.p.: 110 – 112 °C

¹H NMR (400 MHz, CDCl₃) δ 10.40 (d, J = 0.8, 1H, C₂₀), 7.78 (dd, J = 7.6, 1.8, 1H), 7.47 (ddd, J = 8.4, 7.3, 1.8, 1H), 7.21 – 7.09 (m, 5H), 7.07 – 7.00 (m, 2H), 5.36 – 5.18 (m, 2H, C₁₃), 3.87 (dd, J = 6.7, 5.3, 1H, C₁), 3.46 (d, J = 13.7, 1H, C₆), 3.31 (d, J = 13.6, 1H, C₆), 2.83 (dt, J = 11.6, 4.9, 1H, C₅), 2.23 (dt, J = 11.9, 6.3, 1H, C₅), 1.89 – 1.79 (m, 2H, C₂), 1.74 – 1.63 (m, 1H, C₃), 1.60 – 1.52 (m, 2H, C₄), 1.44 – 1.32 (m, 1H, C₃).

¹³C NMR (101 MHz, CDCl₃) δ 188.9 (C₂₀), 168.8 (ArC), 161.8 (ArC), 159.6 (C₁₉), 137.9 (C₇), 135.9 (ArCH), 128.82 (ArCH), 128.87 (ArCH), 128.2 (ArCH), 127.1 (ArCH), 125.5 (C₁₄), 122.4 (ArCH), 112.9 (ArCH), 60.4 (br, C₆ & C₁₃), 57.4 (C₁), 51.1 (C₅), 30.4 (C₂), 25.2 (C₄), 22.2 (C₃).

FT-IR(thin film): $\nu_{\text{max}}(\text{cm}^{-1})$ = 2980, 2886, 1688, 1599, 1483, 1456, 1392, 1286, 1238, 1162, 1104, 1019, 855, 833, 759, 741, 696.

(ESI): m/z calculated for C₂₂H₂₄O₃N₃ requires 378.1812 for [M+H]⁺, found 378.1810.

4-(5-(1-benzylpiperidin-2-yl)-1,3,4-oxadiazol-2-yl)benzenesulfonyl fluoride – 14

Following **general procedure A** (using 1-benzylpiperidin-2-one (**1**) (37.9 mg, 0.20 mmol, 1.0 eq) and Vaska's complex (0.8 mg, 1.0 μ mol, 0.5 mol%), and stirring for 16 h after addition of **S1** (81.7 mg, 0.40 mmol, 2.0 eq) and NIITP (121 mg, 0.40 mmol, 2.0 eq)): after FCC (40% Et₂O/pentane), **14** (32.0 mg, 40%) was afforded as an amber oil.

¹H NMR (400 MHz, CDCl₃) δ 8.24 – 8.18 (m, 2H), 8.10 – 8.05 (m, 2H), 7.23 – 7.13 (m, 4H, C₈ & C₉), 7.10 – 7.04 (m, 1H, C₁₀), 3.95 (t, J = 6.1, 1H, C₁), 3.56 (d, J = 13.7, 1H, C₆), 3.41 (d, J = 13.7, 1H, C₆), 2.94 (dt, J = 11.7, 4.8, 1H, C₅), 2.30 (dt, J = 12.1, 6.2, 1H, C₅), 1.96 – 1.87 (m, 2H, C₂), 1.76 (dt, J = 13.2, 5.2, 1H, C₃), 1.67 – 1.58 (m, 2H, C₄), 1.44 (dt, J = 13.4, 6.7, 1H, C₃).

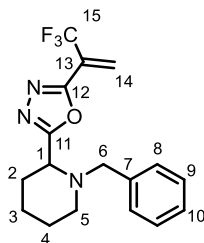
¹⁹F NMR (377 MHz, CDCl₃) δ 66.1.

¹³C NMR (101 MHz, CDCl₃) δ 168.6 (ArC), 162.9 (ArC), 137.9 (ArC), 135.4 (d, J = 25.7, C₁₆), 130.4 (ArC), 129.2 (ArCH), 128.8 (ArCH), 128.2 (ArCH), 127.9 (ArCH), 127.1 (C₁₀), 60.6 (C₆), 57.7 (C₁), 51.6 (C₅), 30.7 (C₂), 25.3 (C₄), 22.4 (C₃).

FT-IR(thin film): ν_{\max} (cm⁻¹) = 2980, 1607, 1550, 1485, 1453, 1415, 1293, 1213, 1171, 1081, 1009, 964, 846, 787, 737, 698, 616.

(ESI): m/z calculated for C₂₀H₂₁O₃N₃FS requires 402.1281 for [M+H]⁺, found 402.1283.

2-(1-benzylpiperidin-2-yl)-5-(3,3,3-trifluoroprop-1-en-2-yl)-1,3,4-oxadiazole – 15



Following **general procedure A** (using 1-benzylpiperidin-2-one (**1**) (37.9 mg, 0.20 mmol, 1.0 eq) and Vaska's complex (0.8 mg, 1.0 μ mol, 0.5 mol%), and stirring for 1 h after addition of 2-(trifluoromethyl)acrylic acid (30.8 mg, 0.22 mmol, 1.1 eq) and NIITP (66.5 mg, 0.22 mmol, 1.1 eq)): after FCC (15% Et₂O/pentane), **15** (29.3 mg, 43%) was afforded as a yellow oil.

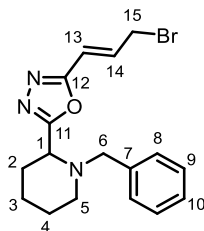
¹H NMR (400 MHz, CDCl₃) δ 7.20 – 7.16 (m, 4H, C₈ & C₉), 7.16 – 7.10 (m, 1H, C₁₀), 6.51 – 6.48 (m, 1H, C₁₄), 6.30 – 6.27 (m, 1H, C₁₄), 3.92 (dd, J = 6.9, 5.0, 1H, C₁), 3.52 (d, J = 13.7, 1H, C₆), 3.38 (d, J = 13.7, 1H, C₆), 2.88 (dt, J = 11.7, 5.0, 1H, C₅), 2.29 (dt, J = 11.9, 6.1, 1H, C₅), 1.91 – 1.83 (m, 2H, C₂), 1.77 – 1.66 (m, 1H, C₃), 1.62 – 1.53 (m, 2H, C₄), 1.49 – 1.37 (m, 1H, C₃).

¹⁹F NMR (377 MHz, CDCl₃) δ -66.1.

¹³C NMR (101 MHz, CDCl₃) δ 167.9 (ArC), 159.2 (ArC), 138.0 (C₇), 128.8 (ArCH), 128.2 (ArCH), 127.1 (C₁₀), 126.9 (q, J = 4.9, C₁₄), 121.0 (q, J = 273.2, C₁₅), 60.5 (C₆), 57.3 (C₁), 51.2 (C₅), 30.5 (C₂), 25.3 (C₄), 22.1 (C₃).

FT-IR(thin film): ν_{\max} (cm⁻¹) = 2980, 2888, 1538, 1454, 1382, 1304, 1253, 1147, 1084, 965, 737, 698.

(ESI): m/z calculated for C₁₇H₂₁ON₃F₃ requires 338.1475 for [M+H]⁺, found 338.1472.

(E)-2-(1-benzylpiperidin-2-yl)-5-(3-bromoprop-1-en-1-yl)-1,3,4-oxadiazole – 16

Following **general procedure A** (using 1-benzylpiperidin-2-one (**1**) (37.9 mg, 0.20 mmol, 1.0 eq) and Vaska's complex (0.8 mg, 1.0 μ mol, 0.5 mol%), and stirring for 1 h after addition of (*E*)-4-bromobut-2-enoic acid (36.3 mg, 0.40 mmol, 2.0 eq) and NIITP (66.5 mg, 0.22 mmol, 1.1 eq)): after FCC (40% Et₂O/pentane), **16** (45.2 mg, 62%) was afforded as a tan powder.

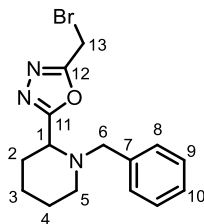
m.p.: 136 – 138 °C

¹H NMR (400 MHz, CDCl₃) δ 7.15 – 7.08 (m, 4H, C₈ & C₉), 7.08 – 7.02 (m, 1H, C₁₀), 6.70 (dt, *J* = 15.8, 7.5, 1H, C₁₄), 6.45 (dt, *J* = 15.8, 1.2, 1H, C₁₃), 3.95 (dd, *J* = 7.5, 1.2, 2H, C₁₅), 3.76 (t, *J* = 6.1, 1H, C₁), 3.44 (d, *J* = 13.6, 1H, C₆), 3.26 (d, *J* = 13.7, 1H, C₆), 2.80 (dt, *J* = 11.7, 4.8, 1H, C₅), 2.15 (dt, *J* = 12.0, 6.2, 1H, C₅), 1.81 – 1.73 (m, 2H, C₂), 1.68 – 1.58 (m, 1H, C₃), 1.54 – 1.44 (m, 2H, C₄), 1.36 – 1.24 (m, 1H, C₃).

¹³C NMR (101 MHz, CDCl₃) δ 167.2 (ArC), 162.7 (ArC), 137.9 (C₇), 136.1 (C₁₄), 128.9 (ArCH), 128.2 (ArCH), 127.1 (C₁₀), 116.3 (C₁₃), 60.4 (C₆), 57.5 (C₁), 51.3 (C₅), 30.6 (C₂), 29.9 (C₁₅), 25.3 (C₄), 22.4 (C₃).

FT-IR(thin film): $\nu_{\max}(\text{cm}^{-1})$ = 2980, 2888, 1529, 1472, 1459, 1382, 1251, 1153, 1072, 955, 814, 732, 701.

(ESI): *m/z* calculated for C₁₇H₂₁ON₃⁷⁹Br requires 362.0863 for [M+H]⁺, found 362.0859.

2-(1-benzylpiperidin-2-yl)-5-(bromomethyl)-1,3,4-oxadiazole – 17

Following **general procedure A** (using 1-benzylpiperidin-2-one (**1**) (37.9 mg, 0.20 mmol, 1.0 eq) and Vaska's complex (0.8 mg, 1.0 μmol , 0.5 mol%), and stirring for 1 h after addition of 2-bromoacetic acid (30.6 mg, 0.22 mmol, 1.1 eq) and NIITP (66.5 mg, 0.22 mmol, 1.1 eq)): after FCC (30% Et₂O/pentane), **17** (32.4 mg, 48%) was afforded as a light yellow semi-solid.

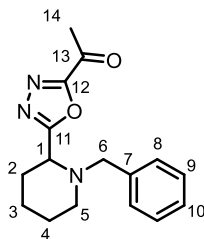
m.p.: 118 – 120 °C

¹H NMR (400 MHz, CDCl₃) δ 7.16 – 7.10 (m, 4H, C₈ & C₉), 7.10 – 7.04 (m, 1H, C₁₀), 4.38 – 4.25 (m, 2H, C₁₃), 3.78 (t, $J = 6.0$, 1H, C₁), 3.44 (d, $J = 13.6$, 1H, C₆), 3.26 (d, $J = 13.6$, 1H, C₆), 2.78 (dt, $J = 11.9, 4.9$, 1H, C₅), 2.17 (dt, $J = 11.9, 6.1$, 1H, C₅), 1.82 – 1.74 (m, 2H, C₂), 1.69 – 1.58 (m, 1H, C₃), 1.55 – 1.44 (m, 2H, C₄), 1.38 – 1.28 (m, 1H, C₃).

¹³C NMR (101 MHz, CDCl₃) δ 168.7 (ArC), 162.6 (ArC), 137.9 (C₇), 128.97 (ArCH), 128.2 (ArCH), 127.1 (C₁₀), 60.4 (C₆), 57.4 (C₁), 51.0 (C₁₃), 30.4 (C₅), 25.3 (C₂), 22.2 (C₄), 16.5 (C₃).

FT-IR(thin film): $\nu_{\text{max}}(\text{cm}^{-1}) = 2980, 1699, 1542, 1492, 1453, 1264, 1161, 1034, 731, 700$.

(ESI): m/z calculated for C₁₅H₁₉ON₃⁷⁹Br requires 336.0706 for [M+H]⁺, found 336.0704.

1-(5-(1-benzylpiperidin-2-yl)-1,3,4-oxadiazol-2-yl)ethan-1-one – 18

Following **general procedure A** (using 1-benzylpiperidin-2-one (**1**) (37.9 mg, 0.20 mmol, 1.0 eq) and Vaska's complex (0.8 mg, 1.0 μ mol, 0.5 mol%), and stirring for 1 h after addition of pyruvic acid (15 μ L, 0.22 mmol, 1.1 eq) and NIITP (66.5 mg, 0.22 mmol, 1.1 eq)): after FCC (20% Et₂O/pentane), **18** (27.1 mg, 48%) was afforded as a yellow oil.

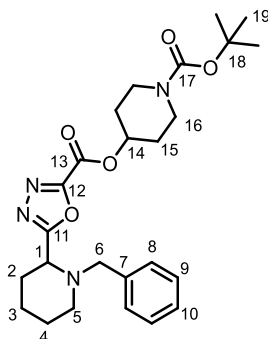
¹H NMR (400 MHz, CDCl₃) δ 7.18 – 7.13 (m, 4H, C₈ & C₉), 7.13 – 7.06 (m, 1H, C₁₀), 3.91 (dd, J = 6.9, 4.8, 1H, C₁), 3.48 (d, J = 13.7, 1H, C₆), 3.37 (d, J = 13.7, 1H, C₆), 2.85 (ddd, J = 12.0, 5.9, 4.4, 1H, C₅), 2.62 (s, 3H, C₁₄), 2.27 (ddd, J = 11.7, 6.9, 4.9, 1H, C₅), 1.91 – 1.80 (m, 2H, C₂), 1.71 – 1.60 (m, 1H, C₃), 1.59 – 1.50 (m, 2H, C₄), 1.44 – 1.34 (m, 1H, C₃).

¹³C NMR (101 MHz, CDCl₃) δ 184.3 (C₁₃), 169.7 (ArC), 161.3 (ArC), 138.0 (C₇), 128.8 (ArCH), 128.2 (ArCH), 127.0 (C₁₀), 60.5 (C₆), 57.4 (C₁), 50.9 (C₅), 30.3 (C₂), 27.2 (C₁₄), 25.3 (C₄), 22.0 (C₃).

FT-IR(thin film): $\nu_{\max}(\text{cm}^{-1})$ = 2981, 2889, 1715, 1493, 1382, 1252, 1152, 1071, 955, 835, 803, 733, 698.

(ESI): m/z calculated for C₁₆H₂₀O₂N₃ requires 286.1550 for [M+H]⁺, found 286.1551.

1-(*tert*-butoxycarbonyl)piperidin-4-yl 5-(1-benzylpiperidin-2-yl)-1,3,4-oxadiazole-2-carboxylate – 19



Following **general procedure A** (using 1-benzylpiperidin-2-one (**1**) (37.9 mg, 0.20 mmol, 1.0 eq) and Vaska's complex (0.8 mg, 1.0 μ mol, 0.5 mol%), and stirring for 16 h after addition of **S2** (109 mg, 0.40 mmol, 2.0 eq) and NIITP (121 mg, 0.40 mmol, 2.0 eq)): after FCC (50% Et₂O/pentane), **19** (51.6 mg, 57%) was afforded as a yellow oil.

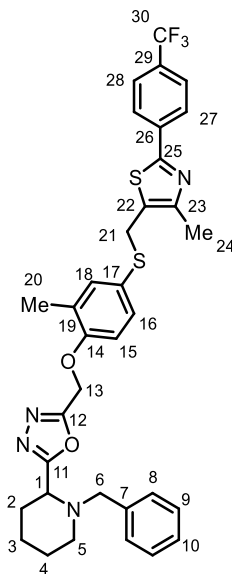
¹H NMR (400 MHz, CDCl₃) δ 7.15 – 7.08 (m, 4H, C₈ & C₉), 7.05 (dt, J = 8.7, 4.2, 1H, C₁₀), 5.11 (tt, J = 8.0, 3.9, 1H, C₁₄), 3.87 (dd, J = 6.7, 5.0, 1H, C₁), 3.72 – 3.59 (m, 2H, C₁₆), 3.43 (d, J = 13.7, 1H, C₆), 3.30 (d, J = 13.7, 1H, C₆), 3.20 – 3.08 (m, 2H, C₁₆), 2.84 – 2.76 (m, 1H, C₅), 2.20 (tt, J = 9.8, 4.4, 1H, C₅), 1.91 – 1.75 (m, 4H, C₂ & C₁₅), 1.73 – 1.55 (m, 3H, C₃ & C₁₅), 1.55 – 1.45 (m, 2H, C₄), 1.32 (s, 10H, C₃ & C₁₉).

¹³C NMR (101 MHz, CDCl₃) δ 169.7 (C₁₃), 156.8 (C), 154.6 (C), 153.7 (C), 137.9 (C₇), 128.8 (ArCH), 128.2 (ArCH), 127.1 (C₁₀), 79.9 (C₁₈), 73.6 (C₁₄), 60.5 (C₆), 57.4 (C₁), 51.0 (C₅), 40.8 (C₁₆), 30.4 (C₁₅), 28.4 (C₁₉), 25.2 (C₄), 22.0 (C₃).

FT-IR(thin film): $\nu_{\max}(\text{cm}^{-1})$ = 2935, 1745, 1691, 1539, 1453, 1422, 1365, 1320, 1274, 1238, 1165, 1135, 941, 770, 736, 699.

(ESI): m/z calculated for C₂₅H₃₅O₅N₄ requires 471.2602 for [M+H]⁺, found 471.2599.

2-(1-benzylpiperidin-2-yl)-5-((2-methyl-4-(((4-methyl-2-(4-(trifluoromethyl)phenyl)thiazol-5-yl)methyl)thio)phenoxy)methyl)-1,3,4-oxadiazole – 20



Following **general procedure A** (using 1-benzylpiperidin-2-one (**1**) (37.9 mg, 0.20 mmol, 1.0 eq) and Vaska's complex (0.8 mg, 1.0 μmol , 0.5 mol%), and stirring for 1 h after addition of 2-[2-methyl-4-[[[4-methyl-2-[4-(trifluoromethyl)phenyl]-5-thiazolyl]methyl]thio]phenoxy]-acetic acid (GW501516) (99.8 mg, 0.22 mmol, 1.1 eq) and NIITP (66.5 mg, 0.22 mmol, 1.1 eq)): after FCC (45% Et₂O/pentane), **20** (94.4 mg, 73%) was afforded as a white powder.

m.p.: 116 – 118 °C

¹H NMR (400 MHz, CDCl₃) δ 7.96 – 7.89 (m, 2H, C₂₇), 7.60 (d, J = 8.2, 2H, C₂₈), 7.24 – 7.08 (m, 7H, C₈ & C₉ & C₁₀ & C₁₅ & C₁₆), 6.80 (d, J = 8.4, 1H, C₁₅), 5.21 – 5.10 (m, 2H, C₁₃), 4.05 (s, 2H, C₂₁), 3.90 (t, J = 6.0, 1H, C₁), 3.49 (d, J = 13.6, 1H, C₆), 3.33 (d, J = 13.6, 1H, C₆), 2.85 (dt, J = 11.7, 4.9, 1H, C₅), 2.29 – 2.20 (m, 1H, C₅), 2.17 (s, 3H, C₂₄), 2.13 (s, 3H, C₂₀), 1.90 – 1.84 (m, 2H, C₂), 1.76 – 1.67 (m, 1H, C₃), 1.63 – 1.54 (m, 2H, C₄), 1.47 – 1.36 (m, 1H, C₃).

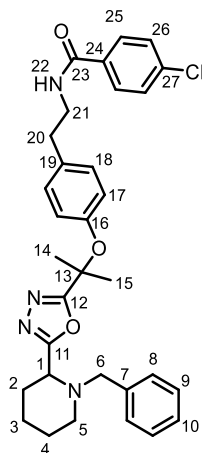
¹⁹F NMR (377 MHz, CDCl₃) δ -62.7.

^{13}C NMR (101 MHz, CDCl_3) δ 168.6 (ArC), 163.1 (ArC), 162.4 (ArC), 155.9 (ArC), 151.4 (ArC), 138.0 (ArC), 136.8 (ArC), 135.9 (ArCH), 131.9 (ArCH), 131.3 (q, $J = 32.4$, C_{29}), 130.6 (ArC), 128.8 (ArCH), 128.4 (ArC), 128.2 (ArCH), 127.0 (ArCH), 126.4 (C_{27}), 126.2 (ArC), 125.9 (q, $J = 3.9$, C_{28}), 124.0 (q, $J = 272.5$, C_{30}), 112.13 (C_{15}), 60.3 (C_6), 60.2 (C_{13}), 57.3 (C_1), 51.0 (C_5), 32.3 (C_{21}), 30.4 (C_2), 25.3 (C_4), 22.2 (C_3), 16.0 (C_{20}), 14.9 (C_{24}).

FT-IR(thin film): $\nu_{\text{max}}(\text{cm}^{-1}) = 2940, 1616, 1591, 1489, 1452, 1323, 1244, 1165, 1124, 1109, 1066, 1001, 844, 734, 696$.

(ESI): m/z calculated for $\text{C}_{34}\text{H}_{34}\text{O}_2\text{N}_4\text{F}_3\text{S}_2$ requires 651.2070 for $[\text{M}+\text{H}]^+$, found 651.2058.

N-(4-((2-(5-(1-benzylpiperidin-2-yl)-1,3,4-oxadiazol-2-yl)propan-2-yl)oxy)phenethyl)-4-chlorobenzamide – 21



Following **general procedure A** (using 1-benzylpiperidin-2-one (**1**) (37.9 mg, 0.20 mmol, 1.0 eq) and Vaska's complex (0.8 mg, 1.0 μ mol, 0.5 mol%), and stirring for 1 h after addition of 2-[4-[2-(4-chlorobenzamido)ethyl]phenoxy]-2-methylpropanoic acid (bezafibrate) (79.6 mg, 0.22 mmol, 1.1 eq) and NIITP (66.5 mg, 0.22 mmol, 1.1 eq)): after FCC (70% Et₂O/pentane), **21** (87.5 mg, 74%) was afforded as a yellow oil.

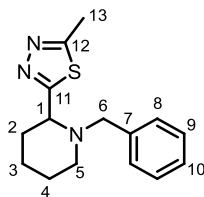
¹H NMR (400 MHz, CDCl₃) δ 7.45 – 7.38 (m, 2H), 7.22 – 7.17 (m, 2H), 7.10 – 6.99 (m, 5H), 6.79 – 6.72 (m, 2H), 6.53 – 6.46 (m, 2H), 6.05 (t, J = 5.9, 1H, N₂₂), 3.74 (t, J = 6.0, 1H, C₁), 3.46 – 3.27 (m, 3H, C₆ & C₂₁), 3.11 (d, J = 13.6, 1H, C₆), 2.70 (dt, J = 11.6, 4.8, 1H, C₅), 2.57 (t, J = 6.9, 2H, C₂₀), 2.09 – 2.01 (m, 1H, C₅), 1.77 – 1.70 (m, 2H, C₂), 1.68 (s, 3H, C₁₄ or C₁₅), 1.66 (s, 3H, C₁₄ or C₁₅), 1.63 – 1.55 (m, 1H, C₃), 1.50 – 1.40 (m, 2H, C₄), 1.33 – 1.23 (m, 1H, C₃).

¹³C NMR (101 MHz, CDCl₃) δ 168.5 (C₂₃), 168.2 (ArC), 166.4 (ArC), 153.4 (ArC), 138.0 (ArC), 137.6 (ArC), 134.1 (ArC), 133.0 (ArC), 129.6 (ArCH), 128.8 (ArCH), 128.3 (ArCH), 128.2 (ArCH), 127.1 (ArCH), 121.3 (ArCH), 75.3 (C₁₃), 60.1 (C₆), 57.4 (C₁), 50.8 (C₅), 41.1 (C₂₁), 34.7 (C₂₀), 30.5 (C₂), 26.3 (C₁₄ or C₁₅), 26.0 (C₁₄ or C₁₅), 25.21 (C₄), 22.3 (C₃).

FT-IR(thin film): $\nu_{\max}(\text{cm}^{-1}) = 2938, 2857, 1639, 1596, 1540, 1506, 1486, 1314, 1224, 1154, 1127, 1067, 984, 881, 846, 757, 698.$

(ESI): m/z calculated for $\text{C}_{32}\text{H}_{36}\text{O}_3\text{N}_4^{35}\text{Cl}$ requires 559.2470 for $[\text{M}+\text{H}]^+$, found 559.2464.

2-(1-benzylpiperidin-2-yl)-5-methyl-1,3,4-thiadiazole – 34



Following **general procedure A** (using 1-benzylpiperidin-2-one (**1**) (37.9 mg, 0.20 mmol, 1.0 eq) and Vaska's complex (0.8 mg, 1.0 μ mol, 0.5 mol%), and stirring for 1 h after addition of thioacetic acid (16 μ L, 0.22 mmol, 1.1 eq) and NIITP (66.5 mg, 0.22 mmol, 1.1 eq)): after FCC (40% Et₂O/pentane), **34** (25.2 mg, 46%) was afforded as a brown semi-solid.

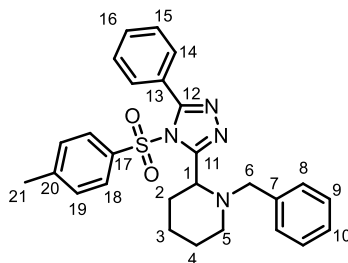
m.p.: 80 – 82 °C

¹H NMR (400 MHz, CDCl₃) δ 7.14 (d, J = 4.4, 4H, C₈ & C₉), 7.07 (dt, J = 5.7, 4.1, 1H, C₁₀), 3.74 (dd, J = 10.6, 3.4, 1H, C₁), 3.59 (d, J = 13.8, 1H, C₆), 2.98 (d, J = 13.8, 1H, C₆), 2.79 (ddt, J = 11.7, 3.6, 1.8, 1H, C₅), 2.59 (s, 3H, C₁₃), 1.95 – 1.85 (m, 2H, C₂ & C₅), 1.69 – 1.61 (m, 1H, C₄), 1.57 – 1.29 (m, 4H, C₂ & C₃ & C₄).

¹³C NMR (101 MHz, CDCl₃) δ 176.1 (ArC), 165.4 (ArC), 138.0 (C₇), 128.1 (ArCH), 127.8 (ArCH), 126.6 (C₁₀), 62.5 (C₁), 59.6 (C₆), 52.0 (C₅), 35.1 (C₂), 24.8 (C₃), 23.4 (C₄), 15.4 (C₁₃).

FT-IR(thin film): ν_{\max} (cm⁻¹) = 2941, 2804, 1494, 1475, 1373, 1244, 1093, 974, 836, 738, 693.

(ESI): m/z calculated for C₁₅H₂₀N₃S requires 274.1372 for [M+H]⁺, found 274.1373.

1-benzyl-2-(5-phenyl-4-tosyl-4*H*-1,2,4-triazol-3-yl)piperidine – 35

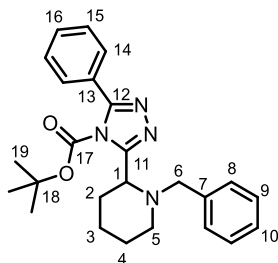
Following **general procedure A** (using 1-benzylpiperidin-2-one (**1**) (37.9 mg, 0.20 mmol, 1.0 eq) and Vaska's complex (1.6 mg, 2.0 μ mol, 1.0 mol%), and stirring for 16 h after addition of **27** (110 mg, 0.40 mmol, 2.0 eq) and NIITP (121 mg, 0.40 mmol, 2.0 eq)): after FCC (40% EtOAc/pentane), **35** (53.4 mg, 57%) was afforded as an amber oil.

^1H NMR (400 MHz, CDCl_3) δ 7.36 – 7.29 (m, 1H), 7.26 – 7.06 (m, 11H), 7.02 – 6.95 (m, 2H), 4.45 (dd, $J = 6.9, 4.6$, 1H, C₁), 3.59 (d, $J = 13.3$, 1H, C₆), 3.19 (d, $J = 13.2$, 1H, C), 3.10 (ddd, $J = 11.1, 6.7, 3.6$, 1H, C₅), 2.24 (s, 4H, C₅ & C₂₁), 1.97 – 1.84 (m, 2H, C₂), 1.76 – 1.63 (m, 1H, C₃), 1.61 – 1.45 (m, 2H, C₄), 1.45 – 1.32 (m, 1H, C₃).

^{13}C NMR (101 MHz, CDCl_3) δ 156.6 (ArC), 153.4 (ArC), 146.6 (ArC), 139.0 (ArC), 134.5 (ArC), 130.8 (ArCH), 130.4 (ArCH), 129.9 (ArCH), 129.0 (ArCH), 128.2 (ArCH), 127.8 (ArCH), 127.7 (ArCH), 127.0 (ArC), 126.9 (ArCH), 59.3 (C₆), 57.9 (C₁), 50.4 (C₅), 31.5 (C₂), 24.7 (C₄), 22.3 (C₃), 21.7 (C₂₁).

FT-IR(thin film): $\nu_{\text{max}}(\text{cm}^{-1}) = 2980, 1595, 1444, 1385, 1265, 1192, 1178, 1121, 1091, 1030, 1010, 909, 813, 731, 698, 664$.

(ESI): m/z calculated for $\text{C}_{27}\text{H}_{29}\text{O}_2\text{N}_4\text{S}$ requires 473.2006 for $[\text{M}+\text{H}]^+$, found 473.2003.

tert-butyl 3-(1-benzylpiperidin-2-yl)-5-phenyl-4H-1,2,4-triazole-4-carboxylate – 36

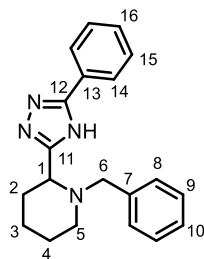
Following **general procedure A** (using 1-benzylpiperidin-2-one (**1**) (37.9 mg, 0.20 mmol, 1.0 eq) and Vaska's complex (0.8 mg, 1.0 μ mol, 0.5 mol%), and stirring for 16 h after addition of **31** (88.5 mg, 0.40 mmol, 2.0 eq) and NiITP (121 mg, 0.40 mmol, 2.0 eq)): after FCC (25% Et₂O/pentane), **36** (30.3 mg, 36%) was afforded as a colourless oil.

¹H NMR (400 MHz, CDCl₃) δ 8.33 – 8.24 (m, 2H, C₁₄), 7.50 – 7.42 (m, 3H, C₁₅ & C₁₆), 7.30 – 7.25 (m, 2H), 7.25 – 7.18 (m, 3H), 4.39 (dd, J = 7.5, 4.1, 1H, C₁), 3.80 (d, J = 13.1, 1H, C₆), 3.46 (d, J = 13.1, 1H, C₆), 3.40 (ddd, J = 10.7, 6.5, 3.5, 1H, C₅), 2.42 (ddd, J = 11.5, 8.1, 3.6, 1H, C₅), 2.03 – 1.92 (m, 1H, C₂), 1.91 – 1.80 (m, 2H, C₂ & C₃), 1.80 – 1.70 (m, 2H, C₃), 1.70 – 1.64 (m, 1H, C₄), 1.61 (s, 9H, C₁₉).

¹³C NMR (101 MHz, CDCl₃) δ 162.2 (ArC), 161.3 (ArC), 147.0 (C₁₇), 138.2 (C₇), 130.03 (C₁₃), 129.96 (C₁₆), 129.3 (ArCH), 128.5 (ArCH), 128.2 (ArCH), 127.3 (ArCH), 127.0 (C₁₀), 86.7 (C₁₈), 59.8 (C₆), 57.4 (C₁), 51.1 (C₅), 31.2 (C₂), 27.8 (C₁₉), 25.5 (C₄), 22.2 (C₃).

FT-IR(thin film): ν_{\max} (cm⁻¹) = 2934, 1777, 1754, 1531, 1448, 1371, 1323, 1258, 1152, 1106, 1044, 988, 967, 910, 843, 770, 736, 699.

(ESI): m/z calculated for C₂₅H₃₁O₂N₄ requires 419.2442 for [M+H]⁺, found 419.2442.

1-benzyl-2-(5-phenyl-4H-1,2,4-triazol-3-yl)piperidine – 37

Following **general procedure A** (using 1-benzylpiperidin-2-one (**1**) (19.0 mg, 0.10 mmol, 1.0 eq) and Vaska's complex (0.4 mg, 0.5 μ mol, 0.5 mol%), and stirring for 16 h after addition of **28** (51.4 mg, 0.20 mmol, 2.0 eq) and NIITP (60.5 mg, 0.20 mmol, 2.0 eq); after reaction completion LiOH (25.2 mg, 0.60 mmol, 6.0 eq) was added to the reaction mixture and stirred for 1 h before following the work up described in **general procedure A**): after FCC (40% EtOAc/pentane), **37** (22.3 mg, 70%) was afforded as a beige powder.

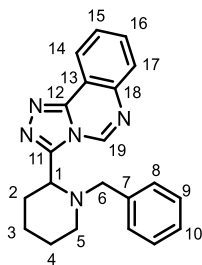
m.p.: 196 – 198 °C

^1H NMR (400 MHz, DMSO) δ 14.02 (s, 1H, NH), 8.03 (d, $J = 7.5$, 2H, C₁₄), 7.53 – 7.34 (m, 3H, C₁₅ & C₁₆), 7.33 – 7.25 (m, 4H, C₈ & C₉), 7.24 – 7.15 (m, 1H, C₁₀), 3.70 – 3.55 (m, 1H, C₁), 3.47 (d, $J = 13.4$, 1H, C₆), 3.10 (d, $J = 13.4$, 1H, C₆), 2.85 (d, $J = 10.8$, 1H, C₅), 2.04 (t, $J = 10.6$, 1H, C₅), 1.92 – 1.70 (m, 3H, C₂ & C₃), 1.65 – 1.44 (m, 2H, C₄), 1.44 – 1.28 (m, 1H, C₃).

^{13}C NMR (101 MHz, DMSO) δ 160.9 (ArC), 159.6 (ArC), 138.8 (C₇), 132.0 (ArCH), 129.2 (ArCH), 129.1 (ArCH), 128.5 (ArCH), 127.3 (ArCH), 126.2 (ArCH), 59.7 (C₆), 59.5 (C₁), 51.8 (C₅), 32.4 (C₂), 25.4 (C₄), 23.7 (C₃).

FT-IR(thin film): $\nu_{\text{max}}(\text{cm}^{-1}) = 2980, 2928, 1472, 1443, 1373, 1316, 1274, 1254, 1130, 1104, 1073, 1063, 1028, 972, 942, 923, 907, 805, 773, 735, 712, 695, 625$.

(ESI): m/z calculated for C₂₀H₂₃N₄ requires 319.1917 for [M+H]⁺, found 319.1917.

3-(1-benzylpiperidin-2-yl)-[1,2,4]triazolo[4,3-c]quinazoline – 39

Following **general procedure A** (using 1-benzylpiperidin-2-one (**1**) (37.9 mg, 0.20 mmol, 1.0 eq) and Vaska's complex (1.6 mg, 2.0 μ mol, 1.0 mol%), and stirring for 16 h after addition of quinazolin-4(3*H*)-one (**38**) (58.5 mg, 0.40 mmol, 2.0 eq) and NIITP (121 mg, 0.40 mmol, 2.0 eq)): after FCC (100% Et₂O \rightarrow 100% EtOAc), **39** (22.8 mg, 33%) was afforded as a yellow crystalline solid.

m.p.; 160 – 162 °C

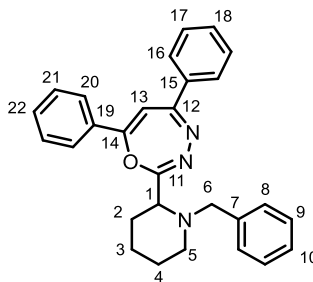
¹H NMR (400 MHz, CDCl₃) δ 9.62 (s, 1H, C₁₉), 8.57 (dd, *J* = 7.9, 1.5, 1H), 7.96 (dd, *J* = 8.1, 1.2, 1H), 7.81 – 7.74 (m, 1H), 7.69 (td, *J* = 7.6, 1.3, 1H), 7.19 – 7.13 (m, 2H, C₈), 7.12 – 7.08 (m, 2H, C₉), 7.08 – 7.02 (m, 1H, C₁₀), 4.21 (dd, *J* = 11.2, 3.5, 1H, C₁), 3.54 (d, *J* = 13.7, 1H, C₆), 3.28 (d, *J* = 13.7, 1H, C₆), 3.17 – 3.09 (m, 1H, C₅), 2.22 – 2.12 (m, 1H, C₅), 2.08 – 2.00 (m, 1H, C₂), 1.98 – 1.87 (m, 2H, C₂ & C₃), 1.82 – 1.73 (m, 1H, C₄), 1.73 – 1.63 (m, 1H, C₄), 1.56 – 1.46 (m, 1H, C₃).

¹³C NMR (101 MHz, CDCl₃) δ 149.8 (ArC), 148.4 (ArC), 140.7 (ArC), 137.1 (ArC), 135.9 (C₁₉), 131.7 (ArCH), 129.4 (ArCH), 128.7 (ArCH), 128.6 (ArCH), 128.3 (ArCH), 127.0 (ArCH), 123.4 (ArCH), 117.2 (ArC), 61.0 (C₆), 60.9 (C₁), 53.5 (C₂), 31.4 (C₂), 25.4 (C₄), 23.9 (C₃).

FT-IR(thin film): ν_{\max} (cm⁻¹) = 2936, 2855, 2801, 1620, 1609, 1527, 1494, 1473, 1453, 1371, 1314, 1302, 1102, 907, 878, 769, 734, 698.

(ESI): *m/z* calculated for C₂₁H₂₂N₅ requires 344.1870 for [M+H]⁺, found 344.1870.

2-(1-benzylpiperidin-2-yl)-5,7-diphenyl-1,3,4-oxadiazepine – 41



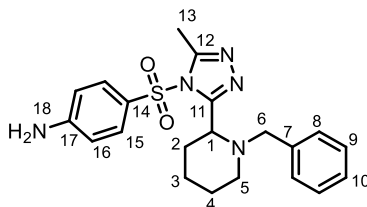
Following **general procedure A** (using 1-benzylpiperidin-2-one (**1**) (37.9 mg, 0.20 mmol, 1.0 eq) and Vaska's complex (1.6 mg, 2.0 μ mol, 1.0 mol%), and stirring for 16 h after addition of 1,3-diphenylpropane-1,3-dione (**40**) (89.7 mg, 0.40 mmol, 2.0 eq) and NIITP (121 mg, 0.40 mmol, 2.0 eq)): after FCC (10% Et₂O/pentane \rightarrow 20% Et₂O/pentane), **41** (23.0 mg, 25%) was afforded as a yellow oil.

¹H NMR (400 MHz, CDCl₃) δ 7.96 – 7.88 (m, 2H), 7.83 – 7.77 (m, 2H), 7.48 – 7.35 (m, 6H), 7.16 – 7.09 (m, 3H), 7.09 – 7.02 (m, 2H), 6.58 (s, 1H, C₁₃), 4.07 (d, J = 13.3, 1H, C₆), 3.34 – 3.25 (m, 2H, C₁ & C₆), 2.97 (dt, J = 11.5, 4.4, 1H, C₅), 2.03 – 1.81 (m, 3H, C₂ & C₅), 1.70 (dt, J = 13.4, 4.7, 1H, C₃), 1.54 – 1.43 (m, 2H, C₄), 1.38 – 1.25 (m, 1H, C₃).

¹³C NMR (101 MHz, CDCl₃) δ 162.8 (ArC), 161.3 (ArC), 154.8 (ArC), 138.5 (ArC), 137.5 (ArC), 132.6 (ArC), 130.8 (ArCH), 130.4 (ArCH), 129.0 (ArCH), 128.7 (ArCH), 128.5 (ArCH), 128.0 (ArCH), 127.4 (ArCH), 126.7 (ArCH), 126.6 (ArCH), 104.5 (C₁₃), 64.6 (C₁), 60.4 (C₆), 50.5 (C₅), 29.2 (C₂), 25.3 (C₄), 22.8 (C₃).

FT-IR(thin film): $\nu_{\max}(\text{cm}^{-1})$ = 3059, 2934, 2855, 1629, 1576, 1524, 1492, 1447, 1342, 1273, 1170, 1105, 1084, 1066, 1028, 837, 766, 737, 605.

(ESI): m/z calculated for C₂₈H₂₈ON₃ requires 422.2227 for [M+H]⁺, found 422.2222.

4-((3-(1-benzylpiperidin-2-yl)-5-methyl-4H-1,2,4-triazol-4-yl)sulfonyl)aniline – 42

Following **general procedure A** (using 1-benzylpiperidin-2-one (**1**) (37.9 mg, 0.20 mmol, 1.0 eq) and Vaska's complex (1.6 mg, 2.0 μ mol, 1.0 mol%), and stirring for 16 h after addition of *N*-(4-aminobenzenesulfonyl)acetamide (sulfacetamide) (85.7 mg, 0.40 mmol, 2.0 eq) and NIITP (121 mg, 0.40 mmol, 2.0 eq)): after FCC (75% EtOAc/pentane) and PTLC (50% EtOAc/CHCl₃), **42** (48.9 mg, 59%) was afforded as a white powder.

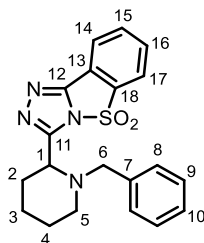
m.p.: 104 – 106 °C

¹H NMR (400 MHz, CDCl₃) δ 7.60 (d, J = 8.8, 2H), 7.26 – 7.14 (m, 5H, C₈ & C₉ & C₁₀), 6.66 (d, J = 8.9, 2H), 4.68 (s, 2H, N₁₈), 4.21 (dd, J = 8.3, 3.2, 1H, C₁), 3.46 (d, J = 13.1, 1H, C₆), 3.13 – 3.04 (m, 1H, C₅), 2.92 (d, J = 13.1, 1H, C₆), 2.65 (s, 3H, C₁₃), 2.14 (ddd, J = 12.0, 8.9, 3.8, 1H, C₅), 1.90 – 1.69 (m, 3H, C₂ & C₃), 1.66 – 1.50 (m, 2H, C₄), 1.44 – 1.32 (m, 1H, C₃).

¹³C NMR (101 MHz, CDCl₃) δ 156.0 (ArC), 153.1 (ArC), 150.6 (ArC), 138.9 (ArC), 130.2 (ArCH), 129.0 (ArCH), 128.0 (ArCH), 126.8 (C₁₀), 124.2 (ArC), 114.0 (ArCH), 59.6 (C₆), 58.4 (C₁), 51.2 (C₅), 32.1 (C₂), 24.9 (C₄), 22.8 (C₃), 13.9 (C₁₃).

FT-IR(thin film): $\nu_{\max}(\text{cm}^{-1})$ = 3657, 2980, 2888, 1596, 1472, 1461, 1380, 1305, 1251, 1195, 1154, 1133, 1080, 954, 833, 738, 700, 682.

(ESI): m/z calculated for C₂₁H₂₆O₂N₅S requires 412.1802 for [M+H]⁺, found 412.1810.

3-(1-benzylpiperidin-2-yl)benzo[4,5]isothiazolo[3,2-c][1,2,4]triazole 5,5-dioxide – 43

Following **general procedure A** (using 1-benzylpiperidin-2-one (**1**) (37.9 mg, 0.20 mmol, 1.0 eq) and Vaska's complex (0.8 mg, 1.0 μ mol, 0.5 mol%), and stirring for 16 h after addition of 2,3-dihydroxy-1,2-benzisothiazol-3-one-1,1-dioxide (saccharin) (73.3 mg, 0.40 mmol, 2.0 eq) and NIITP (121 mg, 0.40 mmol, 2.0 eq): after FCC (45% EtOAc/pentane), **43** (28.9 mg, 38%) was afforded as a white crystalline solid.

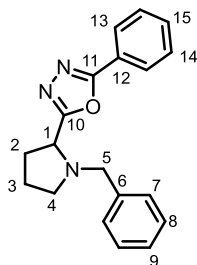
m.p.: 70 – 72 °C

^1H NMR (400 MHz, CDCl_3) δ 8.10 (dt, $J = 7.7, 0.9$, 1H), 7.89 (dt, $J = 7.9, 0.9$, 1H), 7.81 (td, $J = 7.7, 1.1$, 1H), 7.71 (td, $J = 7.7, 1.1$, 1H), 7.40 – 7.35 (m, 2H, C₈), 7.33 – 7.27 (m, 2H, C₉), 7.26 – 7.20 (m, 1H, C₁₀), 3.92 (dd, $J = 10.3, 3.6$, 1H, C₁), 3.83 (d, $J = 13.5$, 1H, C₆), 3.40 (d, $J = 13.5$, 1H, C₆), 3.01 (dtd, $J = 11.8, 4.0, 1.2$, 1H, C₅), 2.16 – 2.03 (m, 2H, C₂ & C₅), 1.95 (dq, $J = 12.8, 4.0$, 1H, C₂), 1.89 – 1.79 (m, 1H, C₃), 1.66 (tt, $J = 7.5, 3.4$, 2H, C₄), 1.45 – 1.30 (m, 1H, C₃).

^{13}C NMR (101 MHz, CDCl_3) δ 156.6 (ArC), 151.9 (ArC), 141.9 (ArC), 136.5 (ArC), 134.9 (ArCH), 132.0 (ArCH), 129.7 (C₈), 128.1 (C₉), 127.1 (C₁₀), 123.3 (ArCH), 123.2 (ArCH), 122.2 (ArC), 60.5 (C₆), 58.8 (C₁), 51.3 (C₅), 31.1 (C₂), 24.6 (C₄), 23.4 (C₃).

FT-IR(thin film): $\nu_{\text{max}}(\text{cm}^{-1}) = 2969, 2931, 2876, 1634, 1436, 1342, 1324, 1298, 1243, 1185, 1165, 1117, 1073, 991, 889, 854, 829, 754, 714, 666$.

(ESI): m/z calculated for $\text{C}_{20}\text{H}_{21}\text{O}_2\text{N}_4\text{S}$ requires 381.1380 for $[\text{M}+\text{H}]^+$, found 381.1376.

2-(1-benzylpyrrolidin-2-yl)-5-phenyl-1,3,4-oxadiazole – 50

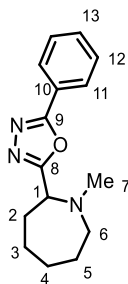
Following **general procedure A** (using 1-benzylpyrrolidin-2-one (35.0 mg, 0.20 mmol, 1.0 eq) and Vaska's complex (0.8 mg, 1.0 μ mol, 0.5 mol%), and stirring for 16 h after addition of benzoic acid (73.3 mg, 0.60 mmol, 3.0 eq) and NIITP (181 mg, 0.60 mmol, 3.0 eq): after FCC (60% EtOAc/pentane), **50** (44.5 mg, 73%) was afforded as an amber oil.

^1H NMR (400 MHz, CDCl_3) δ 8.00 – 7.93 (m, 2H, C₁₃), 7.49 – 7.38 (m, 3H, C₁₄ & C₁₅), 7.24 – 7.13 (m, 4H, C₇ & C₈), 7.13 – 7.06 (m, 1H, C₉), 4.00 (t, J = 7.6, 1H, C₁), 3.82 (d, J = 13.1, 1H, C₅), 3.54 (d, J = 13.1, 1H, C₅), 3.05 (ddd, J = 9.2, 7.9, 3.3, 1H, C₄), 2.53 – 2.41 (m, 1H, C₄), 2.30 – 2.08 (m, 2H, C₂), 2.07 – 1.92 (m, 1H, C₃), 1.91 – 1.78 (m, 1H, C₃).

^{13}C NMR (101 MHz, CDCl_3) δ 167.3 (ArC), 165.1(ArC), 137.9 (ArC), 131.6 (ArCH), 129.0 (ArCH), 128.2 (ArCH), 127.2 (ArCH), 127.0 (ArCH), 124.0 (ArC), 58.8 (C₁), 58.0 (C₅), 53.3 (C₄), 30.1 (C₂), 23.0 (C₃).

FT-IR(thin film): $\nu_{\text{max}}(\text{cm}^{-1})$ = 2980, 2803, 1655, 1609, 1551, 1485, 1449, 1372, 1258, 1176, 1070, 1026, 1007, 777, 740, 690.

(ESI): m/z calculated for $\text{C}_{19}\text{H}_{20}\text{ON}_3$ requires 306.1601 for $[\text{M}+\text{H}]^+$, found 306.1602.

2-(1-methylazepan-2-yl)-5-phenyl-1,3,4-oxadiazole – 51

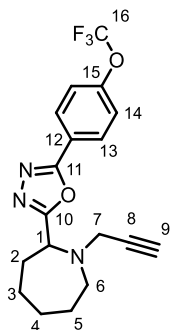
Following **general procedure A** (using 1-methylazepan-2-one (25.4 mg, 0.20 mmol, 1.0 eq) and Vaska's complex (0.8 mg, 1.0 μ mol, 0.5 mol%), and stirring for 1 h after addition of benzoic acid (26.7 mg, 0.22 mmol, 1.1 eq) and NIITP (66.5 mg, 0.22 mmol, 1.1 eq)): after FCC (40% Et₂O/pentane), **51** (35.1 mg, 68%) was afforded as a yellow oil.

¹H NMR (400 MHz, CDCl₃) δ 8.09 – 8.00 (m, 2H, C₁₁), 7.54 – 7.43 (m, 3H, C₁₂ & C₁₃), 4.07 (dd, J = 8.1, 6.3, 1H, C₁), 3.14 – 3.02 (m, 1H, C₆), 2.74 (dt, J = 14.6, 4.9, 1H, C₆), 2.43 (s, 3H, C₇), 2.16 – 2.02 (m, 2H, C₂), 1.92 – 1.81 (m, 1H, C₃), 1.75 – 1.63 (m, 4H, C₃ & C₄ & C₅), 1.59 – 1.46 (m, 1H, C₅).

¹³C NMR (101 MHz, CDCl₃) δ 168.3 (ArC), 164.8 (ArC), 131.5 (C₁₃), 128.9 (C₁₂), 126.9 (C₁₁), 124.1 (C₁₀), 60.7 (C₁), 53.4 (C₅), 43.1 (C₇), 31.9 (C₂), 28.7 (C₅), 28.1 (C₄), 25.5 (C₃).

FT-IR(thin film): $\nu_{\max}(\text{cm}^{-1})$ = 2980, 2930, 1553, 1472, 1449, 1381, 1252, 1152, 1085, 1070, 959, 800, 706, 690.

(ESI): m/z calculated for C₁₅H₂₀ON₃ requires 258.1601 for [M+H]⁺, found 258.1603.

2-(1-(prop-2-yn-1-yl)azepan-2-yl)-5-(4-(trifluoromethoxy)phenyl)-1,3,4-oxadiazole – 52

Following **general procedure A** (using 1-(prop-2-yn-1-yl)azepan-2-one (30.2 mg, 0.20 mmol, 1.0 eq) and Vaska's complex (1.6 mg, 2.0 μ mol, 1.0 mol%), and stirring for 1 h after addition of 4-(trifluoromethoxy)benzoic acid (45.3 mg, 0.22 mmol, 1.1 eq) and NIITP (66.5 mg, 0.22 mmol, 1.1 eq): after FCC (25% Et₂O/pentane), **52** (27.9 mg, 38%) was afforded as an orange crystalline solid.

m.p.: 94 – 96 °C

¹H NMR (400 MHz, CDCl₃) δ 8.14 – 8.08 (m, 2H), 7.37 – 7.31 (m, 2H), 4.39 (dd, J = 8.4, 5.8, 1H, C₁), 3.59 – 3.44 (m, 2H, C₇), 3.09 (ddd, J = 14.7, 7.2, 3.2, 1H, C₆), 2.92 (dt, J = 14.5, 3.8, 1H, C₆), 2.23 – 2.13 (m, 1H, C₂), 2.11 – 2.00 (m, 2H, C₂ & C₉), 1.92 – 1.81 (m, 1H, C₃), 1.79 – 1.64 (m, 4H, C₃ & C₄ & C₅), 1.62 – 1.47 (m, 1H, C₄).

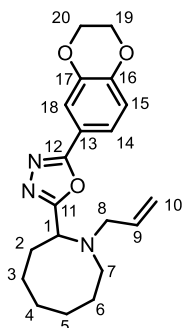
¹⁹F NMR (377 MHz, CDCl₃) δ -57.7.

¹³C NMR (101 MHz, CDCl₃) δ 168.4 (ArC), 163.7 (ArC), 151.5 (C₁₅), 128.7 (ArCH), 122.7 (C₁₂), 121.2 (ArCH), 120.7 (q, J = 259.5, C₁₆), 80.1 (C₈), 72.1 (C₉), 57.7 (C₁), 50.3 (C₆), 45.0 (C₇), 32.5 (C₂), 29.5 (C₃), 29.3 (C₅), 24.8 (C₄).

FT-IR(thin film): ν_{\max} (cm⁻¹) = 2932, 1545, 1498, 1454, 1340, 1254, 1209, 1159, 1111, 1010, 733, 701.

(ESI): m/z calculated for C₁₈H₁₉O₂N₃F₃ requires 366.1424 for [M+H]⁺, found 366.1422.

2-(1-allylazocan-2-yl)-5-(2,3-dihydrobenzo[b][1,4]dioxin-6-yl)-1,3,4-oxadiazole – 53



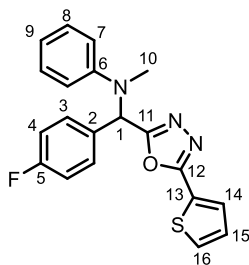
Following **general procedure A** (using **S3** (33.5 mg, 0.20 mmol, 1.0 eq) and Vaska's complex (1.6 mg, 2.0 μ mol, 1.0 mol%), and stirring for 1 h after addition of 2,3-dihydrobenzo[b][1,4]dioxine-6-carboxylic acid (39.6 mg, 0.22 mmol, 1.1 eq) and NIITP (66.5 mg, 0.22 mmol, 1.1 eq)): after FCC (50% Et₂O/pentane), **53** (29.6 mg, 42%) was afforded as a yellow oil.

¹H NMR (400 MHz, CDCl₃) δ 7.56 – 7.51 (m, 2H, C₁₄ & C₁₈), 6.98 – 6.93 (m, 1H, C₁₅), 5.84 (ddt, J = 16.9, 10.0, 6.6, 1H, C₉), 5.17 (dq, J = 17.2, 1.6, 1H, C₁₀), 5.09 (dq, J = 10.0, 1.3, 1H, C₁₀), 4.31 (tt, J = 4.9, 2.6, 4H, C₁₉ & C₂₀), 4.13 (dd, J = 12.0, 5.0, 1H, C₁), 3.29 (ddt, J = 13.8, 6.9, 1.3, 1H, C₈), 3.16 (ddt, J = 13.8, 6.3, 1.4, 1H, C₈), 3.02 (td, J = 10.2, 5.0, 1H, C₇), 2.59 – 2.39 (m, 1H, C₇), 2.16 (m, 1H, C₂), 2.05 – 1.87 (m, 2H), 1.85 – 1.65 (m, 2H), 1.64 – 1.50 (m, 3H) 1.48 – 1.38 (m, 2H).

¹³C NMR (101 MHz, CDCl₃) δ 166.9 (ArC), 164.1 (ArC), 146.5 (ArC), 143.8 (ArC), 136.7 (C₉), 120.5 (ArCH), 118.0 (C₁₅), 117.5 (ArC), 117.3 (C₁₀), 116.1 (ArCH), 64.6 (C₁₉ or C₂₀), 64.3 (C₁₉ or C₂₀), 58.4 (C₈), 57.1 (C₁), 47.1 (C₇), 30.5 (C₂), 28.8 (CH₂), 27.9 (CH₂), 26.6 (CH₂), 25.8 (CH₂).

FT-IR(thin film): ν_{max} (cm⁻¹) = 2980, 2928, 1617, 1593, 1564, 1500, 1418, 1311, 1283, 1252, 1151, 1125, 1065, 966, 894, 870, 818, 733.

(ESI): m/z calculated for C₂₀H₂₆O₃N₃ requires 356.1969 for [M+H]⁺, found 356.1969.

***N*-((4-fluorophenyl)(5-(thiophen-2-yl)-1,3,4-oxadiazol-2-yl)methyl)-*N*-methylaniline – 54**

Following **general procedure A** (using 4-fluoro-*N*-methyl-*N*-phenylbenzamide (45.9 mg, 0.20 mmol, 1.0 eq) and Vaska's complex (7.8 mg, 0.01 mmol, 5.0 mol%), and stirring for 1 h after addition of thiophene-2-carboxylic acid (28.2 mg, 0.22 mmol, 1.1 eq) and NIITP (66.5 mg, 0.22 mmol, 1.1 eq): after FCC (30% Et₂O/pentane), **54** (35.5 mg, 49%) was afforded as a brown oil.

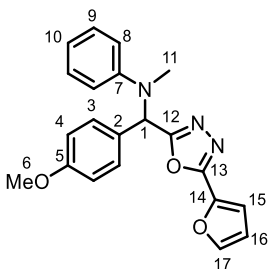
¹H NMR (400 MHz, CDCl₃) δ 7.63 (dd, *J* = 3.8, 1.2, 1H, C₁₆), 7.47 (dd, *J* = 5.0, 1.2, 1H, C₁₄), 7.27 – 7.17 (m, 4H), 7.07 (dd, *J* = 5.0, 3.8, 1H, C₁₅), 7.03 – 6.96 (m, 2H, C₄), 6.90 (dt, *J* = 7.8, 1.0, 2H), 6.78 (tt, *J* = 7.2, 1.0, 1H), 6.39 (s, 1H, C₁), 2.83 (s, 3H, C₁₀).

¹⁹F NMR (377 MHz, CDCl₃) δ -113.4.

¹³C NMR (101 MHz, CDCl₃) δ 164.3 (ArC), 162.6 (d, *J* = 247.9, C₅), 161.4 (ArC), 149.2 (ArC), 131.6 (d, *J* = 3.2, C₂), 130.5 (C₁₄), 130.1 (C₁₆), 129.6 (d, *J* = 8.3, C₃), 129.4 (ArCH), 128.2 (C₁₅), 124.9 (ArC), 119.2 (ArCH), 115.8 (d, *J* = 21.6, C₄), 114.6 (ArCH), 59.1 (C₁), 34.6 (C₁₀).

FT-IR(thin film): $\nu_{\max}(\text{cm}^{-1}) = 2980, 2923, 1596, 1555, 1505, 1424, 1265, 1225, 1159, 1105, 1034, 992, 844, 749, 723, 692.$

(ESI): *m/z* calculated for C₂₀H₁₇ON₃FS requires 366.1071 for [M+H]⁺, found 366.1071.

***N*-((5-(furan-2-yl)-1,3,4-oxadiazol-2-yl)(4-methoxyphenyl)methyl)-*N*-methylaniline – 55**

Following **general procedure A** (using 4-methoxy-*N*-methyl-*N*-phenylbenzamide (48.3 mg, 0.20 mmol, 1.0 eq) and Vaska's complex (7.8 mg, 0.01 mmol, 5.0 mol%), and stirring for 1 h after addition of furan-2-carboxylic acid (24.7 mg, 0.22 mmol, 1.1 eq) and NIITP (66.5 mg, 0.22 mmol, 1.1 eq)): after FCC (35% Et₂O/pentane), **55** (48.0 mg, 66%) was afforded as a dark crystalline solid.

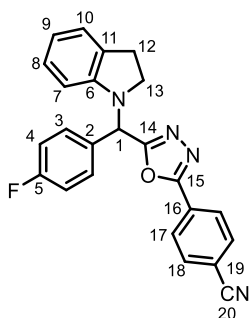
m.p.: 118 – 120 °C

¹H NMR (400 MHz, CDCl₃) δ 7.54 (dd, *J* = 1.8, 0.8, 1H, C₁₇), 7.22 – 7.16 (m, 2H, C₉), 7.16 – 7.11 (m, 2H), 7.06 (dd, *J* = 3.5, 0.8, 1H, C₁₅), 6.91 – 6.86 (m, 2H, C₈), 6.85 – 6.80 (m, 2H), 6.75 (tt, *J* = 7.3, 1.0, 1H, C₁₀), 6.49 (dd, *J* = 3.5, 1.8, 1H, C₁₆), 6.39 (s, 1H, C₁), 3.73 (s, 3H, C₆), 2.82 (s, 3H, C₁₁).

¹³C NMR (101 MHz, CDCl₃) δ 164.8 (ArC), 159.6 (ArC), 157.9 (ArC), 149.3 (ArC), 145.8 (C₁₇), 139.3 (ArC), 129.4 (ArCH), 129.2 (ArCH), 127.7 (ArC), 118.9 (C₁₀), 114.4 (ArCH), 114.3 (C₁₅), 114.2 (ArCH), 112.2 (C₁₆), 59.0 (C₁), 55.3 (C₆), 34.4 (C₁₁).

FT-IR(thin film): $\nu_{\max}(\text{cm}^{-1}) = 2924, 2853, 1636, 1597, 1533, 1455, 1304, 1251, 1176, 1098, 1029, 901, 735, 692.$

(ESI): *m/z* calculated for C₂₁H₂₀O₃N₃ requires 362.1499 for [M+H]⁺, found 362.1500.

4-(5-((4-fluorophenyl)(indolin-1-yl)methyl)-1,3,4-oxadiazol-2-yl)benzonitrile – 56

Following **general procedure A** (using (4-fluorophenyl)(indolin-1-yl)methanone (48.3 mg, 0.20 mmol, 1.0 eq) and Vaska's complex (4.7 mg, 6.0 μ mol, 3.0 mol%) in PhMe (1.0 mL, 0.20 M) for the 1st step, and stirring for 1 h after addition of THF (1.0 mL, 0.10 M total), 4-cyanobenzoic acid (32.4 mg, 0.22 mmol, 1.1 eq) and NIITP (66.5 mg, 0.22 mmol, 1.1 eq)): after FCC (35% Et₂O/pentane), **56** (67.3 mg, 85%) was afforded as a brown crystalline solid.

m.p.: 132 – 134 °C

¹H NMR (400 MHz, CDCl₃) δ 8.12 – 8.05 (m, 2H, C₁₈), 7.78 – 7.71 (m, 2H, C₁₇), 7.47 – 7.40 (m, 2H, C₃), 7.11 – 7.04 (m, 3H, C₄), 7.00 (td, $J = 7.7, 1.3, 1\text{H}$), 6.70 (td, $J = 7.4, 1.0, 1\text{H}$), 6.51 (d, $J = 7.9, 1\text{H}$), 6.15 (s, 1H, C₁), 3.59 (q, $J = 8.9, 1\text{H}, \text{C}_{11}$), 3.34 (td, $J = 8.7, 6.4, 1\text{H}, \text{C}_{11}$), 3.03 – 2.93 (m, 2H, C₁₂).

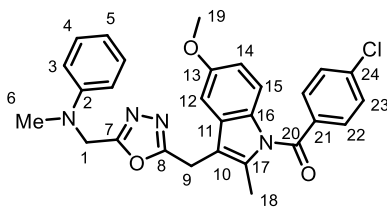
¹⁹F NMR (377 MHz, CDCl₃) δ -112.8.

¹³C NMR (101 MHz, CDCl₃) δ 165.4 (ArC), 163.8 (ArC), 162.8 (d, $J = 248.4, \text{C}_5$), 149.7 (ArC), 132.9 (ArCH), 130.7 (d, $J = 3.4, \text{C}_2$), 130.3 (ArC), 130.0 (d, $J = 8.3, \text{C}_3$), 127.50 (ArCH), 127.47 (ArC), 127.3 (ArCH), 125.0 (ArCH), 119.3 (ArCH), 117.8 (C₁₉), 116.0 (d, $J = 21.8, \text{C}_4$), 115.4 (ArC), 108.0 (ArCH), 56.7 (C₁), 50.2 (C₁₃), 28.2 (C₁₂).

FT-IR(thin film): $\nu_{\text{max}}(\text{cm}^{-1}) = 2980, 2360, 2230, 1605, 1548, 1508, 1487, 1384, 1226, 1159, 1083, 1014, 962, 845, 802, 739, 699.$

(ESI): m/z calculated for $C_{24}H_{18}ON_4F$ requires 397.1459 for $[M+H]^+$, found 397.1459.

(4-chlorophenyl)(5-methoxy-2-methyl-3-((5-((methyl(phenyl)amino)methyl)-1,3,4-oxadiazol-2-yl)methyl)-1*H*-indol-1-yl)methanone – 57



Following **general procedure A** (using *N*-methyl-*N*-phenylformamide (27.0 mg, 0.20 mmol, 1.0 eq) and Vaska's complex (7.8 mg, 0.01 mmol, 5.0 mol%), and stirring for 1 h after addition of 1-(4-chlorobenzoyl)-5-methoxy-2-methyl-3-indoleacetic acid (indomethacin) (78.7 mg, 0.22 mmol, 1.1 eq) and NIITP (66.5 mg, 0.22 mmol, 1.1 eq)): after FCC (40% EtOAc/pentane), **57** (54.3 mg, 69%) was afforded as a brown oil.

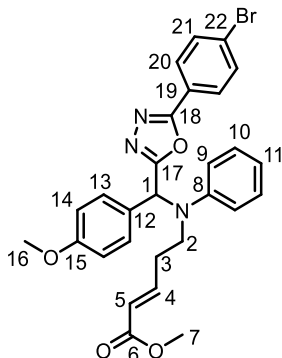
^1H NMR (400 MHz, CDCl_3) δ 7.52 – 7.46 (m, 2H, C₂₂), 7.35 – 7.28 (m, 2H, C₂₃), 7.10 – 7.02 (m, 2H, C₃), 6.80 (d, $J = 2.5$, 1H, C₁₂), 6.70 (d, $J = 9.0$, 1H, C₁₅), 6.68 – 6.59 (m, 3H, C₄ & C₅), 6.53 (dd, $J = 9.0, 2.5$, 1H, C₁₄), 4.46 (s, 2H, C₉), 4.04 (s, 2H, C₁), 3.63 (s, 3H, C₁₉), 2.87 (s, 3H, C₆), 2.24 (s, 3H, C₁₈).

^{13}C NMR (101 MHz, CDCl_3) δ 168.3 (C₂₀), 165.1 (ArC), 164.4 (ArC), 156.2 (ArC), 148.4 (ArC), 139.5 (ArC), 136.0 (ArC), 133.7 (ArC), 131.2 (ArCH), 130.8 (ArC), 130.0 (ArC), 129.3 (C₃), 129.2 (C₂₃), 128.6 (ArCH), 118.3 (C₅), 115.0 (C₁₅), 113.2 (C₄), 112.1 (ArCH), 111.8 (ArC), 100.9 (C₁₂), 55.7 (C₁₉), 47.6 (C₉), 38.9 (C₆), 20.9 (C₁), 13.2 (C₁₈).

FT-IR(thin film): $\nu_{\text{max}}(\text{cm}^{-1}) = 3657, 2980, 2889, 1681, 1599, 1505, 1477, 1455, 1356, 1314, 1176, 1119, 1087, 1067, 1034, 899, 823, 751, 733, 691$.

(ESI): m/z calculated for $\text{C}_{28}\text{H}_{26}\text{O}_3\text{N}_4^{35}\text{Cl}$ requires 501.1688 for $[\text{M}+\text{H}]^+$, found 501.1688.

ethyl (*E*)-5-(((5-(4-bromophenyl)-1,3,4-oxadiazol-2-yl)(4-methoxyphenyl)methyl)(phenyl)amino)pent-2-enoate – 58



Following **general procedure A** (using methyl (*E*)-5-(4-methoxy-*N*-phenylbenzamido)pent-2-enoate (33.9 mg, 0.10 mmol, 1.0 eq) and Vaska's complex (3.9 mg, 5.0 μ mol, 5.0 mol%), and stirring for 1 h after addition of 4-bromobenzoic acid (22.1 mg, 0.11 mmol, 1.1 eq) and NIITP (33.3 mg, 0.11 mmol, 1.1 eq): after FCC (35% Et₂O/pentane), **58** (29.5 mg, 54%) was afforded as a dark oil.

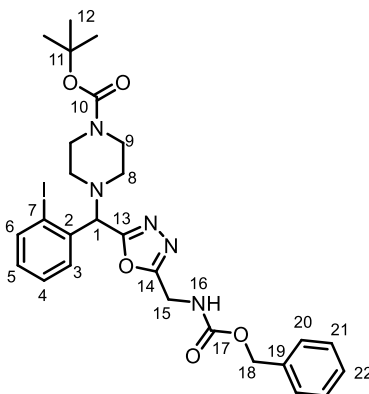
¹H NMR (500 MHz, CDCl₃) δ 7.92 – 7.86 (m, 2H), 7.69 – 7.62 (m, 2H), 7.29 (tq, *J* = 7.2, 2.5, 1.7, 4H), 7.03 – 6.98 (m, 2H), 6.95 – 6.88 (m, 3H), 6.78 (dt, *J* = 15.6, 7.1, 1H, C₄), 6.31 (s, 1H, C₁), 5.71 (dt, *J* = 15.7, 1.5, 1H, C₅), 3.84 (s, 3H, C₇), 3.71 (s, 3H, C₁₆), 3.48 (m, 2H, C₃), 2.35 (m, 1H, C₂), 2.28 – 2.17 (m, 1H, C₂).

¹³C NMR (126 MHz, CDCl₃) δ 166.7 (C₆), 165.8 (ArC), 164.3 (ArC), 159.8 (ArC), 147.5 (ArC), 146.0 (C₄), 132.4 (ArCH), 129.7 (ArCH), 129.5 (ArCH), 128.4 (ArCH), 127.6 (ArC), 126.6 (ArC), 122.6 (ArC), 122.3 (C₅), 120.6 (ArCH), 117.5 (ArCH), 114.3 (ArCH), 60.6 (C₁), 55.3 (C₇), 51.4 (C₁₆), 46.5 (C₃), 30.7 (C₂).

FT-IR(thin film): ν_{max} (cm⁻¹) = 2980, 2889, 1720, 1656, 1601, 1511, 1480, 1436, 1382, 1250, 1175, 1082, 1032, 1008, 966, 833, 749, 732, 694.

(ESI): *m/z* calculated for C₂₈H₂₇O₄N₃⁷⁹Br requires 548.1179 for [M+H]⁺, found 548.1178.

***tert*-butyl 4-((5-(((benzyloxy)carbonyl)amino)methyl)-1,3,4-oxadiazol-2-yl)(2-iodophenyl)methyl)piperazine-1-carboxylate – 59**



Following **general procedure A** (using *tert*-butyl 4-(2-iodobenzoyl)piperazine-1-carboxylate (83.3 mg, 0.20 mmol, 1.0 eq) and Vaska's complex (7.8 mg, 0.01 mmol, 5.0 mol%), and stirring for 1 h after addition of Z-Gly-OH (46.0 mg, 0.22 mmol, 1.1 eq) and NIITP (66.5 mg, 0.22 mmol, 1.1 eq): after FCC (35% EtOAc/pentane), **59** (69.7 mg, 55%) was afforded as an amber colored solid.

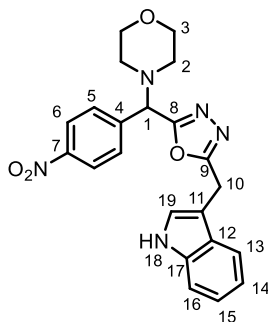
m.p.: 60 – 62 °C

¹H NMR (400 MHz, CDCl₃) δ 7.73 (dd, *J* = 8.0, 1.3, 1H, C₆), 7.52 (d, *J* = 7.8, 1H, C₃), 7.23 – 7.13 (m, 6H, C₄ & C₂₀ & C₂₁ & C₂₂), 6.88 (td, *J* = 7.6, 1.7, 1H, C₅), 5.42 (s, 1H, N₁₆), 5.13 (s, 1H, C₁), 4.99 (s, 2H, C₁₈), 4.45 (d, *J* = 6.0, 2H, C₁₅), 3.34 – 3.20 (m, 4H, C₉), 2.46 – 2.35 (m, 2H, C₈), 2.31 – 2.21 (m, 2H, C₈), 1.29 (s, 9H, C₁₂).

¹³C NMR (101 MHz, CDCl₃) δ 165.1 (ArC), 164.2 (ArC), 156.1 (C), 154.6 (C), 140.3 (C₆), 137.6 (ArC), 136.0 (ArC), 130.3 (C₅), 130.0 (C₃), 128.7 (ArCH), 128.6 (ArCH), 128.3 (ArCH), 128.2 (ArCH), 101.0 (C₇), 79.8 (C₁₁), 69.0 (C₁), 67.4 (C₉), 50.3 (C₈), 43.1 (C₁₈), 36.4 (C₁₅), 28.4 (C₁₂).

FT-IR(thin film): $\nu_{\max}(\text{cm}^{-1}) = 3657, 2980, 2889, 1723, 1689, 1584, 1532, 1456, 1422, 1392, 1366, 1246, 1072, 998, 967, 688, 751, 734, 698.$

(ESI): m/z calculated for $C_{27}H_{33}O_5N_5I$ requires 634.1521 for $[M+H]^+$, found 634.1515.

4-((5-((1*H*-indol-3-yl)methyl)-1,3,4-oxadiazol-2-yl)(4-nitrophenyl)methyl)morpholine – 60

Following **general procedure A** (using morpholino(4-nitrophenyl)methanone (47.2 mg, 0.20 mmol, 1.0 eq) and Vaska's complex (1.6 mg, 2.0 μmol , 1.0 mol%), and stirring for 1 h after addition of 2-(1*H*-indol-3-yl)acetic acid (38.5 mg, 0.22 mmol, 1.1 eq) and NIITP (66.5 mg, 0.22 mmol, 1.1 eq)): after FCC (35% acetone/pentane), **60** (39.8 mg, 47%) was afforded as a dark oil.

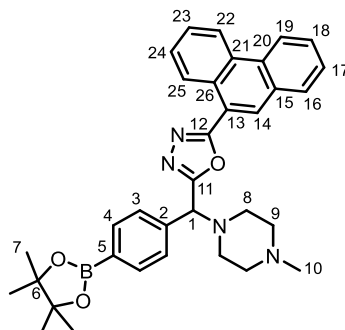
^1H NMR (400 MHz, CDCl_3) δ 8.38 (br, 1H, N₁₈), 8.16 – 8.07 (m, 2H, C₆), 7.64 – 7.57 (m, 2H, C₅), 7.50 (d, $J = 8.0$, 1H, C₁₃), 7.34 (dt, $J = 8.2$, 1.0, 1H, C₁₆), 7.19 (ddd, $J = 8.2$, 7.0, 1.2, 1H, C₁₄), 7.12 (d, $J = 2.5$, 1H, C₁₉), 7.07 (ddd, $J = 8.0$, 7.0, 1.0, 1H, C₁₅), 4.92 (s, 1H, C₁), 4.35 (d, $J = 0.9$, 2H, C₁₀), 3.66 (dd, $J = 5.3$, 4.0, 4H, C₂), 2.46 (dt, $J = 11.6$, 4.7, 2H, C₃), 2.32 (dt, $J = 11.2$, 4.6, 2H, C₃).

^{13}C NMR (101 MHz, CDCl_3) δ 167.1 (ArC), 164.0 (ArC), 148.0 (ArC), 142.6 (ArC), 136.3 (ArC), 129.6 (C₅), 126.5 (ArC), 123.9 (C₆), 123.1 (C₁₉), 122.5 (C₁₄), 119.9 (C₁₅), 118.4 (C₁₃), 111.5 (C₁₆), 107.9 (ArC), 66.6 (C₂), 65.6 (C₁), 51.3 (C₃), 22.3 (C₁₀).

FT-IR(thin film): $\nu_{\text{max}}(\text{cm}^{-1}) = 2980, 2889, 1579, 1521, 1382, 1348, 1264, 1252, 1154, 1114, 955, 880, 835, 810, 732, 700$.

(ESI): m/z calculated for $\text{C}_{22}\text{H}_{22}\text{O}_4\text{N}_5$ requires 420.1666 for $[\text{M}+\text{H}]^+$, found 420.1660.

2-((4-methylpiperazin-1-yl)(4-(4,4,5,5-tetramethyl-1,3,2-dioxaborolan-2-yl)phenyl)methyl)-5-(phenanthren-9-yl)-1,3,4-oxadiazole – 61



Following **general procedure A** (using (4-methylpiperazin-1-yl)(4-(4,4,5,5-tetramethyl-1,3,2-dioxaborolan-2-yl)phenyl)methanone (66.0 mg, 0.20 mmol, 1.0 eq) and Vaska's complex (1.6 mg, 2.0 μ mol, 1.0 mol%), and stirring for 1 h after addition of phenanthrene-9-carboxylic acid (48.9 mg, 0.22 mmol, 1.1 eq) and NIITP (66.5 mg, 0.22 mmol, 1.1 eq)): after FCC (7% MeOH/CH₂Cl₂), **61** (61.7 mg, 55%) was afforded as a dark oil.

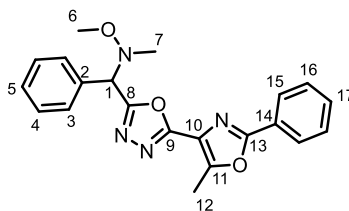
¹H NMR (400 MHz, CDCl₃) δ 9.22 – 9.15 (m, 1H), 8.74 – 8.67 (m, 1H), 8.65 (d, *J* = 8.3, 1H), 8.37 (s, 1H, C₁₄), 7.95 (dd, *J* = 8.0, 1.4, 1H), 7.91 – 7.85 (m, 2H), 7.75 – 7.67 (m, 3H), 7.67 – 7.58 (m, 3H), 5.06 (s, 1H, C₁), 2.76 (br, s, 2H, C₈), 2.63 (br, s, 6H, C₈ & C₉), 2.36 (s, 3H, C₁₀), 1.32 (s, 12H, C₇).

¹³C NMR (101 MHz, CDCl₃) δ 165.3 (ArC), 164.9 (ArC), 138.9 (ArC), 135.4 (ArCH), 131.7 (ArC), 130.9 (ArCH), 130.6 (ArC), 130.2 (ArC), 129.8 (ArCH), 128.9 (ArCH), 128.1 (ArCH), 127.9 (ArC), 127.8 (ArCH), 127.4 (ArCH), 127.2 (ArCH), 127.0 (ArCH), 122.9 (ArCH), 122.7 (ArCH), 119.3 (ArC), 84.0 (C₆), 66.5 (C₁), 54.7 (C₉), 50.6 (C₈), 45.4 (C₁₀), 24.9 (C₇).

FT-IR(thin film): $\nu_{\max}(\text{cm}^{-1})$ = 2980, 2888, 1611, 1539, 1472, 1380, 1359, 1293, 1264, 1142, 1088, 962, 857, 814, 768, 733, 565.

(ESI): *m/z* calculated for C₃₄H₃₈O₃N₄¹⁰B requires 561.3036 for [M+H]⁺, found 561.3027.

***N,O*-dimethyl-*N*-((5-(5-methyl-2-phenyloxazol-4-yl)-1,3,4-oxadiazol-2-yl)(phenyl)methyl)hydroxylamine – 62**



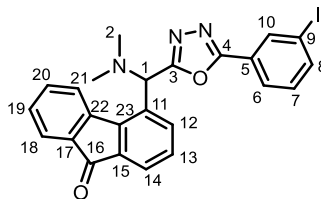
Following **general procedure A** (using *N*-methoxy-*N*-methylbenzamide (33.0 mg, 0.20 mmol, 1.0 eq) and Vaska's complex (1.6 mg, 2.0 μ mol, 1.0 mol%), and stirring for 1 h after addition of 5-methyl-2-phenyloxazole-4-carboxylic acid (44.7 mg, 0.22 mmol, 1.1 eq) and NIITP (66.5 mg, 0.22 mmol, 1.1 eq)): after FCC (40% Et₂O/pentane), **62** (32.0 mg, 43%) was afforded as a brown oil.

¹H NMR (400 MHz, CDCl₃) δ 7.99 – 7.83 (m, 2H, C₁₅), 7.50 – 7.38 (m, 2H, C₃), 7.38 – 7.24 (m, 3H, C₁₆ & C₁₇), 7.24 – 7.12 (m, 3H, C₄ & C₅), 4.98 (s, 1H, C₁), 3.33 (s, 3H, C₆), 2.61 (s, 3H, C₁₂), 2.42 (s, 3H, C₇).

¹³C NMR (101 MHz, CDCl₃) δ 165.1 (ArC), 160.9 (ArC), 159.7 (ArC), 151.8 (ArC), 135.1 (ArC), 130.9 (ArCH), 129.05 (ArCH), 128.96 (ArCH), 128.8 (ArCH), 126.6 (ArCH), 126.5 (ArC), 123.6 (ArC), 69.2 (C₁), 60.3 (C₆), 42.7 (C₇), 11.9 (C₁₂).

FT-IR(thin film): $\nu_{\max}(\text{cm}^{-1}) = 3062, 2980, 2890, 1644, 1564, 1546, 1489, 1450, 1333, 1197, 1088, 1072, 1057, 1042, 958, 812, 776, 708, 694.$

(ESI): m/z calculated for C₂₁H₂₁O₃N₄ requires 377.1608 for [M+H]⁺, found 377.1608.

4-((dimethylamino)(5-(3-iodophenyl)-1,3,4-oxadiazol-2-yl)methyl)-9H-fluoren-9-one – 63

Following **general procedure A** (using *N,N*-dimethyl-9-oxo-9*H*-fluorene-4-carboxamide (50.3 mg, 0.20 mmol, 1.0 eq) and Vaska's complex (1.6 mg, 2.0 μ mol, 1.0 mol%), and stirring for 1 h after addition of 3-iodobenzoic acid (54.6 mg, 0.22 mmol, 1.1 eq) and NIITP (66.5 mg, 0.22 mmol, 1.1 eq): after FCC (40% Et₂O/pentane), **63** (61.1 mg, 60%) was afforded as a yellow crystalline solid.

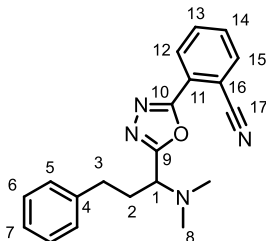
m.p.: 70 – 72 °C

¹H NMR (400 MHz, CDCl₃) δ 8.32 (t, *J* = 1.7, 1H), 8.09 (d, *J* = 7.7, 1H), 7.99 (dt, *J* = 7.8, 1.3, 1H), 7.85 (ddd, *J* = 7.9, 1.8, 1.0, 1H), 7.82 (dd, *J* = 8.0, 1.2, 1H), 7.75 – 7.71 (m, 1H), 7.69 (dd, *J* = 7.3, 1.2, 1H), 7.60 (td, *J* = 7.6, 1.3, 1H), 7.39 – 7.33 (m, 2H), 7.22 (t, *J* = 7.9, 1H), 5.48 (s, 1H, C₁), 2.44 (s, 6H, C₂).

¹³C NMR (101 MHz, CDCl₃) δ 193.3 (C₁₆), 164.8 (ArC), 163.9 (ArC), 143.7 (ArC), 143.0 (ArC), 140.8 (ArCH), 135.6 (ArCH), 135.5 (ArC), 135.1 (ArCH), 135.0 (ArCH), 134.6 (ArC), 132.7 (ArC), 130.7 (ArCH), 129.3 (ArCH), 129.2 (ArCH), 126.1 (ArCH), 125.4 (ArCH), 124.4 (ArCH), 124.3 (ArCH), 94.3 (C₉), 63.2 (C₁), 43.1 (C₂).

FT-IR(thin film): $\nu_{\max}(\text{cm}^{-1})$ = 2980, 1711, 1605, 1575, 1542, 1463, 1425, 1239, 1169, 1094, 1039, 994, 961, 888, 811, 792, 766, 734, 721, 678.

(ESI): *m/z* calculated for C₂₄H₁₉O₂N₃I requires 508.0516 for [M+H]⁺, found 508.0516.

2-(5-(1-(dimethylamino)-3-phenylpropyl)-1,3,4-oxadiazol-2-yl)benzonitrile – 64

Following **general procedure A** (using *N,N*-dimethyl-3-phenylpropanamide (35.4 mg, 0.20 mmol, 1.0 eq) and Vaska's complex (1.6 mg, 2.0 μ mol, 1.0 mol%), and stirring for 16 h after addition of 2-cyanobenzoic acid (58.9 mg, 0.40 mmol, 2.0 eq) and NIITP (121 mg, 0.40 mmol, 2.0 eq)): after FCC (45% EtOAc/pentane), **64** (32.8 mg, 49%) was afforded as an amber oil.

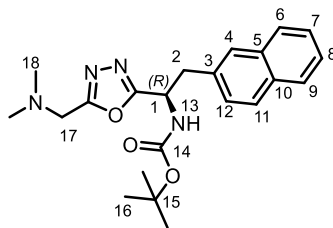
^1H NMR (400 MHz, CDCl_3) δ 8.21 (ddd, $J = 8.0, 1.4, 0.5$, 1H), 7.79 (ddd, $J = 7.7, 1.4, 0.5$, 1H), 7.69 (td, $J = 7.8, 1.4$, 1H), 7.58 (td, $J = 7.7, 1.3$, 1H), 7.19 (tdd, $J = 7.2, 2.2, 1.0$, 2H), 7.16 – 7.11 (m, 2H), 7.11 – 7.06 (m, 1H, C_7), 3.93 (t, $J = 7.6$, 1H, C_1), 2.74 – 2.61 (m, 2H, C_3), 2.30 (s, 6H, C_8), 2.29 – 2.22 (m, 2H, C_2).

^{13}C NMR (101 MHz, CDCl_3) δ 166.2 (ArC), 162.5 (ArC), 140.9 (ArC), 134.8 (ArCH), 133.1 (ArCH), 131.7 (ArCH), 129.5 (ArCH), 128.6 (ArCH), 128.5 (ArCH), 126.11 (ArC), 126.08 (ArCH), 117.0 (C_{17}), 110.5 (C_{16}), 59.5 (C_1), 41.4 (C_8), 32.2 (C_3), 32.1 (C_2).

FT-IR(thin film): $\nu_{\text{max}}(\text{cm}^{-1}) = 2941, 2866, 2832, 2786, 2361, 2229, 1601, 1541, 1493, 1468, 1453, 1437, 1157, 1029, 965, 775, 747, 699$.

(ESI): m/z calculated for $\text{C}_{20}\text{H}_{21}\text{ON}_4$ requires 333.1710 for $[\text{M}+\text{H}]^+$, found 333.1709.

***tert*-butyl (*R*)-(1-(5-((dimethylamino)methyl)-1,3,4-oxadiazol-2-yl)-2-(naphthalen-2-yl)ethyl)carbamate – 65**



Following **general procedure A** (using *N,N*-dimethylformamide (14.6 mg, 0.20 mmol, 1.0 eq) and Vaska's complex (0.8 mg, 1.0 μ mol, 0.5 mol%), and stirring for 1 h after addition of (*R*)-2-((*tert*-butoxycarbonyl)amino)-3-(naphthalen-2-yl)propanoic acid (69.4 mg, 0.22 mmol, 1.1 eq) and NIITP (66.5 mg, 0.22 mmol, 1.1 eq)): after FCC (40% acetone/pentane) and PTLC (85% EtOAc/Hexane), **65** (46.3 mg, 58%) was afforded as a colourless oil.

ee: >99.5% [HPLC CHIRALPAK[®] AD-H, Hexane/IPA = 85/15, 1 mL/min, λ = 220 nm, $t_{(S)}$ = 16.5 min, $t_{(R)}$ = 19.0 min].

¹H NMR (400 MHz, CDCl₃) δ 7.83 – 7.70 (m, 3H), 7.56 (s, 1H, C₄), 7.49 – 7.41 (m, 2H), 7.22 (dd, J = 8.4, 1.8, 1H), 5.45 – 5.31 (m, 1H, C₁), 5.25 – 5.10 (m, 1H, N₁₃), 3.69 (s, 2H, C₁₇), 3.41 (d, J = 6.5, 2H, C₂), 2.23 (s, 6H, C₁₈), 1.38 (s, 9H, C₁₆).

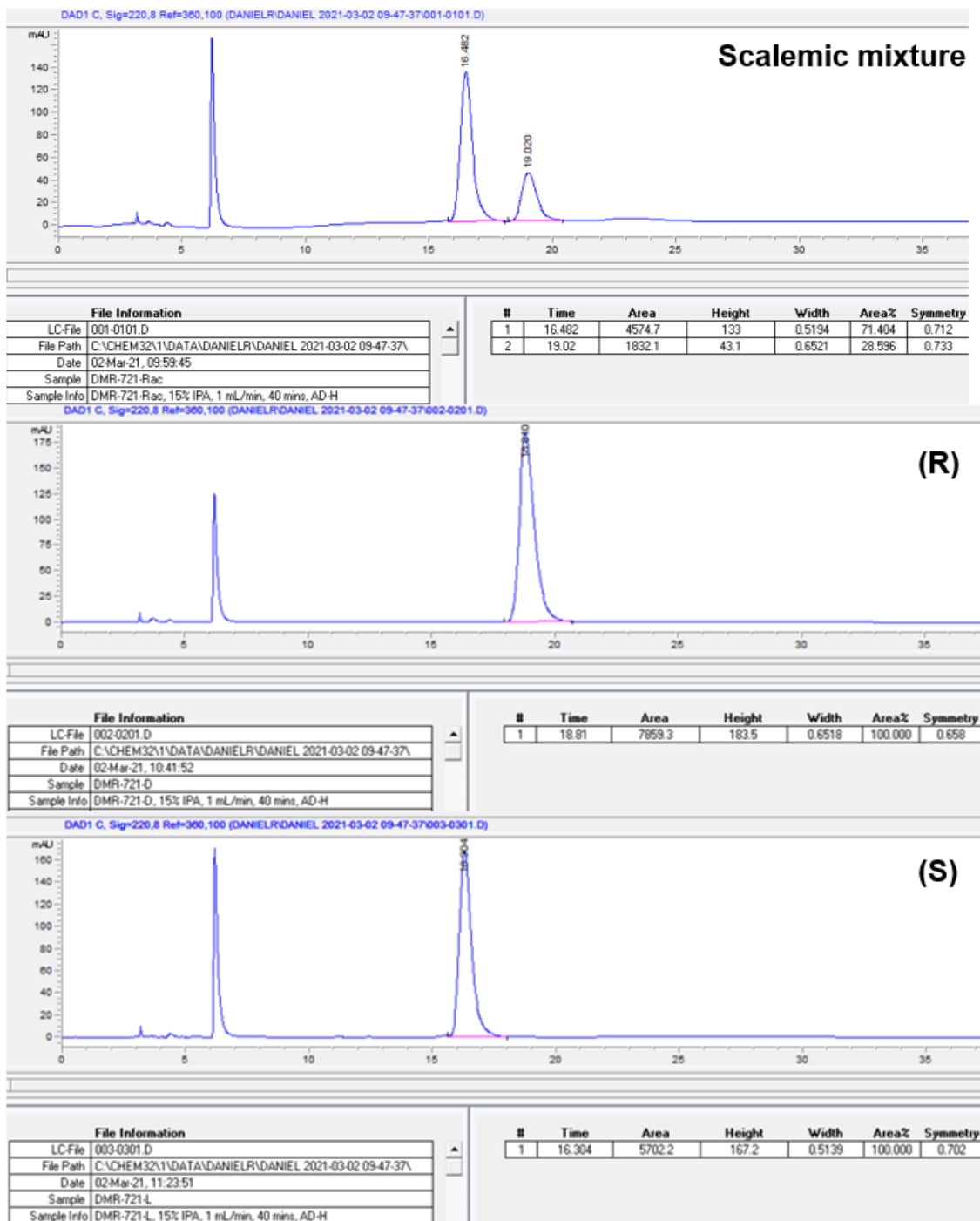
¹³C NMR (101 MHz, CDCl₃) δ 167.0 (ArC), 164.0 (ArC), 133.4 (ArC), 132.8 (ArC), 132.6 (ArC), 128.5 (ArCH), 128.2 (ArCH), 127.6 (ArCH), 127.6 (ArCH), 127.2 (ArCH), 126.2 (ArCH), 125.9 (ArCH), 80.5 (C₁₅), 52.7 (C₁₇), 48.5 (C₁), 44.9 (C₁₈), 40.2 (C₂), 28.2 (C₁₆).

FT-IR(thin film): $\nu_{\max}(\text{cm}^{-1})$ = 3348, 2977, 2771, 1693, 1509, 1459, 1365, 1326, 1279, 1265, 1243, 1162, 1047, 1024, 869, 847, 821, 772, 750, 645.

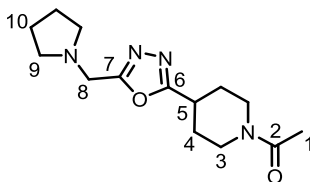
(ESI): m/z calculated for C₂₂H₂₉O₃N₄ requires 397.2234 for [M+H]⁺, found 397.2236.

$[\alpha]_{\text{D}}^{25}$ = 35.5 (c = 0.21, CHCl₃).

Enantiopurity was of **(R)**-**65** was confirmed by synthesis of **(S)**-**65** starting from *(S)*-2-((*tert*-butoxycarbonyl)amino)-3-(naphthalen-2-yl)propanoic acid and combining with **(R)**-**65** to create a scalemic mixture for separation by chiral HPLC. Relevant HPLC traces are below.



1-(4-(5-(pyrrolidin-1-ylmethyl)-1,3,4-oxadiazol-2-yl)piperidin-1-yl)ethan-1-one – 66



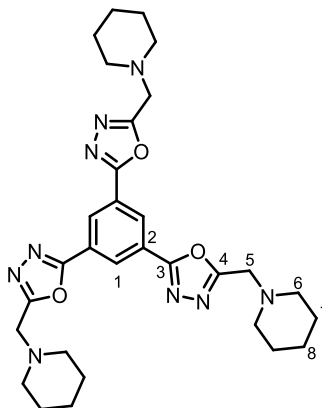
Following **general procedure A** (using pyrrolidine-1-carbaldehyde (198 mg, 2.0 mmol, 1.0 eq) and Vaska's complex (15.6 mg, 0.02 mmol, 1.0 mol%), and stirring for 1 h after addition of 1-acetylpiperidine-4-carboxylic acid (377 mg, 2.2 mmol, 1.1 eq) and NIITP (665 mg, 2.2 mmol, 1.1 eq): after FCC (EtOAc → 10% MeOH/CH₂Cl₂), **66** (292 mg, 58%) was afforded as a dark oil.

¹H NMR (400 MHz, CDCl₃) δ 4.45 (dtd, *J* = 13.6, 4.3, 1.6, 1H, C₃), 3.91 (s, 2H, C₈), 3.86 (dtd, *J* = 14.0, 4.3, 1.5, 1H, C₃), 3.24 (ddd, *J* = 14.0, 11.1, 3.0, 1H, C₃), 3.15 (tt, *J* = 10.6, 4.0, 1H, C₅), 2.91 (ddd, *J* = 13.9, 11.1, 3.1, 1H, C₃), 2.72 – 2.63 (m, 4H, C₉), 2.16 – 2.03 (m, 5H, C₁ & C₄), 1.95 – 1.73 (m, 6H, C₄ & C₁₀).

¹³C NMR (101 MHz, CDCl₃) δ 168.9 (C₂), 168.7 (ArC), 164.1 (ArC), 54.0 (C₉), 49.1 (C₈), 45.5 (C₃), 40.6 (C₃), 33.2 (C₅), 29.3 (C₄), 28.8 (C₄), 23.7 (C₁₀), 21.4 (C₁).

FT-IR(thin film): $\nu_{\max}(\text{cm}^{-1}) = 2970, 2801, 1635, 1586, 1561, 1435, 1372, 1295, 1272, 1229, 1181, 1143, 1117, 1044, 978, 875, 722, 697.$

(ESI): *m/z* calculated for C₁₄H₂₃O₂N₄ requires 279.1816 for [M+H]⁺, found 279.1816.

1,3,5-tris(5-(piperidin-1-ylmethyl)-1,3,4-oxadiazol-2-yl)benzene – 67

To an oven-dried screw cap vial equipped with magnetic stirrer, *N*-formylpiperidine (67.9 mg, 0.60 mmol, 6.0 eq), and Vaska's complex (4.7 mg, 6.0 μ mol, 1.0 mol% with respect to the amide) were added. The vial was evacuated and backfilled with nitrogen (x3). Then anhydrous THF (3.0 mL) was added followed in quick succession by TMDS (216 μ L, 1.2 mmol, 12 eq), and the vial was capped and stirred at rt. After 30 mins, the vial was opened and a suspension of NIITP (182 mg, 0.60 mmol, 6.0 eq) in THF (3.0 mL) added, followed by 1,3,5-benzenetricarboxylic acid (21.0 mg, 0.10 mmol, 1.0 eq) as a single portion. The vial was recapped and stirred at rt for 80 mins. After this time, CH_2Cl_2 (10 mL) was added and the reaction washed with saturated aqueous NaHCO_3 (20 mL), then the aqueous was extracted with CH_2Cl_2 (3 x 10 mL). The combined organics were dried (MgSO_4), filtered, and concentrated *in vacuo* to afford the crude product. The crude was purified by FCC (EtOAc \rightarrow 10% MeOH/ CH_2Cl_2) to afford the *title compound* (36.6 mg, 64%) as a tan powder.

m.p.: 154 – 156 $^\circ\text{C}$

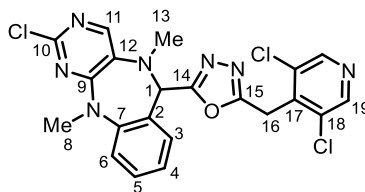
^1H NMR (400 MHz, CDCl_3) δ 8.91 (s, 3H, C₁), 3.90 (s, 6H, C₅), 2.59 (t, $J = 5.3$, 12H, C₆), 1.64 (p, $J = 5.5$, 12H, C₇), 1.44 (m, 6H, C₈).

^{13}C NMR (101 MHz, CDCl_3) δ 164.5 (ArC), 163.5 (ArC), 127.6 (C₁), 126.1 (ArC), 54.3 (C₆), 52.7 (C₅), 25.7 (C₇), 23.7 (C₈).

FT-IR(thin film): $\nu_{\max}(\text{cm}^{-1}) = 2980, 2935, 2889, 1713, 1605, 1574, 1544, 1463, 1438, 1381, 1300, 1251, 1154, 1110, 1072, 961, 803, 733, 680.$

(ESI): m/z calculated for $\text{C}_{30}\text{H}_{40}\text{O}_3\text{N}_9$ requires 574.3249 for $[\text{M}+\text{H}]^+$, found 574.3248.

2-(2-chloro-5,11-dimethyl-6,11-dihydro-5*H*-benzo[e]pyrimido[5,4-b][1,4]diazepin-6-yl)-5-((3,5-dichloropyridin-4-yl)methyl)-1,3,4-oxadiazole – 68



Following **general procedure A** (using 2-chloro-5,11-dimethyl-5,11-dihydro-6*H*-benzo[e]pyrimido[5,4-b][1,4]diazepin-6-one (19.2 mg, 0.07 mmol, 1.0 eq) and Vaska's complex (2.7 mg, 3.5 μ mol, 5.0 mol%), and stirring for 1 h after addition of 2-(3,5-dichloropyridin-4-yl)acetic acid (28.8 mg, 0.14 mmol, 2.0 eq) and NIITP (42.3 mg, 0.14 mmol, 2.0 eq): after PTLC (90% EtOAc/Hexane), **68** (14.7 mg, 43%) was afforded as a beige crystalline solid.

m.p.: 98 – 100 °C

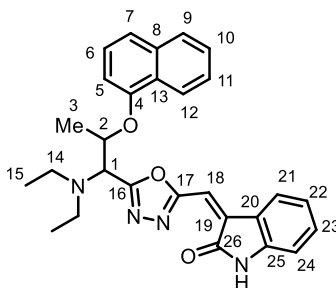
^1H NMR (400 MHz, CDCl_3) δ 8.53 (s, 2H, C₁₉), 7.67 (s, 1H, C₁₁), 7.43 (ddd, $J = 8.2, 7.4, 1.6$, 1H), 7.24 (d, $J = 1.6$, 1H), 7.20 – 7.11 (m, 2H), 5.29 (s, 1H, C₁), 4.44 (s, 2H, C₁₆), 3.24 (s, 3H, C₈), 2.98 (s, 3H, C₁₃).

^{13}C NMR (101 MHz, CDCl_3) δ 165.0 (ArC), 162.2 (ArC), 154.4 (ArC), 151.1 (ArC), 147.9 (C₁₉), 146.4 (C₁₁), 145.2 (ArC), 138.3 (ArC), 133.0 (ArC), 131.2 (ArC), 130.4 (ArCH), 129.4 (ArC), 128.9 (ArCH), 124.5 (ArCH), 123.1 (ArCH), 64.0 (C₁), 43.3 (C₁₃), 40.0 (C₈), 27.0 (C₁₆).

FT-IR(thin film): $\nu_{\text{max}}(\text{cm}^{-1}) = 2980, 2917, 1556, 1532, 1497, 1476, 1448, 1403, 1344, 1241, 1204, 1174, 1141, 1119, 1095, 1038, 949, 887, 798, 767, 729, 706, 668$.

(ESI): m/z calculated for $\text{C}_{21}\text{H}_{17}^{35}\text{Cl}_3\text{ON}_7$ requires 488.0555 for $[\text{M}+\text{H}]^+$, found 488.0554.

(Z)-3-((5-(1-(diethylamino)-2-(naphthalen-1-yloxy)propyl)-1,3,4-oxadiazol-2-yl)methylene)indolin-2-one – 69



Following **general procedure A** (using *N,N*-Diethyl-2-(1-naphthyloxy)propanamide (napropamide) (54.3 mg, 0.20 mmol, 1.0 eq) and Vaska's complex (1.6 mg, 2.0 μ mol, 1.0 mol%), and stirring for 16 h after addition of (*Z*)-2-(2-oxoindolin-3-ylidene)acetic acid (75.7 mg, 0.40 mmol, 2.0 eq) and NIITP (121 mg, 0.40 mmol, 2.0 eq)): after FCC (60% Et₂O/pentane), **69** (50.1 mg, 53%) as a 2.4:1 mixture of diastereomers was afforded as an orange crystalline solid.

m.p.: 74 – 76 °C

The integral ratios are given as observed - ¹H NMR (400 MHz, CDCl₃) δ 9.04 – 8.98 (m, 0.4H), 8.92 – 8.85 (m, 1H), 8.72 (s, 0.4H), 8.63 (s, 1H), 8.29 – 8.22 (m, 0.4H), 7.93 (dd, *J* = 8.3, 1.4, 1H), 7.84 – 7.77 (m, 0.4H), 7.74 – 7.67 (m, 1H), 7.53 – 7.27 (m, 9H), 7.08 (td, *J* = 7.7, 1.1, 0.5H), 7.05 – 6.95 (m, 3H), 6.94 – 6.89 (m, 0.5H), 6.89 – 6.83 (m, 1H), 5.37 – 5.27 (m, 0.5H, C₂), 5.27 – 5.17 (m, 1H, C₂), 4.60 (d, *J* = 7.5, 0.4H, C₁), 4.54 (d, *J* = 9.5, 1H, C₁), 2.99 (dq, *J* = 13.2, 7.2, 0.9H, C₁₄), 2.89 (dq, *J* = 13.0, 7.3, 2.2H, C₁₄), 2.68 (dq, *J* = 13.8, 6.9, 0.9H, C₁₄), 2.45 (dq, *J* = 13.5, 6.8, 2.2H, C₁₄), 1.68 (d, *J* = 6.0, 3.2H, C₃), 1.53 (d, *J* = 6.1, 1.3H, C₃), 1.19 (t, *J* = 7.1, 6.4H, C₁₅), 1.09 (t, *J* = 7.1, 2.7H, C₁₅).

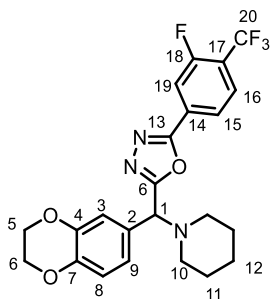
¹³C NMR (101 MHz, CDCl₃) δ 169.2 (C₂₆), 166.1 (ArC), 165.9 (ArC), 163.1 (ArC), 162.9 (ArC), 153.4 (ArC), 153.1 (ArC), 143.0 (ArC), 142.7 (ArC), 134.8 (ArC), 134.6 (ArC), 134.0 (ArC),

133.6 (ArC), 132.5 (ArCH), 132.3 (ArCH), 128.5 (ArCH), 128.4 (ArCH), 127.5 (ArCH), 127.4 (ArCH), 126.4 (ArCH), 126.4 (ArCH), 126.3 (ArCH), 126.3 (ArC), 125.8 (ArCH), 125.7 (ArCH), 125.3 (ArCH), 125.2 (ArCH), 123.0 (ArCH), 122.9 (ArCH), 122.3 (ArCH), 121.6 (ArCH), 120.9 (ArCH), 120.7 (ArC), 120.7 (ArCH), 112.2 (ArCH), 112.1 (ArCH), 110.2 (ArCH), 110.0 (ArCH), 106.8 (ArCH), 106.1 (ArCH), 74.2 (C₂), 73.3 (C₂), 61.6 (C₁), 45.4 (C₁₄), 45.1 (C₁₄), 18.1 (C₃), 17.5 (C₃), 14.1 (C₁₅), 13.9 (C₁₅).

FT-IR(thin film): $\nu_{\max}(\text{cm}^{-1}) = 2657, 2980, 2888, 1712, 1611, 1462, 1382, 1251, 1154, 1072, 953, 815, 794, 772, 734, 677, 607.$

(ESI): m/z calculated for C₂₈H₂₉O₃N₄ requires 469.2234 for [M+H]⁺, found 469.2234.

2-((2,3-dihydrobenzo[b][1,4]dioxin-6-yl)(piperidin-1-yl)methyl)-5-(3-fluoro-4-(trifluoromethyl)phenyl)-1,3,4-oxadiazole – 70



Following **general procedure A** (using **S4** (49.5 mg, 0.20 mmol, 1.0 eq) and Vaska's complex (1.6 mg, 2.0 μ mol, 1.0 mol%), and stirring for 1 h after addition of 3-fluoro-4-(trifluoromethyl)benzoic acid (45.8 mg, 0.22 mmol, 1.1 eq) and NIITP (66.5 mg, 0.22 mmol, 1.1 eq)): after FCC (25% Et₂O/pentane), **70** (80.6 mg, 87%) was afforded as an orange oil.

¹H NMR (400 MHz, CDCl₃) δ 7.98 – 7.92 (m, 1H, C₁₅), 7.90 – 7.85 (m, 1H, C₁₉), 7.74 (t, J = 7.6, 1H, C₁₆), 7.06 (d, J = 2.2, 1H, C₃), 6.96 (dd, J = 8.4, 2.2, 1H, C₉), 6.84 (d, J = 8.3, 1H, C₈), 4.82 (s, 1H, C₁), 4.24 (s, 4H, C₅ & C₆), 2.58 – 2.47 (m, 2H, C₁₀), 2.39 – 2.28 (m, 2H, C₁₀), 1.65 – 1.54 (m, 4H, C₁₁), 1.48 – 1.39 (m, 2H, C₁₂).

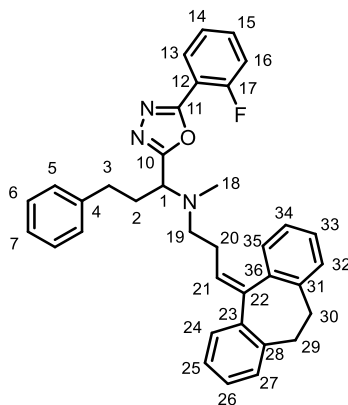
¹⁹F NMR (377 MHz, CDCl₃) δ -61.7 (d, J = 12.9, C₂₀), -112.2 (q, J = 13.1, C₁₈).

¹³C NMR (101 MHz, CDCl₃) δ 167.0 (C₆), 163.0 (d, J = 3.1, C₁₃), 159.9 (dq, J = 259.8, 2.1, C₁₈), 143.73 (ArC), 143.66 (ArC), 129.4 (d, J = 8.7, C₁₄), 129.2 (ArC), 128.2 – 128.0 (m, C₁₆), 122.6 (d, J = 4.0, C₁₅), 121.5 (C₉), 117.4 (C₈), 117.3 (C₃), 115.4 (d, J = 23.6, C₁₉), 66.4 (C₁), 64.34 (C₅ or C₆), 64.32 (C₅ or C₆), 52.4 (C₁₀), 25.9 (C₁₁), 24.2 (C₁₂).

FT-IR(thin film): $\nu_{\max}(\text{cm}^{-1})$ = 2980, 2888, 1633, 1591, 1563, 1505, 1472, 1416, 132, 1284, 1255, 1130, 1068, 1047, 955, 887, 734.

(ESI): m/z calculated for C₂₃H₂₂O₃N₃F₄ requires 464.1592 for [M+H]⁺, found 464.1590.

***N*-(3-(10,11-dihydro-5*H*-dibenzo[*a,d*][7]annulen-5-ylidene)propyl)-1-(5-(2-fluorophenyl)-1,3,4-oxadiazol-2-yl)-*N*-methyl-3-phenylpropan-1-amine – 71**



Following **general procedure A** (using *N*-(3-(10,11-dihydro-5*H*-dibenzo[*a,d*][7]annulen-5-ylidene)propyl)-*N*-methyl-3-phenylpropanamide (79.1 mg, 0.20 mmol, 1.0 eq) and Vaska's complex (1.6 mg, 2.0 μ mol, 1.0 mol%), and stirring for 16 h after addition of 2-fluorobenzoic acid (56.0 mg, 0.40 mmol, 2.0 eq) and NIITP (121 mg, 0.40 mmol, 2.0 eq): after FCC (12% EtOAc/pentane), **71** (64.1 mg, 59%) was afforded as a yellow oil.

^1H NMR (400 MHz, CDCl_3) δ 7.87 (td, $J = 7.5, 1.8, 1\text{H}$), 7.40 – 7.32 (m, 1H), 7.15 – 7.05 (m, 5H), 7.04 – 6.93 (m, 9H), 6.90 – 6.85 (m, 1H), 5.74 (t, $J = 7.3, 1\text{H}, \text{C}_{21}$), 3.82 (t, $J = 7.6, 1\text{H}, \text{C}_1$), 3.26 (br, 1H, C_{29} or C_{30}), 3.13 (br, 1H, C_{29} or C_{30}), 2.88 – 2.71 (br, 1H, C_{29} or C_{30}), 2.69 – 2.45 (m, 4H, C_3 & C_{19} & C_{29} or C_{30}), 2.39 – 2.25 (m, 1H, C_{19}), 2.21 – 2.10 (m, 4H, C_2 & C_{20}), 2.09 (s, 3H, C_{18}).

^{19}F NMR (377 MHz, CDCl_3) δ -110.2.

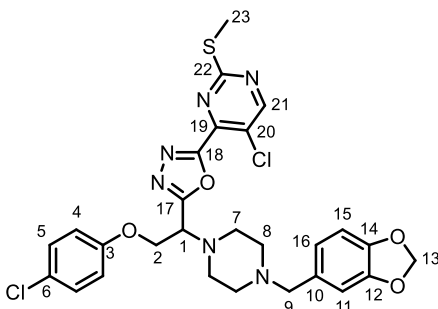
^{13}C NMR (101 MHz, CDCl_3) δ 166.1 (C_{10}), 161.7 (d, $J = 4.8, \text{C}_{11}$), 160.0 (d, $J = 258.2, \text{C}_{17}$), 143.7 (ArC), 141.4 (ArC), 141.1 (ArC), 140.1 (ArC), 139.4 (ArC), 137.1 (ArC), 133.47 (d, $J = 8.6, \text{C}_{13}$), 130.0 (ArCH), 129.8 (ArCH), 129.4 (ArCH), 128.6 (ArCH), 128.5 (ArCH), 128.3 (ArCH), 128.1 (ArCH), 127.4 (ArCH), 127.1 (ArCH), 126.0 (ArCH), 125.8 (ArCH), 124.66 (d, J

= 3.7, C₁₄), 116.98 (d, $J = 20.9$, C₁₆), 112.53 (d, $J = 11.6$, C₁₂), 58.9 (C₁), 54.2 (C₁₉), 53.6 (C₁₉), 37.9 (C₁₈), 37.2 (C₁₈), 33.8 (C₂₉ or C₃₀), 32.3 (C₃), 32.1 (C₂₉ or C₃₀), 32.0 (C₂₀), 28.3 (C₂).

FT-IR(thin film): $\nu_{\max}(\text{cm}^{-1}) = 2980, 1621, 1589, 1543, 1494, 1472, 1462, 1362, 1265, 1225, 1157, 1111, 1065, 964, 822, 766, 755, 735, 699.$

(ESI): m/z calculated for C₃₆H₃₅ON₃F requires 544.2759 for [M+H]⁺, found 544.2750.

2-(1-(4-(benzo[d][1,3]dioxol-5-ylmethyl)piperazin-1-yl)-2-(4-chlorophenoxy)ethyl)-5-(5-chloro-2-(methylthio)pyrimidin-4-yl)-1,3,4-oxadiazole – 72



Following **general procedure A** (using 1-(2-[4-Chlorophenoxy]acetyl)-4-(3,4-methylenedioxybenzyl)piperazine (fipexide) (73.9 mg, 0.19 mmol, 1.0 eq) and Vaska's complex (1.5 mg, 1.9 μ mol, 1.0 mol%), and stirring for 16 h after addition of 5-chloro-2-(methylthio)pyrimidine-4-carboxylic acid (77.8 mg, 0.38 mmol, 2.0 eq) and NIITP (115 mg, 0.38 mmol, 2.0 eq)): after FCC (45% EtOAc/pentane), **72** (77.8 mg, 69%) was afforded as a golden crystalline solid.

m.p.: 54 – 56 °C

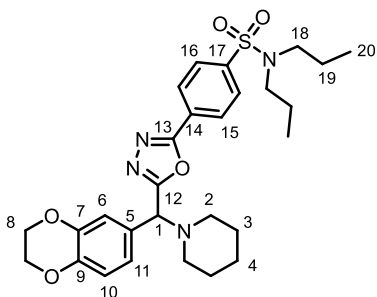
^1H NMR (400 MHz, CDCl_3) δ 8.71 (s, 1H, C₂₁), 7.25 – 7.19 (m, 2H, C₅), 6.86 – 6.80 (m, 2H, C₄), 6.79 (d, J = 1.4, 1H, C₁₁), 6.71 (dd, J = 4.0, 1.0, 2H, C₁₅ & C₁₆), 5.92 (s, 2H, C₁₃), 4.59 (dd, J = 8.5, 7.8, 1H, C₂), 4.53 (dd, J = 7.8, 5.1, 1H, C₁), 4.45 (dd, J = 8.5, 5.1, 1H, C₂), 3.39 (s, 2H, C₉), 2.81 – 2.72 (m, 2H, C₇), 2.72 – 2.64 (m, 2H, C₇), 2.59 (s, 3H, C₂₃), 2.47 (s, 4H, C₈).

^{13}C NMR (101 MHz, CDCl_3) δ 171.4 (ArC), 165.0 (ArC), 159.1 (C₂₁), 156.7 (ArC), 147.7 (ArC), 146.8 (ArC), 146.7 (ArC), 131.7 (ArC), 129.4 (C₅), 126.5 (ArC), 124.5 (ArC), 122.2 (ArCH), 116.3 (C₄), 109.4 (C₁₁), 107.9 (ArCH), 100.9 (C₁₃), 67.0 (C₂), 62.6 (C₉), 59.8 (C₁), 53.0 (C₈), 50.0 (C₇), 14.6 (C₂₃).

FT-IR(thin film): $\nu_{\text{max}}(\text{cm}^{-1})$ = 2980, 2882, 1700, 1541, 1489, 1439, 1399, 1367, 1337, 1300, 1242, 1212, 1165, 1037, 1006, 933, 889, 885, 826, 803, 776, 729, 668.

(ESI): m/z calculated for $C_{27}H_{27}O_4N_6^{35}Cl_2S$ requires 601.1186 for $[M+H]^+$, found 601.1180.

**4-(5-((2,3-dihydrobenzo[b][1,4]dioxin-6-yl)(piperidin-1-yl)methyl)-1,3,4-oxadiazol-2-yl)-
N,N-dipropylbenzenesulfonamide – 78**



Following **general procedure A** (using **S4** (989 mg, 4.0 mmol, 1.0 eq) and Vaska's complex (31.2 mg, 0.04 mmol, 1.0 mol%), and stirring for 1 h after addition of probenecid (1.26 g, 4.4 mmol, 1.1 eq) and NIITP (1.33 g, 4.4 mmol, 1.1 eq)): after FCC (50% Et₂O/pentane), **78** (1.73 g, 80%) was afforded as a white crystalline solid.

m.p.: 50 – 52 °C

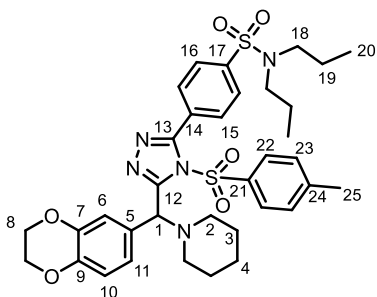
¹H NMR (400 MHz, CDCl₃) δ 8.17 (d, *J* = 8.5, 2H, C₁₅), 7.92 (d, *J* = 8.5, 2H, C₁₆), 7.06 (d, *J* = 2.1, 1H, C₆), 6.97 (dd, *J* = 8.4, 2.1, 1H, C₁₁), 6.83 (d, *J* = 8.3, 1H, C₁₀), 4.81 (s, 1H, C₁), 4.24 (s, 4H, C₈), 3.13 – 3.06 (m, 4H, C₁₈), 2.51 (dt, *J* = 11.1, 5.3, 2H, C₂), 2.33 (dt, *J* = 10.3, 4.8, 2H, C₂), 1.64 – 1.48 (m, 8H, C₃ & C₁₉), 1.44 (td, *J* = 6.7, 2.8, 2H, C₄), 0.87 (t, *J* = 7.4, 6H, C₂₀).

¹³C NMR (101 MHz, CDCl₃) δ 166.7 (ArC), 163.9 (ArC), 143.7 (ArC), 143.6 (ArC), 143.1 (ArC), 129.4 (ArC), 127.6 (C₁₆), 127.5 (C₁₅), 127.3 (ArC), 121.5 (C₁₁), 117.4 (C₁₀), 117.3 (C₆), 66.4 (C₁), 64.3 (C₈), 52.4 (C₂), 49.9 (C₁₈), 25.9 (C₃), 24.3 (C₄), 21.9 (C₁₉), 11.2 (C₂₀).

FT-IR(thin film): $\nu_{\max}(\text{cm}^{-1}) = 2933, 1699, 1505, 1455, 1381, 1339, 1283, 1257, 1212, 1155, 1091, 1066, 992, 980, 886, 838, 729, 699.$

(ESI): *m/z* calculated for C₂₈H₃₇O₅N₄S requires 541.2479 for [M+H]⁺, found 541.2474.

4-(5-((2,3-dihydrobenzo[b][1,4]dioxin-6-yl)(piperidin-1-yl)methyl)-4-tosyl-4*H*-1,2,4-triazol-3-yl)-*N,N*-dipropylbenzenesulfonamide – 90



Following **general procedure A** (using **S4** (49.5 mg, 0.20 mmol, 1.0 eq) and Vaska's complex (1.6 mg, 2.0 μ mol, 1.0 mol%), and stirring for 16 h after addition of **87** (175 mg, 0.40 mmol, 2.0 eq) and NIITP (121 mg, 0.40 mmol, 2.0 eq)): after FCC (50% EtOAc/pentane) and PTLC (50% EtOAc/Hexane), **90** (38.4 mg, 28%) was afforded as a tan powder.

m.p.: 114 – 116 °C

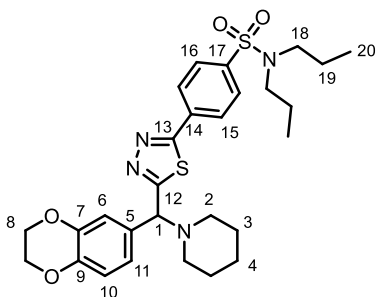
^1H NMR (400 MHz, CDCl_3) δ 7.77 (d, $J = 8.4$, 2H, C_{15}), 7.42 (d, $J = 8.4$, 2H, C_{16}), 7.10 – 7.02 (m, 5H, C_6 & C_{22} & C_{23}), 6.97 (dd, $J = 8.4$, 2.1, 1H, C_{11}), 6.83 (d, $J = 8.3$, 1H, C_{10}), 5.61 (s, 1H, C_1), 4.26 (s, 4H, C_8), 3.12 – 3.06 (m, 4H, C_{18}), 2.77 – 2.62 (m, 2H, C_2), 2.56 – 2.43 (m, 2H, C_2), 2.35 (s, 3H, C_{25}), 1.65 – 1.49 (m, 8H, C_3 & C_{19}), 1.46 – 1.37 (m, 2H, C_4), 0.88 (t, $J = 7.4$, 6H, C_{20}).

^{13}C NMR (101 MHz, CDCl_3) δ 152.2 (ArC), 147.0 (ArC), 143.5 (ArC), 143.2 (ArC), 142.1 (ArC), 134.2 (ArC), 131.7 (C_{16}), 130.8 (ArC), 129.8 (ArCH), 127.8 (ArCH), 126.2 (C_{15}), 123.5 (C_{11}), 119.3 (C_6), 116.8 (C_{10}), 65.4 (C_1), 64.3 (C_8), 51.8 (C_2), 50.1 (C_{18}), 26.2 (C_3), 24.4 (C_4), 22.0 (C_{19}), 21.7 (C_{25}), 11.2 (C_{20}).

FT-IR(thin film): $\nu_{\text{max}}(\text{cm}^{-1}) = 2967, 2934, 2875, 1697, 1627, 1592, 1507, 1458, 1386, 1338, 1287, 1258, 1184, 1157, 1081, 1017, 992, 888, 813, 735, 701, 666$.

(ESI): m/z calculated for $C_{35}H_{44}O_6N_5S_2$ requires 694.2728 for $[M+H]^+$, found 694.2720.

**4-(5-((2,3-dihydrobenzo[b][1,4]dioxin-6-yl)(piperidin-1-yl)methyl)-1,3,4-thiadiazol-2-yl)-
N,N-dipropylbenzenesulfonamide – 91**



Following **general procedure A** (using **S4** (49.5 mg, 0.20 mmol, 1.0 eq) and Vaska's complex (1.6 mg, 2.0 μ mol, 1.0 mol%), and stirring for 1 h after addition of **89** (121 mg, 0.40 mmol, 2.0 eq) and NIITP (121 mg, 0.40 mmol, 2.0 eq)): after FCC (55% Et₂O/pentane), **91** (70.8 mg, 62%) was afforded as an orange crystalline solid.

m.p.: 60 – 62 °C

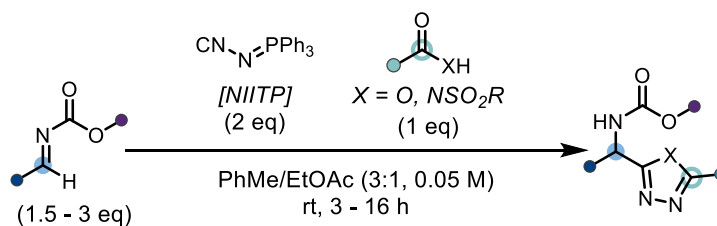
¹H NMR (400 MHz, CDCl₃) δ 8.06 (d, *J* = 8.5, 2H, C₁₅), 7.87 (d, *J* = 8.5, 2H, C₁₆), 6.98 (d, *J* = 2.1, 1H, C₆), 6.92 (dd, *J* = 8.4, 2.1, 1H, C₁₁), 6.82 (d, *J* = 8.3, 1H, C₁₀), 4.84 (s, 1H, C₁₁), 4.23 (s, 4H, C₈), 3.13 – 3.07 (m, 4H, C₁₈), 2.61 – 2.45 (m, 2H, C₂), 2.45 – 2.29 (m, 2H, C₂), 1.65 – 1.50 (m, 8H, C₃ & C₁₉), 1.49 – 1.41 (m, 2H, C₄), 0.86 (t, *J* = 7.4, 6H, C₂₀).

¹³C NMR (101 MHz, CDCl₃) δ 176.0 (ArC), 167.8 (ArC), 143.7 (ArC), 143.5 (ArC), 142.3 (ArC), 133.9 (ArC), 131.5 (ArC), 128.3 (C₁₅), 127.7 (C₁₆), 121.5 (C₁₁), 117.5 (C₁₀), 117.2 (C₆), 70.6 (C₁), 64.3 (C₈), 52.8 (C₂), 49.9 (C₁₈), 26.1 (C₃), 24.3 (C₄), 21.9 (C₁₉), 11.2 (C₂₀).

FT-IR(thin film): ν_{\max} (cm⁻¹) = 2933, 1699, 1588, 1504, 1455, 1381, 1283, 1257, 1212, 1155, 1066, 992, 979, 923, 886, 776, 729, 669.

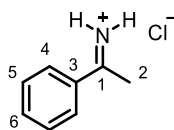
(ESI): *m/z* calculated for C₂₈H₃₇O₄N₄S₂ requires 557.2251 for [M+H]⁺, found 557.2245.

5.3 Experimental Details for Chapter 3

5.3.1 General Procedure B: Synthesis of *N*-Carbamoyl α -Amino Heterodiazoles

To an oven-dried screw cap vial equipped with magnetic stirrer NIITP (60.5 mg, 0.20 mmol, 2.0 eq) was added. Then anhydrous PhMe (1.0 mL, 0.20 M) was added followed firstly by addition of *N*-Boc aldimine (1.5 – 3.0 eq) as a solution in PhMe (0.5 mL, 0.75 M total), and subsequently the appropriate *O*-, or *N*-Brønsted acid (0.10 mmol, 1.0 eq) was added dropwise as a solution in EtOAc (0.5 mL, 0.05 M total); or if insoluble in EtOAc the acid was added as a single portion, followed in quick succession by EtOAc (0.5 mL, 0.05 M total). The vial was capped and stirred at rt for the specified time, typically 3 – 16 h. After this time, the solvent was removed and the crude product purified by FCC, to afford the pure *N*-carbamoyl α -amino heterodiazole products.

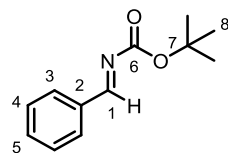
5.3.2 Synthesis of Starting Materials

1-phenylethaniminium chloride – 95

To an oven-dried rbf was added benzonitrile (2.6 mL, 25 mmol, 1.0 eq), and anhydrous THF (25 mL, 1.0 M). The reaction was cooled to $-78\text{ }^{\circ}\text{C}$ and methyl lithium (1.6 M in Et_2O , 25 mL, 40 mmol, 1.6 eq) added over 1 h using a syringe pump. Then the reaction was stirred at $-78\text{ }^{\circ}\text{C}$ for a further 2 h, and afterwards anhydrous MeOH (6.0 mL) was added dropwise. After complete addition the reaction warmed to rt and stirred for 2 h. The reaction mixture was then filtered through celite and the filtrate concentrated *in vacuo*. The residue was uptaken into anhydrous MTBE (25 mL), and HCl (4.0 M in 1,4-dioxane, 6.3 mL, 25 mmol, 1.0 eq) added. After stirring at rt for 30 mins the precipitate formed was isolated by filtration, washed with MTBE (2 x 10 mL), and dried *in vacuo* to afford the *title compound* (3.60 g, 92%) as a pale-yellow solid. Data was consistent with that found in the literature.³⁷⁴

^1H NMR (400 MHz, CDCl_3) δ 8.29 (d, $J = 7.6$, 2H, C_4), 7.76 (t, $J = 7.6$, 1H, C_6), 7.63 (t, $J = 7.6$, 2H C_5), 3.00 (s, 3H, C_2).

^{13}C NMR (101 MHz, CDCl_3) δ 183.3 (C_1), 136.4 (C_6), 129.8, 129.7, 129.6 (C_3), 21.3 (C_2).

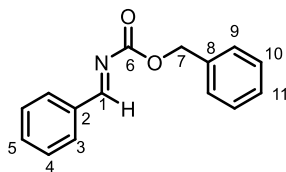
tert-butyl benzylidenecarbamate – 96

To an rbf was added benzaldehyde (10 mL, 102 mmol, 1.02 eq), sodium benzenesulfinate (16.7 g, 102 mmol, 1.02 eq), *tert*-butyl carbamate (11.7 g, 100 mmol, 1.0 eq), THF (44 mL, 2.3 M), water (88 mL, 1.1 M), and formic acid (22 mL, 4.5 M). The reaction was then stirred at rt for 23 h and the precipitate that formed was isolated by filtration. The precipitate was then washed with water (40 mL), CH₂Cl₂:hexane (1:9, 2 x 40 mL), and then dried *in vacuo* to afford the α -amino sulfone (27.5 g, 79%) as a white solid which was used without further purification.

To an oven-dried rbf was added the α -amino sulfone (5.39 g, 15.5 mmol, 1.0 eq), anhydrous potassium carbonate (16.6 g, 120 mmol, 7.7 eq), anhydrous sodium sulfate (19.9 g, 140 mmol, 9.0 eq), and anhydrous THF (200 mL, 0.08 M). The reaction was then heated to 60 °C and stirred for 18 h. The reaction was then cooled to rt, filtered through celite, washing with pentane (3 x 100 mL), and the filtrate concentrated *in vacuo* to afford the *title compound* (3.27 g, quant.) as a colourless oil. Data was consistent with that found in the literature.³⁷⁵

¹H NMR (400 MHz, CDCl₃) δ 8.87 (s, 1H, C₁), 7.91 (dd, *J* = 8.3, 1.2, 2H, C₃), 7.59 – 7.51 (m, 1H, C₅), 7.51 – 7.42 (m, 2H, C₄), 1.59 (s, 9H, C₈).

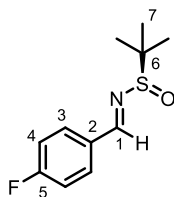
¹³C NMR (101 MHz, CDCl₃) δ 169.6 (C₁), 162.7 (C₆), 134.1 (C₂), 133.5 (C₅), 130.2 (C₃), 128.9 (C₄), 82.3 (C₇), 27.9 (C₈).

benzyl benzylidenecarbamate – 97

To an oven-dried rbf was added benzyl (phenyl(phenylsulfonyl)methyl)carbamate (1.91 g, 5.0 mmol, 1.0 eq), anhydrous cesium fluoride (2.28 g, 15 mmol, 3.0 eq), and anhydrous THF (50 mL, 0.10 M). The reaction was then heated to 60 °C for 2 h, before being cooled to rt and filtered through celite, washing with Et₂O. The filtrate was concentrated *in vacuo* to afford the *title compound* (1.16 g, 97%) as a colourless oil. Data was consistent with that found in the literature.³⁷⁶

¹H NMR (400 MHz, CDCl₃) δ 8.86 (s, 1H, C₁), 7.88 – 7.81 (m, 2H, C₃), 7.53 – 7.46 (m, 1H, C₅), 7.44 – 7.35 (m, 4H), 7.33 – 7.22 (m, 3H), 5.24 (s, 2H, C₇).

¹³C NMR (101 MHz, CDCl₃) δ 171.2 (C₁), 163.7 (C₆), 135.4 (C₂), 133.9 (C₅), 130.4 (C₃), 129.0 (ArCH), 128.6 (ArCH), 128.6 (ArCH), 128.5 (ArCH), 68.9 (C₇).

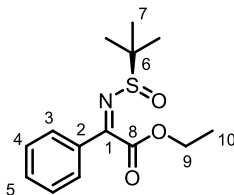
(R)-N-(4-fluorobenzylidene)-2-methylpropane-2-sulfinamide – 98

To an oven-dried rbf was added (*R*)-(+)-2-methyl-2-propanesulfinamide (606 mg, 5.0 mmol, 1.0 eq), anhydrous cesium carbonate (2.17 g, 6.0 mmol, 1.2 eq), and anhydrous CH₂Cl₂ (25 mL, 0.20 M). Then 4-fluorobenzaldehyde (640 μL, 6.0 mmol, 1.2 eq) was added, and the reaction heated at reflux for 19 h. After this time the reaction was cooled to rt and filtered through celite, washing with CH₂Cl₂, and the filtrate concentrated *in vacuo* to afford the crude product. The crude was purified by FCC (20% EtOAc/pentane) to afford the *title compound* (522 mg, 46%) as a colourless oil. Data was consistent with that found in the literature.³⁷⁷

¹H NMR (400 MHz, CDCl₃) δ 8.53 (s, 1H, C₁), 7.84 (ddd, *J* = 8.2, 5.2, 2.4, 2H, C₃), 7.20 – 7.09 (m, 2H, C₄), 1.24 (s, 9H, C₇).

¹⁹F NMR (376 MHz, CDCl₃) δ -105.9.

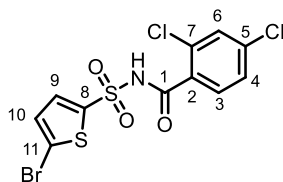
¹³C NMR (101 MHz, CDCl₃) δ 165.3 (d, *J* = 254.2, C₅), 161.3 (C₁), 131.5 (d, *J* = 9.1, C₃), 130.6 (d, *J* = 3.1, C₂), 116.2 (d, *J* = 22.1, C₄), 57.8 (C₆), 22.6 (C₇).

ethyl (*R*)-2-((*tert*-butylsulfinyl)imino)-2-phenylacetate – 99

According to a modified literature procedure,³⁷⁸ to an oven-dried rbf was added (*R*)-(+)-2-methyl-2-propanesulfonamide (636 mg, 5.3 mmol, 1.05 eq), ethyl 2-oxo-2-phenylacetate (794 μ L, 5.0 mmol, 1.0 eq), and $\text{Ti}(\text{OEt})_4$ (2.1 mL). The reaction was then put under vacuum (~ 10 mbar) and heated to 50 $^\circ\text{C}$ for 100 mins. The reaction was then cooled to rt and diluted with THF (50 mL), and brine (2.0 mL). The suspension that formed was then filtered through celite, washing with THF, and the filtrate was concentrated *in vacuo* to afford the crude product. The crude product was purified by FCC (10% EtOAc/pentane) to afford the *title compound* (825 mg, 59%) as a colourless oil. Data was consistent with that found in the literature.³⁷⁹

^1H NMR (400 MHz, CDCl_3) δ 7.81 – 7.74 (m, 2H, C₃), 7.56 – 7.49 (m, 1H, C₅), 7.48 – 7.41 (m, 2H, C₄), 4.53 – 4.38 (m, 2H, C₉), 1.41 (t, $J = 7.2$, 3H, C₁₀), 1.34 (s, 9H, C₇).

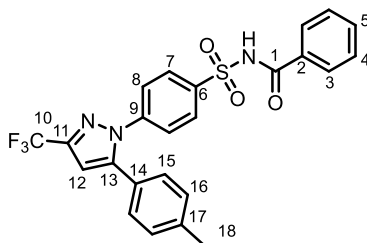
^{13}C NMR (101 MHz, CDCl_3) δ 165.8 (C₈), 163.3 (C₁), 133.2 (C₂), 132.6 (C₅), 128.9 (C₄), 127.9 (C₃), 62.3 (C₉), 59.5 (C₆), 23.0 (C₇), 14.0 (C₁₀).

***N*-((5-bromothiophen-2-yl)sulfonyl)-2,4-dichlorobenzamide – Tasisulam – 152**

To an oven-dried rbf, 5-bromothiophene-2-sulfonamide (1.00 g, 4.1 mmol, 1.1 eq) and DMAP (23.0 mg, 0.19 mmol, 5.0 mol%) were added, followed by triethylamine (1.1 mL, 7.5 mmol, 2.0 eq) and a mixture of PhMe/EtOAc (3:1, 4.7 mL:1.9 mL, 1.8 M). Lastly, 2,4-dichlorobenzoic acid (526 μ L, 3.75 mmol, 1.0 eq) was added and the reaction was heated to 55 $^{\circ}$ C for 2 h. The reaction was quenched by addition of aqueous HCl (2.0 M, 25 mL), extracted with EtOAc (4 x 10 mL), and the combined organics dried (MgSO_4), filtered, and concentrated *in vacuo* to afford the crude product. The crude was purified by trituration with pentane: Et_2O (1:1) to afford the *title compound* (1.46 g, 94%). Data was consistent with that found in the literature.³⁸⁰

^1H NMR (400 MHz, CDCl_3) δ 9.25 (s, 1H, NH), 7.70 (d, $J = 4.1$, 1H, C₉), 7.67 (d, $J = 8.4$, 1H, C₃), 7.42 (d, $J = 1.6$, 1H, C₆), 7.33 (dd, $J = 8.4, 1.7$, 1H, C₄), 7.12 (d, $J = 4.1$, 1H, C₁₀).

^{13}C NMR (101 MHz, CDCl_3) δ 162.5 (C₁), 139.3 (ArC), 138.6 (ArC), 136.0 (C₉), 132.11 (C₃), 132.08 (ArC), 130.6 (C₆), 130.5 (C₁₀), 129.6 (ArC), 128.0 (C₄), 123.2 (ArC).

***N*-((4-(5-(*p*-tolyl)-3-(trifluoromethyl)-1*H*-pyrazol-1-yl)phenyl)sulfonyl)benzamide – 153**

To an oven-dried rbf 4-(5-(*p*-tolyl)-3-(trifluoromethyl)-1*H*-pyrazol-1-yl)benzenesulfonamide (celecoxib) (466 mg, 1.22 mmol, 1.0 eq), and DMAP (8.0 mg, 0.07 mmol, 5.0 mol%) were added, followed by triethylamine (370 μ L, 2.6 mmol, 2.1 eq) and a mixture of PhMe/EtOAc (3:1, 1.5 mL:0.5 mL, 1.8 M). Lastly, benzoyl chloride (150 μ L, 1.3 mmol, 1.05 eq) was added and the reaction was heated to 55 $^{\circ}$ C for 2 h. The reaction was quenched by addition of aqueous HCl (2.0 M, 25 mL), extracted with EtOAc (4 x 10 mL), and the combined organics were dried (MgSO_4), filtered, and concentrated *in vacuo* to afford the crude product. The crude was purified by FCC (pentane \rightarrow 50% EtOAc/pentane) and the product fractions concentrated *in vacuo*. The resulting residue was then uptaken into aqueous HCl (2.0 M, 25 mL), extracted with CH_2Cl_2 (4 x 10 mL), and the combined organics dried (MgSO_4), filtered, and concentrated *in vacuo* to afford the *title compound* (338 mg, 57%) as a white crystalline solid.

m.p.: 80 – 82 $^{\circ}$ C

^1H NMR (400 MHz, CDCl_3) δ 9.58 (s, 1H, NH), 8.12 – 8.05 (m, 2H, C_7), 7.80 (dd, $J = 8.3, 1.1$, 2H, C_3), 7.59 – 7.52 (m, 1H, C_5), 7.50 – 7.36 (m, 4H, C_4 & C_8), 7.16 (d, $J = 7.9$, 2H, C_{15}), 7.10 (d, $J = 8.2$, 2H, C_{16}), 6.74 (s, 1H, C_{12}), 2.36 (s, 3H, C_{18}).

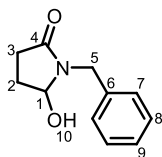
^{19}F NMR (376 MHz, CDCl_3) δ -62.4.

^{13}C NMR (101 MHz, CDCl_3) δ 164.5 (C_1), 145.4 (ArC), 144.2 (q, $J = 38.8$, C_{11}), 143.4 (ArC), 139.9 (ArC), 137.8 (ArC), 133.8 (ArC), 133.6 (C_5), 131.1 (ArC), 130.2 (ArC), 129.82 (ArCH),

129.79 (ArCH), 128.9 (ArCH), 128.7 (ArC), 128.5 (C₁₆), 128.0 (C₃), 125.6 (ArC), 125.1 (ArCH),
121.0 (q, $J = 269.1$, C₁₀), 106.5 (C₁₂), 21.3 (C₁₈).

FT-IR(thin film): $\nu_{\max}(\text{cm}^{-1}) = 3248, 1700, 1452, 1373, 1235, 1163, 1132, 886, 827, 809$.

(ESI): m/z calculated for C₂₄H₁₉O₃N₃F₃S requires 486.1094 for [M+H]⁺, found 486.1093.

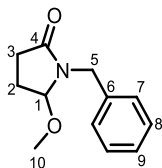
1-benzyl-5-hydroxypyrrolidin-2-one – 174

To an oven-dried rbf was added succinimide (3.00 g, 30 mmol, 1.0 eq), anhydrous potassium carbonate (5.74 g, 36 mmol, 1.2 eq), and acetone (60 mL, 0.50 M). Then benzyl bromide (4.0 mL, 33 mmol 1.1 eq) was added as a single portion and the reaction heated to reflux for 16 h. The reaction was then cooled to rt and filtered through celite, washing with EtOAc, and concentrated *in vacuo* to afford crude 1-benzylpyrrolidine-2,5-dione (assumed quantitative yield), as a white solid which was used without further purification.

To an rbf was added crude 1-benzylpyrrolidine-2,5-dione (5.73 g, 30 mmol, 1.0 eq) and MeOH (150 mL, 0.20 M). The mixture was cooled to 0 °C, and NaBH₄ (5.72 g, 150 mmol, 5.0 eq) added portionwise. At 120 mins, a further portion of NaBH₄ (2.82 g, 76 mmol, 2.5 eq) was added. At 150 mins, H₂O (40 mL) was added and the solvent removed *in vacuo*. The residue was uptaken into CH₂Cl₂ (150 mL) and H₂O (150 mL). The aqueous layer was extracted with CH₂Cl₂ (3 x 50 mL), the combined organics were washed with brine (100 mL), dried (MgSO₄), filtered, and concentrated *in vacuo* to give the crude product. The solid crude was triturated with cold (-15 °C) EtOAc and collected by filtration to afford the *title compound* (3.74 g, 65%) as a white solid. Data was consistent with that found in the literature values.³⁸¹

¹H NMR (400 MHz, CDCl₃) δ 7.36 – 7.25 (m, 5H, C₇ & C₈ & C₉), 5.08 (ddd, *J* = 7.4, 6.3, 2.3, 1H, C₁), 4.83 (d, *J* = 14.8, 1H, C₅), 4.21 (d, *J* = 14.8, 1H, C₅), 3.00 (d, *J* = 7.5, 1H, O₁₀), 2.70 – 2.53 (m, 1H, C₃), 2.42 – 2.21 (m, 2H, C₂ & C₃), 1.95 – 1.84 (m, 1H, C₂).

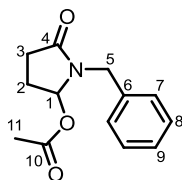
¹³C NMR (101 MHz, CDCl₃) δ 174.6 (C₄), 136.6 (C₆), 128.8 (C₇), 128.3 (C₈), 127.7 (C₉), 82.6 (C₁), 43.6 (C₅), 28.9 (C₃), 28.2 (C₂).

1-benzyl-5-methoxypyrrolidin-2-one – 175

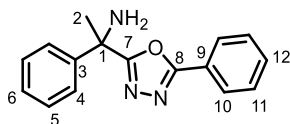
To an oven-dried rbf was added **174** (1.91 g, 10 mmol, 1.0 eq), MeOH (100 mL, 0.10 M) and pyridinium p-toluenesulfonate (502 mg, 2.0 mmol, 0.20 eq). The reaction was stirred at rt for 2 h then triethylamine (2 mL) was added and the reaction was concentrated *in vacuo*. The residue was uptaken into CH₂Cl₂ (200 mL) and washed with saturated aqueous NaHCO₃ (2 x 100 mL) and brine (75 mL), then dried (MgSO₄), filtered, and concentrated *in vacuo* to afford the *title compound* (2.39 g, quant.) as a pale-yellow oil. Data was consistent with that found in the literature values.³⁸²

¹H NMR (400 MHz, CDCl₃) δ 7.38 – 7.25 (m, 5H, C₇ & C₈ & C₉), 4.97 (d, *J* = 14.7, 1H, C₅), 4.75 (dd, *J* = 6.3, 1.6, 1H, C₁), 4.03 (dd, *J* = 14.8, 1.0, 1H, C₅), 3.23 (s, 3H, C₁₀), 2.66 – 2.53 (m, 1H, C₃), 2.40 (ddd, *J* = 17.3, 9.9, 3.3, 1H, C₃), 2.15 – 2.06 (m, 1H, C₂), 2.04 – 1.95 (m, 1H, C₂).

¹³C NMR (101 MHz, CDCl₃) δ 174.8 (C₄), 136.5 (C₆), 128.7 (C₇), 128.4 (C₈), 127.6 (C₉), 89.0 (C₁), 52.9 (C₁₀), 43.8 (C₅), 29.0 (C₂), 23.8 (C₃).

1-benzyl-5-methoxypyrrolidin-2-one – 176

To an oven-dried rbf was added **174** (19.1 mg, 0.10 mmol, 1.0 eq), triethylamine (18 μ L, 0.13 mmol, 1.3 eq), DMAP (1.2 mg, 0.01 mmol, 10 mol%), and CH_2Cl_2 (380 μ L, 0.26 M). Acetic anhydride (11 μ , 0.11 mmol, 1.1 eq) was added as a single portion and the reaction was stirred at rt for 50 mins, at which point TLC analysis indicated complete consumption of **173**. The reaction mixture was filtered through a short silica plug, washing with Et_2O , and the filtrate concentrated using a stream of nitrogen to afford the *title compound* (assumed quantitative yield) which was then used immediately without further analysis or purification.

5.3.3 Synthesis of *N*-Carbamoyl α -Amino Heterodiazoles Products**1-phenyl-1-(5-phenyl-1,3,4-oxadiazol-2-yl)ethan-1-amine – 93**

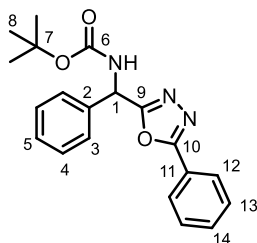
To an oven-dried vial was added benzonitrile (20 μ L, 0.20 mmol, 1.0 eq) and anhydrous THF (200 μ L, 1.0 M). The reaction was then cooled to -78 $^{\circ}$ C and MeLi (1.6 M in Et₂O, 130 μ L, 0.30 mmol, 1.5 eq) was added. The reaction was stirred at -78 $^{\circ}$ C for 2 h, and subsequently anhydrous MeOH (50 μ L) was added and the reaction warmed to rt. The reaction was diluted with anhydrous THF (800 μ L), and subsequently benzoic acid (36.6 mg, 0.30 mmol, 1.5 eq) and NIITP (90.7 mg, 0.30 mmol, 1.5 eq) were added. After stirring at rt for 17.5 h the reaction was diluted with aqueous HCl (2.0 M, 10 mL), and the aqueous layer was extracted with CH₂Cl₂ (3 x 10 mL). The aqueous layer was then basified using aqueous NaOH (12 M) and extracted with CH₂Cl₂ (3 x 10 mL), and these organics combined, dried (MgSO₄), filtered, and concentrated *in vacuo* to afford the crude product. The crude was purified by FCC (80% Et₂O/pentane) to afford the *title compound* (6.1 mg, 12%) as a colourless oil.

¹H NMR (400 MHz, CDCl₃) δ 8.04 – 7.97 (m, 2H, C₁₀), 7.56 – 7.43 (m, 5H, C₄ & C₁₁ & C₁₂), 7.36 (tt, *J* = 8.4, 1.8, 2H, C₅), 7.33 – 7.27 (m, 1H, C₆), 2.56 – 2.30 (m, 2H, NH₂), 1.99 (s, 3H, C₂).

¹³C NMR (101 MHz, CDCl₃) δ 171.5 (ArC), 165.3 (ArC), 143.8 (C₉), 131.7 (ArCH), 129.0 (ArCH), 128.7 (C₅), 127.9 (C₆), 127.0 (C₁₀), 125.5 (ArCH), 125.2 (C₃), 123.9 (ArCH), 55.7 (C₁), 29.3 (C₂).

FT-IR(thin film): ν_{\max} (cm⁻¹) = 3289, 3060, 2917, 2848, 1608, 1557, 1490, 1448, 1289, 1193, 1068, 1002, 767, 702.

(ESI): *m/z* calculated for C₁₆H₁₆ON₃ requires 266.1288 for [M+H]⁺, found 266.1289.

tert-butyl (phenyl(5-phenyl-1,3,4-oxadiazol-2-yl)methyl)carbamate – 102

To an oven-dried vial was added **96** (20.5 mg, 0.10 mmol, 1.0 eq), and CDCl_3 (1.0 mL, 0.10 M). Then benzoic acid (24.4 mg, 0.20 mmol, 2.0 eq), and NIITP (60.5 mg, 0.20 mmol, 2.0 eq) were added in quick succession. The reaction was then allowed to stir at rt for 100 mins, before a further addition of benzoic acid (12.2 mg, 0.10 mmol, 1.0 eq) and NIITP (30.2 mg, 0.10 mmol, 1.0 eq). After a total of 135 min had elapsed, the reaction was diluted with saturated aqueous NaHCO_3 (20 mL). The aqueous was extracted with CH_2Cl_2 (3 x 10 mL), and the combined organics washed with brine (10 mL), dried (MgSO_4), filtered, and concentrated *in vacuo* to afford the crude product. The crude was purified by FCC (40% Et_2O /pentane) to afford the *title compound* (17.8 mg, 51%) as a colourless oil.

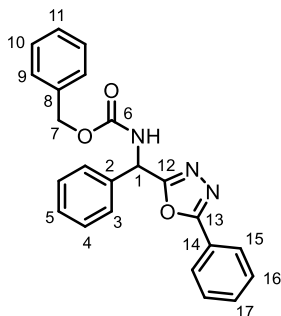
^1H NMR (400 MHz, CDCl_3) δ 8.00 (dd, $J = 8.1, 1.4$, 2H, C_{12}), 7.59 – 7.44 (m, 3H), 7.44 – 7.29 (m, 5H), 6.20 (d, $J = 6.5$, 1H, C_1), 5.74 (s, 1H, NH), 1.45 (s, 9H, C_8).

^{13}C NMR (101 MHz, CDCl_3) δ 165.7 (ArC), 165.3 (ArC), 154.7 (C_6), 136.9 (C_{11}), 131.9 (ArCH), 129.2 (ArCH), 129.0 (ArCH), 128.9 (ArCH), 127.2 (ArCH), 127.0 (ArCH), 123.6 (C_2), 80.8 (C_7), 51.6 (C_1), 28.3 (C_8).

FT-IR(thin film): $\nu_{\text{max}}(\text{cm}^{-1}) = 3289, 3064, 2935, 1713, 1521, 1491, 1451, 1366, 1246, 1168, 1018, 883, 755, 654$.

(ESI): m/z calculated for $\text{C}_{20}\text{H}_{22}\text{O}_3\text{N}_3$ requires 352.1656 for $[\text{M}+\text{H}]^+$, found 352.1655.

HPLC – CHIRALPAK® AD-H, Hexane/IPA = 90/10, 1 mL/min, $\lambda = 220$ nm, $t_{(1)} = 29.2$ min, $t_{(2)} = 36.0$ min.

benzyl (phenyl(5-phenyl-1,3,4-oxadiazol-2-yl)methyl)carbamate – 103

To an oven-dried vial was added **97** (23.9 mg, 0.10 mmol, 1.0 eq) and CDCl_3 (600 μL , 0.60 M). Then benzoic acid (24.4 mg, 0.20 mmol, 2.0 eq), and NIITP (60.5 mg, 0.20 mmol, 2.0 eq) were added in quick succession. After stirring at rt for 1 h, the reaction mixture was purified by FCC (40% Et_2O /pentane) to afford the *title compound* (16.8 mg, 44%) as a colourless oil.

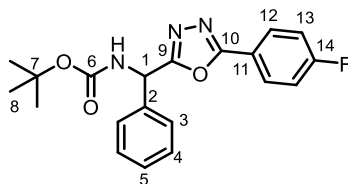
^1H NMR (400 MHz, CDCl_3) δ 8.04 – 7.95 (m, 2H, C₁₅), 7.57 – 7.27 (m, 13H), 6.27 (d, J = 8.0, 1H, C₁), 6.14 (d, J = 7.5, 1H, NH), 5.15 (d, J = 2.1, 2H, C₇).

^{13}C NMR (101 MHz, CDCl_3) δ 165.5 (ArC), 165.3 (ArC), 155.4 (C₆), 136.5 (ArC), 133.4 (ArC), 132.0 (ArCH), 129.3 (ArCH), 129.0 (ArCH), 128.6 (ArCH), 128.4 (ArCH), 128.3 (ArCH), 128.2 (ArCH), 127.2 (ArCH), 127.0 (ArCH), 123.5 (ArC), 67.5 (C₇), 52.1 (C₁).

FT-IR(thin film): $\nu_{\text{max}}(\text{cm}^{-1})$ = 3288, 2940, 2911, 1718, 1528, 1450, 1304, 1213, 1106, 876, 748.

(ESI): m/z calculated for $\text{C}_{23}\text{H}_{20}\text{O}_3\text{N}_3$ requires 386.1499 for $[\text{M}+\text{H}]^+$, found 386.1499.

HPLC – CHIRALPAK® OD-H, Hexane/IPA = 80/20, 1 mL/min, λ = 220 nm, $t_{(1)}$ = 16.8 min, $t_{(2)}$ = 34.4 min.

tert-butyl ((5-(4-fluorophenyl)-1,3,4-oxadiazol-2-yl)(phenyl)methyl)carbamate – 104

Following **general procedure B** (using 4-fluorobenzoic acid (14.0 mg, 0.10 mmol, 1.0 eq), **96** (30.8 mg, 0.15 mmol, 1.5 eq), and stirring for 16 h): after FCC (30% Et₂O/pentane), **104** (29.0 mg, 79%) was afforded as a cream-colored solid.

m.p.: 130 – 133 °C

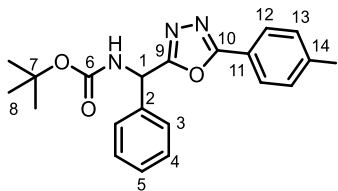
¹H NMR (400 MHz, CDCl₃) δ 8.03 – 7.95 (m, 2H, C₁₂), 7.45 – 7.30 (m, 5H, C₃ & C₄ & C₅), 7.19 – 7.11 (m, 2H, C₁₃), 6.17 (s, 1H, C₁), 5.77 (s, 1H, NH), 1.44 (s, 9H, C₈).

¹⁹F NMR (376 MHz, CDCl₃) δ -106.6.

¹³C NMR (101 MHz, CDCl₃) δ 165.7 (ArC), 164.9 (d, *J* = 253.5, C₁₄), 164.5 (ArC), 154.7 (C₆), 136.8 (C₂), 129.3 (d, *J* = 9.0, C₁₂), 129.2 (ArCH), 128.9 (ArCH), 127.2 (ArCH), 119.9 (d, *J* = 3.3, C₁₁), 116.4 (d, *J* = 22.4, C₁₃), 80.8 (C₇), 51.6 (C₁), 28.3 (C₈).

FT-IR(thin film): $\nu_{\max}(\text{cm}^{-1}) = 3298, 2979, 1715, 1612, 1499, 1242, 1160$.

(ESI): *m/z* calculated for C₂₀H₂₁O₃N₃F requires 370.1561 for [M+H]⁺, found 370.1566.

tert-butyl ((5-(4-iodophenyl)-1,3,4-oxadiazol-2-yl)(phenyl)methyl)carbamate – 107

Following **general procedure B** (using 4-iodobenzoic acid (24.8 mg, 0.10 mmol, 1.0 eq), **96** (30.8 mg, 0.15 mmol, 1.5 eq), and stirring for 3 h): after FCC (30% EtOAc/pentane), **107** (31.9 mg, 67%) was afforded as a cream-colored solid.

m.p.: 146 – 148 °C

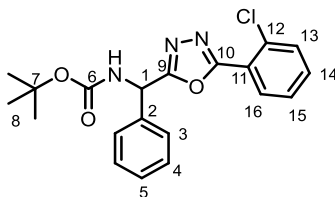
¹H NMR (400 MHz, CDCl₃) δ 7.84 – 7.80 (m, 2H, C₁₂), 7.73 – 7.68 (m, 2H, C₁₃), 7.43 – 7.31 (m, 5H, C₃ & C₄ & C₅), 6.18 (d, *J* = 7.3, 1H, C₁), 5.73 (d, *J* = 7.3, 1H, NH), 1.45 (s, 9H, C₈).

¹³C NMR (101 MHz, CDCl₃) δ 165.9 (ArC), 164.8 (ArC), 154.7 (C₆), 138.3 (C₁₂), 136.7 (C₂), 129.2 (ArCH), 129.0 (C₅), 128.3 (C₁₃), 127.2 (ArCH), 123.0 (C₁₁), 98.8 (C₁₄), 80.8 (C₇), 51.6 (C₁), 28.3 (C₈).

FT-IR(thin film): $\nu_{\max}(\text{cm}^{-1}) = 3297, 2975, 2919, 2849, 2362, 1716, 1601, 1478, 1367, 1248, 1166.$

(ESI): *m/z* calculated for C₂₀H₂₁O₃N₃I requires 478.0622 for [M+H]⁺, found 478.0621.

Scale-up procedure: In an oven-dried rbf NIITP (2.42 g, 8.0 mmol, 2.0 eq) was suspended in PhMe (40 mL, 0.10 M). *Tert*-butyl-(*E*)-benzylidenecarbamate (1.23 g, 6.0 mmol, 1.5 eq) was added as a solution in PhMe (20 mL, 0.75 M total), followed by a suspension of 4-iodobenzoic acid (992 mg, 4.0 mmol, 1.0 eq) in EtOAc (20 mL, 0.05 M total), and the reaction allowed to stir at rt for 18 hours after which time the reaction was concentrated *in vacuo* to afford the crude product. The crude was purified by FCC (30% Et₂O/pentane) to afford the *title compound* (1.63 g, 85%) as a cream-colored solid.

tert-butyl ((5-(2-chlorophenyl)-1,3,4-oxadiazol-2-yl)(phenyl)methyl)carbamate – 108

Following **general procedure B** (using 2-chlorobenzoic acid (15.7 mg, 0.10 mmol, 1.0 eq), **96** (30.8 mg, 0.15 mmol, 1.5 eq), and stirring for 16 h): after FCC (40% Et₂O/pentane), **108** (30.7 mg, 80%) was afforded as a cream-colored solid.

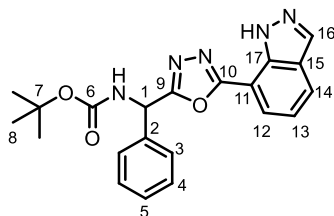
m.p.: 108 – 110 °C

¹H NMR (400 MHz, CDCl₃) δ 7.92 (dd, *J* = 7.8, 1.7, 1H, C₁₆), 7.51 (dd, *J* = 8.0, 1.2, 1H), 7.47 – 7.30 (m, 7H), 6.22 (s, 1H, C₁), 5.75 (s, 1H, NH), 1.45 (s, 9H, C₈).

¹³C NMR (101 MHz, CDCl₃) δ 166.1 (ArC), 163.7 (ArC), 154.7 (C₆), 136.8 (C₂), 133.2 (C₁₁), 132.5 (ArCH), 131.3 (ArCH), 131.2 (ArCH), 129.2 (ArCH), 128.9 (ArCH), 127.1 (ArCH), 127.0 (ArCH), 123.0 (C₁₂), 80.8 (C₇), 51.6 (C₁), 28.3 (C₈).

FT-IR(thin film): $\nu_{\max}(\text{cm}^{-1}) = 3300, 2926, 2851, 2360, 1715, 1498, 1392, 1248, 1166$.

(ESI): *m/z* calculated for C₂₀H₂₁O₃N₃³⁵Cl requires 386.1266 for [M+H]⁺, found 386.1268.

tert-butyl ((5-(1*H*-indazol-7-yl)-1,3,4-oxadiazol-2-yl)(phenyl)methyl)carbamate – 111

Following **general procedure B** (using 1*H*-indazole-7-carboxylic acid (16.2 mg, 0.10 mmol, 1.0 eq), **96** (61.6 mg, 0.30 mmol, 3.0 eq), and stirring for 16 h): after FCC (35% EtOAc/pentane), **111** (23.7 mg, 61%) was afforded as a white solid.

m.p.: 210 – 212 °C

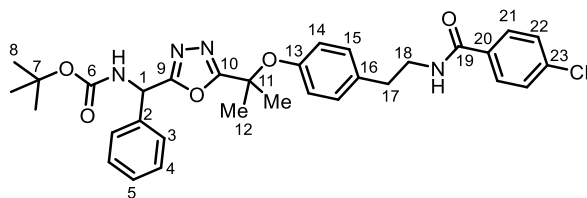
¹H NMR (600 MHz, CDCl₃) δ 8.21 (s, 1H, C₁₆), 7.97 (d, *J* = 8.0, 1H, C₁₂), 7.91 (d, *J* = 7.2, 1H, C₁₄), 7.50 (d, *J* = 7.3, 2H, C₃), 7.38 (t, *J* = 7.4, 2H, C₄), 7.36 – 7.32 (m, 1H, C₅), 7.28 (t, *J* = 7.7, 1H, C₁₃), 6.96 (s, 1H, NH), 6.34 (s, 1H, C₁), 1.44 (s, 9H, C₈).

¹³C NMR (151 MHz, CDCl₃) δ 166.0 (ArC), 163.7 (ArC), 155.2 (C₆), 136.9 (ArC), 136.6 (ArC), 134.9 (ArCH), 129.2 (C₄), 128.9 (C₅), 127.3 (C₃), 125.3 (ArCH), 125.2 (ArCH), 124.2 (ArCH), 120.7 (ArCH), 106.3 (ArC), 80.5 (C₇), 51.7 (C₁), 28.3 (C₈).

FT-IR(thin film): $\nu_{\max}(\text{cm}^{-1}) = 3270, 2926, 2855, 1708, 1538, 1499, 1366, 1252, 1167$.

(ESI): *m/z* calculated for C₂₁H₂₂O₃N₅ requires 392.1717 for [M+H]⁺, found 392.1712.

tert-butyl ((5-(2-(4-(2-(4-chlorobenzamido)ethyl)phenoxy)propan-2-yl)-1,3,4-oxadiazol-2-yl)(phenyl)methyl)carbamate – 124



Following **general procedure B** (using bezafibrate (36.2 mg, 0.10 mmol, 1.0 eq), **96** (30.8 mg, 0.15 mmol, 1.5 eq), and stirring for 3 h): after FCC (40% EtOAc/pentane), **124** (26.6 mg, 45%) was afforded as a white solid.

m.p.: 60 – 62 °C

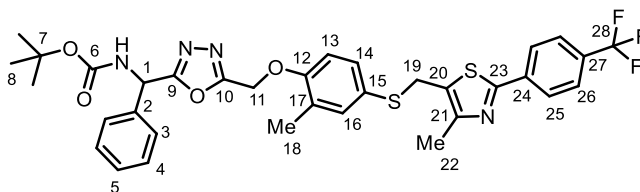
¹H NMR (400 MHz, CDCl₃) δ 7.64 – 7.56 (m, 2H, C₂₁), 7.42 – 7.36 (m, 2H, C₂₂), 7.36 – 7.27 (m, 5H, C₃ & C₄ & C₅), 6.96 – 6.88 (m, 2H, C₁₅), 6.54 – 6.47 (m, 2H, C₁₄), 6.09 (br, s, 2H, NH & C₁), 5.62 (br, s, 1H, NH), 3.62 (q, *J* = 6.6, 2H, C₁₈), 2.81 (t, *J* = 6.8, 2H, C₁₇), 1.78 (s, 3H, C₁₂), 1.77 (s, 3H, C₁₂), 1.43 (s, 9H, C₈).

¹³C NMR (101 MHz, CDCl₃) δ 168.8 (C₁₉), 166.7 (ArC), 166.4 (ArC), 153.1 (C₆), 137.7 (ArC), 136.6 (ArC), 134.4 (ArC), 133.0 (ArC), 129.6 (C₁₅), 129.2 (C₄), 128.9 (C₅), 128.9 (C₂₂), 128.3 (C₂₁), 127.1 (C₃), 122.2 (C₁₄), 80.8 (C₇), 75.5 (C₁₁), 51.7 (C₁), 41.1 (C₁₈), 34.8 (C₁₇), 28.3 (C₈), 26.3 (C₁₂), 25.8 (C₁₂).

FT-IR(thin film): $\nu_{\max}(\text{cm}^{-1}) = 3307, 2980, 2932, 1708, 1644, 1535, 1506, 1487, 1389, 1225, 1160, 731$.

(ESI): *m/z* calculated for C₃₂H₃₅O₅N₄³⁵ClNa requires 613.2188 for [M+Na]⁺, found 613.2186.

***tert*-butyl ((5-((2-methyl-4-(((4-methyl-2-(4-(trifluoromethyl)phenyl)thiazol-5-yl)methyl)thio)phenoxy)methyl)-1,3,4-oxadiazol-2-yl)(phenyl)methyl)carbamate – 125**



Following **general procedure B** (using GW501516 (45.4 mg, 0.10 mmol, 1.0 eq), **96** (30.8 mg, 0.15 mmol, 1.5 eq), and stirring for 3 h): after FCC (65% Et₂O/pentane), **125** (46.7 mg, 68%) was afforded as a beige solid.

m.p.: 146 – 148 °C

¹H NMR (400 MHz, CDCl₃) δ 7.96 (d, *J* = 8.1, 2H, C₂₅), 7.65 (d, *J* = 8.2, 2H, C₂₆), 7.40 – 7.27 (m, 5H, C₃ & C₄ & C₅), 7.20 – 7.10 (m, 2H, C₁₃ & C₁₄), 6.81 (d, *J* = 8.4, 1H, C₁₆), 6.13 (br, s, 1H, C₁), 5.69 (br, s, 1H, NH), 5.19 (d, *J* = 2.6, 2H, C₁₁), 4.11 (s, 2H, C₁₉), 2.21 (s, 3H, C₂₂), 2.11 (s, 3H, C₁₈), 1.43 (s, 9H, C₈).

¹⁹F NMR (376 MHz, CDCl₃) δ -62.7.

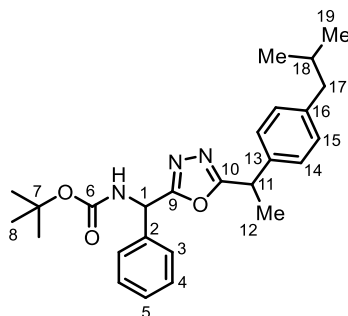
¹³C NMR (101 MHz, CDCl₃) δ 167.0 (ArC), 163.2 (ArC), 162.9 (ArC), 155.8 (ArC), 154.6 (C₆), 151.3 (ArC), 136.4 (ArC), 135.9 (ArCH), 131.9 (ArCH), 131.4 (q, *J* = 32.5, C₂₇), 130.6 (ArC), 129.2 (C₄), 129.0 (C₅), 128.6 (ArC), 127.1 (C₃), 126.4 (C₂₅), 126.3 (ArC), 125.9 (q, *J* = 3.8, C₂₆), 123.9 (q, *J* = 272.2, C₂₈), 112.4 (C₁₆), 80.9 (C₇), 60.2 (C₁₁), 51.6 (C₁), 32.3 (C₁₉), 28.3 (C₈), 16.0 (C₁₈), 14.8 (C₂₂).

FT-IR(thin film): $\nu_{\max}(\text{cm}^{-1}) = 3357, 2980, 1708, 1685, 1520, 1490, 1325, 1247, 1165, 1124, 1067, 864, 731.$

(ESI): *m/z* calculated for C₃₄H₃₄O₄N₄F₂S₂ requires 683.1968 for [M+H]⁺, found 683.1968.

tert-butyl ((5-(1-(4-isobutylphenyl)ethyl)-1,3,4-oxadiazol-2-yl)(phenyl)methyl)carbamate

– 126



Following **general procedure B** (using 2-(4-isobutylphenyl)propanoic acid (ibuprofen) (20.6 mg, 0.10 mmol, 1.0 eq), **96** (30.8 mg, 0.15 mmol, 1.5 eq), and stirring for 16 h): after FCC (35% Et₂O/pentane), **126** (28.0 mg, 64%) was afforded as a yellow oil. d.r: 50:50 as determined by integration of the ¹H signals at 4.31 and 4.24 ppm.

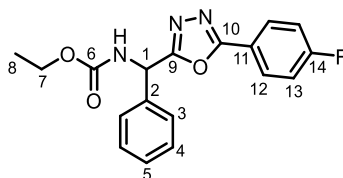
The integral ratios are given as observed - ¹H NMR (400 MHz, CDCl₃) δ 7.36 – 7.26 (m, 5H, C₃ & C₄ & C₅), 7.16 – 7.04 (m, 4H, C₁₄ & C₁₅), 6.06 (s, 1H, C₁), 5.68 (s, 0.4H, NH), 5.62 (s, 0.4H, NH), 4.31 (q, *J* = 7.2, 0.5H, C₁₁), 4.24 (q, *J* = 7.1, 0.5H, C₁₁), 2.44 (dd, *J* = 7.1, 2.2, 2H, C₁₇), 1.89 – 1.79 (m, 1H, C₁₈), 1.70 (t, *J* = 7.5, 3H, C₁₂), 1.42 (s, 9H, C₈), 0.89 (dd, *J* = 6.6, 3.0, 6H, C₁₉).

¹³C NMR (101 MHz, CDCl₃) δ 169.73 (ArC), 169.69 (ArC), 165.8 (ArC), 154.6 (C₆), 141.01 (ArC), 140.98 (ArC), 137.4 (ArC), 137.2 (ArC), 137.0 (ArC), 129.63 (ArCH), 129.59 (ArCH), 129.56 (ArCH), 129.02 (ArCH), 129.01 (ArCH), 128.68 (ArCH), 128.67 (ArCH), 127.1 (ArCH), 127.0 (ArCH), 126.92 (ArCH), 126.90 (ArCH), 80.6 (C₇), 51.4 (C₁), 51.3 (C₁), 45.0 (C₁₇), 37.1 (C₁₁), 37.0 (C₁₁), 30.2 (C₁₈), 28.4 (C₈), 28.3 (C₈), 22.4 (C₁₉), 19.63 (C₁₂), 19.58 (C₁₂).

FT-IR(thin film): $\nu_{\max}(\text{cm}^{-1}) = 3297, 2924, 2851, 1713, 1512, 1497, 1366, 1246, 1167, 1019, 698.$

(ESI): m/z calculated for $C_{26}H_{34}O_3N_3$ requires 436.2595 for $[M+H]^+$, found 436.2594.

ethyl ((5-(4-fluorophenyl)-1,3,4-oxadiazol-2-yl)(phenyl)methyl)carbamate – 141



Following **general procedure B** (using 4-fluorobenzoic acid (16.8 mg, 0.12 mmol, 1.0 eq), **127** (60.2 mg, 0.34 mmol, 2.8 eq), and stirring for 16 h): after FCC (50% Et₂O/pentane), **141** (40.3 mg, 98%) was afforded as a yellow crystalline solid.

m.p.: 112 – 114 °C

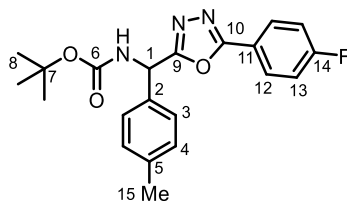
¹H NMR (400 MHz, CDCl₃) δ 7.95 – 7.87 (m, 2H, C₁₂), 7.38 – 7.21 (m, 5H, C₃ & C₄ & C₅), 7.11 – 7.03 (m, 2H, C₁₃), 6.16 (d, *J* = 8.1, 1H, C₁), 5.96 (d, *J* = 7.3, 1H, NH), 4.07 (d, *J* = 6.6, 2H, C₇), 1.16 (d, *J* = 7.0, 3H, C₈).

¹⁹F NMR (376 MHz, CDCl₃) δ -106.4

¹³C NMR (101 MHz, CDCl₃) δ 165.5 (ArC), 164.9 (d, *J* = 253.5, C₁₄), 164.6 (ArC), 155.6 (C₆), 136.6 (C₂), 129.3 (d, *J* = 8.9, C₁₂), 129.2 (C₄), 129.0 (C₅), 127.2 (C₃), 119.9 (d, *J* = 3.3, C₁₁), 116.4 (d, *J* = 22.4, C₁₃), 61.7 (C₇), 51.9 (C₁), 14.5 (C₈).

FT-IR(thin film): $\nu_{\max}(\text{cm}^{-1}) = 3297, 2982, 1702, 1611, 1524, 1497, 1237, 1045, 845, 698.$

(ESI): *m/z* calculated for C₁₈H₁₆O₃N₃FNa requires 364.1068 for [M+Na]⁺, found 364.1069.

tert-butyl ((5-(4-fluorophenyl)-1,3,4-oxadiazol-2-yl)(p-tolyl)methyl)carbamate – 142

Following **general procedure B** (using 4-fluorobenzoic acid (14.0 mg, 0.10 mmol, 1.0 eq), **128** (32.9 mg, 0.15 mmol, 1.5 eq), and stirring for 88 h): after FCC (33% Et₂O/pentane), **142** (33.7 mg, 88%) was afforded as a white crystalline solid.

m.p.: 46 – 48 °C

¹H NMR (400 MHz, CDCl₃) δ 8.08 – 7.95 (m, 2H, C₁₂), 7.35 – 7.25 (m, 2H, C₃), 7.25 – 7.13 (m, 4H, C₄ & C₁₃), 6.16 (d, *J* = 8.2, 1H, C₁), 5.72 (d, *J* = 8.0, 1H, NH), 2.36 (s, 3H, C₁₅), 1.47 (s, 9H, C₈).

¹⁹F NMR (376 MHz, CDCl₃) δ -106.7.

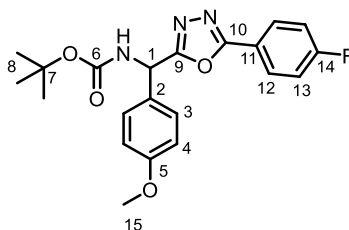
¹³C NMR (101 MHz, CDCl₃) δ 165.9 (ArC), 164.8 (d, *J* = 235.1, C₁₄), 164.4 (ArC), 154.7 (C₆), 138.9 (ArC), 133.8 (ArC), 129.9 (C₄), 129.3 (d, *J* = 8.8, C₁₂), 127.1 (C₃), 120.0 (d, *J* = 3.4, C₁₁), 116.4 (d, *J* = 22.3, C₁₃), 80.7 (C₇), 51.4 (C₁), 28.3 (C₈), 21.1 (C₁₅).

FT-IR(thin film): $\nu_{\max}(\text{cm}^{-1}) = 3288, 2978, 2929, 1705, 1612, 1498, 1391, 1240, 1159, 1014, 844, 732$.

(ESI): *m/z* calculated for C₂₁H₂₂O₃N₃FNa requires 406.1537 for [M+Na]⁺, found 406.1537.

tert-butyl ((5-(4-fluorophenyl)-1,3,4-oxadiazol-2-yl)(4-methoxyphenyl)methyl)carbamate

– 143



Following **general procedure B** (using 4-fluorobenzoic acid (14.0 mg, 0.10 mmol, 1.0 eq), **129** (35.3 mg, 0.15 mmol, 1.5 eq), and stirring for 16 h): after FCC (40% Et₂O/pentane), **143** (35.7 mg, 89%) was afforded as a white crystalline solid.

m.p.: 134 – 136 °C

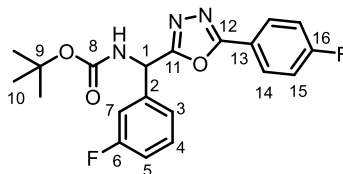
¹H NMR (400 MHz, CDCl₃) δ 7.96 – 7.88 (m, 2H, C₁₂), 7.30 – 7.21 (m, 2H, C₃), 7.13 – 7.04 (m, 2H, C₁₃), 6.87 – 6.76 (m, 2H, C₄), 6.04 (d, *J* = 8.1, 1H, C₁), 5.60 (s, 1H, NH), 3.72 (s, 3H, C₁₅), 1.37 (s, 9H, C₈).

¹⁹F NMR (376 MHz, CDCl₃) δ -106.7

¹³C NMR (101 MHz, CDCl₃) δ 166.0 (ArC), 164.8 (d, *J* = 253.1, C₁₄), 164.4 (ArC), 160.0 (C₅), 154.7 (C₆), 129.3 (d, *J* = 8.8, C₁₂), 128.8 (C₂), 128.5 (C₃), 120.0 (d, *J* = 3.3, C₁₁), 116.4 (d, *J* = 22.4, C₁₃), 114.5, 80.7 (C₇), 55.4 (C₁₅), 55.3 (C₁₅), 51.1 (C₁), 28.3 (C₈).

FT-IR(thin film): $\nu_{\max}(\text{cm}^{-1}) = 2977, 1706, 1611, 1512, 1498, 1392, 1241, 1159, 1029, 843, 733.$

(ESI): *m/z* calculated for C₂₁H₂₂O₄N₃FNa requires 422.1487 for [M+Na]⁺, found 422.1487.

tert-butyl ((3-fluorophenyl)(5-(4-fluorophenyl)-1,3,4-oxadiazol-2-yl)methyl)carbamate –**144**

Following **general procedure B** (using 4-fluorobenzoic acid (14.0 mg, 0.10 mmol, 1.0 eq), **130** (33.5 mg, 0.15 mmol, 1.5 eq), and stirring for 16 h): after FCC (30% Et₂O/pentane), **144** (25.2 mg, 65%) was afforded as a white crystalline solid.

m.p.: 118 – 120 °C

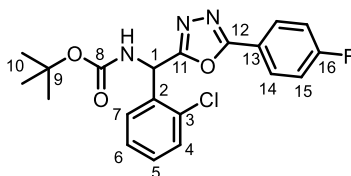
¹H NMR (400 MHz, CDCl₃) δ 8.06 – 7.95 (m, 2H, C₁₄), 7.41 – 7.30 (m, 1H), 7.23 – 7.10 (m, 4H), 7.08 – 7.00 (m, 1H), 6.19 (d, *J* = 8.2, 1H, C₁), 5.85 – 5.74 (m, 1H, NH), 1.45 (s, 9H, C₈).

¹⁹F NMR (376 MHz, CDCl₃) δ -106.27, -111.25 (td, *J* = 9.1, 5.6).

¹³C NMR (101 MHz, CDCl₃) δ 165.1 (ArC), 164.9 (d, *J* = 235.1, C₁₆), 164.7 (ArC), 163.0 (d, *J* = 248.2, C₆), 154.6 (C₈), 139.2 (d, *J* = 7.1, ArC), 130.8 (d, *J* = 8.1, ArCH), 129.3 (d, *J* = 8.9, C₁₄), 122.8 (d, *J* = 3.0, ArCH), 119.8 (d, *J* = 3.4, C₁₃), 116.5 (d, *J* = 22.4, C₁₅), 115.9 (d, *J* = 21.1, ArCH), 114.3 (d, *J* = 22.7, ArCH), 81.1 (C₉), 51.1 (C₁), 28.3 (C₁₀).

FT-IR(thin film): $\nu_{\max}(\text{cm}^{-1}) = 3297, 2980, 1702, 1612, 1498, 1368, 1242, 1158, 1014, 844, 784, 694.$

(ESI): *m/z* calculated for C₂₀H₁₉O₃N₃F₂Na requires 410.1287 for [M+Na]⁺, found 410.1287.

tert-butyl ((2-chlorophenyl)(5-(4-fluorophenyl)-1,3,4-oxadiazol-2-yl)methyl)carbamate –**145**

Following **general procedure B** (using 4-fluorobenzoic acid (14.0 mg, 0.10 mmol, 1.0 eq), **131** (47.9 mg, 0.20 mmol, 2.0 eq), and stirring for 16 h): after FCC (35% Et₂O/pentane), **145** (34.0 mg, 84%) was afforded as a beige solid.

m.p.: 126 – 128 °C

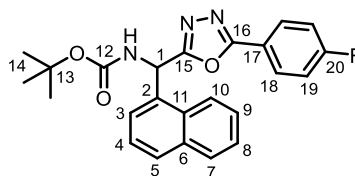
¹H NMR (400 MHz, CDCl₃) δ 7.97 – 7.87 (m, 2H, C₁₄), 7.39 – 7.32 (m, 2H), 7.26 – 7.19 (m, 2H), 7.08 (dd, *J* = 9.5, 7.8, 2H, C₁₅), 6.51 (d, *J* = 7.6, 1H, C₁), 5.83 (d, *J* = 8.1, 1H, NH), 1.37 (s, 9H, C₈).

¹⁹F NMR (376 MHz, CDCl₃) δ -106.5.

¹³C NMR (101 MHz, CDCl₃) δ 165.3 (ArC), 164.9 (d, *J* = 253.5, C₁₆), 164.6 (ArC), 154.6 (C₈), 133.6 (ArC), 130.3 (ArCH), 130.2 (ArCH), 129.3 (d, *J* = 8.9, C₁₄), 129.0 (ArCH), 127.5 (ArCH), 119.9 (d, *J* = 3.3, C₁₃), 116.4 (d, *J* = 22.4, C₁₅), 80.9 (C₉), 79.6 (C₃), 49.3 (C₁), 28.3 (C₁₀), 28.2 (C₁₀).

FT-IR(thin film): $\nu_{\max}(\text{cm}^{-1}) = 3286, 1703, 1611, 1497, 1367, 1240, 1158, 1051, 1014, 844, 755, 735.$

(ESI): *m/z* calculated for C₂₀H₂₀O₃N₃F³⁵Cl requires 404.1172 for [M+H]⁺, found 404.1171.

tert-butyl ((5-(4-fluorophenyl)-1,3,4-oxadiazol-2-yl)(naphthalen-1-yl)methyl)carbamate –**146**

Following **general procedure B** (using 4-fluorobenzoic acid (14.0 mg, 0.10 mmol, 1.0 eq), **132** (38.3 mg, 0.15 mmol, 1.5 eq), and stirring for 3 h): after FCC (40% Et₂O/pentane), **146** (27.6 mg, 66%) was afforded as a white solid.

m.p.: 180 – 182 °C

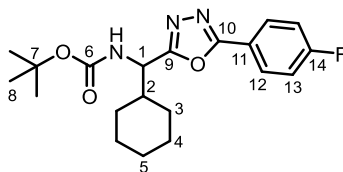
¹H NMR (400 MHz, CDCl₃) δ 8.26 (d, *J* = 8.5, 1H), 8.02 – 7.95 (m, 2H, C₁₈), 7.92 (dd, *J* = 8.3, 1.4, 1H), 7.88 (d, *J* = 8.3, 1H), 7.64 (ddd, *J* = 8.4, 6.8, 1.5, 1H), 7.57 (ddd, *J* = 8.1, 6.8, 1.2, 1H), 7.42 (t, *J* = 7.7, 1H), 7.31 (d, *J* = 7.2, 1H), 7.19 – 7.09 (m, 2H, C₁₉), 6.97 (d, *J* = 8.7, 1H, C₁), 5.66 (d, *J* = 8.7, 1H, NH), 1.47 (s, 9H, C₈).

¹⁹F NMR (376 MHz, CDCl₃) δ -106.6.

¹³C NMR (101 MHz, CDCl₃) δ 166.1 (ArC), 164.8 (d, *J* = 253.5, C₂₀), 164.6 (ArC), 154.8 (C₁₂), 134.1 (ArC), 132.4 (ArC), 130.7 (ArC), 129.9 (ArCH), 129.3 (d, *J* = 8.9, C₁₈), 129.1 (ArCH), 127.3 (ArCH), 126.4 (ArCH), 125.6 (ArCH), 125.3 (ArCH), 122.9 (ArCH), 120.0 (d, *J* = 3.2, C₁₇), 116.4 (d, *J* = 22.4, C₁₉), 80.9 (C₁₃), 48.8 (C₁), 28.3 (C₁₄).

FT-IR(thin film): $\nu_{\max}(\text{cm}^{-1}) = 3314, 2977, 1707, 1612, 1498, 1367, 1239, 1159, 1051, 844, 779, 733.$

(ESI): *m/z* calculated for C₂₄H₂₂O₃N₃FNa requires 442.1537 for [M+Na]⁺, found 442.1536.

tert-butyl (cyclohexyl(5-(4-fluorophenyl)-1,3,4-oxadiazol-2-yl)methyl)carbamate – 149

Following **general procedure B** (using 4-fluorobenzoic acid (14.0 mg, 0.10 mmol, 1.0 eq), **135** (42.2 mg, 0.20 mmol, 2.0 eq), and stirring for 88 h): after FCC (30% Et₂O/pentane), **149** (36.2 mg, 96%) was afforded as a white crystalline solid.

m.p.: 44 – 46 °C

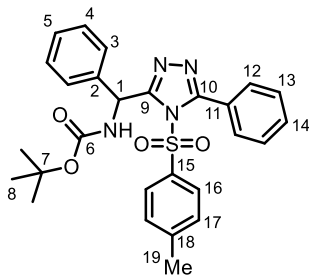
¹H NMR (400 MHz, CDCl₃) δ 8.02 – 7.92 (m, 2H, C₁₂), 7.17 – 7.07 (m, 2H, C₁₃), 5.19 (d, *J* = 9.5, 1H, NH), 4.88 (dd, *J* = 9.5, 6.3, 1H, C₁), 1.90 – 1.76 (m, 1H, C₂), 1.76 – 1.64 (m, 3H), 1.64 – 1.48 (m, 2H), 1.43 – 1.30 (m, 9H, C₈), 1.25 – 0.95 (m, 5H).

¹⁹F NMR (376 MHz, CDCl₃) δ -106.9.

¹³C NMR (101 MHz, CDCl₃) δ 166.4 (ArC), 164.8 (d, *J* = 253.5, C₁₄), 164.0 (ArC), 155.3 (C₆), 129.2 (d, *J* = 8.9, C₁₂), 120.2 (d, *J* = 3.4, C₁₁), 116.4 (d, *J* = 22.3, C₁₃), 80.3 (C₇), 52.1 (C₁), 41.9 (C₂), 29.3 (CH₂), 28.4 (C₈), 28.3 (C₈), 28.2 (CH₂), 26.0 (CH₂), 25.8 (CH₂), 25.8 (CH₂).

FT-IR(thin film): $\nu_{\max}(\text{cm}^{-1}) = 3294, 2977, 2928, 2854, 1703, 1612, 1498, 1366, 1242, 1158, 1013, 844, 732.$

(ESI): *m/z* calculated for C₂₀H₂₇O₃N₃F requires 376.2031 for [M+H]⁺, found 376.2031.

tert-butyl (phenyl(5-phenyl-4H-1,2,4-triazol-3-yl)methyl)carbamate – 151

Following **general procedure B** (using **27** (27.5 mg, 0.10 mmol, 1.0 eq), **96** (30.8 mg, 0.15 mmol, 1.5 eq), and stirring for 16 h): after FCC (30% EtOAc/pentane), **151** (34.3 mg, 68%) was afforded as a beige powder.

m.p.: 156 – 158 °C

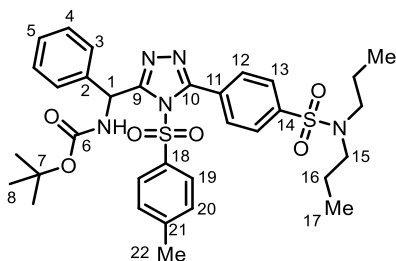
^1H NMR (400 MHz, CDCl_3) δ 7.53 – 7.45 (m, 3H), 7.43 – 7.37 (m, 3H), 7.37 – 7.32 (m, 2H), 7.28 – 7.23 (m, 2H), 6.95 (d, $J = 8.1$, 2H), 6.88 (d, $J = 9.2$, 1H, C_1), 6.82 (d, $J = 8.1$, 2H), 6.03 (d, $J = 9.1$, 1H, NH), 2.32 (s, 3H, C_{19}), 1.47 (s, 9H, C_8).

^{13}C NMR (101 MHz, CDCl_3) δ 155.3 (C), 154.8 (C), 154.2 (C), 146.6 (ArC), 138.8 (ArC), 133.7 (ArC), 131.1 (ArCH), 130.7 (ArCH), 129.6 (ArCH), 129.0 (ArCH), 128.4 (ArCH), 128.3 (ArCH), 128.1 (ArCH), 127.8 (ArCH), 126.1 (ArC), 80.2 (C_7), 52.1 (C_1), 28.4 (C_8), 21.7 (C_{19}).

FT-IR(thin film): $\nu_{\text{max}}(\text{cm}^{-1}) = 3289, 2973, 1700, 1526, 1492, 1392, 1323, 1308, 1194, 1179, 890, 724, 698$.

(ESI): m/z calculated for $\text{C}_{27}\text{H}_{29}\text{O}_4\text{N}_4\text{S}$ requires 505.1904 for $[\text{M}+\text{H}]^+$, found 505.1903.

tert-butyl ((5-(4-(*N,N*-dipropylsulfamoyl)phenyl)-4-tosyl-4*H*-1,2,4-triazol-3-yl)(phenyl)methyl)carbamate – 154



Following **general procedure B** (using **87** (43.9 mg, 0.10 mmol, 1.0 eq), **96** (30.8 mg, 0.15 mmol, 1.5 eq), and stirring for 16 h): after FCC (30% EtOAc/pentane), **154** (31.0 mg, 46%) was afforded as a yellow oil.

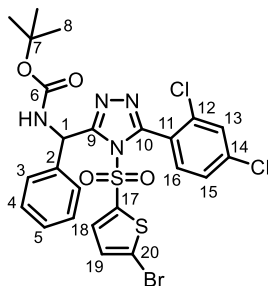
^1H NMR (400 MHz, CDCl_3) δ 7.76 – 7.69 (m, 2H), 7.43 – 7.38 (m, 2H), 7.38 – 7.30 (m, 5H), 6.97 – 6.88 (m, 2H), 6.86 – 6.75 (m, 2H, C_1), 5.88 (d, $J = 9.1$, 1H, NH), 3.09 – 2.98 (m, 4H, C_{15}), 2.27 (s, 3H, C_{22}), 1.50 (h, $J = 7.4$, 4H, C_{16}), 1.40 (s, 9H, C_8), 0.82 (t, $J = 7.4$, 6H, C_{17}).

^{13}C NMR (101 MHz, CDCl_3) δ 155.9 (C), 154.8 (C), 152.8 (C), 147.2 (ArC), 142.5 (ArC), 138.3 (ArC), 133.6 (ArC), 131.8 (ArCH), 130.0 (ArC), 129.9 (ArCH), 129.1 (ArCH), 128.5 (ArCH), 128.4 (ArCH), 128.0 (ArCH), 126.3 (ArCH), 80.3 (C_7), 52.1 (C_1), 50.1 (C_{15}), 28.4 (C_8), 22.0 (C_{16}), 21.7 (C_{22}), 11.2 (C_{17}).

FT-IR(thin film): $\nu_{\text{max}}(\text{cm}^{-1}) = 2970, 2933, 2876, 1708, 1492, 1390, 1340, 1159, 1019, 757, 666$.

(ESI): m/z calculated for $\text{C}_{33}\text{H}_{42}\text{O}_6\text{N}_5\text{S}_2$ requires 668.2571 for $[\text{M}+\text{H}]^+$, found 668.2566.

***tert*-butyl ((4-((5-bromothiophen-2-yl)sulfonyl)-5-(2,4-dichlorophenyl)-4*H*-1,2,4-triazol-3-yl)(phenyl)methyl)carbamate – 155**



Following **general procedure B** (using **152** (41.5 mg, 0.10 mmol, 1.0 eq), **96** (30.8 mg, 0.15 mmol, 1.5 eq), and stirring for 16 h): after FCC (40% Et₂O/pentane), **155** (48.3 mg, 75%) was afforded as a yellow crystalline solid.

m.p.: 76 – 78 °C

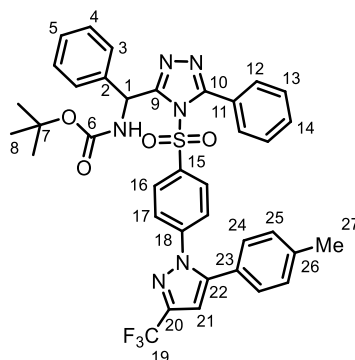
¹H NMR (400 MHz, CDCl₃) δ 7.38 (m, 8H), 6.90 – 6.82 (m, 1H), 6.74 (d, *J* = 9.1, 1H, C₁), 6.56 (s, 1H), 5.98 (s, 1H, NH), 1.45 (s, 9H, C₈).

¹³C NMR (101 MHz, CDCl₃) δ 154.8 (C), 150.1 (C), 138.4 (ArC), 138.2 (ArC), 137.2 (ArCH), 136.9 (ArC), 136.0 (ArC), 134.0 (ArC), 130.9 (ArCH), 129.2 (ArCH), 128.7 (ArCH), 128.4 (ArCH), 126.9 (ArCH), 126.5 (ArCH), 124.2 (ArC), 80.4 (C₇), 52.1 (C₁), 28.4 (C₈).

FT-IR(thin film): $\nu_{\max}(\text{cm}^{-1}) = 2977, 1707, 1597, 1489, 1392, 1181, 1152, 908, 808, 729, 676.$

(ESI): *m/z* calculated for C₂₄H₂₂O₄N₄S₂⁷⁹Br³⁵Cl₂ requires 642.9637 for [M+H]⁺, found 642.9635.

***tert*-butyl (phenyl(5-phenyl-4-((4-(5-(*p*-tolyl)-3-(trifluoromethyl)-1*H*-pyrazol-1-yl)phenyl)sulfonyl)-4*H*-1,2,4-triazol-3-yl)methyl)carbamate – 156**



Following **general procedure B** (using **153** (48.5 mg, 0.10 mmol, 1.0 eq), **96** (61.6 mg, 0.30 mmol, 3.0 eq), and stirring for 16 h): after FCC (45% Et₂O/pentane), **156** (46.2 mg, 65%) was afforded as a red crystalline solid.

m.p.: 98 – 100 °C

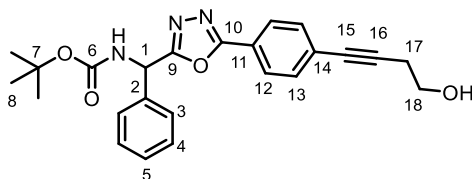
¹H NMR (400 MHz, CDCl₃) δ 7.50 – 7.44 (m, 3H), 7.41 – 7.33 (m, 3H), 7.33 – 7.19 (m, 7H), 7.15 – 7.09 (m, 2H), 7.03 (d, *J* = 8.0, 2H), 6.86 (dd, *J* = 14.1, 8.9, 2H, C₁), 6.70 (s, 1H, C₂₁), 6.00 (d, *J* = 9.0, 1H, NH), 2.42 (s, 3H, C₂₇), 1.45 (s, 9H, C₈).

¹⁹F NMR (376 MHz, CDCl₃) δ -62.6

¹³C NMR (101 MHz, CDCl₃) δ 155.4 (C), 154.9 (C), 154.0 (C), 145.4 (ArC), 144.3 (ArC), 140.1 (ArC), 138.4 (ArC), 135.5 (ArC), 131.1 (ArCH), 131.0 (ArCH), 129.95 (ArCH), 129.86 (ArCH), 129.2 (ArCH), 129.1 (ArCH), 128.8 (ArCH), 128.7 (ArCH), 128.5 (ArCH), 128.4 (ArCH), 128.1 (ArCH), 127.9 (ArCH), 125.8 (ArC), 125.6 (ArC), 125.5 (ArCH), 124.9 (ArCH), 107.0 (C₂₁), 80.3 (C₇), 52.2 (C₁), 28.4 (C₈), 21.3 (C₂₇).

FT-IR(thin film): ν_{\max} (cm⁻¹) = 3034, 1708, 1495, 1472, 1368, 1237, 1163, 1139, 732.

(ESI): *m/z* calculated for C₃₇H₃₄O₄N₆F₃S requires 715.2309 for [M+H]⁺, found 715.2302.

5.3.4 Derivatization of α -Amino 1,3,4-Oxadiazole Products***tert*-butyl ((5-(4-(4-hydroxybut-1-yn-1-yl)phenyl)-1,3,4-oxadiazol-2-yl)(phenyl)methyl)carbamate – 157**

To an oven-dried screw-cap vial was added **107** (47.7 mg, 0.10 mmol, 1.0 eq), bis(triphenylphosphine)palladium(II) dichloride (3.5 mg, 5.0 μ mol, 5.0 mol%), and copper(I) iodide (1.9 mg, 0.01 mmol, 10 mol%). The vial was then evacuated and backfilled with N_2 (x3). THF (1 mL, 0.10 M) was then added followed by but-3-yn-1-ol (15 μ L, 0.20 mmol, 2.0 eq), and lastly diisopropylamine (42 μ L, 0.30 mmol, 3 eq). The vial was then capped and stirred at rt for 22 h. After this time the reaction was concentrated *in vacuo* and then purified by FCC (85% Et_2O /pentane) to afford the *title compound* (42.4 mg, quant.) as a yellow crystalline solid.

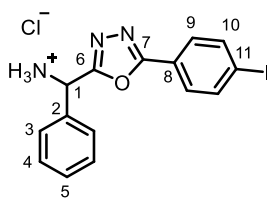
m.p.: 60 – 62 $^{\circ}C$

1H NMR (400 MHz, $CDCl_3$) δ 7.90 (d, J = 8.4, 2H, C_{12}), 7.47 (d, J = 8.5, 2H, C_{13}), 7.43 – 7.31 (m, 5H, C_3 & C_4 & C_5), 6.18 (d, J = 7.2, 1H, C_1), 5.82 (d, J = 5.9, 1H, NH), 3.83 (t, J = 6.3, 2H, C_{18}), 2.70 (t, J = 6.3, 2H, C_{17}), 1.44 (s, 9H, C_8).

^{13}C NMR (101 MHz, $CDCl_3$) δ 165.8 (ArC), 164.9 (ArC), 154.7 (C_6), 136.7 (C_2), 132.2 (C_{13}), 129.2 (C_4), 128.9 (C_5), 127.2 (C_3), 126.8 (C_{12}), 122.6 (C_{11}), 90.1 (C), 81.5 (C), 80.8 (C_7), 61.0 (C_{18}), 51.6 (C_1), 28.3 (C_8), 23.9 (C_{17}).

FT-IR(thin film): $\nu_{max}(cm^{-1})$ = 3304, 1698, 1493, 1367, 1164, 1049, 1015, 846, 731.

(ESI): m/z calculated for $C_{24}H_{25}O_4N_3Na$ requires 442.1737 for $[M+Na]^+$, found 442.1736.

(5-(4-iodophenyl)-1,3,4-oxadiazol-2-yl)(phenyl)methanaminium chloride – 158

In an oven-dried rbf was added **107** (1.26 g, 2.65 mmol, 1.0 eq) and HCl (4.0 M in 1,4-dioxane, 27 mL, 0.10 M), and the reaction stirred at rt. After 1 h, the reaction was concentrated *in vacuo* to afford the *title compound* (1.15 g, quant.) as a white solid.

m.p.: 190 – 192 °C (decomposition).

¹H NMR (400 MHz, MeOD) δ 7.93 – 7.88 (m, 2H, C₉), 7.76 – 7.72 (m, 2H, C₁₀), 7.64 – 7.58 (m, 2H, C₃), 7.57 – 7.50 (m, 3H, C₄ & C₅), 6.15 (s, 1H, C₁), 4.93 (s, 3H, NH).

¹³C NMR (101 MHz, MeOD) δ 165.8 (ArC), 162.7 (ArC), 138.5 (C₉), 131.8 (C₂), 130.4 (C₅), 129.5 (C₄), 128.1 (ArCH), 128.1 (ArCH), 122.2 (C₈), 99.0 (C₁₁), 50.6 (C₁).

FT-IR(thin film): $\nu_{\max}(\text{cm}^{-1}) = 3387, 2850, 1599, 1478, 1403, 1080, 1006, 828, 726, 697.$

(ESI): m/z calculated for C₁₅H₁₃ON₃I requires 378.0098 for [M+H]⁺, found 378.0099.

Note: The free base of **158** was used for some of the below reactions and was available by a basic workup using saturated aqueous NaHCO₃, extracting with CH₂Cl₂, and subsequently drying (MgSO₄), filtering, and concentrating *in vacuo* to afford **158** (freebase) as a beige solid.

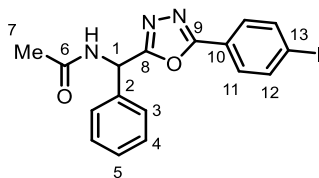
m.p.: 154 – 156 °C

¹H NMR (400 MHz, CDCl₃) δ 7.81 (d, *J* = 8.7, 2H, C₉), 7.69 (d, *J* = 8.6, 2H, C₁₀), 7.49 – 7.43 (m, 2H, C₃), 7.42 – 7.30 (m, 3H, C₄ & C₅), 5.45 (s, 1H, C₁), 2.28 (s, 2H, NH₂).

^{13}C NMR (101 MHz, CDCl_3) δ 168.5 (ArC), 164.7 (ArC), 139.4 (C_2), 138.3 (C_9), 129.1 (ArCH), 128.6 (C_5), 128.3 (C_{10}), 126.9 (ArCH), 123.2 (C_8), 98.7 (C_{11}), 52.7 (C_1).

FT-IR(thin film): $\nu_{\text{max}}(\text{cm}^{-1}) = 3290, 3082, 2927, 1601, 1479, 1085, 1005, 907, 831, 731$.

(ESI): m/z calculated for $\text{C}_{15}\text{H}_{13}\text{ON}_3\text{I}$ requires 378.0098 for $[\text{M}+\text{H}]^+$, found 378.0098.

N-((5-(4-iodophenyl)-1,3,4-oxadiazol-2-yl)(phenyl)methyl)acetamide – 159

To an oven-dried screw-cap vial was added **158** (41.4 mg, 0.10 mmol 1.0 eq), DMAP (1.2 mg, 0.01 mmol, 10 mol%), CH₂Cl₂ (1.0 mL, 0.10 M), triethylamine (42 μL, 0.30 mmol, 3.0 eq), and lastly acetic anhydride (19 μL, 0.20 mmol, 2.0 eq); then the vial capped and stirred at rt for 19 h. The reaction was then diluted with EtOAc (15 mL) and washed with saturated aqueous NaHCO₃ (10 mL), water (2 x 10 mL), and brine (10 mL). The combined organics were dried (MgSO₄), filtered, and concentrated *in vacuo* to afford the *title compound* (41.3 mg, quant.) as a white powder.

m.p.: 216 – 218 °C

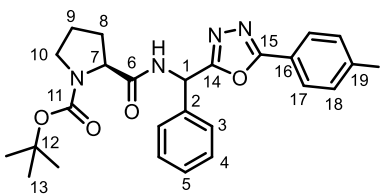
¹H NMR (400 MHz, CDCl₃ & DMSO-D₆) δ 9.04 (d, *J* = 7.9, 1H, NH), 7.83 (d, *J* = 8.5, 2H, C₁₁), 7.68 (d, *J* = 8.5, 2H, C₁₂), 7.42 – 7.34 (m, 3H, C₂ & C₅), 7.32 – 7.26 (m, 2H, C₄), 6.40 (d, *J* = 7.9, 1H, C₁), 1.97 (s, 3H, C₇).

¹³C NMR (101 MHz, CDCl₃ & DMSO-D₆) δ 169.2 (C₆), 165.6 (ArC), 163.7 (ArC), 137.8 (C₁₂), 136.2 (C₂), 128.3 (C₄), 128.0 (C₅), 127.7 (C₃), 127.1 (C₁₁), 122.5 (C₁₀), 98.5 (C₁₃), 48.8 (C₁), 22.0 (C₇).

FT-IR(thin film): $\nu_{\max}(\text{cm}^{-1}) = 3293, 2917, 2849, 1651, 1538, 1006, 831, 729, 694.$

(ESI): *m/z* calculated for C₁₇H₁₅O₂N₃I requires 420.0203 for [M+H]⁺, found 420.0202.

***tert*-butyl (2S)-2-(((5-(4-iodophenyl)-1,3,4-oxadiazol-2-yl)(phenyl)methyl)carbamoyl)pyrrolidine-1-carboxylate – 160**



To an oven-dried screw-cap vial was added **158** (41.4 mg, 0.10 mmol 1.0 eq), Boc-*L*-proline (23.6 mg, 0.11 mmol, 1.1 eq), CH₂Cl₂ (0.50 mL, 0.20 M), triethylamine (42 μL, 0.30 mmol, 3.0 eq), and lastly propylphosphonic anhydride solution (50% wt. in EtOAc, 90 μL, 0.15 mmol, 1.5 eq), then the vial capped and stirred at rt for 4.5 h. The reaction was then diluted with EtOAc (15 mL) and washed with saturated aqueous NaHCO₃ (10 mL), water (2 x 10 mL), and brine (10 mL). The combined organics were dried (MgSO₄), filtered, and concentrated *in vacuo* to afford the crude product. The crude was purified by FCC (40% EtOAc/pentane) to afford the *title compound* (46.8 mg, 82%) as a white crystalline solid. d.r: 51:49 as determined by integration of the ¹H signals at 7.94 – 7.91 and 7.91 – 7.88 ppm.

m.p.: 72 – 74 °C

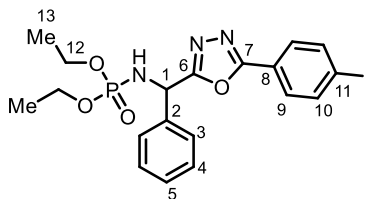
The integral ratios are given as observed - ¹H NMR (400 MHz, MeOD) δ 7.95 – 7.87 (m, 2H, C₁₇), 7.82 – 7.67 (m, 2H, C₁₈), 7.51 – 7.45 (m, 2H), 7.45 – 7.33 (m, 3H), 6.63 – 6.39 (m, 1H, C₁), 4.40 – 4.25 (m, 1H, C₇), 3.51 (s, 1H), 3.46 – 3.36 (m, 1H), 2.38 – 2.13 (m, 1H), 2.11 – 2.01 (m, 0.5H), 1.99 – 1.78 (m, 2.6H), 1.48 – 1.27 (m, 9H, C₁₃).

¹³C NMR (101 MHz, MeOD) δ 175.1 (C₆), 166.3 (ArC), 155.9 (C₁₁), 139.8 (ArCH), 137.5 (ArC), 130.1 (ArCH), 129.9 (ArCH), 129.3 (ArCH), 129.0 (ArCH), 128.6 (ArCH), 124.1 (ArC), 99.8 (C₁₉), 81.4 (C₁₂), 61.6 (C₇), 61.3 (C₇), 51.3 (C₁), 50.8 (C₁), 47.9 (CH₂), 32.5 (CH₂), 31.2 (CH₂), 28.6 (C₁₃), 25.4 (CH₂), 24.6 (CH₂).

FT-IR(thin film): $\nu_{\max}(\text{cm}^{-1}) = 2974, 1669, 1400, 1365, 1162, 1123, 1085, 980, 697.$

(ESI): m/z calculated for $\text{C}_{25}\text{H}_{28}\text{O}_4\text{N}_4\text{I}$ requires 575.1150 for $[\text{M}+\text{H}]^+$, found 575.1144.

diethyl ((5-(4-iodophenyl)-1,3,4-oxadiazol-2-yl)(phenyl)methyl)phosphoramidate – 161



To an oven-dried screw-cap vial was added **158** (free base) (37.7 mg, 0.10 mmol 1.0 eq), DMAP (1.2 mg, 0.01 mmol, 10 mol%), CH₂Cl₂ (0.50 mL, 0.20 M), triethylamine (28 μL, 0.20 mmol, 2.0 eq), and lastly diethyl chlorophosphate (17 μL, 0.12 mmol, 1.2 eq), then the vial capped and stirred at rt for 18 h. After this time, additional DMAP (1.2 mg, 0.01 mmol, 10 mol%), triethylamine (42 μL, 0.30 mmol, 3.0 eq), CH₂Cl₂ (0.5 mL, 0.10 M total), and diethyl chlorophosphate (43 μL, 0.30 mmol, 3.0 eq) were added, and the reaction stirred for a further 3 h. The reaction was then diluted with CH₂Cl₂ (10 mL), washed with saturated aqueous NaHCO₃ (30 mL), and extracted with CH₂Cl₂ (3 x 10 mL). The combined organics were dried (MgSO₄), filtered, and concentrated *in vacuo* to afford the crude product. The crude was purified by FCC (60% → 80% EtOAc/pentane) to afford the *title compound* (40.8 mg, 80%) as a white powder.

m.p.: 170 – 172 °C

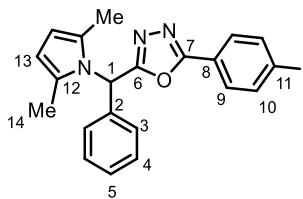
¹H NMR (400 MHz, CDCl₃) δ 7.85 – 7.80 (m, 2H, C₉), 7.74 – 7.67 (m, 2H, C₁₀), 7.46 – 7.41 (m, 2H, C₃), 7.41 – 7.31 (m, 3H, C₄ & C₅), 5.77 (t, *J* = 9.0, 1H, C₁), 4.18 – 3.90 (m, 4H, C₁₂), 1.28 – 1.17 (m, 6H, C₁₃).

³¹P NMR (162 MHz, CDCl₃) δ 5.7

¹³C NMR (101 MHz, CDCl₃) δ 166.5 (d, *J* = 6.5, C₆), 164.8 (C₇), 138.4 (C₉), 137.8 (d, *J* = 5.2, C₂), 129.1 (C₄), 128.8 (C₅), 128.3 (C₁₀), 126.8 (C₃), 123.0 (C₈), 98.8 (C₁₁), 62.9 (d, *J* = 5.3, C₁₂), 62.8 (d, *J* = 5.9, C₁₂), 52.3 (d, *J* = 1.7, C₁), 16.0 (d, *J* = 7.1, C₁₃).

FT-IR(thin film): ν_{max}(cm⁻¹) = 3195, 2924, 2852, 1600, 1477, 1455, 1234, 1055, 1027, 972.

(ESI): m/z calculated for C₁₉H₂₂O₄N₃P requires 514.0387 for [M+H]⁺, found 514.0386.

2-((2,5-dimethyl-1H-pyrrol-1-yl)(phenyl)methyl)-5-(4-iodophenyl)-1,3,4-oxadiazole – 162

To an oven-dried screw-cap vial was added **158** (free base) (37.7 mg, 0.10 mmol 1.0 eq), MeOH (0.50 mL, 0.20 M), hexane-2,5-dione (36 μ L, 0.30 mmol, 3.0 eq), and acetic acid (6.0 μ L, 0.05 mmol, 0.50 eq). The vial was then capped and stirred at rt for 22 h. After this time the reaction mixture was purified by FCC (15% Et₂O/pentane) to afford the *title compound* (37.5 mg, 82%) as a white solid.

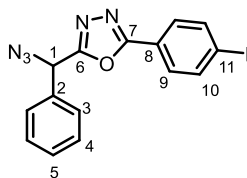
m.p.: 142 – 144 °C

¹H NMR (400 MHz, CDCl₃) δ 7.86 (d, J = 8.3, 2H, C₉), 7.74 (d, J = 8.4, 2H, C₁₀), 7.41 – 7.33 (m, 3H, C₄ & C₅), 7.15 – 7.08 (m, 2H, C₃), 6.93 (s, 1H, C₁), 5.89 (s, 2H, C₁₃), 2.14 (s, 6H, C₁₄).

¹³C NMR (101 MHz, CDCl₃) δ 165.1 (ArC), 164.4 (ArC), 138.4 (C₉), 135.4 (ArC), 129.0 (ArC), 128.9 (C₄), 128.4 (C₅), 128.4 (C₁₀), 126.7 (C₃), 122.9 (ArC), 107.5 (C₁₃), 99.0 (C₁₁), 54.0 (C₁), 13.5 (C₁₄).

FT-IR(thin film): ν_{\max} (cm⁻¹) = 2925, 1599, 1450, 1392, 1289, 1056, 1005, 828, 761, 728, 696.

(ESI): m/z calculated for C₂₁H₁₉ON₃I requires 456.0567 for [M+H]⁺, found 456.0565.

2-(azido(phenyl)methyl)-5-(4-iodophenyl)-1,3,4-oxadiazole – 163

To an oven-dried screw-cap vial was added **158** (free base) (37.7 mg, 0.10 mmol 1.0 eq), copper(II) sulfate (1.3 mg, 5.0 μmol , 5.0 mol%), potassium carbonate (7.0 mg, 0.05 mmol, 5.0 mol%), and MeOH (0.25 mL, 0.25 M). Imidazole-1-sulfonyl azide (0.83 M in EtOAc, 140 μL , 0.12 mmol, 1.2 eq)³⁵⁰ was added, and the reaction stirred open to air at rt. After 30 mins, EtOAc (0.5 mL, 0.13 M total) was added, and after 135 mins additional copper(II) sulfate (1.3 mg, 5.0 μmol , 5.0 mol%) and imidazole-1-sulfonyl azide (0.83 M in EtOAc, 400 μL , 0.33 mmol, 3.3 eq)³⁵⁰ were added. After 22 h total, the reaction mixture was purified by FCC (20% Et₂O/pentane), to afford the *title compound* (24.6 mg, 61%) as a white powder.

m.p.: 64 – 66 °C

¹H NMR (400 MHz, CDCl₃) δ 7.88 – 7.83 (m, 2H, C₉), 7.76 – 7.72 (m, 2H, C₁₀), 7.52 – 7.40 (m, 5H, C₃ & C₄ & C₅), 5.94 (s, 1H, C₁).

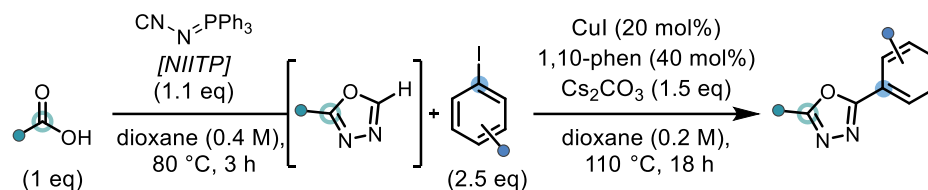
¹³C NMR (101 MHz, CDCl₃) δ 165.2 (ArC), 163.8 (ArC), 138.4 (C₉), 133.6 (ArC), 129.7 (C₅), 129.3 (C₄), 128.4 (C₁₀), 127.6 (C₅), 122.8 (ArC), 99.1 (C₁₁), 59.7 (C₁).

FT-IR(thin film): $\nu_{\text{max}}(\text{cm}^{-1}) = 2980, 2104, 1600, 1477, 1402, 1182, 1083, 1006, 908, 829, 730$.

(ESI): m/z calculated for C₁₅H₁₁ON₃I requires 375.9947 for [M+H-N₂]⁺, found 375.9942.

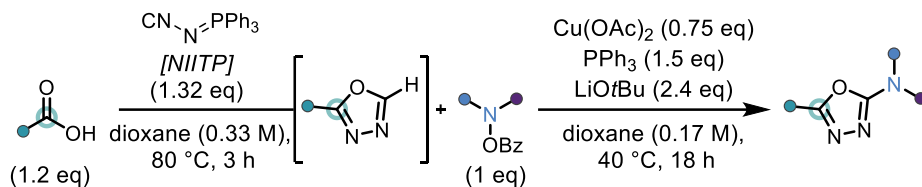
5.4 Experimental Details for Chapter 4

5.4.1 General Procedure C: One-Pot 1,3,4-Oxadiazole Construction-Arylation



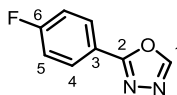
To a dry Schlenk tube under nitrogen was added carboxylic acid (0.20 mmol, 1.0 eq), and NIITP (66.5 mg, 0.22 mmol, 1.1 eq). The Schlenk tube was then evacuated and backfilled with nitrogen (x4) and then anhydrous 1,4-dioxane (0.50 mL, 0.40 M) was added. The Schlenk tube was then sealed and put into an oil bath preheated at 80 °C and stirred for 3 h. After this time the reaction was cooled to rt and aryl iodide (0.50 mmol, 2.5 eq), 1,10-phenanthroline (14.4 mg, 0.08 mmol, 40 mol%), cesium carbonate (97.7 mg, 0.30 mmol, 1.5 eq), copper(I) iodide (7.6 mg, 0.04 mmol, 20 mol%), and anhydrous 1,4-dioxane (0.50 mL, 0.20 M total) were added sequentially. The Schlenk tube was then sealed and put into an oil bath preheated at 110 °C and stirred for 18 h. After this time the reaction was cooled to rt and filtered through a silica plug, washing with EtOAc, and then concentrated *in vacuo* to afford the crude product. The crude product was purified by FCC, and subsequent PTLC when required, to afford the pure 2,5-disubstituted 1,3,4-oxadiazole product.

5.4.2 General Procedure D: One-Pot 1,3,4-Oxadiazole Construction-Amination



To a dry Schlenk tube under nitrogen was added carboxylic acid (0.20 mmol, 1.2 eq), and NIITP (66.5 mg, 0.22 mmol, 1.32 eq). The Schlenk tube was then evacuated and backfilled with nitrogen (x4) and the anhydrous 1,4-dioxane (0.50 mL, 0.33 M) added. The Schlenk tube was then sealed and put into an oil bath preheated at 80 °C and stirred for 3 h. After this time the reaction was cooled to rt and O-benzoyl hydroxylamine (0.167 mmol, 1.0 eq), triphenylphosphine (65.6 mg, 0.25 mmol, 1.5 eq), lithium *tert*-butoxide (32.0 mg, 0.40 mmol, 2.4 eq), copper(II) acetate (22.7 mg, 0.13 mmol, 0.75 eq), and anhydrous 1,4-dioxane (0.50 mL, 0.17 M total) were added sequentially. The Schlenk tube was then sealed and put into an oil bath preheated at 40 °C and stirred for 18 h. After this time the reaction was cooled to rt and filtered through a silica plug, washing with EtOAc, and then concentrated *in vacuo* to afford the crude product. The crude product was purified by FCC, and subsequent PTLC when required, to afford the pure 2-amino-5-substituted 1,3,4-oxadiazole product.

5.4.3 Synthesis of Starting Materials

2-(4-fluorophenyl)-1,3,4-oxadiazole – 105

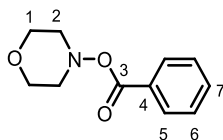
To an oven-dried rbf was added 4-fluorobenzohydrazide (3.01 g, 19.5 mmol, 1.0 eq), and triethyl orthoformate (17 mL, 103 mmol, 5.3 eq). The reaction was then heated to 150 °C and stirred for 19.5 h. After this time the reaction was cooled to rt and diluted with EtOAc (300 mL), and then washed with saturated aqueous NaHCO₃ (100 mL), water (3 x 100 mL), and brine (100 mL), before being dried (MgSO₄), filtered, and concentrated *in vacuo* to afford the crude product. The crude was purified by FCC (50% Et₂O/pentane) to afford the *title compound* (2.74 g, 86%) as a white solid. Data was consistent with that found in the literature.³⁸³

¹H NMR (400 MHz, CDCl₃) δ 8.46 (s, 1H, C₁), 8.13 – 8.04 (m, 2H, C₄), 7.24 – 7.15 (m, 2H, C₅).

¹⁹F NMR (377 MHz, CDCl₃) δ -106.4.

¹³C NMR (101 MHz, CDCl₃) δ 165.0 (d, *J* = 253.6, C₆), 164.0 (C₂), 152.6 (C₁), 129.4 (d, *J* = 8.9, C₄), 119.9 (d, *J* = 3.4, C₃), 116.5 (d, *J* = 22.4, C₅).

morpholino benzoate – 206

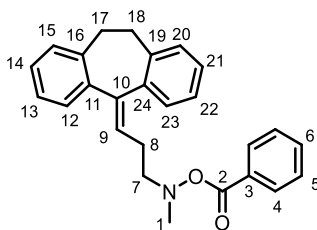


To an oven-dried rbf was added benzoyl peroxide (75% with 25% H₂O, 3.23 g, 10 mmol, 1.0 eq), K₂HPO₄ (3.48 g, 20 mmol, 2.0 eq), and anhydrous DMF (50 mL, 0.20 M). Then morpholine (960 μL, 11 mmol, 1.1 eq) was added and the reaction stirred at rt for 23 h. After this time the reaction was diluted with water (300 mL) and extracted with EtOAc (3 x 100 mL). The combined organics were then washed with water (4 x 100 mL), and brine (100 mL), then dried (MgSO₄), filtered, and concentrated *in vacuo* to afford the crude product. The crude was purified by FCC (40% EtOAc/pentane) to afford the *title compound* (1.64 g, 79%) as a white solid. Data was consistent with that found in the literature.³⁸⁴

¹H NMR (400 MHz, CDCl₃) δ 8.05 – 7.95 (m, 2H, C₅), 7.59 – 7.52 (m, 1H, C₇), 7.48 – 7.37 (m, 2H, C₆), 4.03 – 3.77 (m, 4H, C₁), 3.43 (d, *J* = 9.2, 2H, C₂), 3.04 (d, *J* = 8.5, 2H, C₂).

¹³C NMR (101 MHz, CDCl₃) δ 164.6 (C₃), 133.2 (C₇), 129.4 (C₆), 129.2 (C₄), 128.4 (C₅), 65.8 (C₁), 57.0 (C₂).

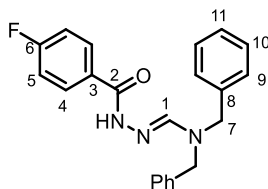
O-benzoyl-N-(3-(10,11-dihydro-5H-dibenzo[a,d][7]annulen-5-ylidene)propyl)-N-methylhydroxylamine – 213



To an oven-dried rbf was added nortriptyline hydrochloride (1.00 g, 3.34 mmol, 1.1 eq), benzoyl peroxide (75% with 25% H₂O, 970 mg, 3.0 mmol, 1.0 eq), dipotassium phosphate (1.59 g, 9.1 mmol, 3.0 eq), and anhydrous DMF (15 mL, 0.22 M). The reaction was allowed to stir at rt for 19.5 h, and then was diluted with water (150 mL) and extracted with EtOAc (3 x 50 mL). The combined organics were washed with water (2 x 50 mL), and brine (50 mL), then dried (MgSO₄), filtered, and concentrated *in vacuo* to afford the crude product. The crude was purified by FCC (pentane → 30% Et₂O/pentane), and subsequently triturated with pentane and filtered to afford the *title compound* (730 mg, 63%) as a white powder. Data was consistent with that found in the literature.³⁶⁵

¹H NMR (400 MHz, CDCl₃) δ 7.94 (d, *J* = 7.2, 2H, C₄), 7.59 (t, *J* = 7.4, 1H, C₆), 7.43 (t, *J* = 7.8, 2H, C₅), 7.31 (dd, *J* = 7.0, 2.1, 1H), 7.22 – 7.09 (m, 6H), 7.06 (dd, *J* = 6.9, 1.8, 1H), 5.98 (t, *J* = 7.5, 1H, C₉), 3.47 – 3.23 (m, 2H, C₁₇ & C₁₈), 3.22 – 3.04 (m, 2H, C₇), 3.04 – 2.94 (m, 1H), 2.91 (s, 3H, C₁), 2.76 (d, *J* = 13.4, 1H), 2.54 (q, *J* = 7.0, 2H, C₈).

¹³C NMR (101 MHz, CDCl₃) δ 165.1 (C₂), 144.4 (ArC), 141.0 (ArC), 139.9 (ArC), 139.3 (ArC), 137.1 (ArC), 133.0 (ArCH), 130.0 (ArCH), 129.4 (ArCH), 129.3 (ArC), 128.6 (ArCH), 128.4 (ArCH), 128.1 (C₉), 128.0 (ArCH), 127.4 (ArCH), 127.1 (ArCH), 126.0 (ArCH), 125.8 (ArCH), 60.8 (C₇), 46.9 (C₁), 33.8 (C₁₇ or C₁₈), 32.0 (C₁₇ or C₁₈), 27.4 (C₈).

***N,N*-dibenzyl-*N*-(4-fluorobenzoyl)formohydrazoneamide – 214**

To an oven-dried vial was added **105** (32.8 mg, 0.20 mmol, 1.0 eq), and dibenzylamine (120 μL , 0.60 mmol, 3.0 eq). The vial was capped, and the reaction stirred at 110 $^{\circ}\text{C}$ for 17 h, then cooled to rt and then reaction purified by FCC (EtOAc) to afford the *title compound* (23.7 mg, 33%) as a white solid.

m.p.: 188 – 190 $^{\circ}\text{C}$

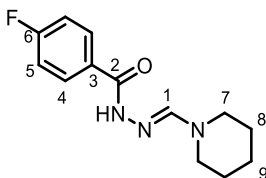
^1H NMR (400 MHz, CDCl_3) δ 8.42 (s, 1H, C₁), 8.25 (s, 1H, NH), 7.79 (dt, $J = 11.1, 5.6$, 2H, C₄), 7.38 – 7.26 (m, 8H), 7.26 – 7.19 (m, 2H), 7.11 (t, $J = 8.6$, 2H), 4.39 (s, 4H, C₇).

^{19}F NMR (377 MHz, CDCl_3) δ -108.5.

^{13}C NMR (151 MHz, CDCl_3) δ 164.6 (d, $J = 251.8$, C₆), 164.2 (C₂), 158.8 (C₁), 136.5 (C₈), 129.0 (d, $J = 8.7$, C₄), 128.8 (ArCH), 128.0 (ArCH), 127.7 (ArCH), 126.3 (C₃), 115.7 (d, $J = 21.9$, C₅), 59.4 (C₇).

FT-IR(thin film): $\nu_{\text{max}}(\text{cm}^{-1}) = 3030, 2922, 1647, 1615, 1585, 1506, 1363, 1226, 1161, 698$.

(ESI): m/z calculated for $\text{C}_{22}\text{H}_{21}\text{ON}_3\text{F}$ requires 362.1663 for $[\text{M}+\text{H}]^+$, found 362.1660.

4-fluoro-*N*-(piperidin-1-ylmethylene)benzohydrazide – 215

To an oven-dried vial was added **105** (32.8 mg, 0.20 mmol, 1.0 eq), and piperidine (60 μ L, 0.60 mmol, 3.0 eq). The vial was capped, and the reaction stirred at 110 $^{\circ}$ C for 17 h, then cooled to rt and the reaction was purified by FCC (EtOAc) to afford the *title compound* (7.4 mg, 15%) as a yellow oil.

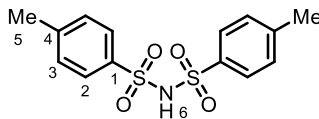
^1H NMR (400 MHz, CDCl_3) δ 7.85 (s, 1H, C₁), 7.79 – 7.72 (m, 2H, C₄), 7.08 (t, J = 8.6, 2H, C₅), 3.35 – 3.22 (m, 4H, C₇), 1.72 – 1.49 (m, 6H, C₈ & C₉).

^{19}F NMR (377 MHz, CDCl_3) δ -108.8.

^{13}C NMR (151 MHz, CDCl_3) δ 163.5 (d, J = 251.1, C₆), 162.8 (C₂), 156.3 (C₁), 128.0 (d, J = 8.8, C₄), 114.6 (d, J = 21.8, C₅), 112.9 (C₃), 47.8 (C₇), 25.6 (C₈), 24.4 (C₉).

FT-IR(thin film): $\nu_{\text{max}}(\text{cm}^{-1})$ = 3233, 2936, 2855, 1652, 1615, 1506, 1449, 1257, 850, 668.

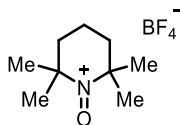
(ESI): m/z calculated for $\text{C}_{13}\text{H}_{17}\text{ON}_3\text{F}$ requires 250.1350 for $[\text{M}+\text{H}]^+$, found 250.1349.

4-methyl-*N*-tosylbenzenesulfonamide – S5

To a solution of 4-methylbenzenesulfonamide (1.58 g, 9.2 mmol, 1.0 eq) in PhMe (20 mL, 0.50 M) was added triethylamine (1.7 mL, 12.0 mmol, 1.3 eq), DMAP (224 mg, 1.8 mmol, 20 mol%), and 4-toluenesulfonyl chloride (1.93 g, 10.1 mmol, 1.1 eq). The reaction was heated at 70 °C for 22 h, then cooled to rt and aqueous HCl (2.0 M, 50 mL) added. The layers were separated and the aqueous extracted with EtOAc (3 x 30 mL). The combined organics were dried (MgSO₄), filtered, and concentrated *in vacuo* to give the crude product. The crude product was recrystallized from CHCl₃:hexane (1:1) to afford the *title compound* (1.57 g, 52%) as an off-white solid. Data was consistent with that found in the literature.³⁸⁵

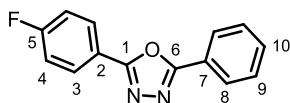
¹H NMR (400 MHz, DMSO-*d*₆) δ 9.62 (s, 1H, N₆), 7.63 – 7.44 (m, 4H, C₂), 7.23 (d, *J* = 8.0, 4H, C₃), 2.34 (s, 6H, C₅).

¹³C NMR (101 MHz, DMSO-*d*₆) δ 142.1 (C₄), 141.2 (C₁), 129.3 (C₃), 127.0 (C₂), 21.4 (C₅).

2,2,6,6-tetramethylpiperidine-1-oxoammonium tetrafluoroborate – TEMPO⁺BF₄⁻ – S6

According to a literature procedure,¹⁷⁸ TEMPO (8.00 g, 51.2 mmol, 1.0 eq) was suspended in Et₂O (40 mL, 0.78 M) and cooled to 0 °C and then tetrafluoroboric acid (50% in H₂O, 14.4 mL, 111 mmol, 2.2 eq) added dropwise. The resulting suspension was warmed to rt and allowed to stir for 90 mins. The precipitate that formed was isolated by filtration, washing with cold Et₂O (100 mL), to afford the *title compound* (5.20 g, 84%) as a bright yellow solid, which was used without further analysis or purification.

5.4.4 Synthesis of 2,5-Disubstituted 1,3,4-Oxadiazole Products

2-(4-fluorophenyl)-5-phenyl-1,3,4-oxadiazole – 180

Following **general procedure C** (using 4-fluorobenzoic acid (28.0 mg, 0.20 mmol, 1.0 eq), and iodobenzene (56 μ L, 0.50 mmol, 2.5 eq)): after FCC (20% Et₂O/pentane), **180** (37.3 mg, 78%) was afforded as a white solid. Data was consistent with that found in the literature.¹⁰¹

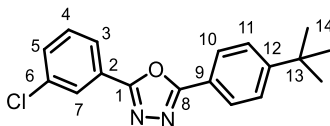
m.p.: 154 – 156 °C

¹H NMR (400 MHz, CDCl₃) δ 8.19 – 8.09 (m, 4H, C₃ & C₈), 7.60 – 7.50 (m, 3H, C₉ & C₁₀), 7.28 – 7.19 (m, 2H, C₄).

¹⁹F NMR (376 MHz, CDCl₃) δ -106.8.

¹³C NMR (101 MHz, CDCl₃) δ 164.8 (d, J = 253.2, C₅), 164.6 (ArC), 163.8 (ArC), 131.8 (C₁₀), 129.2 (d, J = 8.9, C₃), 129.1 (C₉), 126.9 (C₈), 123.8 (C₇), 120.3 (J = 3.6, C₂), 116.5 (d, J = 22.3, C₄).

During reaction optimization a reference sample was obtained using the following procedure: To an oven-dried vial was added 4-fluorobenzoic acid (28.0 mg, 0.20 mmol, 1.0 eq), benzohydrazide (27.2 mg, 0.20 mmol, 1.0 eq), EtOAc (500 μ L, 0.40 M), triethylamine (83 μ L, 0.60 mmol, 3.0 eq), and lastly propylphosphonic anhydride solution (50% in EtOAc, 300 μ L, 0.50 mmol, 2.5 eq). The vial was then sealed and heated at 80 °C for 24 h. After this time the reaction mixture was purified by FCC (15% EtOAc/pentane) to afford the *title compound* (24.0 mg, 50%) as a white solid.

2-(4-(*tert*-butyl)phenyl)-5-(3-chlorophenyl)-1,3,4-oxadiazole – 182

Following **general procedure C** (using 3-chlorobenzoic acid (31.3 mg, 0.20 mmol, 1.0 eq), and 1-(*tert*-butyl)-4-iodobenzene (89 μ L, 0.50 mmol, 2.5 eq)): after FCC (20% Et₂O/pentane), **182** (36.6 mg, 59%) was afforded as a beige powder.

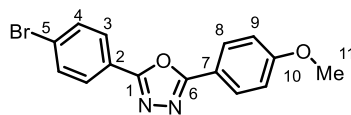
m.p.: 112 – 114 °C

¹H NMR (400 MHz, CDCl₃) δ 8.11 (t, J = 1.6, 1H, C₃), 8.08 – 8.01 (m, 3H, C₇ & C₁₀), 7.58 – 7.53 (m, 2H, C₁₁), 7.53 – 7.49 (m, 1H, C₄), 7.49 – 7.44 (m, 1H, C₅), 1.37 (s, 9H, C₁₄).

¹³C NMR (101 MHz, CDCl₃) δ 165.0 (ArC), 163.2 (ArC), 155.6 (ArC), 135.2 (ArC), 131.6 (C₄), 130.4 (C₅), 126.9 (C₁₀), 126.8 (C₃), 126.1 (C₁₁), 125.7 (C₂), 125.0 (C₇), 120.8 (C₆), 35.1 (C₁₃), 31.1 (C₁₄).

FT-IR(thin film): ν_{max} (cm⁻¹) = 2964, 1615, 1575, 1546, 1494, 1413, 1271, 1018, 839, 749, 724.

(ESI): m/z calculated for C₁₈H₁₈ON₂³⁵Cl requires 313.1102 for [M+H]⁺, found 313.1104.

2-(4-bromophenyl)-5-(4-methoxyphenyl)-1,3,4-oxadiazole – 183

Following **general procedure C** (using 4-bromobenzoic acid (40.2 mg, 0.20 mmol, 1.0 eq), and 1-iodo-4-methoxybenzene (117 mg, 0.50 mmol, 2.5 eq)): after FCC (40% → 50% Et₂O/pentane), **183** (44.8 mg, 68%) was afforded as a beige powder.

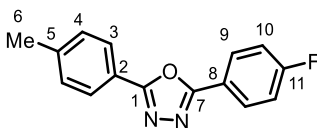
m.p.: 144 – 146 °C

¹H NMR (400 MHz, CDCl₃) δ 8.08 – 8.01 (m, 2H, C₈), 7.99 – 7.94 (m, 2H, C₃), 7.68 – 7.62 (m, 2H, C₄), 7.04 – 6.98 (m, 2H, C₉), 3.87 (s, 3H, C₁₁).

¹³C NMR (101 MHz, CDCl₃) δ 164.7 (ArC), 163.4 (ArC), 162.5 (ArC), 132.4 (C₄), 128.7 (C₈), 128.2 (C₃), 126.2 (ArC), 123.0 (ArC), 116.2 (ArC), 114.6 (C₉), 55.5 (C₁₁).

FT-IR(thin film): $\nu_{\max}(\text{cm}^{-1}) = 2917, 1611, 1495, 1477, 1258, 1172, 1074, 832, 723$.

(ESI): m/z calculated for C₁₅H₁₂O₂N₂⁷⁹Br requires 331.0077 for [M+H]⁺, found 331.0078.

2-(4-fluorophenyl)-5-(*p*-tolyl)-1,3,4-oxadiazole – 184

Following **general procedure C** (using 4-methylbenzoic acid (27.2 mg, 0.20 mmol, 1.0 eq), and 1-fluoro-4-iodobenzene (58 μ L, 0.50 mmol, 2.5 eq)): after FCC (25% Et₂O/pentane), **184** (40.6 mg, 80%) was afforded as a white powder.

m.p.: 166 – 168 °C

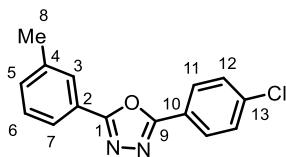
¹H NMR (400 MHz, CDCl₃) δ 8.16 – 8.09 (m, 2H, C₉), 8.03 – 7.96 (m, 2H, C₃), 7.32 (d, J = 8.0, 2H, C₁₀), 7.24 – 7.17 (m, 2H, C₄), 2.43 (s, 3H, C₆).

¹⁹F NMR (376 MHz, CDCl₃) δ -107.0.

¹³C NMR (101 MHz, CDCl₃) δ 164.8 (ArC), 164.7 (d, J = 253.1, C₁₁), 163.5 (ArC), 142.4 (ArC), 129.8 (C₁₀), 129.1 (d, J = 8.9, C₉), 126.9 (C₉), 121.1 (ArC), 120.4 (d, J = 3.4, C₈), 116.4 (d, J = 22.3, C₁₀), 21.7 (C₆).

FT-IR(thin film): ν_{\max} (cm⁻¹) = 1608, 1494, 1418, 1227, 1159, 1096, 1069, 1013, 843, 824, 740.

(ESI): m/z calculated for C₁₅H₁₂ON₂F requires 255.0928 for [M+H]⁺, found 255.0929.

2-(4-chlorophenyl)-5-(*m*-tolyl)-1,3,4-oxadiazole – 185

Following **general procedure C** (using 3-methylbenzoic acid (27.2 mg, 0.20 mmol, 1.0 eq), and 1-chloro-4-iodobenzene (119 mg, 0.50 mmol, 2.5 eq)): after FCC (25% Et₂O/pentane), **185** (47.0 mg, 87%) was afforded as a beige powder.

m.p.: 130 – 132 °C

¹H NMR (400 MHz, CDCl₃) δ 8.09 – 8.02 (m, 2H, C₁₁), 7.94 – 7.91 (m, 1H, C₃), 7.90 (d, *J* = 7.6, 1H, C₇), 7.51 – 7.46 (m, 2H, C₁₂), 7.40 (t, *J* = 7.6, 1H, C₆), 7.34 (d, *J* = 7.6, 1H, C₅), 2.44 (s, 3H, C₈).

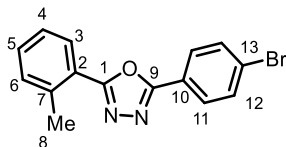
¹³C NMR (101 MHz, CDCl₃) δ 164.9 (ArC), 163.7 (ArC), 139.0 (ArC), 137.9 (ArC), 132.7 (C₅), 129.5 (C₁₂), 129.0 (C₆), 128.2 (C₁₁), 127.5 (C₃), 124.1 (C₇), 123.6 (ArC), 122.5 (ArC), 21.3 (C₈).

FT-IR(thin film): $\nu_{\max}(\text{cm}^{-1}) = 1597, 1543, 1481, 1405, 1089, 1012, 908, 839, 790, 734, 687.$

(ESI): *m/z* calculated for C₁₅H₁₂O₂N³⁵Cl requires 271.0633 for [M+H]⁺, found 271.0633.

Scale-up procedure: To an oven-dried rbf was added 3-methylbenzoic acid (681 mg, 5.0 mmol, 1.0 eq), and NIITP (1.67 g, 5.5 mmol, 1.1 eq). The rbf was then evacuated and backfilled with nitrogen (x4) before the addition of anhydrous 1,4-dioxane (25 mL, 0.20 M). The rbf was put into an oil bath, preheated to 80 °C, and stirred for 3 h. After this time the reaction was cooled to rt and anhydrous 1,4-dioxane (15 mL, 0.14 M total), 1-chloro-4-iodobenzene (2.98 g, 12.5 mmol, 2.5 eq), 1,10-phenanthroline (360 mg, 2.0 mmol, 40 mol%), cesium carbonate (2.44 g, 7.5 mmol, 1.5 eq), copper(I) iodide (190 mg, 1.0 mmol, 20 mol%), and anhydrous 1,4-dioxane

(10 mL, 0.10 M total) were added sequentially. The rbf was then put into an oil bath preheated at 120 °C and stirred for 17 h. After this time, the reaction was cooled to rt and filtered through a silica plug, washing with EtOAc (200 mL), and then concentrated *in vacuo* to afford the crude product. The crude product was purified by FCC (25% → 35% Et₂O/pentane) to afford the *title compound* (1.01 g, 74%) as a beige powder.

2-(4-bromophenyl)-5-(*o*-tolyl)-1,3,4-oxadiazole – 186

Following **general procedure C** (using 2-methylbenzoic acid (27.2 mg, 0.20 mmol, 1.0 eq), and 1-bromo-4-iodobenzene (141 mg, 0.50 mmol, 2.5 eq)): after FCC (15% Et₂O/pentane), **186** (43.2 mg, 69%) was afforded as a white powder.

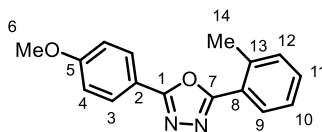
m.p.: 138 – 140 °C

¹H NMR (400 MHz, CDCl₃) δ 8.04 – 7.96 (m, 3H, C₃ & C₁₁), 7.70 – 7.64 (m, 2H, C₁₂), 7.46 – 7.40 (m, 1H, C₅), 7.39 – 7.31 (m, 2H, C₄ & C₆), 2.76 (s, 3H, C₈).

¹³C NMR (101 MHz, CDCl₃) δ 165.0 (ArC), 163.4 (ArC), 138.5 (ArC), 132.5 (C₁₂), 131.9 (ArCH), 131.4 (C₅), 129.0 (C₃), 128.3 (C₁₁), 126.4 (ArC), 126.2 (ArCH), 122.9 (ArC), 122.8 (ArC), 22.1 (C₈).

FT-IR(thin film): $\nu_{\max}(\text{cm}^{-1}) = 2980, 1600, 1538, 1452, 1097, 1068, 1009, 959, 730$.

(ESI): m/z calculated for C₁₅H₁₂ON₂⁷⁹Br requires 315.0128 for [M+H]⁺, found 315.0128.

2-(4-methoxyphenyl)-5-(*o*-tolyl)-1,3,4-oxadiazole – 187

Following **general procedure C** (using 4-methoxybenzoic acid (30.4 mg, 0.20 mmol, 1.0 eq), and 1-iodo-2-methylbenzene (64 μ L, 0.50 mmol, 2.5 eq)): after FCC (30% \rightarrow 50% Et₂O/pentane), **187** (43.8 mg, 82%) was afforded as a white powder.

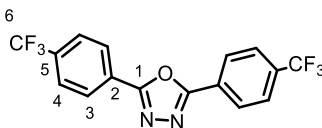
m.p.: 118 – 120 °C

¹H NMR (400 MHz, CDCl₃) δ 8.09 – 8.03 (m, 2H, C₃), 8.03 – 7.99 (m, 1H, C₉), 7.45 – 7.37 (m, 1H, C₁₀), 7.37 – 7.29 (m, 2H, C₉ & C₁₁), 7.06 – 6.98 (m, 2H, C₄), 3.87 (s, 3H, C₆), 2.75 (s, 3H, C₁₄).

¹³C NMR (101 MHz, CDCl₃) δ 164.4 (ArC), 164.1 (ArC), 162.3 (ArC), 138.3 (ArC), 131.8 (ArCH), 131.0 (C₁₀), 128.9 (C₉), 128.7 (C₃), 126.1 (ArCH), 123.2 (ArC), 116.5 (ArC), 114.5 (C₄), 55.5 (C₆), 22.1 (C₁₄).

FT-IR(thin film): $\nu_{\max}(\text{cm}^{-1}) = 1613, 1502, 1260, 1253, 1020, 844, 798, 723$.

(ESI): m/z calculated for C₁₆H₁₅O₂N₂ requires 267.1128 for [M+H]⁺, found 267.1126.

2,5-bis(4-(trifluoromethyl)phenyl)-1,3,4-oxadiazole – 188

Following **general procedure C** (using 4-(trifluoromethyl)benzoic acid (38.0 mg, 0.20 mmol, 1.0 eq), and 1-iodo-4-(trifluoromethyl)benzene (73 μ L, 0.50 mmol, 2.5 eq)): after FCC (12% Et₂O/pentane), **188** (45.9 mg, 64%) was afforded as a white powder.

m.p.: 150 °C (decomposition)

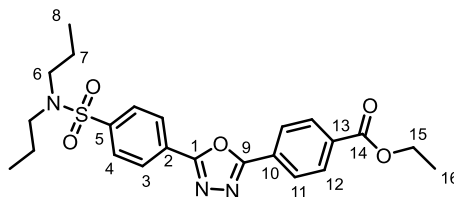
¹H NMR (400 MHz, CDCl₃) δ 8.27 (d, J = 8.1, 4H, C₃), 7.81 (d, J = 8.2, 4H, C₄).

¹⁹F NMR (376 MHz, CDCl₃) δ -63.2.

¹³C NMR (101 MHz, CDCl₃) δ 164.0 (C₁), 133.7 (q, J = 33.0, C₅), 127.4 (C₃), 126.8 (C₂), 126.2 (q, J = 3.7, C₄), 123.5 (q, J = 272.5, C₆).

FT-IR(thin film): $\nu_{\max}(\text{cm}^{-1})$ = 1324, 1317, 1169, 1137, 1105, 1083, 1063, 1015, 850, 755, 713, 667.

(ESI): m/z calculated for C₁₆H₉ON₂F₆ requires 359.0614 for [M+H]⁺, found 359.0611.

ethyl 4-(5-(4-(*N,N*-dipropylsulfamoyl)phenyl)-1,3,4-oxadiazol-2-yl)benzoate – 189

Following **general procedure C** (using probenecid (57.1 mg, 0.20 mmol, 1.0 eq), and ethyl 4-iodobenzoate (84 μ L, 0.50 mmol, 2.5 eq)): after FCC (20% \rightarrow 30% EtOAc/pentane), **189** (39.8 mg, 44%) was afforded as a yellow crystalline solid.

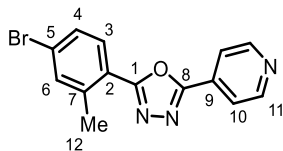
m.p.: 164 – 166 $^{\circ}$ C

^1H NMR (400 MHz, CDCl_3) δ 8.31 – 8.25 (m, 2H), 8.21 (s, 4H), 8.01 – 7.94 (m, 2H), 4.42 (q, $J = 7.1$, 2H, C_{15}), 3.18 – 3.08 (m, 4H, C_6), 1.56 (h, $J = 7.4$, 4H, C_7), 1.42 (t, $J = 7.1$, 3H, C_{16}), 0.87 (t, $J = 7.4$, 6H, C_8).

^{13}C NMR (101 MHz, CDCl_3) δ 165.5 (C_{14}), 164.5 (ArC), 163.8 (ArC), 143.5 (ArC), 133.6 (ArC), 130.3 (ArCH), 127.8 (ArCH), 127.6 (ArCH), 127.1 (ArC), 127.0 (ArCH), 61.6 (C_{15}), 49.9 (C_6), 21.9 (C_7), 14.3 (C_{16}), 11.2 (C_8).

FT-IR(thin film): $\nu_{\text{max}}(\text{cm}^{-1}) = 2969, 1718, 1341, 1273, 1158, 1074, 688, 612$.

(ESI): m/z calculated for $\text{C}_{23}\text{H}_{28}\text{O}_5\text{N}_3\text{S}$ requires 458.1744 for $[\text{M}+\text{H}]^+$, found 458.1742.

2-(4-bromo-2-methylphenyl)-5-(pyridin-4-yl)-1,3,4-oxadiazole – 190

Following **general procedure C** (using 4-bromo-2-methylbenzoic acid (42.6 mg, 0.20 mmol, 1.0 eq), and 4-iodopyridine (103 mg, 0.50 mmol, 2.5 eq)): after FCC (20% → 30% acetone/pentane), **190** (42.4 mg, 67%) was afforded as a white powder.

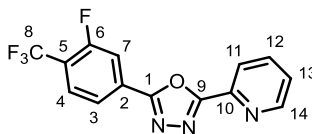
m.p.: 180 – 182 °C

¹H NMR (400 MHz, CDCl₃) δ 8.86 – 8.79 (m, 2H, C₁₀), 7.98 – 7.92 (m, 2H, C₁₁), 7.88 (d, *J* = 8.4, 1H, C₃), 7.56 – 7.53 (m, 1H, C₆), 7.49 (dd, *J* = 8.4, 1.9, 1H, C₄), 2.73 (s, 3H, C₁₂).

¹³C NMR (101 MHz, CDCl₃) δ 165.1 (ArC), 162.4 (ArC), 151.0 (C₁₀), 140.7 (ArC), 134.9 (C₆), 130.8 (ArC), 130.3 (C₃), 129.6 (C₄), 126.4 (ArC), 121.4 (ArC), 120.3 (C₁₁), 22.0 (C₁₂).

FT-IR(thin film): $\nu_{\max}(\text{cm}^{-1}) = 2980, 1596, 1539, 1478, 1413, 827, 743, 704$.

(ESI): *m/z* calculated for C₁₄H₁₁ON₂⁷⁹Br requires 316.0080 for [M+H]⁺, found 316.0081.

2-(3-fluoro-4-(trifluoromethyl)phenyl)-5-(pyridin-2-yl)-1,3,4-oxadiazole – 191

Following **general procedure C** (using 3-fluoro-4-(trifluoromethyl)benzoic acid (41.6 mg, 0.20 mmol, 1.0 eq), and 2-iodopyridine (53 μ L, 0.50 mmol, 2.5 eq)): after FCC (40% EtOAc/pentane), **191** (34.3 mg, 55%) was afforded as a beige powder.

m.p.: 156 – 158 $^{\circ}$ C

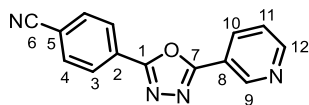
^1H NMR (400 MHz, CDCl_3) δ 8.82 (ddd, $J = 4.8, 1.7, 0.9$, 1H, C_{11}), 8.33 (dt, $J = 7.9, 1.0$, 1H, C_{14}), 8.11 (d, $J = 8.2$, 1H, C_3), 8.06 (d, $J = 10.5$, 1H, C_7), 7.92 (td, $J = 7.8, 1.7$, 1H, C_{13}), 7.78 (t, $J = 7.6$, 1H, C_4), 7.51 (ddd, $J = 7.7, 4.8, 1.2$, 1H, C_{12}).

^{19}F NMR (376 MHz, CDCl_3) δ -61.7 (d, $J = 12.8$, 3F, C_8), -112.0 – -112.1 (m, 1F, C_6).

^{13}C NMR (101 MHz, CDCl_3) δ 164.6 (ArC), 163.4 (d, $J = 3.1$, C_1), 159.9 (d, $J = 256.3$, C_6), 150.5 (C_{11}), 143.1 (ArC), 137.4 (C_{13}), 129.1 (d, $J = 9.0$, C_2), 128.3 (dd, $J = 4.7, 2.0$, C_4), 126.3 (C_{12}), 123.6 (C_{14}), 122.8 (d, $J = 4.0$, C_3), 122.0 (d, $J = 272.5$, C_8), 115.7 (d, $J = 23.8$, C_7).

FT-IR(thin film): $\nu_{\text{max}}(\text{cm}^{-1}) = 1556, 1444, 1324, 1127, 1046, 658, 741, 728$.

(ESI): m/z calculated for $\text{C}_{14}\text{H}_8\text{ON}_3\text{F}$ requires 310.0598 for $[\text{M}+\text{H}]^+$, found 310.0598.

4-(5-(pyridin-3-yl)-1,3,4-oxadiazol-2-yl)benzonitrile – 192

Following **general procedure C** (using 4-cyanobenzoic acid (29.4 mg, 0.20 mmol, 1.0 eq), and 3-iodopyridine (103 mg, 0.50 mmol, 2.5 eq)): after FCC (30% acetone/pentane), **192** (24.0 mg, 48%) was afforded as a beige powder.

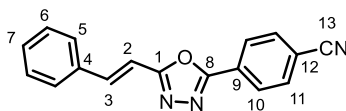
m.p.: 182 – 184 °C

^1H NMR (400 MHz, CDCl_3) δ 9.37 – 9.33 (m, 1H, C₉), 8.82 (dd, $J = 4.9, 1.6$, 1H, C₁₂), 8.44 (dt, $J = 8.0, 2.0$, 1H, C₁₀), 8.30 – 8.24 (m, 2H, C₃), 7.89 – 7.82 (m, 2H, C₄), 7.51 (ddd, $J = 8.0, 4.9, 0.8$, 1H, C₁₁).

^{13}C NMR (101 MHz, CDCl_3) δ 163.6 (ArC), 163.3 (ArC), 152.9 (C₁₂), 148.0 (C₉), 134.3 (C₁₀), 133.0 (C₄), 127.5 (C₃), 127.4 (ArC), 123.9 (C₁₁), 120.0 (ArC), 117.8 (ArC), 115.6 (ArC).

FT-IR(thin film): $\nu_{\text{max}}(\text{cm}^{-1}) = 2231, 1601, 1493, 1410, 1273, 852, 741, 718, 702$.

(ESI): m/z calculated for $\text{C}_{14}\text{H}_9\text{ON}_4$ requires 249.0771 for $[\text{M}+\text{H}]^+$, found 249.0770.

(E)-4-(5-styryl-1,3,4-oxadiazol-2-yl)benzonitrile – 193

Following **general procedure C** (using cinnamic acid (29.6 mg, 0.20 mmol, 1.0 eq), and 4-iodobenzonitrile (115 mg, 0.50 mmol, 2.5 eq)): after FCC (20% → 30% EtOAc/pentane), **193** (43.8 mg, 80%) was afforded as a beige powder.

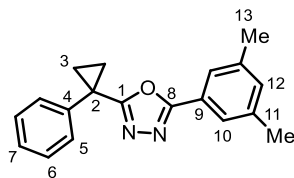
m.p.: 184 – 186 °C

^1H NMR (400 MHz, CDCl_3) δ 8.26 – 8.18 (m, 2H, C₁₀), 7.85 – 7.77 (m, 2H, C₁₁), 7.66 (d, J = 16.5, 1H, C₂), 7.60 – 7.54 (m, 2H, C₅), 7.47 – 7.37 (m, 3H, C₆ & C₇), 7.08 (d, J = 16.5, 1H, C₃).

^{13}C NMR (101 MHz, CDCl_3) δ 165.0 (ArC), 162.5 (ArC), 140.1 (C₂), 134.5 (ArC), 132.9 (C₁₁), 130.4 (C₇), 129.1 (C₆), 127.73 (ArC), 127.67 (C₅), 127.4 (C₁₀), 117.9 (ArC), 115.2 (ArC), 109.4 (C₃).

FT-IR(thin film): $\nu_{\text{max}}(\text{cm}^{-1})$ = 3062, 2228, 1642, 1520, 1490, 1087, 1015, 966, 842, 751, 694, 684.

(ESI): m/z calculated for C₁₇H₁₂ON₃ requires 274.0975 for [M+H]⁺, found 274.0975.

2-(3,5-dimethylphenyl)-5-(1-phenylcyclopropyl)-1,3,4-oxadiazole – 194

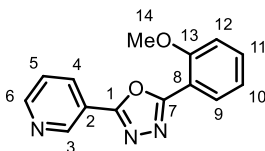
Following **general procedure C** (using 1-phenyl-1-cyclopropanecarboxylic acid (32.4 mg, 0.20 mmol, 1.0 eq), and 1-iodo-3,5-dimethylbenzene (72 μ L, 0.50 mmol, 2.5 eq)): after FCC (30% Et₂O/pentane), **194** (41.3 mg, 71%) was afforded as a yellow oil.

¹H NMR (400 MHz, CDCl₃) δ 7.59 – 7.55 (m, 2H, C₁₀), 7.50 – 7.44 (m, 2H, C₅), 7.38 (ddd, *J* = 7.5, 6.1, 1.3, 2H, C₆), 7.34 – 7.29 (m, 1H, C₇), 7.13 – 7.09 (m, 1H, C₁₂), 2.35 (s, 6H, C₁₃), 1.79 – 1.74 (m, 2H, C₃), 1.51 – 1.46 (m, 2H, C₃).

¹³C NMR (101 MHz, CDCl₃) δ 169.3 (ArC), 165.0 (ArC), 138.9 (ArC), 138.6 (C₁₁), 133.2 (C₁₂), 129.5 (C₅), 128.7 (C₆), 127.7 (C₇), 124.5 (C₁₀), 123.8 (ArC), 22.4 (C₂), 21.2 (C₁₃), 16.0 (C₃).

FT-IR(thin film): $\nu_{\max}(\text{cm}^{-1})$ = 2918, 1569, 1549, 1447, 1160, 1033, 1024, 857, 743, 698.

(ESI): *m/z* calculated for C₁₉H₁₉ON₂ requires 291.1492 for [M+H]⁺, found 291.1489.

2-(2-methoxyphenyl)-5-(pyridin-3-yl)-1,3,4-oxadiazole – 195

Following **general procedure C** (using nicotinic acid (24.6 mg, 0.20 mmol, 1.0 eq), and 1-iodo-2-methoxybenzene (65 μ L, 0.50 mmol, 2.5 eq)): after FCC (30% acetone/pentane) and PTLC (50% EtOAc/ CHCl_3), **195** (30.6 mg, 60%) was afforded as a white crystalline solid.

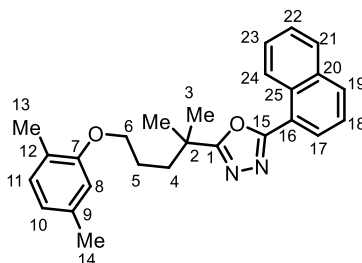
m.p.: 114 – 116 $^{\circ}\text{C}$

^1H NMR (400 MHz, CDCl_3) δ 9.34 (d, $J = 1.6$, 1H, C_3), 8.76 (dd, $J = 4.9$, 1.6, 1H, C_6), 8.42 (dt, $J = 8.0$, 1.9, 1H, C_4), 8.02 (dd, $J = 7.7$, 1.7, 1H, C_9), 7.53 (ddd, $J = 8.4$, 7.5, 1.8, 1H, C_{11}), 7.47 (ddd, $J = 8.0$, 4.9, 0.7, 1H, C_5), 7.13 – 7.04 (m, 2H, C_{10} & C_{12}), 3.99 (s, 3H, C_{14}).

^{13}C NMR (101 MHz, CDCl_3) δ 164.0 (ArC), 162.3 (ArC), 158.0 (ArC), 152.2 (C_6), 147.9 (C_3), 134.1 (C_4), 133.4 (C_{11}), 130.6 (C_9), 123.8 (C_5), 120.8 (C_{10}), 120.7 (ArC), 112.7 (ArC), 112.1 (C_{12}), 56.1 (C_{14}).

FT-IR(thin film): $\nu_{\text{max}}(\text{cm}^{-1}) = 2971, 1604, 1588, 1496, 1475, 1287, 1264, 1022, 749, 721, 704$.

(ESI): m/z calculated for $\text{C}_{14}\text{H}_{12}\text{O}_2\text{N}_3$ requires 254.0924 for $[\text{M}+\text{H}]^+$, found 254.0924.

2-(5-(2,5-dimethylphenoxy)-2-methylpentan-2-yl)-5-(naphthalen-1-yl)-1,3,4-oxadiazole –**196**

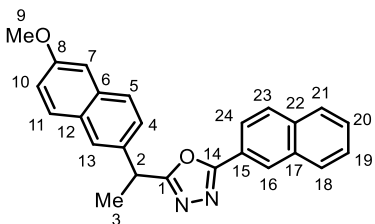
Following **general procedure C** (using 5-(2,5-dimethylphenoxy)-2,2-dimethylpentanoic acid (gemfibrozil) (50.1 mg, 0.20 mmol, 1.0 eq), and 1-iodonaphthalene (73 μ L, 0.50 mmol, 2.5 eq)): after FCC (20% Et₂O/pentane), **196** (63.0 mg, 79%) was afforded as a yellow oil.

¹H NMR (400 MHz, CDCl₃) δ 9.24 (d, J = 8.7, 1H, C₁₇), 8.15 (dd, J = 7.3, 1.2, 1H, C₂₄), 8.03 (d, J = 8.2, 1H, C₂₁), 7.94 (d, J = 8.1, 1H, C₁₉), 7.69 (ddd, J = 8.5, 6.9, 1.4, 1H, C₁₈), 7.64 – 7.53 (m, 2H, C₂₂ & C₂₃), 6.98 (d, J = 7.5, 1H, C₁₁), 6.63 (d, J = 7.5, 1H, C₁₀), 6.60 (s, 1H, C₈), 3.96 (t, J = 6.1, 2H, C₆), 2.28 (s, 3H), 2.17 (s, 3H), 2.10 – 2.02 (m, 2H, C₄), 1.91 – 1.81 (m, 2H, C₅), 1.60 (s, 6H, C₃).

¹³C NMR (101 MHz, CDCl₃) δ 171.9 (ArC), 164.8 (ArC), 156.9 (ArC), 136.5 (ArC), 133.9 (ArC), 132.4 (C₂₁), 130.3 (C₁₁), 130.1 (ArC), 128.7 (C₁₉), 128.2 (C₂₄), 128.1 (C₁₈), 126.7 (ArCH), 126.3 (C₁₇), 124.8 (ArCH), 123.5 (ArC), 120.8 (C₁₀), 111.9 (C₈), 67.6 (C₆), 38.1 (C₄), 35.8 (C₂), 26.3 (C₃), 25.0 (C₅), 21.4 (ArCH₃), 15.8 (ArCH₃).

FT-IR(thin film): ν_{\max} (cm⁻¹) = 2972, 1537, 1509, 1264, 1157, 1126, 1047, 805, 775.

(ESI): m/z calculated for C₂₆H₂₉O₂N₂ requires 401.2224 for [M+H]⁺, found 401.2235.

2-(1-(6-methoxynaphthalen-2-yl)ethyl)-5-(naphthalen-2-yl)-1,3,4-oxadiazole – 197

Following **general procedure C** (using 2-(6-methoxy-2-naphthyl)propionic acid (naproxen) (46.1 mg, 0.20 mmol, 1.0 eq), and 2-iodonaphthalene (127 mg, 0.50 mmol, 2.5 eq)): after FCC (25% EtOAc/pentane), **197** (52.5 mg, 69%) was afforded as a beige crystalline solid.

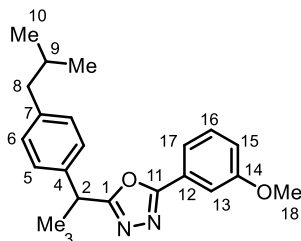
m.p.: 58 – 60 °C

^1H NMR (400 MHz, CDCl_3) δ 8.46 – 8.44 (m, 1H, C₁₆), 8.08 (dd, J = 8.6, 1.7, 1H, C₂₄), 7.89 (dd, J = 9.1, 2.5, 2H), 7.86 – 7.81 (m, 1H), 7.78 – 7.72 (m, 3H), 7.59 – 7.45 (m, 3H), 7.20 – 7.11 (m, 2H), 4.61 (q, J = 7.2, 1H, C₂), 3.91 (s, 3H, C₉), 1.94 (d, J = 7.2, 3H, C₃).

^{13}C NMR (101 MHz, CDCl_3) δ 169.0 (ArC), 165.3 (ArC), 157.9 (ArC), 135.5 (ArC), 134.6 (ArC), 133.9 (ArC), 132.8 (ArC), 129.3 (ArCH), 129.0 (ArC), 128.9 (ArCH), 128.8 (ArCH), 127.93 (ArCH), 127.86 (ArCH), 127.6 (ArCH), 127.2 (C₁₆), 127.0 (ArCH), 125.92 (ArCH), 125.89 (ArCH), 123.2 (C₂₄), 121.3 (ArC), 119.3 (ArCH), 105.7 (ArCH), 55.3 (C₉), 37.6 (C₂), 19.7 (C₃).

FT-IR(thin film): $\nu_{\text{max}}(\text{cm}^{-1})$ = 2980, 1606, 1485, 1392, 1267, 1231, 1217, 1174, 1063, 1031, 907, 730.

(ESI): m/z calculated for $\text{C}_{25}\text{H}_{21}\text{O}_2\text{N}_2$ requires 381.1598 for $[\text{M}+\text{H}]^+$, found 381.1600.

2-(1-(4-isobutylphenyl)ethyl)-5-(3-methoxyphenyl)-1,3,4-oxadiazole – 198

Following **general procedure C** (using ibuprofen (41.3 mg, 0.20 mmol, 1.0 eq), and 1-iodo-3-methoxybenzene (60 μ L, 0.50 mmol, 2.5 eq)): after FCC (35% Et₂O/pentane), **198** (40.1 mg, 60%) was afforded as a yellow oil.

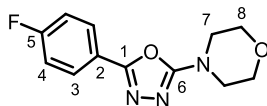
¹H NMR (400 MHz, CDCl₃) δ 7.60 – 7.53 (m, 2H, C₁₃ & C₁₇), 7.37 (t, J = 8.0, 1H, C₁₅), 7.29 – 7.23 (m, 2H, C₅), 7.13 (d, J = 8.2, 2H, C₆), 7.05 (ddd, J = 8.3, 2.6, 0.9, 1H, C₁₆), 4.42 (q, J = 7.2, 1H, C₂), 3.87 (s, 3H, C₁₈), 2.46 (d, J = 7.2, 2H, C₈), 1.87 (dt, J = 13.5, 6.7, 1H, C₉), 1.82 (d, J = 7.3, 3H, C₃), 0.90 (d, J = 6.6, 6H, C₁₀).

¹³C NMR (101 MHz, CDCl₃) δ 169.0 (ArC), 164.9 (ArC), 159.9 (ArC), 141.0 (ArC), 137.6 (ArC), 130.1 (C₁₅), 129.6 (C₆), 127.0 (C₅), 125.2 (ArC), 119.3 (C₁₇), 117.9 (C₁₆), 111.6 (C₁₃), 55.5 (C₁₈), 45.0 (C₈), 37.2 (C₂), 30.2 (C₉), 22.4 (C₁₀), 19.7 (C₃).

FT-IR(thin film): $\nu_{\max}(\text{cm}^{-1})$ = 2953, 2868, 1566, 1550, 1466, 1242, 1043, 852, 727, 686.

(ESI): m/z calculated for C₂₁H₂₅O₂N₂ requires 337.1911 for [M+H]⁺, found 337.1909.

5.4.5 Synthesis of 2-Amino-5-substituted 1,3,4-Oxadiazole Products

2-(4-fluorophenyl)-5-(piperidin-1-yl)-1,3,4-oxadiazole – 207

Following **general procedure D** (using 4-fluorobenzoic acid (28.0 mg, 0.20 mmol, 1.2 eq), and **206** (34.6 mg, 0.167 mmol, 1.0 eq)): after FCC (25% acetone/pentane) and PTLC (75% EtOAc/Hexane), **207** (26.7 mg, 64%) was afforded as a white powder.

m.p.: 136 – 138 °C

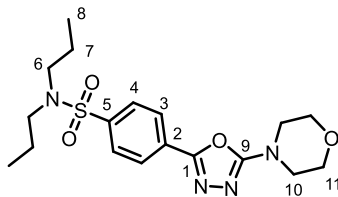
^1H NMR (400 MHz, CDCl_3) δ 7.94 – 7.86 (m, 2H, C₃), 7.18 – 7.10 (m, 2H, C₄), 3.87 – 3.81 (m, 4H, C₈), 3.59 (dd, $J = 5.6, 4.2$, 4H, C₇).

^{19}F NMR (377 MHz, CDCl_3) δ -108.5

^{13}C NMR (101 MHz, CDCl_3) δ 164.1 (d, $J = 251.7$, C₅), 164.1 (ArC), 158.8 (ArC), 128.0 (d, $J = 8.6$, C₃), 120.8 (d, $J = 3.4$, C₂), 116.2 (d, $J = 22.3$, C₄), 65.9 (C₈), 46.3 (C₇).

FT-IR(thin film): $\nu_{\text{max}}(\text{cm}^{-1}) = 2865, 1618, 1608, 1502, 1274, 1121, 912, 816, 732, 617$.

(ESI): m/z calculated for $\text{C}_{12}\text{H}_{13}\text{O}_2\text{N}_3\text{F}$ requires 250.0986 for $[\text{M}+\text{H}]^+$, found 250.0987.

4-(5-morpholino-1,3,4-oxadiazol-2-yl)-*N,N*-dipropylbenzenesulfonamide – 208

Following **general procedure D** (using probenecid (57.1 mg, 0.20 mmol, 1.2 eq), and **206** (34.6 mg, 0.167 mmol, 1.0 eq)): after FCC (30% MeCN/CH₂Cl₂), **208** (29.0 mg, 44%) was afforded as a white powder.

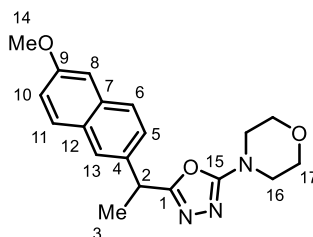
m.p.: 108 – 110 °C.

¹H NMR (400 MHz, CDCl₃) δ 8.02 (d, *J* = 8.7, 2H, C₃), 7.87 (d, *J* = 8.7, 2H, C₄), 3.87 – 3.80 (m, 4H, C₁₁), 3.64 – 3.57 (m, 4H, C₁₀), 3.14 – 3.04 (m, 4H, C₆), 1.54 (h, *J* = 7.4, 4H, C₇), 0.86 (t, *J* = 7.4, 6H, C₈).

¹³C NMR (101 MHz, CDCl₃) δ 164.3 (ArC), 158.3 (ArC), 142.0 (ArC), 127.8 (ArC), 127.6 (C₄), 126.1 (C₃), 65.9 (C₁₁), 49.9 (C₆), 46.2 (C₁₀), 21.9 (C₇), 11.2 (C₈).

FT-IR(thin film): $\nu_{\max}(\text{cm}^{-1}) = 2967, 1613, 1339, 1274, 1156, 1117, 913, 754, 729.$

(ESI): *m/z* calculated for C₁₈H₂₇O₄N₄S requires 395.1748 for [M+H]⁺, found 395.1745.

4-(5-(1-(6-methoxynaphthalen-2-yl)ethyl)-1,3,4-oxadiazol-2-yl)morpholine – 209

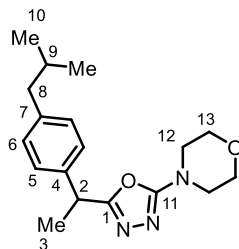
Following **general procedure D** (using naproxen (41.6 mg, 0.20 mmol, 1.2 eq), and **206** (34.6 mg, 0.167 mmol, 1.0 eq)): after FCC (40% acetone/pentane) and PTLC (70% EtOAc/CHCl₃), **209** (27.9 mg, 49%) was afforded as a colourless oil.

¹H NMR (400 MHz, CDCl₃) δ 7.70 (dd, *J* = 8.7, 3.1, 2H), 7.64 (s, 1H, C₁₃), 7.37 (dd, *J* = 8.5, 1.8, 1H), 7.15 (dd, *J* = 8.9, 2.5, 1H), 7.11 (d, *J* = 2.4, 1H, C₈), 4.32 (q, *J* = 7.2, 1H, C₂), 3.91 (s, 3H, C₃), 3.77 – 3.68 (m, 4H, C₁₇), 3.46 – 3.36 (m, 4H, C₁₆), 1.77 (d, *J* = 7.2, 3H, C₃).

¹³C NMR (101 MHz, CDCl₃) δ 164.5 (ArC), 163.5 (ArC), 157.8 (ArC), 135.8 (ArC), 133.8 (ArC), 129.3 (ArCH), 128.9 (ArC), 127.4 (ArCH), 125.9 (ArCH), 125.7 (C₁₃), 119.2 (ArCH), 105.7 (C₈), 65.9 (C₁₇), 55.3 (C₁₄), 46.1 (C₁₆), 37.5 (C₂), 19.4 (C₃).

FT-IR(thin film): $\nu_{\max}(\text{cm}^{-1}) = 2974, 2858, 1620, 1568, 1452, 1266, 1216, 1118, 1029, 912, 853$.

(ESI): *m/z* calculated for C₁₉H₂₂O₃N₃ requires 340.1656 for [M+H]⁺, found 340.1653.

4-(5-(1-(4-isobutylphenyl)ethyl)-1,3,4-oxadiazol-2-yl)morpholine – 210

Following **general procedure D** (using ibuprofen (41.3 mg, 0.20 mmol, 1.2 eq), and **206** (34.6 mg, 0.167 mmol, 1.0 eq)): after FCC (20% MeCN/CH₂Cl₂ → 10% MeOH/CH₂Cl₂) and PTLC (33% acetone/PhMe), **210** (24.4 mg, 46%) was afforded as a yellow oil.

¹H NMR (400 MHz, CDCl₃) δ 7.18 (d, *J* = 8.1, 2H, C₅), 7.10 (d, *J* = 8.1, 2H, C₄), 4.17 (q, *J* = 7.2, 1H, C₂), 3.79 – 3.71 (m, 4H, C₁₃), 3.46 – 3.39 (m, 4H, C₁₂), 2.44 (d, *J* = 7.2, 2H, C₈), 1.90 – 1.78 (m, 1H, C₉), 1.68 (d, *J* = 7.3, 3H, C₃), 0.89 (d, *J* = 6.6, 6H, C₁₀).

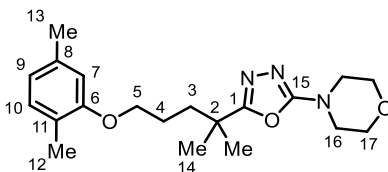
¹³C NMR (101 MHz, CDCl₃) δ 164.4 (ArC), 163.5 (ArC), 140.8 (ArC), 137.9 (ArC), 129.5 (C₅), 126.9 (C₆), 65.9 (C₁₃), 46.1 (C₁₂), 45.0 (C₈), 37.1 (C₂), 30.2 (C₉), 22.4 (C₁₀), 19.5 (C₃).

FT-IR(thin film): $\nu_{\max}(\text{cm}^{-1}) = 2957, 2865, 1620, 1569, 1453, 1274, 1118, 913$.

(ESI): *m/z* calculated for C₁₈H₂₆O₂N₃ requires 316.2020 for [M+H]⁺, found 316.2018.

4-(5-(5-(2,5-dimethylphenoxy)-2-methylpentan-2-yl)-1,3,4-oxadiazol-2-yl)morpholine –

211



Following **general procedure D** (using gemfibrozil (50.1 mg, 0.20 mmol, 1.2 eq), and **206** (34.6 mg, 0.167 mmol, 1.0 eq)): after FCC (25% acetone/pentane) and FCC (75% EtOAc/pentane), **211** (31.8 mg, 53%) was afforded as a colourless oil.

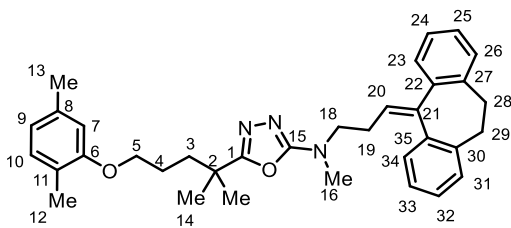
^1H NMR (400 MHz, CDCl_3) δ 6.99 (d, $J = 7.5$, 1H, C_{10}), 6.65 (d, $J = 7.5$, 1H, C_9), 6.58 (s, 1H, C_7), 3.90 (t, $J = 5.9$, 2H, C_5), 3.82 – 3.74 (m, 4H, C_{17}), 3.49 – 3.40 (m, 4H, C_{16}), 2.30 (s, 3H), 2.16 (s, 3H), 1.84 (qd, $J = 6.3$, 2.7, 2H, C_3), 1.80 – 1.70 (m, 2H, C_4), 1.39 (s, 6H, C_{14}).

^{13}C NMR (101 MHz, CDCl_3) δ 166.8 (ArC), 164.3 (ArC), 156.9 (ArC), 136.5 (ArC), 130.3 (C_{10}), 123.4 (ArC), 120.8 (C_9), 111.9 (C_7), 67.6 (C_5), 65.9 (C_{17}), 46.2 (C_{16}), 37.6 (C_3), 35.5 (C_2), 25.9 (C_{14}), 24.9 (C_4), 21.4 (Ar CH_3), 15.8 (Ar CH_3).

FT-IR(thin film): $\nu_{\text{max}}(\text{cm}^{-1}) = 2970, 2921, 1615, 1565, 1509, 1453, 1263, 1157, 1119, 1046, 912$.

(ESI): m/z calculated for $\text{C}_{20}\text{H}_{30}\text{O}_3\text{N}_3$ requires 360.2282 for $[\text{M}+\text{H}]^+$, found 360.2278.

***N*-(3-(10,11-dihydro-5*H*-dibenzo[*a,d*][7]annulen-5-ylidene)propyl)-5-(5-(2,5-dimethylphenoxy)-2-methylpentan-2-yl)-*N*-methyl-1,3,4-oxadiazol-2-amine – 212**



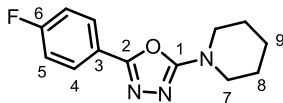
Following **general procedure D** (using gemfibrozil (50.1 mg, 0.20 mmol, 1.2 eq), and **213** (64.0 mg, 0.167 mmol, 1.0 eq)): after FCC (30% → 60% EtOAc/pentane), **212** (62.3 mg, 70%) was afforded as a yellow oil.

^1H NMR (400 MHz, CDCl_3) δ 7.27 – 7.06 (m, 7H), 7.04 – 6.96 (m, 2H), 6.66 (d, $J = 7.5$, 1H, C₉), 6.58 (s, 1H, C₇), 5.83 (t, $J = 7.5$, 1H, C₂₀), 3.83 (t, $J = 5.9$, 2H, C₅), 3.55 – 3.18 (m, 4H), 3.00 – 2.86 (m, 1H), 2.90 (s, 3H, C₁₆), 2.82 – 2.68 (m, 1H), 2.53 – 2.35 (m, 2H), 2.31 (s, 3H), 2.17 (s, 3H), 1.83 – 1.75 (m, 2H, C₃), 1.74 – 1.65 (m, 2H, C₄), 1.31 (s, 6H, C₁₄).

^{13}C NMR (151 MHz, CDCl_3) δ 165.9 (ArC), 164.4 (ArC), 157.0 (ArC), 145.4 (ArC), 140.9 (ArC), 139.7 (ArC), 139.4 (ArC), 137.1 (ArC), 136.5 (ArC), 130.3 (ArCH), 130.1 (ArCH), 128.5 (ArCH), 128.2 (ArCH), 128.0 (ArCH), 127.7 (ArCH), 127.3 (ArCH), 127.1 (ArCH), 126.1 (ArCH), 125.8 (ArCH), 123.5 (ArC), 120.7 (C₉), 111.9 (C₇), 67.7 (C₅), 50.6 (CH₂), 37.6 (C₃), 35.7 (C₁₆), 35.4 (C₂), 33.7 (CH₂), 32.0 (CH₂), 27.6 (CH₂), 25.9 (C₁₄), 24.9 (C₄), 21.5 (ArCH₃), 15.8 (ArCH₃).

FT-IR(thin film): $\nu_{\text{max}}(\text{cm}^{-1}) = 2973, 1633, 1572, 1508, 1265, 1128, 1042, 909, 730$.

(ESI): m/z calculated for $\text{C}_{35}\text{H}_{42}\text{O}_2\text{N}_3$ requires 536.3272 for $[\text{M}+\text{H}]^+$, found 536.3264.

2-(4-fluorophenyl)-5-(piperidin-1-yl)-1,3,4-oxadiazole – 216

To an oven-dried vial was added 4-fluorobenzoic acid (28.0 mg, 0.2 mmol, 1.0 eq) and NIITP (66.5 mg, 0.22 mmol, 1.1 eq), and anhydrous 1,4-dioxane (750 μ L, 0.30 M). The vial was then capped and stirred at 80 $^{\circ}$ C for 3 h. The vial was cooled to rt and piperidine (60 μ L, 0.60 mmol, 3.0 eq) and dibenzenesulfonamide (11.9 mg, 0.04 mmol, 20 mol%) added; then the vial recapped and stirred at 110 $^{\circ}$ C for 16 h. After this time the vial was cooled to rt, and the volatile reaction components, and solvent, removed using a stream of nitrogen. The residue was uptaken into anhydrous MeCN (1.0 mL, 0.20 M) and 2,2,6,6-tetramethylpiperidine (135 μ L, 0.80 mmol, 4.0 eq) added. A solution of TEMPO $^{+}$ BF $_4^{-}$ (195 mg, 0.80 mmol, 4.0 eq) in anhydrous MeCN (1.0 mL, 0.10 M total) was then added dropwise, and after complete addition the reaction was stirred at rt for 30 mins. After this time saturated aqueous NaHCO $_3$ (20 mL) was added, and the layers separated. The aqueous layer was extracted with CH $_2$ Cl $_2$ (3 x 10 mL), and subsequent the combined organics were dried (MgSO $_4$), filtered, and concentrated *in vacuo* to afford the crude product. The crude was purified by FCC (40% EtOAc/pentane) to afford the *title compound* (21.5 mg, 51%) as a white powder.

m.p.: 142 – 144 $^{\circ}$ C

1 H NMR (400 MHz, CDCl $_3$) δ 7.93 – 7.85 (m, 2H, C $_4$), 7.17 – 7.07 (m, 2H, C $_5$), 3.60 – 3.49 (m, 4H, C $_7$), 1.74 – 1.61 (m, 6H, C $_8$ & C $_9$).

19 F NMR (377 MHz, CDCl $_3$) δ -109.3.

13 C NMR (101 MHz, CDCl $_3$) δ 164.4 (ArC), 163.9 (d, J = 251.0, C $_6$), 158.2 (ArC), 127.8 (d, J = 8.6, C $_4$), 121.2 (d, J = 3.6, C $_3$), 116.1 (d, J = 22.3, C $_5$), 47.2 (C $_7$), 24.9 (C $_8$), 23.8 (C $_9$).

FT-IR(thin film): $\nu_{\max}(\text{cm}^{-1}) = 2939, 2857, 1618, 1607, 1502, 1264, 1160, 906, 857$.

(ESI): m/z calculated for $\text{C}_{13}\text{H}_{15}\text{ON}_3\text{F}$ requires 248.1194 for $[\text{M}+\text{H}]^+$, found 248.1193.

Chapter 6: References

1. N. A. Meanwell, *J. Med. Chem.*, 2011, **54**, 2529-2591.
2. K. Goldberg, S. Groombridge, J. Hudson, A. G. Leach, P. A. MacFaul, A. Pickup, R. Poultney, J. S. Scott, P. H. Svensson and J. Sweeney, *MedChemComm*, 2012, **3**, 600-604.
3. K. E. Andersen, B. F. Lundt, A. S. Jørgensen and C. Braestrup, *Eur. J. Med. Chem.*, 1996, **31**, 417-425.
4. K. Andersen, A. Jørgensen and C. Bræstrup, *Eur. J. Med. Chem.*, 1994, **29**, 393-399.
5. G. D. Diana, D. L. Volkots, T. J. Nitz, T. R. Bailey, M. A. Long, N. Vescio, S. Aldous, D. C. Pevear and F. J. Dutko, *J. Med. Chem.*, 1994, **37**, 2421-2436.
6. M. T. Nguyen, A. F. Hegarty and J. Elguero, *Angew. Chem. Int. Ed.*, 1985, **24**, 713-715.
7. H. Khalilullah, M. J. Ahsan, M. Hedaitullah, S. Khan and B. Ahmed, *Mini-Rev. Med. Chem.*, 2012, **12**, 789-801.
8. A. K. Mishra, A. Kumar and J. K. Sahu, *Lett. Org. Chem.*, 2020, **17**, 409.
9. J. Boström, A. Hogner, A. Llinàs, E. Wellner and A. T. Plowright, *J. Med. Chem.*, 2012, **55**, 1817-1830.
10. D. A. Price, J. Blagg, L. Jones, N. Greene and T. Wager, *Expert Opin. Drug Metab. Toxicol.*, 2009, **5**, 921-931.
11. F. Omar, N. Mahfouz and M. Rahman, *Eur. J. Med. Chem.*, 1996, **31**, 819-825.
12. D. H. Boschelli, D. T. Connor, D. A. Bornemeier, R. D. Dyer, J. A. Kennedy, P. J. Kuipers, G. C. Okonkwo, D. J. Schrier and C. D. Wright, *J. Med. Chem.*, 1993, **36**, 1802-1810.
13. M. Akhter, A. Husain, B. Azad and M. Ajmal, *Eur. J. Med. Chem.*, 2009, **44**, 2372-2378.

14. B. Narayana, B. V. Ashalatha, K. K. Vijay, R. J. Fernandes and B. K. Sarojini, *Biorg. Med. Chem.*, 2005, **13**, 4638-4644.
15. A. A. Kadi, N. R. El-Brollosy, O. A. Al-Deeb, E. E. Habib, T. M. Ibrahim and A. A. El-Emam, *Eur. J. Med. Chem.*, 2007, **42**, 235-242.
16. S. Bajaj, P. P. Roy and J. Singh, *Anticancer Agents Med. Chem.*, 2017, **17**.
17. A. Vaidya, D. Pathak and K. Shah, *Chem. Biol. Drug Des.*, 2020, **97**, 572-591.
18. A. H. Abadi, A. A. H. Eissa and G. S. Hassan, *Chem. Pharm. Bull.*, 2003, **51**, 838-844.
19. Q.-Z. Zheng, X.-M. Zhang, Y. Xu, K. Cheng, Q.-C. Jiao and H.-L. Zhu, *Biorg. Med. Chem.*, 2010, **18**, 7836-7841.
20. X.-M. Zhang, M. Qiu, J. Sun, Y.-B. Zhang, Y.-S. Yang, X.-L. Wang, J.-F. Tang and H.-L. Zhu, *Biorg. Med. Chem.*, 2011, **19**, 6518-6524.
21. A. S. Aboraia, H. M. Abdel-Rahman, N. M. Mahfouz and M. A. El-Gendy, *Biorg. Med. Chem.*, 2006, **14**, 1236-1246.
22. X. Ouyang, E. L. Piatnitski, V. Pattaropong, X. Chen, H.-Y. He, A. S. Kiselyov, A. Velankar, J. Kawakami, M. Labelle, L. S. II, J. Lohman, S. P. Lee, A. Malikzay, J. Fleming, J. Gerlak, Y. Wang, R. L. Rosler, K. Zhou, S. Mitelman, M. Camara, D. Surguladze, J. F. Doody and M. C. Tuma, *Bioorg. Med. Chem. Lett.*, 2006, **16**, 1191-1196.
23. N. C. Desai, N. Bhatt, H. Somani and A. Trivedi, *Eur. J. Med. Chem.*, 2013, **67**, 54-59.
24. A. Kocabalkanli, Ö. Ateş and G. Ötükçü, *Il Farmaco*, 2001, **56**, 975-979.
25. Salahuddin, A. Mazumder and M. Shaharyar, *Med. Chem. Res.*, 2015, **24**, 2514-2528.
26. A. Rauf, S. Sharma and S. Gangal, *Chin. Chem. Lett.*, 2008, **19**, 5-8.

27. Salahuddin, A. Mazumder, M. S. Yar, R. Mazumder, G. S. Chakraborty, M. J. Ahsan and M. U. Rahman, *Synth. Commun.*, 2017, **47**, 1805-1847.
28. S. Bala, S. Kamboj and A. Kumar, *J. Pharm. Res.*, 2010, **3**, 2993-2997.
29. A. Siwach and P. K. Verma, *BMC Chemistry*, 2020, **14**, 1-40.
30. R. R. Somani and O. Y. Shirodkar, *Der Pharma Chemica*, 2009, **1**, 130-140.
31. Z. Li, P. Zhan and X. Liu, *Mini-Rev. Med. Chem.*, 2011, **11**, 1130-1142.
32. C. S. de Oliveira, B. F. Lira, J. M. Barbosa-Filho, J. G. F. Lorenzo and P. F. de Athayde-Filho, *Molecules*, 2012, **17**, 10192-10231.
33. J. Sun, J. Makawana and H.-L. Zhu, *Mini-Rev. Med. Chem.*, 2013, **13**, 1725-1743.
34. S. Bajaj, P. P. Roy and J. Singh, *Anticancer Agents Med. Chem.*, 2018, **17**, 1869-1883.
35. G. Verma, M. F. Khan, W. Akhtar, M. M. Alam, M. Akhter and M. Shaquiquzzaman, *Mini-Rev. Med. Chem.*, 2019, **19**, 477-509.
36. C. Knox, V. Law, T. Jewison, P. Liu, S. Ly, A. Frolkis, A. Pon, K. Banco, C. Mak, V. Neveu, Y. Djoumbou, R. Eisner, A. C. Guo and D. S. Wishart, *Nucleic Acids Res.*, 2011, **39**, D1035-D1041.
37. V. Law, C. Knox, Y. Djoumbou, T. Jewison, A. C. Guo, Y. Liu, A. Maciejewski, D. Arndt, M. Wilson, V. Neveu, A. Tang, G. Gabriel, C. Ly, S. Adamjee, Z. T. Dame, B. Han, Y. Zhou and D. S. Wishart, *Nucleic Acids Res.*, 2014, **42**, D1091-D1097.
38. D. S. Wishart, Y. D. Feunang, A. C. Guo, E. J. Lo, A. Marcu, J. R. Grant, T. Sajed, D. Johnson, C. Li, Z. Sayeeda, N. Assempour, I. Iynkkaran, Y. Liu, A. Maciejewski, N. Gale, A. Wilson, L. Chin, R. Cummings, D. Le, A. Pon, C. Knox and M. Wilson, *Nucleic Acids Res.*, 2018, **46**, D1074-D1082.

39. D. S. Wishart, C. Knox, A. C. Guo, S. Shrivastava, M. Hassanali, P. Stothard, Z. Chang and J. Woolsey, *Nucleic Acids Res.*, 2006, **34**, D668-D672.
40. D. S. Wishart, C. Knox, A. C. Guo, D. Cheng, S. Shrivastava, D. Tzur, B. Gautam and M. Hassanali, *Nucleic Acids Res.*, 2008, **36**, D901-D906.
41. N. A. McGrath, M. Brichacek and J. T. Njardarson, *J. Chem. Educ.*, 2010, **87**, 1348-1349.
42. E. Ko, J. Liu, L. M. Perez, G. Lu, A. Schaefer and K. Burgess, *J. Am. Chem. Soc.*, 2011, **133**, 462-477.
43. S. Borg, G. Estenne-Bouhtou, K. Luthman, I. Csoeregh, W. Hesselink and U. Hacksell, *J. Org. Chem.*, 1995, **60**, 3112-3120.
44. S. D. Appavoo, T. Kaji, J. R. Frost, C. C. G. Scully and A. K. Yudin, *J. Am. Chem. Soc.*, 2018, **140**, 8763-8770.
45. J. R. Frost, C. C. G. Scully and A. K. Yudin, *Nat. Chem.*, 2016, **8**, 1105-1111.
46. R. Stollé, *Journal für Praktische Chemie*, 1904, **69**, 145-160.
47. F. N. Hayes, B. S. Rogers and D. G. Ott, *J. Am. Chem. Soc.*, 1955, **77**, 1850-1852.
48. E. Baltazzi and A. J. Wysocki, *Chem. Ind.*, 1963, 1080-1081.
49. J. C. Thurman, *Chem. Ind.*, 1964, 752.
50. J. K. Augustine, V. Vairaperumal, S. Narasimhan, P. Alagarsamy and A. Radhakrishnan, *Tetrahedron*, 2009, **65**, 9989-9996.
51. G. Nagendra, R. S. Lamani, N. Narendra and V. V. Sureshbabu, *Tetrahedron Lett.*, 2010, **51**, 6338-6341.

52. P. Stabile, A. Lamonica, A. Ribecai, D. Castoldi, G. Guercio and O. Curcuruto, *Tetrahedron Lett.*, 2010, **51**, 4801-4805.
53. B. Rigo, P. Cauliez, D. Fasseur and D. Couturier, *Synth. Commun.*, 1986, **16**, 1665-1669.
54. C. I. Chiriac, *Rev. Roum. Chim.*, 1986, **31**, 159-162.
55. C. I. Chiriac, *Rev. Roum. Chim.*, 1986, **31**, 51-55.
56. C. I. Chiriac, *Rev. Roum. Chim.*, 1987, **32**, 223-226.
57. B. Rigo, P. Cauliez, D. Fasseur and D. Couturier, *Synth. Commun.*, 1988, **18**, 1247-1251.
58. C. T. Brain, J. M. Paul, Y. Loong and P. J. Oakley, *Tetrahedron Lett.*, 1999, **40**, 3275-3278.
59. S. Lutun, B. Hasiak and D. Couturier, *Synth. Commun.*, 1999, **29**, 111-116.
60. S. Liras, M. P. Allen and B. E. Segelstein, *Synth. Commun.*, 2000, **30**, 437-443.
61. C. T. Brain and S. A. Brunton, *Synlett*, 2001, **2001**, 382-384.
62. X. Min and C. Qiong, *Huaxue Tongbao*, 2002, **65**, 554-556.
63. C. A. James, B. Poirier, C. Grisé, A. Martel and E. H. Ruediger, *Tetrahedron Lett.*, 2006, **47**, 511-514.
64. Y. Wang, D. R. Sauer and S. W. Djuric, *Tetrahedron Lett.*, 2006, **47**, 105-108.
65. Z. Li, A. Zhu, X. Mao, X. Sun and X. Gong, *J. Braz. Chem. Soc.*, 2008, **19**, 1622-1626.
66. D. Ellis, P. S. Johnson, A. Nortcliffe and S. Wheeler, *Synth. Commun.*, 2010, **40**, 3021-3026.

67. H. Lei-Lei and C. Lian-Qing, *Guangzhou Huagong*, 2012, **40**, 129-131.
68. M.-F. Pouliot, L. Angers, J.-D. Hamela and J.-F. Paquin, *Org. Biomol. Chem.*, 2012, **10**, 988-993.
69. T. L. Andersen, W. Caneschi, A. Ayoub, A. T. Lindhardt, M. R. C. Couri and T. Skrydstrup, *Adv. Synth. Catal.*, 2014, **356**, 3074-3082.
70. M. Zarei and F. Rasooli, *Org. Prep. Proced. Int.*, 2017, **49**, 355-362.
71. M. J. Goldfogel, C. R. Jamison, S. A. Savage, M. W. Haley, S. Mukherjee, C. Sfougataki, M. Gujjar, J. Mohan, S. Rakshit and R. Vaidyanathan, *Org. Process Res. Dev.*, 2021, DOI: 10.1021/acs.oprd.1c00088.
72. M. Golden, D. Legg, D. Milne, K. D. Arun Bharadwaj M., M. Gopal, N. Dokka, S. Nambiar, P. Ramachandra, U. Santhosh, P. Sharma, R. Sridharan, M. Sulur, M. Linderberg, A. Nilsson, R. Sohlberg, J. Kremers, S. Oliver and D. Patra, *Org. Process Res. Dev.*, 2016, **20**, 675-682.
73. S. Karlsson, R. Bergman, C. Löfberg, P. R. Moore, F. Pontén, J. Tholander and H. Sörensen, *Org. Process Res. Dev.*, 2015, **19**, 2067-2074.
74. W. A. F. Gladstone, J. B. Aylward and R. O. C. Norman, *J. Chem. Soc. C*, 1969, **1969**, 2587-2598.
75. R. Milcent and G. Barbier, *J. Heterocycl. Chem.*, 1983, **20**, 77-80.
76. P. S. N. Reddy and P. P. Reddy, *Indian J. Chem., Sect B*, 1987, **26B**, 890-891.
77. S. P. Hiremath, K. Shivaramayya, K. R. Sekhar and M. G. Purohit, *Indian J. Chem., Sect B*, 1990, **29B**, 1118-1124.

78. M. A. E. Sallam, M. A. Mostafa, N. A. R. Hussein and L. B. Townsend, *Alex. J. Pharm. Sci.*, 1990, **4**, 18-21.
79. S. K. Srivastava, R. B. Pathak and S. C. Bahel, *J. Indian Chem. Soc.*, 1991, **68**, 113-114.
80. R. Yang and L. Dai, *J. Org. Chem.*, 1993, **58**, 3381-3383.
81. Z. Shang, *Synth. Commun.*, 2006, **36**, 2927-2937.
82. C. Dobrotă, C. C. Paraschivescuoana, D. Mihaela, M. Baciuc and L. L. Ruță, *Tetrahedron Lett.*, 2009, **50**, 1886-1888.
83. E. Jedlovská and J. Leško, *Synth. Commun.*, 1994, **24**, 1879-1885.
84. S. Guin, T. Ghosh, S. K. Rout, A. Banerjee and B. K. Patel, *Org. Lett.*, 2011, **13**, 5976-5979.
85. H. Jiang, X. Li, X. Pan and P. Zhou, *Pure Appl. Chem.*, 2012, **84**, 553-559.
86. G. Zhang, Y. Yu, Y. Zhao, X. Xie and C. Ding, *Synlett*, 2017, **28**, 1373-1377.
87. A. K. Yadav and L. D. S. Yadav, *Tetrahedron Lett.*, 2014, **55**, 2065-2069.
88. J. Chauhan, M. K. Ravva and S. Sen, *Org. Lett.*, 2019, **21**, 6562-6565.
89. S. Basak, S. Dutta and D. Maiti, *Chem. - Eur. J.*, 2021, **27**, 10533-10557.
90. S. Chen, P. Ranjan, L. G. Voskressensky, E. V. Van der Eycken and U. K. Sharma, *Molecules*, 2020, **25**, 4970.
91. M. Jeganmohan and P. Knochel, *Angew. Chem. Int. Ed.*, 2010, **49**, 8520-8524.
92. C. J. Rohbogner, S. H. Wunderlich, G. C. Clososki and P. Knochel, *Eur. J. Org. Chem.*, 2009, **2009**, 1781-1795.

93. S. H. Wunderlich, M. Kienle and P. Knochel, *Angew. Chem. Int. Ed.*, 2009, **48**, 7256-7260.
94. S. H. Wunderlich and P. Knochel, *Chem. - Eur. J.*, 2010, **16**, 3304-3307.
95. A. Whitehead, Y. Zhang, J. M. Dunn, E. C. Sherer, Y.-h. Lam, J. Stelmach, A. Sun, M. Shiroda, R. K. Orr, S. T. Waddell and S. Raghavan, *Org. Lett.*, 2017, **19**, 4448-4451.
96. S. Lee and Y. Lee, *Eur. J. Org. Chem.*, 2019, **2019**, 3045-3050.
97. S. L. McDonald, C. E. Hendrick and Q. Wang, *Angew. Chem. Int. Ed.*, 2014, **53**, 4667-4670.
98. K. Schwärzer, C. P. Tüllmann, S. Graßl, B. Górski, C. E. Brocklehurst and P. Knochel, *Org. Lett.*, 2020, **22**, 1899-1902.
99. S. H. Wunderlich and P. Knochel, *Angew. Chem. Int. Ed.*, 2007, **46**, 7685-7688.
100. K. P. Harish, K. N. Mohana, L. Mallesha and B. N. P. kumar, *Eur. J. Med. Chem.*, 2013, **65**, 276-283.
101. T. Kawano, T. Yoshizumi, K. Hirano, T. Satoh and M. Miura, *Org. Lett.*, 2009, **11**, 3072-3075.
102. S. Shin, Y. Kim, K. Kim and S. Hong, *Org. Biomol. Chem.*, 2014, **12**, 5719-5726.
103. N. S. Reddy, P. R. Reddy and B. Das, *Synthesis*, 2015, **47**, 2831-2838.
104. R. Tadikonda, M. Nakka, S. Rayavarapu, S. P. K. Kalidindi and S. Vidavalur, *Tetrahedron Lett.*, 2015, **56**, 690-692.
105. F. Yang, J. Koeller and L. Ackermann, *Angew. Chem. Int. Ed.*, 2016, **55**, 4759-4762.
106. H. Hachiya, K. Hirano, T. Satoh and M. Miura, *ChemCatChem*, 2010, **2**, 1403-1406.

107. B. Liu, X. Qin, K. Li, X. Li, Q. Guo, J. Lan and J. You, *Chem. - Eur. J.*, 2010, **16**, 11836-11839.
108. N. Salvanna, G. C. Reddy and B. Das, *Tetrahedron*, 2013, **69**, 2220-2225.
109. H. Hachiya, K. Hirano, T. Satoh and M. Miura, *Angew. Chem. Int. Ed.*, 2010, **49**, 2202-2205.
110. B. Liu, Q. Guo, Y. Cheng, J. Lan and J. You, *Chem. - Eur. J.*, 2011, **17**, 13415-13419.
111. M. Wang, D. Li, W. Zhou and L. Wang, *Tetrahedron*, 2012, **68**, 1926-1930.
112. C. Li, P. Li, J. Yang and L. Wang, *Chem. Commun.*, 2012, **48**, 4214-4216.
113. B. Liu, J. Li, F. Song and J. You, *Chem. - Eur. J.*, 2012, **18**, 10830-10833.
114. D. M. Ferguson, S. R. Rudolph and D. Kalyani, *ACS Catalysis*, 2014, **4**, 2395-2401.
115. D. Kumar, M. Pilania, V. Arun and S. Pooniya, *Org. Biomol. Chem.*, 2014, **12**, 6340-6344.
116. F. Zhu, J.-L. Tao and Z.-X. Wang, *Org. Lett.*, 2015, **17**, 4926-4929.
117. K.-J. Wei, Z.-J. Quan, Z. Zhang, Y.-X. Da and X.-C. Wang, *RSC Adv.*, 2016, **6**, 78059-78063.
118. M. G. Hanson, N. M. Olson, Z. Yi, G. Wilson and D. Kalyani, *Org. Lett.*, 2017, **19**, 4271-4274.
119. Y. B. Bhujabal, K. S. Vadagaonkar and A. R. Kapdi, *Asian J. Org. Chem.*, 2019, **8**, 289-295.
120. J. Yang, *Tetrahedron*, 2019, **75**, 2182-2187.

121. C. Liu, Z. Wang, L. Wang, P. Li and Y. Zhang, *Org. Biomol. Chem.*, 2019, **17**, 9209-9216.
122. P.-X. Zhou, S. Shi, J. Wang, Y. Zhang, C. Li and C. Ge, *Org. Chem. Front.*, 2019, **6**, 1942-1947.
123. M. Nishino, K. Hirano, T. Satoh and M. Miura, *Angew. Chem. Int. Ed.*, 2013, **52**, 4457-4461.
124. D. Yu, L. Lu and Q. Shen, *Org. Lett.*, 2013, **15**, 940-943.
125. L.-H. Zou, J. Mottweiler, D. L. Priebbenow, J. Wang, J. A. Stubenrauch and C. Bolm, *Chem. - Eur. J.*, 2013, **19**, 3302-3305.
126. R. Odani, K. Hirano, T. Satoh and M. Miura, *Angew. Chem. Int. Ed.*, 2014, **53**, 10784-10788.
127. G. Tan, S. He, X. Huang, X. Liao, Y. Cheng and J. You, *Angew. Chem. Int. Ed.*, 2016, **55**, 10414-10418.
128. Y. Li, J. Jin, W. Qian and W. Bao, *Org. Biomol. Chem.*, 2010, **8**, 326-330.
129. H.-Q. Do and O. Daugulis, *J. Am. Chem. Soc.*, 2011, **133**, 13577-13586.
130. Z. Mao, Z. Wang, Z. Xu, F. Huang, Z. Yu and R. Wang, *Org. Lett.*, 2012, **14**, 3854-3857.
131. X. Qin, B. Feng, J. Dong, X. Li, Y. Xue, J. Lan and J. You, *J. Org. Chem.*, 2012, **77**, 7677-7683.
132. W. Chen, M. Wang, P. Li and L. Wang, *Tetrahedron*, 2011, **67**, 5913-5919.
133. X. Qin, X. Cong, D. Zhao, J. You and J. Lan, *Chem. Commun.*, 2011, **47**, 5611-5613.
134. H. Hachiya, K. Hirano, T. Satoh and M. Miura, *Org. Lett.*, 2011, **13**, 3076-3079.

135. Y. Oda, N. Matsuyama, K. Hirano, T. Satoh and M. Miura, *Synthesis*, 2012, **44**, 1515-1520.
136. B. Das, G. C. Reddy, P. Balasubramanyam and N. Salvanna, *Tetrahedron*, 2012, **68**, 300-305.
137. C. Schneider, D. Masi, S. Couve-Bonnaire, X. Pannecoucke and C. Hoarau, *Angew. Chem. Int. Ed.*, 2013, **52**, 3246-3249.
138. K. Rousée, C. Schneider, S. Couve-Bonnaire, X. Pannecoucke, V. Levacher and C. Hoarau, *Chem. - Eur. J.*, 2014, **20**, 15000-15004.
139. J.-B. E. Y. Rouchet, M. Hachem, C. Schneider and C. Hoarau, *ACS Catalysis*, 2017, **7**, 5363-5369.
140. N. Salvanna, P. R. Reddy and B. Das, *Synlett*, 2018, **29**, 71-74.
141. T. Mukai, K. Hirano, T. Satoh and M. Miura, *J. Org. Chem.*, 2009, **74**, 6410-6413.
142. Z. Ding and N. Yoshikai, *Org. Lett.*, 2010, **12**, 4180-4183.
143. U. K. Sharma, N. Sharma, Y. Kumar, B. K. Singh and E. V. Van der Eycken, *Chem. - Eur. J.*, 2015, **22**, 481-485.
144. J. Zheng, F. Hosseini-Eshbala, Y.-X. Dong and B. Breit, *Chem. Commun.*, 2019, **55**, 624-627.
145. F. Besselièvre and S. Piguel, *Angew. Chem. Int. Ed.*, 2009, **48**, 9553-9556.
146. T. Kawano, N. Matsuyama, K. Hirano, T. Satoh and M. Miura, *J. Org. Chem.*, 2010, **75**, 1764-1766.
147. G. C. Reddy, P. Balasubramanyam, N. Salvanna and B. Das, *Eur. J. Org. Chem.*, 2012, **2012**, 471-474.

148. C. Theunissen and G. Evans, *Org. Lett.*, 2014, **16**, 4488-4491.
149. M. Kitahara, K. Hirano, H. Tsurugi, T. Satoh and M. Miura, *Chem. - Eur. J.*, 2010, **16**, 1772-1775.
150. L. M. Reddy, P. R. Reddy and C. K. Reddy, *Synthesis*, 2017, **49**, 1675-1679.
151. T. Mukai, K. Hirano, T. Satoh and M. Miura, *Org. Lett.*, 2010, **12**, 1360-1363.
152. Y. Makida, H. Ohmiya and M. Sawamura, *Angew. Chem. Int. Ed.*, 2012, **51**, 4122-4127.
153. P. Xie, H. Huang, Y. Xie, S. Guo and C. Xia, *Adv. Synth. Catal.*, 2012, **354**, 1692-1700.
154. W.-J. P. Z.-X. Wang, *Asian J. Org. Chem.*, 2018, **7**, 1626-1634.
155. G.-W. Wang, A.-X. Zhou, J.-J. Wang, R.-B. Hu and S.-D. Yang, *Org. Lett.*, 2013, **15**, 5270-5273.
156. N. Salvann, G. C. Reddy, B. R. Rao and B. Das, *RSC Adv.*, 2013, **3**, 20538-20544.
157. X.-L. Su, L. Ye, J.-J. Chen, X.-D. Liu, S.-P. Jiang, F.-L. Wang, L. Liu, C.-J. Yang, X.-Y. Chang, Z.-L. Li, Q.-S. Gu and X.-Y. Liu, *Angew. Chem. Int. Ed.*, 2020, **60**, 380-384.
158. D. D. Vachhani, A. Sharma and E. Van der Eycken, *Angew. Chem. Int. Ed.*, 2013, **52**, 2547-2550.
159. L. Chu and F.-L. Qing, *J. Am. Chem. Soc.*, 2012, **134**, 1298-1304.
160. S.-Q. Zhu, Y.-L. Liu, H. Li, X.-H. Xu and F.-L. Qing, *J. Am. Chem. Soc.*, 2018, **140**, 11613-11617.
161. L. J. Sebren, I. James J. Devery and C. R. J. Stephenson, *ACS Catalysis*, 2014, **4**, 703-716.
162. L. F. Tietze, *Chem. Rev.*, 1996, **96**, 115-136.

163. H. A. Döndaş, M. d. G. Retamosa and J. M. Sansano, *Organometallics*, 2019, **38**, 1828-1867.
164. H. Clavier and H. Pellissier, *Adv. Synth. Catal.*, 2012, **354**, 3347-3403.
165. H. Pellissier, *Adv. Synth. Catal.*, 2016, **358**, 2194-2259.
166. X. Bao, Q. Wang and J. Zhu, *Angew. Chem. Int. Ed.*, 2017, **56**, 9577-9582.
167. W. Kong, Q. Wang and J. Zhu, *J. Am. Chem. Soc.*, 2015, **137**, 16028-16031.
168. S. Tong, A. Limouni, Q. Wang, M.-X. Wang and J. Zhu, *Angew. Chem. Int. Ed.*, 2017, **56**, 14192-14196.
169. J. Hédouin, C. Schneider, I. Gillaizeau and C. Hoarau, *Org. Lett.*, 2018, **20**, 6027-6032.
170. K. Ishu, D. Kumar, N. K. Maurya, S. Yadav, D. Chaudhary and M. R. Kuram, *Org. Biomol. Chem.*, 2020, **19**, 2243-2253.
171. W. Kong, Q. Wang and J. Zhu, *Angew. Chem. Int. Ed.*, 2016, **55**, 9714-9718.
172. U. K. Sharma, N. Sharma, J. Xu, G. Song and E. V. Van der Eycken, *Chem. - Eur. J.*, 2015, **21**, 4908-4912.
173. J. Y. Kim, S. H. Cho, J. Joseph and S. Chang, *Angew. Chem. Int. Ed.*, 2010, **49**, 9899-9903.
174. S. Guo, B. Qian, Y. Xie, C. Xia and H. Huang, *Org. Lett.*, 2011, **13**, 522-525.
175. J. Joseph, J. Y. Kim and S. Chang, *Chem. - Eur. J.*, 2011, **17**, 8294-8298.
176. M. Miyasaka, K. Hirano, T. Satoh, R. Kowalczyk, C. Bolm and M. Miura, *Org. Lett.*, 2011, **13**, 359-361.

177. J. Wang, J.-T. Hou, J. Wen, J. Zhang and X.-Q. Yu, *Chem. Commun.*, 2011, **47**, 3652-3654.
178. S. Wertz, S. Kodama and A. Studer, *Angew. Chem. Int. Ed.*, 2011, **50**, 11511-11515.
179. Y. Oda, K. Hirano, T. Satoh and M. Miura, *Org. Lett.*, 2012, **14**, 664-667.
180. Y. Qiu, J. Struwe, T. H. Meyer, J. C. A. Oliveira and L. Ackermann, *Chem. - Eur. J.*, 2018, **24**, 12784-12789.
181. M. Henrion, S. Smolders and D. E. De Vos, *Catal. Sci. Technol.*, 2020, **10**, 940-943.
182. T. Kawano, K. Hirano, T. Satoh and M. Miura, *J. Am. Chem. Soc.*, 2010, **132**, 6900-6901.
183. N. Matsuda, K. Hirano, T. Satoh and M. Miura, *Org. Lett.*, 2011, **13**, 2860-2863.
184. W. Xie, J. H. Yoon and S. Chang, *J. Am. Chem. Soc.*, 2016, **138**, 12605-12614.
185. L.-H. Zou, J. Reball, J. Mottweiler and C. Bolm, *Chem. Commun.*, 2012, **48**, 11307-11309.
186. J. Rafique, S. Saba, A. R. Rosário, G. Zenib and A. L. Braga, *RSC Adv.*, 2014, **4**, 51648-51652.
187. J. Rafique, S. Saba, A. R. Rosário and A. L. Braga, *Chem. - Eur. J.*, 2016, **22**, 11854-11862.
188. A.-X. Zhou, X.-Y. Liu, K. Yang, S.-C. Zhao and Y.-M. Liang, *Org. Biomol. Chem.*, 2011, **9**, 5456-5462.
189. M. M. Peterle, M. R. Scheide, L. T. Silva, S. Saba, J. Rafique and A. L. Braga, *ChemistrySelect*, 2018, **3**, 13191-13196.

190. E. V. Zarudnitskii, I. I. Pervak, A. S. Merkulov, A. A. Yurchenko, A. A. Tolmachev and A. M. Pinchuk, *Synthesis*, 2006, **2006**, 1279-1282.
191. E. V. Zarudnitskii, I. I. Pervak, A. S. Merkulov, A. A. Yurchenko and A. A. Tolmachev, *Tetrahedron*, 2008, **64**, 10431-10442.
192. R. Huisgen, J. Sauer and H. J. Sturm, *Angew. Chem.*, 1958, **70**, 272-273.
193. L. Green, K. Livingstone, S. Bertrand, S. Peace and C. Jamieson, *Chem. - Eur. J.*, 2020, **26**, 14866-14870.
194. B. Reichart and C. O. Kappe, *Tetrahedron Lett.*, 2012, **53**, 952-955.
195. J. Cao and L. Wang, *Chin. J. Chem.*, 2015, **33**, 1239-1243.
196. L. Wang, J. Cao, Q. Chen and M. He, *J. Org. Chem.*, 2015, **80**, 4743-4748.
197. Z. Li and L. Wang, *Adv. Synth. Catal.*, 2015, **357**, 3469-3473.
198. S. E. John, S. Gulatia and N. Shankaraiah, *Org. Chem. Front.*, 2021, **8**, 4237-4287.
199. A. Maleki and A. Sarvary, *RSC Adv.*, 2015, **5**, 60938-60955.
200. Q. Wang, K. C. Mgimpatsang, M. Konstantinidou, S. V. Shishkina and A. Dömling, *Org. Lett.*, 2019, **21**, 7320-7323.
201. S. Kurhade, M. Konstantinidou, F. Sutanto, K. Kurpiewska, J. Kalinowska-Tłuścik and A. Dömling, *Eur. J. Org. Chem.*, 2019, **2019**, 2029-2034.
202. K. Kumar, *ChemistrySelect*, 2020, **5**, 10298-10328.
203. T. Kurihara, S. Satake, M. Hatano, K. Ishihara, T. Yoshino and S. Matsunaga, *Chemistry - An Asian Journal*, 2018, **13**, 2378-2381.

204. M. Giustiniano, A. Basso, V. Mercalli, A. Massarotti, E. Novellino, G. C. Tron and J. Zhu, *Chem. Soc. Rev.*, 2017, **46**, 1295-1357.
205. M. M. Bio, G. Javadi and Z. J. Song, *Synthesis*, 2005, **2005**, 19-21.
206. G. Ojeda-Carralero, L. Ceballos, J. Coro and D. Rivera, *ACS Combinatorial Science*, 2020, **22**, 475-494.
207. Y. Wang and C. Zhang, *ChemistrySelect*, 2020, **5**, 171-177.
208. A. Souldozi and A. Ramazani, *Tetrahedron Lett.*, 2007, **48**, 1549-1551.
209. M. Rouhani, A. Ramazani and S. W. Joo, *Ultrason. Sonochem.*, 2014, **21**, 262-267.
210. A. Ramazani and A. Souldozi, *ARKIVOC*, 2008, **2008**, 235-242.
211. A. Ramazani and A. Souldozi, *Phosphorus, Sulfur Silicon Relat. Elem.*, 2009, **184**, 3191-3198.
212. H. Ahankar, A. Ramazani, I. Amini, Y. Ahmadi and A. Souldozi, *Heteroat. Chem*, 2011, **22**, 612-616.
213. A. Ramazani and A. Souldozi, *Phosphorus, Sulfur Silicon Relat. Elem.*, 2009, **184**, 2344-2350.
214. A. Souldozi, K. Ślepokura, T. Lis and A. Ramazani, *Zeitschrift für Naturforschung B*, 2014, **62**, 835-840.
215. N. Takahashi, K. Hayashi, Y. Nakagawa, Y. Furutani, M. Toguchi, Y. Shiozaki-Sato, M. Sudoh, S. Kojima and H. Kakeya, *Biorg. Med. Chem.*, 2019, **27**, 470-478.
216. M. Adib, E. Sheikhi, M. Karimzadeh, H. R. Bijanzadeh and M. Amanlou, *Helv. Chim. Acta*, 2012, **95**, 788-794.

217. M. Adib, M. R. Kesheh, S. Ansari and H. R. Bijanzadeh, *Synlett*, 2009, **2009**, 1575-1578.
218. M. Adib, E. Sheikhi, A. Kavooosi and H. R. Bijanzadeh, *Synthesis*, 2010, **2010**, 4082-4086.
219. A. Ramazani, Y. Ahmadi, M. Rouhani, N. Shajari and A. Souldozi, *Heteroat. Chem*, 2010, **21**, 368-372.
220. A. Ramazani, N. Shajari, A. T. Mahyari, M. Khoobi, Y. Ahmadi and A. Souldozi, *Phosphorus, Sulfur Silicon Relat. Elem.*, 2010, **185**, 2496-2502.
221. A. Ramazani, Y. Ahmadi and A. Mahyari, *Synth. Commun.*, 2011, **41**, 2273-2282.
222. A. Ramazani, F. Z. Nasrabadi, A. M. Malekzadeh and Y. Ahmadi, *Monatshefte für Chemie - Chemical Monthly volume* 2011, **142**, 625-630.
223. A. Ramazani, M. Rouhani, A. Rezaei, N. Shajari and A. Souldozi, *Helv. Chim. Acta*, 2011, **94**, 282-288.
224. M. V. Holagh, A. M. O. Maharramov, M. A. O. Allahverdiyev, A. Ramazani, Y. Ahmadi and A. Souldozi, *Turk. J. Chem.*, 2012, **36**, 179-188.
225. A. Ramazani, Y. Ahmadi, Z. Karimi and A. Rezaei, *J. Heterocycl. Chem.*, 2012, **49**, 1447-1451.
226. A. Ramazani, B. Abdian, F. Z. Nasrabadi and M. Rouhani, *Phosphorus, Sulfur, and Silicon and the Related Elements* 2013, **188**, 642-648.
227. A. Jafari, A. Ramazani, P. A. Asiabi, F. Sadri and S. W. Joo, *Phosphorus, Sulfur Silicon Relat. Elem.*, 2015, **190**, 2246-2254.

228. A. Ramazani, M. Rouhani, F. Z. Nasrabadi and F. Gouranlou, *Phosphorus, Sulfur Silicon Relat. Elem.*, 2015, **190**, 20-28.
229. M. Rouhani, A. Ramazani and S. W. Joo, *Ultrason. Sonochem.*, 2015, **22**, 391-396.
230. A. Souldozi, *J. Chem. Res.*, 2015, **39**, 177-179.
231. A. Jafari, A. Ramazani, F. Sadri and S. W. Joo, *Phosphorus, Sulfur Silicon Relat. Elem.*, 2016, **191**, 316-321.
232. A. Souldozi and S. Karami, *Phosphorus, Sulfur Silicon Relat. Elem.*, 2016, **191**, 867-870.
233. A. Ramazani, F. Z. Nasrabadi, B. Abdian and M. Rouhani, *Bull. Korean Chem. Soc.*, 2011, **33**, 453-458.
234. A. Jafari, A. Ramazani, H. Ahankar, P. A. Asiabi, F. Sadri and S. W. Joo, *Phosphorus, Sulfur Silicon Relat. Elem.*, 2016, **191**, 373-380.
235. A. Ramazani and A. Rezaei, *Org. Lett.*, 2010, **12**, 2852-2855.
236. A. R. Kazemizadeh, N. Shajari, R. Shapouri, N. Adibpour, R. Teimuri-Mofrad and P. Dinmohammadi, *Appl. Organomet. Chem.*, 2015, **30**, 148-153.
237. A. Ramazani, B. Abdian, F. Z. Nasrabadi, N. Shajari and Z. Ranjdoost, *Bull. Korean Chem. Soc.*, 2012, **33**, 3701-3705.
238. A. Ramazani, M. Khoobi, A. Torkaman, F. Zeinali Nasrabadi, H. Forootanfar, M. Shakibaie, M. Jafari, A. Ameri, S. Emami, M. A. Faramarzi, A. Foroumadi and A. Shafiee, *Eur. J. Med. Chem.*, 2014, **78**, 151-156.
239. A. Ramazani, F. Zeinalia Nasrabadi and Y. Ahmadi, *Helv. Chim. Acta*, 2011, **94**, 1024-1029.

240. A. Ramazani, Y. Ahmadi, A. M. Malekzadeh and A. Rezaei, *Heteroat. Chem*, 2011, **22**, 692-698.
241. A. Ramazani, Y. Ahmadi and R. Tarasi, *Heteroat. Chem*, 2011, **22**, 79-84.
242. A. Ramazani, R. Kalhor, A. Rezaei and Z. Karimi, *Heteroat. Chem*, 2012, **23**, 315-321.
243. A. Ramazani, Y. Ahmadi, F. Z. Nasrabadi and M. Rouhani, *J. Heterocycl. Chem.*, 2013, **50**, 1294-1298.
244. A. R. Kazemizadeh, N. Shajari, R. Shapouri, N. Adibpour and R. Teimuri-Mofrad, *J. Iran. Chem. Soc.*, 2016, **2016**, 1349-1355.
245. N. Shajari, A. R. Kazemizadeh and A. Ramazani, *J. Serb. Chem. Soc.*, 2012, **77**, 1175-1180.
246. A. Ramazani, N. Shajari, A. Mahyari and Y. Ahmadi, *Mol. Divers.*, 2010, **2011**, 521-527.
247. V. B. K. Kunig, C. Ehrh, A. Dömling and A. Brunschweiler, *Org. Lett.*, 2019, **21**, 7238-7243.
248. H. Ahankar, A. Ramazani and Y. Ahmadi, *Phosphorus, Sulfur Silicon Relat. Elem.*, 2014, **189**, 914-923.
249. H. Ahankar, A. Ramazani, Y. Ahmadi and I. Amini, *Phosphorus, Sulfur Silicon Relat. Elem.*, 2013, **188**, 886-894.
250. A. Ahmadi, A. Bagherzadeh, A. Ramazani, Y. Ahmadi, S. W. Joo and H. Ahankar, *Phosphorus, Sulfur Silicon Relat. Elem.*, 2016, **191**, 871-875.
251. M. Ashtary, A. Ramazani, A. R. Kazemizadeh, N. Shajari, N. Fattahi and S. W. Joo, *Phosphorus, Sulfur Silicon Relat. Elem.*, 2016, **191**, 1402-1407.

252. A. Ramazani, Y. Ahmadi, N. Fattahi, H. Ahankar, M. Pakzad, H. Aghahosseini, A. Rezaei, S. T. Fardood and S. W. Joo, *Phosphorus, Sulfur Silicon Relat. Elem.*, 2016, **191**, 1057-1062.
253. A. Ramazani, M. Ashtari, A. Souldozi and Y. Ahmadi, *Phosphorus, Sulfur Silicon Relat. Elem.*, 2011, **187**, 1064-1073.
254. A. Ramazani, N. Fattahi, M. Ashtari, A. Rezaei and S. W. Joo, *Phosphorus, Sulfur Silicon Relat. Elem.*, 2016, **191**, 908-912.
255. A. Ramazani, F. Z. Nasrabadi, H. Ahankar, P. A. Asiabi, F. Sadri and S. W. Joo, *Phosphorus, Sulfur Silicon Relat. Elem.*, 2016, **191**, 230-223.
256. A. Ramazani, A. Rezaei and Y. Ahmadi, *Phosphorus, Sulfur Silicon Relat. Elem.*, 2012, **187**, 22-31.
257. A. Ramazani, F. Z. Nasrabadi, Z. Karimi and M. Rouhani, *Synth. Commun.*, 2013, **43**, 1818-1830.
258. A. Ramazani, Y. Ahmadi and F. Z. Nasrabadi, *Zeitschrift für Naturforschung B*, 2011, **2011**, 184-190.
259. A. T. Londregan, K. A. Farley, C. Limberakis, P. B. Mullins and D. W. Piotrowski, *Org. Lett.*, 2012, **14**, 2890-2893.
260. H. A. Brown and R. M. Waymouth, *Acc. Chem. Res.*, 2013, **46**, 2585-2596.
261. L. Guo, S. H. Lahasky, K. Ghale and D. Zhang, *J. Am. Chem. Soc.*, 2012, **134**, 9163-9171.
262. M. Sun, L. Zhao, Y.-L. Yu and M.-W. Ding, *Synthesis*, 2021, **53**, 1365-1371.

263. C. Russo, R. Cannalire, P. Luciano, F. Brunelli, G. C. Tron and M. Giustiniano, *Synthesis*, 2021, **53**, 4419-4427.
264. F. Z. Nasrabadi, A. Ramazani and Y. Ahmadi, *Mol. Divers.*, 2011, **2011**, 791-798.
265. F. Brockmeyer, D. v. Gerven, W. Saak and J. Martens, *Synthesis*, 2014, **46**, 1603-1612.
266. N. Shajari, A. R. Kazemizadeh and A. Ramazani, *Turk. J. Chem.*, 2015, **2015**, 874-879.
267. K. P. Jethava, J. Fine, Y. Chen, A. Hossain and G. Chopra, *Org. Lett.*, 2020, **22**, 8480-8486.
268. L. Cui, Q. Liu, J. Yu, C. Ni and H. Yu, *Tetrahedron Lett.*, 2011, **52**, 5530-5533.
269. E. G. Arnott, in *Comprehensive Organic Synthesis*, eds. P. Knochel and A. G. Molander, Elsevier, Oxford, 2 edn., 2014, vol. 8, pp. 390-399.
270. J. Seyden-Penne, *Reductions by the Alumino- and Borohydrides in Organic Synthesis*, Wiley-VCH, New-York, 2 edn., 1997.
271. S. Werkmeister, K. Junge and M. Beller, *Org. Process Res. Dev.*, 2014, **18**, 289-302.
272. A. Volkov, F. Tinnis, T. Slagbrand, P. Trilloa and H. Adolfsson, *Chem. Soc. Rev.*, 2016, **45**, 6685-6697.
273. A. Chardon, E. Morisset, J. Rouden and J. Blanchet, *Synthesis*, 2018, **50**, 984-997.
274. A. M. Smith and R. Whyman, *Chem. Rev.*, 2014, **114**, 5477-5510.
275. D. J. A. Schedler, A. G. Godfrey and B. Ganem, *Tetrahedron Lett.*, 1993, **34**, 5035-5038.
276. J. T. Spletstoser, J. M. White, A. R. Tunoori and G. I. Georg, *J. Am. Chem. Soc.*, 2007, **129**, 3408-3419.

277. Y. Oda, T. Sato and N. Chida, *Org. Lett.*, 2012, **14**, 950-953.
278. S. L. Buchwald, S. J. LaMaire, R. B. Nielsen, B. T. Watson and S. M. King, *Org. Synth.*, 1993, **71**, 73.
279. T. Dombrey, C. Helleu, C. Darcel and J.-B. Sortais, *Adv. Synth. Catal.*, 2013, **355**, 3358-3362.
280. S. Das, B. Join, K. Junge and M. Beller, *Chem. Commun.*, 2012, **48**, 2683-2685.
281. S. Zhou, K. Junge, D. Addis, S. Das and M. Beller, *Angew. Chem. Int. Ed.*, 2009, **48**, 9507-9510.
282. Y. Sunada, H. Kawakami, T. Imaoka, Y. Motoyama and H. Nagashima, *Angew. Chem. Int. Ed.*, 2009, **48**, 9511-9514.
283. S. Das, B. Wendt, K. Möller, K. Junge and M. Beller, *Angew. Chem. Int. Ed.*, 2012, **51**, 1662-1666.
284. A. Volkov, F. Tinnis, T. Slagbrand, I. Pershagen and H. Adolfsson, *Chem. Commun.*, 2014, **50**, 14508-14511.
285. R. Kuwano, M. Takahashi and Y. Ito, *Tetrahedron Lett.*, 1998, **39**, 1017-1020.
286. B. Li, J.-B. Sortais and C. Darcel, *Chem. Commun.*, 2013, **49**, 3691-3693.
287. S. Das, D. Addis, S. Zhou, K. Junge and M. Beller, *J. Am. Chem. Soc.*, 2010, **132**, 1770-1771.
288. S. Das, D. Addis, K. Junge and M. Beller, *Chem. - Eur. J.*, 2011, **17**, 12186-12192.
289. L. Vaska and J. W. DiLuzio, *J. Am. Chem. Soc.*, 1961, **83**, 2784-2785.
290. Y. Motoyama, M. Aoki, N. Takaoka, R. Aoto and H. Nagashima, *Chem. Commun.*, 2009, 1574-1576.

291. D. Matheau-Raven, P. Gabriel, J. A. Leitch, Y. A. Almeahmadi, K. Yamazaki and D. J. Dixon, *ACS Catalysis*, 2020, **10**, 8880-8897.
292. P. J. Czerwiński and B. Furman, *Frontiers in Chemistry*, 2021, **9**, 655849.
293. A. Tahara and H. Nagashima, *Tetrahedron Lett.*, 2020, **61**, 151423-151423.
294. A. W. Gregory, A. Chambers, A. Hawkins, P. Jakubec and D. J. Dixon, *Chem. - Eur. J.*, 2015, **21**, 111-114.
295. M. Nakajima, T. Sato and N. Chida, *Org. Lett.*, 2015, **17**, 1696-1699.
296. K. Shirokane, T. Wada, M. Yoritate, R. Minamikawa, N. Takayama, T. Sato and N. Chida, *Angew. Chem. Int. Ed.*, 2013, **53**, 512-516.
297. P. Q. Huang, W. Ou and F. Han, *Chem. Commun.*, 2016, **52**, 11967-11970.
298. S. Katahara, S. Kobayashi, K. Fujita, T. Matsumoto, T. Sato and N. Chida, *J. Am. Chem. Soc.*, 2016, **138**, 5246-5249.
299. Á. L. Fuentes de Arriba, E. Lenci, M. Sonawane, O. Formery and D. J. Dixon, *Angew. Chem. Int. Ed.*, 2017, **56**, 3655-3659.
300. L. G. Xie and D. J. Dixon, *Chem. Sci.*, 2017, **8**, 7492-7497.
301. P. Gabriel, L.-G. Xie, D. J. Dixon, K. R. Holman and S. E. Reisman, *Org. Synth*, 2019, **96**, 511-527.
302. X. N. Hu, T. L. Shen, D. C. Cai, J. F. Zheng and P. Q. Huang, *Org. Chem. Front.*, 2018, **5**, 2051-2056.
303. L. G. Xie and D. J. Dixon, *Nat. Commun.*, 2018, **9**, 1-8.
304. P. Gabriel, A. W. Gregory and D. J. Dixon, *Org. Lett.*, 2019, **21**, 6658-6662.

305. Y. Takahashi, T. Sato and N. Chida, *Chem. Lett.*, 2019, **48**, 1138-1141.
306. Z. P. Yang, G. S. Lu, J. L. Ye and P. Q. Huang, *Tetrahedron*, 2019, **75**, 1624-1631.
307. W. Ou, G. S. Lu, D. An, F. Han and P. Q. Huang, *Eur. J. Org. Chem.*, 2020, **2020**, 52-56.
308. P. Biallas, K. Yamazaki and D. J. Dixon, *Org. Lett.*, 2022, **24**, 2002-2007.
309. P. Gabriel, Y. A. Almeahmadi, Z. R. Wong and D. J. Dixon, *J. Am. Chem. Soc.*, 2021, **143**, 10828-10835.
310. Y. He and X. Wang, *Org. Lett.*, 2021, **23**, 225-230.
311. Z. Li, F. Zhao, W. Ou, P.-Q. Huang and X. Wang, *Angew. Chem. Int. Ed.*, 2021, DOI: 10.1002/anie.202111029.
312. K. Yamazaki, P. Gabriel, G. D. Carmine, J. Pedroni, M. Farizyan, T. A. Hamlin and D. J. Dixon, *ACS Catalysis*, 2021, **11**, 7489-7497.
313. T. Rogova, P. Gabriel, S. Zavitsanou, J. A. Leitch, F. Duarte and D. J. Dixon, *ACS Catalysis*, 2020, **10**, 11436-11447.
314. H. Kobayashi, Y. Sasano, N. Kanoh, E. Kwon and Y. Iwabuchi, *Eur. J. Org. Chem.*, 2016, **2016**, 270-273.
315. Z. P. Yang, Q. He, J. L. Ye and P. Q. Huang, *Org. Lett.*, 2018, **20**, 4200-4203.
316. C. L. Hugelshofer, V. Palani and R. Sarpong, *J. Org. Chem.*, 2019, **84**, 14069-14091.
317. C. L. Hugelshofer, V. Palani and R. Sarpong, *J. Am. Chem. Soc.*, 2019, **141**, 8431-8435.
318. N.-P. Li, M. Liu, X.-J. Huang, X.-Y. Gong, W. Zhang, M.-J. Cheng, W.-C. Ye and L. Wang, *J. Org. Chem.*, 2018, **83**, 5707-5714.

319. W. B. Motherwell, M. J. Tozer and B. C. Ross, *J. Chem. Soc., Chem. Commun.*, 1989, **1989**, 1437-1439.
320. S. Purser, P. R. Moore, S. Swallow and V. Gouverneur, *Chem. Soc. Rev.*, 2008, **37**, 320-330.
321. D. O'Hagan, *Chem. Soc. Rev.*, 2008, **37**, 308-319.
322. E. Vitaku, D. T. Smith and J. T. Njardarson, *J. Med. Chem.*, 2014, **57**, 10257-10274.
323. M. Baumann and I. R. Baxendale, *Beilstein J. Org. Chem.*, 2013, **9**, 2265-2319.
324. M. M. Heravi and V. Zadsirjan, *RSC Adv.*, 2020, **10**, 44247-44311.
325. N. Kerru, L. Gummidi, S. Maddila, K. K. Gangu and S. B. Jonnalagadda, *Molecules*, 2020, **25**, 1909.
326. A. Souldozi, A. Ramazani, N. Bouslimani and R. Welter, *Tetrahedron Lett.*, 2007, **48**, 2617-2620.
327. M. Adib, S. Ansari, S. Feizi and H. R. Bijanzadeh, *Synlett*, 2010, **2010**, 921-923.
328. K.-I. Tanaka, S. Yoshifuji and Y. Nitta, *Chem. Pharm. Bull.*, 1988, **36**, 3125-3129.
329. A. Ammazalorso, B. D. Filippis, L. Giampietro and R. Amoroso, *Chem. Biol. Drug Des.*, 2017, **90**, 1094-1105.
330. A. Tahara, Y. Miyamoto, R. Aoto, K. Shigeta, Y. Une, Y. Sunada, Y. Motoyama and H. Nagashima, *Organometallics*, 2015, **34**, 4895-4907.
331. A. Tahara, I. Kitahara, D. Sakata, Y. Kuninobu and H. Nagashima, *J. Org. Chem.*, 2019, **84**, 15236-15254.
332. Y. Une, A. Tahara, Y. Miyamoto, Y. Sunada and H. Nagashima, *Organometallics*, 2019, **38**, 852-862.

333. M. Saitoh, J. Kunitomo, E. Kimura, H. Iwashita, Y. Uno, T. Onishi, N. Uchiyama, T. Kawamoto, T. Tanaka, C. D. Mol, D. R. Dougan, G. P. Textor, G. P. Snell, M. Takizawa, F. Itoh and M. Kori, *J. Med. Chem.*, 2009, **52**, 6270-6286.
334. N. Linganna and K. M. LokanathaRai, *Synth. Commun.*, 1998, **28**, 4611-4617.
335. F. Thalhammer, U. Wallfahrer and J. Sauer, *Tetrahedron Lett.*, 1988, **29**, 3231-3234.
336. G. I. Elliott, J. R. Fuchs, B. S. J. Blagg, H. Ishikawa, H. Tao, Z.-Q. Yuan and D. L. Boger, *J. Am. Chem. Soc.*, 2006, **128**, 10589-10595.
337. J. E. Sears and D. L. Boger, *Acc. Chem. Res.*, 2016, **49**, 241-251.
338. Y. Rao, X. Li, P. Nagorny, J. Hayashida and S. J. Danishefsky, *Tetrahedron Lett.*, 2009, **50**, 6684-6686.
339. D. Matheau-Raven and D. J. Dixon, *Angew. Chem. Int. Ed.*, 2021, **60**, 19725-19729.
340. J. Vesely and R. Rios, *Chem. Soc. Rev.*, 2013, **43**, 611-630.
341. E. Marcantoni and M. Petrini, *Adv. Synth. Catal.*, 2016, **358**, 3657-3682.
342. R. Appel and H. Mayr, *J. Am. Chem. Soc.*, 2011, **133**, 8240-8251.
343. H. Mayr, T. Bug, M. F. Gotta, N. Hering, B. Irrgang, B. Janker, B. Kempf, R. Loos, A. R. Ofial, G. Remennikov and H. Schimmel, *J. Am. Chem. Soc.*, 2001, **123**, 9500-9512.
344. H. Mayr and M. Patz, *Angew. Chem. Int. Ed.*, 1994, **33**, 938-957.
345. R. Appel, S. Chelli, T. Tokuyasu, K. Troshin and H. Mayr, *J. Am. Chem. Soc.*, 2013, **135**, 6579-6587.
346. T. Kano, T. Yurino, D. Asakawa and K. Maruoka, *Angew. Chem. Int. Ed.*, 2013, **52**, 5532-5534.

347. L. Knorr, *Ber. Dtsch. Chem. Ges.*, 1884, **17**, 2863-2870.
348. C. Paal, *Ber. Dtsch. Chem. Ges.*, 1884, **17**, 2756-2767.
349. E. D. Goddard-Borger and R. V. Stick, *Org. Lett.*, 2007, **9**, 3797-3800.
350. H. Ye, R. Liu, D. Li, Y. Liu, H. Yuan, W. Guo, L. Zhou, X. Cao, H. Tian, J. Shen and P. G. Wang, *Org. Lett.*, 2013, **15**, 18-21.
351. Y.-N. Li, F. Xiao, Y. Guo and Y.-F. Zeng, *Eur. J. Org. Chem.*, 2020, **2021**, 1215-1228.
352. J. T. M. Correia, V. A. Fernandes, B. T. Matsuo, J. A. C. Delgado, W. C. de Souza and M. W. Paixão, *Chem. Commun.*, 2020, **56**, 503-514.
353. J. A. Andrews, L. R. E. Pantaine, C. F. Palmer, D. L. Poole and M. C. Willis, *Org. Lett.*, 2021, **23**, 8488-8493.
354. M. A. Fouad, H. Abdel-Hamid and M. S. Ayoup, *RSC Adv.*, 2020, **10**, 42644-42681.
355. J. Li, C. Kornhaaß and L. Ackermann, *Chem. Commun.*, 2012, **48**, 11343-11345.
356. J. A. Leitch, P. B. Wilson, C. L. McMullin, M. F. Mahon, Y. Bhonoah, I. H. Williams and C. G. Frost, *ACS Catalysis*, 2016, **6**, 5520-5529.
357. T. Akiyama and K. Mori, *Chem. Rev.*, 2015, **115**, 9277-9306.
358. T. Akiyama, *Chem. Rev.*, 2007, **107**, 5744-5758.
359. X. Yu and W. Wang, *Chem. Asian J.*, 2008, **3**, 516-532.
360. T. James, M. van Gemmeren and B. List, *Chem. Rev.*, 2015, **115**, 9388-9409.
361. D. Matheau-Raven, E. Boulter, T. Rogova and D. J. Dixon, *Org. Lett.*, 2021, **23**, 8209-8213.
362. C. G. Saluste, R. J. Whitby and M. Furber, *Tetrahedron Lett.*, 2001, **42**, 6191-6194.

363. H. Jiang, B. Liu, Y. Li, A. Wang and H. Huang, *Org. Lett.*, 2011, **13**, 1028-1031.
364. B. Wang, D. He, B. Ren and T. Yao, *Chem. Commun.*, 2020, **56**, 900-903.
365. S. Graßl, Y.-H. Chen, C. Hamze, C. P. Tüllmann and P. Knochel, *Org. Lett.*, 2019, **21**, 494-497.
366. E. Boulter, Part II Thesis, University of Oxford, 2021.
367. T. Zhong, M.-K. Pang, Z.-D. Chen, B. Zhang, J. Weng and G. Lu, *Org. Lett.*, 2020, **22**, 3072-3078.
368. X. Zhang and D. W. C. MacMillan, *J. Am. Chem. Soc.*, 2016, **138**, 13862-13865.
369. L. Yang, S. Li, L. Cai, Y. Ding, L. Fu, Z. Cai, H. Ji and G. Li, *Org. Lett.*, 2017, **19**, 2746-2749.
370. K. Osowska-pacewicka, S. Zawadzki and A. Zwierzak, *Phosphorus, Sulfur Silicon Relat. Elem.*, 1993, **82**, 49-54.
371. N. Ohmura, A. Nakamura, A. Hamasaki and M. Tokunaga, *Eur. J. Org. Chem.*, 2008, **2008**, 5042-4045.
372. P. Hermange, A. T. Lindhardt, R. H. Taaning, K. Bjerglund, D. Lupp and T. Skrydstrup, *J. Am. Chem. Soc.*, 2011, **133**, 6061-6071.
373. F. Cumine, S. Zhou, T. Tuttle and J. A. Murphy, *Org. Biomol. Chem.*, 2017, **15**, 3324-3336.
374. G. Hou, F. Gosselin, W. Li, J. C. McWilliams, Y. Sun, M. Weisel, P. D. O'Shea, C.-Y. Chen and I. W. D. X. Zhang, *J. Am. Chem. Soc.*, 2009, **131**, 9882-9883.
375. L. C. Morrill, J. Douglas, T. Lebl, A. M. Z. Slawin, D. J. Fox and A. D. Smith, *Chem. Sci.*, 2013, **4**, 4146-4155.

376. C. G. Goodman, D. T. Do and J. S. Johnson, *Org. Lett.*, 2013, **15**, 2446-2449.
377. T. Mita, M. Sugawara, K. Saito and Y. Sato, *Org. Lett.*, 2014, **16**, 3028-3031.
378. S. Tabet, N. Rodeville, J.-G. Boiteau and I. Cardinaud, *Org. Process Res. Dev.*, 2016, **20**, 1383-1387.
379. J. F. Collados, E. Toledano, D. Guijarro and M. Yus, *J. Org. Chem.*, 2012, **77**, 5744-5750.
380. E. Dubost, V. Babin, F. Benoist, A. Hébert, P. Barbey, C. Chollet, J.-P. Bouillon, A. Manrique, G. Pieters, F. Fabis and T. Cailly, *Org. Lett.*, 2018, **20**, 6302-6305.
381. D. Susanti, L. L. R. Ng and P. W. H. Chan, *Adv. Synth. Catal.*, 2014, **356**, 353-358.
382. J. R. Cabrero-Antonino, I. Sorribes, K. Junge and M. Beller, *Angew. Chem. Int. Ed.*, 2015, **55**, 387-391.
383. Y. Fan, Y. He, X. Liu, T. Hu, H. Ma, X. Yang, X. Luo and G. Huang, *J. Org. Chem.*, 2016, **81**, 6820-6825.
384. Z.-L. Yao, L. Wang, N.-Q. Shao, Y.-L. Guo and D.-H. Wang, *ACS Catalysis*, 2019, **9**, 7343-7349.
385. Y. Jeong, J. Ban, M. Lim and H. Rhee, *Synthesis*, 2018, **50**, 1867-1874.